



2000 NASA Seal/Secondary Air System Workshop

The NASA STI Program Office . . . in Profile

Since its founding, NASA has been dedicated to the advancement of aeronautics and space science. The NASA Scientific and Technical Information (STI) Program Office plays a key part in helping NASA maintain this important role.

The NASA STI Program Office is operated by Langley Research Center, the Lead Center for NASA's scientific and technical information. The NASA STI Program Office provides access to the NASA STI Database, the largest collection of aeronautical and space science STI in the world. The Program Office is also NASA's institutional mechanism for disseminating the results of its research and development activities. These results are published by NASA in the NASA STI Report Series, which includes the following report types:

- **TECHNICAL PUBLICATION.** Reports of completed research or a major significant phase of research that present the results of NASA programs and include extensive data or theoretical analysis. Includes compilations of significant scientific and technical data and information deemed to be of continuing reference value. NASA's counterpart of peer-reviewed formal professional papers but has less stringent limitations on manuscript length and extent of graphic presentations.
- **TECHNICAL MEMORANDUM.** Scientific and technical findings that are preliminary or of specialized interest, e.g., quick release reports, working papers, and bibliographies that contain minimal annotation. Does not contain extensive analysis.
- **CONTRACTOR REPORT.** Scientific and technical findings by NASA-sponsored contractors and grantees.

- **CONFERENCE PUBLICATION.** Collected papers from scientific and technical conferences, symposia, seminars, or other meetings sponsored or cosponsored by NASA.
- **SPECIAL PUBLICATION.** Scientific, technical, or historical information from NASA programs, projects, and missions, often concerned with subjects having substantial public interest.
- **TECHNICAL TRANSLATION.** English-language translations of foreign scientific and technical material pertinent to NASA's mission.

Specialized services that complement the STI Program Office's diverse offerings include creating custom thesauri, building customized data bases, organizing and publishing research results . . . even providing videos.

For more information about the NASA STI Program Office, see the following:

- Access the NASA STI Program Home Page at <http://www.sti.nasa.gov>
- E-mail your question via the Internet to help@sti.nasa.gov
- Fax your question to the NASA Access Help Desk at 301-621-0134
- Telephone the NASA Access Help Desk at 301-621-0390
- Write to:
NASA Access Help Desk
NASA Center for Aerospace Information
7121 Standard Drive
Hanover, MD 21076



2000 NASA Seal/Secondary Air System Workshop

Proceedings of a conference held at and sponsored by
NASA Glenn Research Center
Cleveland, Ohio
October 25–26, 2000

National Aeronautics and
Space Administration

Glenn Research Center

Trade names or manufacturers' names are used in this report for identification only. This usage does not constitute an official endorsement, either expressed or implied, by the National Aeronautics and Space Administration.

Available from

NASA Center for Aerospace Information
7121 Standard Drive
Hanover, MD 21076

National Technical Information Service
5285 Port Royal Road
Springfield, VA 22100

Available electronically at <http://gltrs.grc.nasa.gov/GLTRS>

Executive Summary

Volume I

The 2000 NASA Seal/Secondary Air System Workshop covered four main areas:

- (i) overviews of NASA-sponsored Ultra-Efficient Engine Technology (UEET) and Access to Space Programs, with emphasis on program goals and seal needs
- (ii) review of turbine engine seal issues from the perspective of end users such as United Airlines
- (iii) reviews of sealing concepts, test results, experimental facilities, and numerical predictions
- (iv) reviews of material development programs relevant to advanced seals development

The NASA UEET overview illustrates for the reader the importance of advanced technologies, including seals, in meeting future engine system efficiency and emission goals. The NASA UEET program goals include an 8- to 15-percent reduction in fuel burn, a 15-percent reduction in CO₂, a 70-percent reduction in NO_x, CO, and unburned hydrocarbons, and a 30-dB noise reduction relative to program baselines.

General Electric, Pratt & Whitney, and Honeywell presented advanced seal development work being performed within their organizations. The NASA-funded GE/Stein Seal team has successfully demonstrated a large (3-ft. diam) aspirating seal that can withstand all anticipated pressures, speeds, and rotor runouts anticipated for a GE90 L.P. turbine balance piston location. Laboratory tests at GE-CRD demonstrated the seal could accommodate a 1-in-5000 hour severe maneuver tilt-load without rubbing, in which the rotor tilts 0.080 in. toward the seal face! GE/Stein Seal are fabricating a full-scale seal to be tested in a GE-90 ground test engine in early 2002. Pratt & Whitney and Stein Seal are investigating carbon seals to accommodate large radial movements anticipated in future geared-fan gearbox locations.

Honeywell presented a finger seal design being considered for a high-temperature static combustor location incorporating ceramic finger elements. Mohawk presented a foil seal arrangement that applies foil-bearing technology to arrive at a noncontacting very low leakage seal. This foil seal is being developed by Mohawk under a NASA SBIR contract and exploits NASA Glenn's advanced solid film lubricant developments. PerkinElmer presented analytical work being performed on a noncontacting face seal. Technetics presented abradable tip seal experimental results and indicated a need for an industry standard for abradable material assessments.

Space Seal Developments: Successful demonstration of the braided carbon rope thermal barriers to extreme temperatures (5500 °F) for short durations provide a new form of very high temperature barrier for future Shuttle solid rocket motor nozzle joints. The X-37, X-38, and future highly reusable launch vehicles pose challenging control surface seal demands that require new seal concepts made from emerging high-temperature ceramics and other materials.

TABLE OF CONTENTS

Volume I

Overview of NASA Glenn Seal Development Program Bruce M. Steinetz and Robert C. Hendricks, NASA Glenn Research Center	1
Welcome to the Airline Industry Sherry Soditus, United Airlines	23
Design of Critical Components Robert C. Hendricks and Erwin V. Zaretsky, NASA Glenn Research Center	29
Overview of Ultra-Efficient Engine Technology (UEET) Program Joe Shaw, NASA Glenn Research Center	33
Development of an Enhanced Thermal Barrier for RSRM Nozzle Joints Paul H. Bauer, Thiokol Propulsion	61
Advanced Seals at GE Research and Development Center Ray Chupp and Norm Turnquist, General Electric Corporate Research and Development	91
GE90 Demonstration of Aspirating Seal T.W. Tseng, General Electric Aircraft Engines	105
Advanced Aspirating Seal Alan D. McNickle, Stein Seal Company	113
Development of High Misalignment Carbon Seals: Overview Lou Dobek, Pratt & Whitney	137
Development of High Misalignment Carbon Seals: Designs George Szymborski, Stein Seal Company	147
Finger Seal Development for a Combustor Application Arun Kumar, Honeywell Engines & Systems	157
High Temperature Performance Evaluation of a Compliant Foil Seal Mohsen Salehi, Hooshang Heshmat, and James F. Walton II, Mohawk Innovative Technology, Inc. (MiTi)	171
Large-Diameter Spiral Groove Face Seal Development Xiaoqing Zheng and Gerald Berard, PerkinElmer Fluid Sciences	199
Abradable Seal Developments at Technetics Doug Chappel and Harold Howe, Technetics Corporation	227
High Temperature Metallic Seal Development Amit Datta, Advanced Components and Materials, Inc., and D. Greg More, The Advanced Products Company	247
Investigation of a Shrouded Rotor-Stator Disk Cavity Ram P. Roy, G. Xu, and J. Feng, Arizona State University	263

X-38 Seal Development	
Donald M. Curry and Ronald K. Lewis, NASA Johnson Space Center, and Jeffrey D. Hagen, Lockheed Martin Space Operations	283
Rudder/Fin Seal Investigations for the X-38 Re-Entry Vehicle	
Patrick H. Dunlap, Jr. and Bruce M. Steinetz, NASA Glenn Research Center, and Donald M. Curry, NASA Johnson Space Center	315
Control Surface Seal Development for Future Re-Entry Vehicles	
Chuck Newquist, Juris Verzemnieks, and Pete Keller, The Boeing Company	331
Thermal Barriers	
Dennis Barber, Oceaneering Thermal Systems	353
Overview of Thermal Barrier/Seal Development at Hi-Temp Insulation	
James Joyce and Sieg Bork, Hi-Temp Insulation, Inc.	373
Rope Seal Developments	
Bruce Bond, Albany International Techniweave, Inc.; John Xia, Siemens Westinghouse; and Margaret Kowal, University of New Hampshire	387
NASA GRC Cryogenic Seal Test Rig Capability	
Margaret Proctor, NASA Glenn Research Center	405
Overview of CMC Development Activities in NASA's Ultra-Efficient Engine Technology (UEET) Program	
Dave Brewer, NASA Glenn Research Center	423
Overview of NASA Studies on High-Temperature Ceramic Fibers	
James A. DiCarlo and Hee Mann Yun, NASA Glenn Research Center	439
High Temperature Ceramic Fiber Development and Trends	
David Wilson, 3M	449
An Introduction to TRIZ	
Dana W. Clarke, Sr., Ideation International Inc.	463

OVERVIEW OF NASA GLENN SEAL DEVELOPMENT PROGRAM

Bruce M. Steinetz and Robert C. Hendricks
National Aeronautics and Space Administration
Glenn Research Center
Cleveland, Ohio

2000 NASA Seal/Secondary Air System Workshop

Dr. Bruce M. Steinetz
NASA Glenn Research Center
Cleveland, OH 44135

Mr. Robert C. Hendricks
NASA Glenn Research Center
Cleveland, OH 44135

Contributors
Margaret Proctor, Patrick Dunlap, Irebert Delgado

October 25-26, 2000
NASA Glenn Research Center
Administration Bldg. Auditorium

CD-00-80927

NASA Glenn hosted the Seals/Secondary Air System Workshop on October 25-26, 2000. Each year NASA and our industry and university partners share their respective seal technology developments. We use these workshops as a technical forum to exchange recent advancements and “lessons-learned” in advancing seal technology and solving problems of common interest. As in the past we are publishing two volumes. Volume I will be publicly available and individual papers will be made available on-line through the web page address listed at the end of this chapter. Volume II will be restricted under International Traffic and Arms Regulations (I.T.A.R.)

2000 NASA Seal/Secondary Air System Workshop

Wednesday, Oct. 25, Morning:

Registration

7:15 a.m.–8:00 a.m.

Introductions

Introductions
Welcome to NASA Glenn
Overview of NASA Glenn Seal Development Program

8:00 a.m.–8:30 a.m.

Dr. Bruce Steinetz, Bob Hendricks/NASA GRC
Dr. Woodrow Whitlow, R&T Dir./NASA GRC
Dr. Bruce Steinetz/NASA GRC

Program Overviews and Requirements

Welcome to the Airline Industry
Design of Critical Components

Overview of Ultra-Efficient Engine Technology (UEET) Program
Overview of USAF Propulsion
Overview of NASA's Access to Space Programs

8:30 a.m.–10:30 a.m.

Ms. Sherry Soditus /Mr. Jim Uhl/United Airlines
Bob Hendricks,Erv Zaretsky/NASA GRC
Ms. Sherry Soditus/United Airlines
Dr. Joe Shaw/NASA GRC
Dr. Otha Davenport/WPAFB
Mr. Harry Cikanek/NASA GRC

Break

10:30–10:45 a.m.

Advanced Seal Development Session I

Development of an Enhanced Thermal Barrier
for RSRM Nozzle Joints
Advanced Seals at GE Research & Development Center
GE90 Demonstration of Aspirating Seal
Advanced Aspirating Seal
Development of High Misalignment Carbon Seals (UEET)

10:45 a.m.–12:30 p.m.

Mr. Paul Bauer/Thiokol

Dr. Ray Chupp, Norm Turnquist/GE-CRD
Dr. Tom Tseng/GEAE
Mr. Alan McNickle/Stein Seal
Mr. Lou Dobek/PW; G. Szymborski/Stein Seal

Lunch Main Cafe

12:30 p.m.–1:30 p.m.

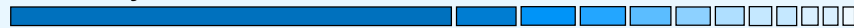
CD-00-80927

The first day of presentations included overviews of a variety of NASA, commercial airline, military and Access to Space programs. Dr. Steinetz presented the the NASA seal development program. Ms. Soditus presented United Airline's end-user's perspective of turbine engine seal/secondary air systems. Mr. Davenport summarized some recent Air Force experience with turbine engine seal and secondary air systems. Mr. Cikanek of NASA's Space Project office summarized NASA's Access to Space Programs citing areas where advanced seals are required.

Representatives from GE, P&W and Honeywell engine companies provided insight into their advanced seal development programs. Thiokol presented results of investigations applying the NASA braided carbon rope as a thermal barrier for the Shuttle Reusable Solid Rocket Motor Nozzle redesigned joints to prevent hot gas effects on critical Viton O-rings.

2000 NASA Seal/Secondary Air System Workshop

Wednesday, Oct. 25, Afternoon:



Advanced Seal Development Session II

Finger Seal Development for a Combustor Application
High Temperature Performance Evaluation
of a Compliant Foil Seal
Large-diameter Spiral Groove Face Seal Development
Abradable Seal Developments at Technetics
High Temperature Metallic Seal Development
NASA High Temperature Turbine Seal Rig Development

Calibration of Optical Pyrometer System for
Non-Contacting Temperature Measurement

Break

Turbine Cavity Seal Flow Studies

UTRC Turbine Rim Seal Ingestion
and Platform Cooling Experiments
Investigation of a Shrouded Rotor-Stator Disk Cavity
Coupled Main/Cavity Flow Calculations Using
TURBO/SCISEAL

Social Hour at GRC

Dinner at Mallorca restaurant with individual checks

1:30 p.m.–4:00 p.m.

Dr. Arun Kumar/Honeywell Engines
Dr. James F. Walton III, H. Heshmat/Mohawk

Dr. Xiaoping Zheng/Perkin-Elmer
Mr. Doug Chappel, H. Howe/Technetics
Dr. Amit Datta/Adv. Components & Materials
Mr. Irebert Delgado/NASA Army Program
M. Proctor, B. Steinetz/NASA GRC
Mr. Jay Oswald/CWRU, B. Steinetz/NASA

4:00 p.m.–4:15 p.m.

4:15 p.m.–5:15 p.m.

Dr. John Feiereisen/UTRC

Dr. Ram Roy/Arizona State Univ
Dr. Mahesh Athavale/CFDRC

5:30 p.m.–6:00 p.m.

7:00 p.m.–?

CD-00-80927

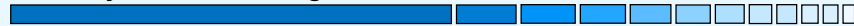
Representatives from seal vendors Stein Seal, Perkin-Elmer, Technetics, Advanced Components and Materials presented their company's recent seal development status.

Researchers from NASA Glenn presented a status review of the new High Temperature, High Speed Turbine Seal rig and associated non-contacting rotor temperature measurement system.

Researchers from United Technology Research Center, Arizona State and CFDRC presented experimental and analytical investigations into the complex flow patterns in rim seal/cavity locations in modern turbine engines. Studies have shown that excessive amounts of flow (up to 2-3% core flow) go through rim seals beyond that which is needed for cooling purposes (Munson and Steinetz, 1994). Hence SFC reductions are possible by reducing flows to what is needed for cooling purposes. New concepts and analytical methods are being developed to limit cooling to the appropriate level and provide positive out-flow of coolant preventing ingestion of hot combustion gases into the turbine rim cavity due to unsteady effects.

2000 NASA Seal/Secondary Air System Workshop

Thursday, Oct. 26, Morning:



Registration

7:45 a.m.–8:30 a.m.

Space Propulsion/Vehicle Seal Development I

Overview of X-37 Program and Seal Development
X-38 Seal Development

Rudder/Fin Seal Investigations for the X-38 Re-entry Vehicle

Control Surface Seal Development for Future Re-entry Vehicles

8:30 a.m.–10:00 a.m.

Dr. Todd Steyer/Boeing

Dr. Don Curry, R. Lewis/NASA JSC;

J. Hagan/Lockheed-Martin

Mr. Pat Dunlap, B. Steinetz/NASA GRC

D. Curry/NASA JSC

Mr. Juris Verzemnieks, C. Newquist/Boeing

Break

10:00 a.m.–10:15 a.m.

Space Propulsion/Vehicle Seal Development II

Thermal Barriers

Overview of Thermal Barrier/Seal Development
at HiTemp Insulation

Rope Seal Developments

NASA GRC Cryogenic Seal Test Rig Capability

10:15 a.m.–12:00 a.m.

Mr. Dennis Barber/Oceaneering

Mr. Sieg Bork/HiTemp Insulation

Mr. Bruce Bond/Albany Techniweave

Ms. Margaret Proctor/NASA GRC

Lunch Main Cafeteria

12:00 a.m.–1:15 p.m.

CD-00-80927

Presentations on the second day concentrated on space vehicle/propulsion seal developments. NASA is developing both the X-37 and X-38 vehicles to demonstrate technologies for each of their respective missions. Both vehicles will be taken to low earth orbit via the Space Shuttle and demonstrate on-orbit and re-entry technologies. Boeing presented an overview of the joint NASA/Air Force X-37 program, control surface seal requirements, and candidate seal approaches. NASA Johnson presented an overview of the X-38 program, control surface seal requirements, and candidate seal approaches. The X-38 is an X-vehicle that is a precursor vehicle to the Space Station Emergency Crew Return Vehicle. Dunlap and Verzemnieks presented work on developing and testing control surface seals for the X-vehicles mentioned.

Representatives from Oceaneering, HiTemp Insulation, and Albany-Techniweave presented structural seals developed for space vehicle thermal protections systems and turbine engine applications.

Proctor presented an overview of NASA Glenn's cryogenic seal test capabilities.

2000 NASA Seal/Secondary Air System Workshop

Thursday, Oct. 26, Afternoon:



Advanced Materials Development

Overview of CMC Development Activities in
NASA's Ultra-Efficient Engine Technology (UEET) Program
Overview of NASA Studies on High-Temperature Ceramic Fibers
High Temperature Ceramic Fiber Development and Trends

1:30 p.m.–2:30 p.m.

Mr. David Brewer/NASA/Army Program

Dr. James DiCarlo/NASA GRC
Dr. David Wilson/3M

Special Topics

An Introduction to TRIZ

2:30 p.m.–3:00 p.m.

Mr. Dana Clarke/Ideation Int'l

Tour of NASA Seal Facilities

3:00 p.m.–4:00 p.m.

Adjourn

4:00 p.m.

CD-00-80927

Representatives from NASA Glenn presented GRC's high temperature ceramic matrix composite and ceramic fiber developments. 3-M presented property comparisons for their Nextel fibers and YAG fibers.

Ideation presented an overview of the Theory of Inventive Problem Solution (TRIZ/TIPS). TRIZ problem solution is based on research done by Genrich Altshuller (Altshuller, 1996) who extracted cause and effect solution methods from the patent literature to arrive at a systematic solution approach to obtain elegant solutions in both the original field and quite different fields of application.

Scope of Activities: Turbine Seals



Objective:

Develop durable, low-leakage turbomachinery seals to meet demands of next generation subsonic and supersonic engines

Specific Goals:

- Develop seal technology to reduce specific fuel consumption (SFC) • 2%
- Validate seal performance and design models through lab. testing under simulated speeds to (1500 fps), temperatures (to 1500°F) and pressures
- Investigate non-contacting, non-wearing seals to meet life and speed requirements
- Demonstrate seal performance in full scale engine tests
- Transition seals to engine service by 2005

Key Facilities:

In House:

- Turbine engine seal test rig upgraded to 1500°F, 1500 fps speed
- Army T-700 & T-55 engines

Contractor: Numerous laboratory facilities including full scale engine tests (GE90)

Partners:

GE; PW; Allison; Air Force; Army; UTRC; Honeywell (AlliedSignal); Williams; Perkin Elmer (EG&G); Stein Seal; Mohawk

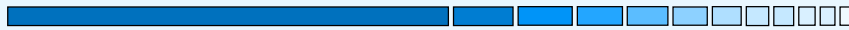
CD-00-80927

The objective of the NASA Glenn turbine engine seal development program is to develop durable, low-leakage seals to meet demands of next generation subsonic and supersonic engines.

Advanced seals that include film riding aspirating, compliant foil, and advanced finger seals are being investigated to demonstrate non-contacting, low-leakage operation. Advanced test rigs such as NASA GRC's unique high speed (1500 fps) and high temperature (1500°F) turbine seal rig will be used to assess performance characteristics of these new seals. Under contract, GE will perform engine tests of a full scale (36" diameter) aspirating seal in a ground-based GE-90 engine.

Analytical methods such as the coupled TURBO/SCISEAL code are being developed under contract with CFDRC to perform coupled main-flow (TURBO) and secondary air/seal (SCISEAL) calculations.

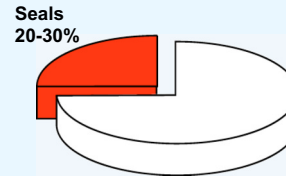
Why Seals?



AST Study Results: Expected Seal Technology Payoffs		
Seal Technology	Study Engine/ Company	System Level Benefits
Large diameter aspirating seals (Multiple locations)	GE90-Transport/ GE	-1.86% SFC -0.69% DOC+1
Interstage seals (Multiple locations)	GE90-Transport/ GE	-1.25% SFC -0.36% DOC+1
Film riding seals (Turbine inter-stage seals)	Regional-AE3007/ Allison	> -0.9% SFC > -0.89% DOC+1
Advanced finger seals	AST Regional/ Honeywell	-1.4% SFC -0.7% DOC+1

UEET Program Goal

Reduce Fuel Burn by 8-15%



- Seals provide high return on technology \$ investment
Same performance goals possible through modest investment in the technology development
Example: 1/5th to 1/4th cost of obtaining same performance improvements of re-designing/re-qualifying the compressor
- Seal contribution to program goals: 2 to 3% SFC reduction

Advanced Seal Technology: An Important Player

CD-00-80927

Cycle studies have shown the benefits of increasing engine pressure ratios and cycle temperatures to decrease engine weight and improve performance in next generation turbine engines. Advanced seals have been identified as critical in meeting engine goals for specific fuel consumption, thrust-to-weight, emissions, durability and operating costs. NASA and the industry are identifying and developing engine and sealing technologies that will result in dramatic improvements and address each of these goals for engines entering service in the 2005-2007 time frame.

General Electric, Allison and AlliedSignal Engines all performed detailed engine system studies to assess the potential benefits of implementing advanced seals. The study results were compelling. Implementing advanced seals into modern turbine engines will net large reductions in both specific fuel consumption (SFC) and direct operating costs including interest (DOC+I) as shown in the chart (Steinetz et al, 1998).

Applying the seals to just several engine locations would reduce SFC 2 to 3% . This represents a significant (20-30%) contribution toward meeting the overall goals of NASA's Ultra-Efficient Engine Technology (UEET) program.

Aspirating Seal Development: GE90 Demo Program Funded UEET Seal Development Program

- **Goal:**

- Complete aspirating seal development by conducting full scale (36 in. diameter) aspirating seal demonstration tests in GE90 engine.

- **Payoffs:**

- Leakage <1/5th labyrinth seal
- Operates without contact under severe conditions:
 - 10 mil TIR
 - 0.25°/0.8 sec tilt maneuver loads (0.08" deflection!)
- Decrease SFC by 1.86% for three locations

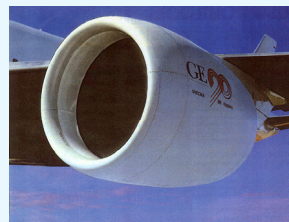
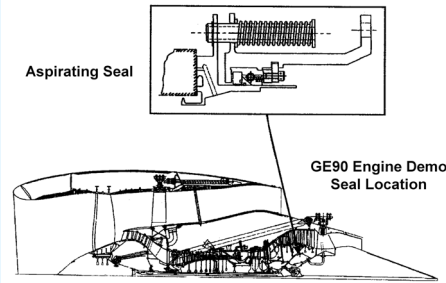
- **Approach:**

- Seal and runner design and fabrication
- Seal system CFD analysis
- Instrumentation and installation
- GE90 engine test
- Data analysis and report

- **Schedule:**

- Design and analyses by 1Q FY01
- Hardware fabrication by 3Q FY01
- GE90 engine test from 4Q FY01 to 1Q FY02
- Data analysis and report by 1Q FY02

- **Partners:** GE/Stein Seal/CFDRC/NASA GRC



General Electric GE90

CD-00-80927

General Electric is developing a low leakage aspirating face seal for a number of locations within modern turbine applications. (see also Tseng, 2001 in this workshop proceeding for further details). This seal shows promise both for compressor discharge and balance piston locations. The seal consists of an axially translating mechanical face that seals the face of a high speed rotor. The face rides on a hydrostatic cushion of air supplied through ports on the seal face connected to the high pressure side of the seal. The small clearance (0.001-0.002 in.) between the seal and rotor results in low leakage (1/5th that of new labyrinth seals). Applying the seal to 3 locations in a GE90 engine can lead to >1.8% SFC reduction. GE Corporate Research and Development tested the seal under a number of conditions to demonstrate the seal's rotor tracking ability. The seal was able to follow a 0.010 in. rotor face total indicator run-out (TIR) and could dynamically follow a 0.25° tilt maneuver (simulating a hard maneuver load) all without face seal contact.

The NASA GRC Ultra Efficient Engine Technology (UEET) Program is funding GE to demonstrate this seal in a ground-based GE-90 demonstrator engine in early 2002.

PW Bearing Compartment Seal Program PW-11

Funded UEET Seal Development Program



Objectives:

- Develop high misalignment seals capable of handling extremely large radial displacements due to angular and radial misalignment.
- Develop high speed seals that will meet life requirements at high temperatures
- Develop large diameter (up to 16 in.) seals operating at low delta P
- Develop seal technology ready for 2004 demonstrator

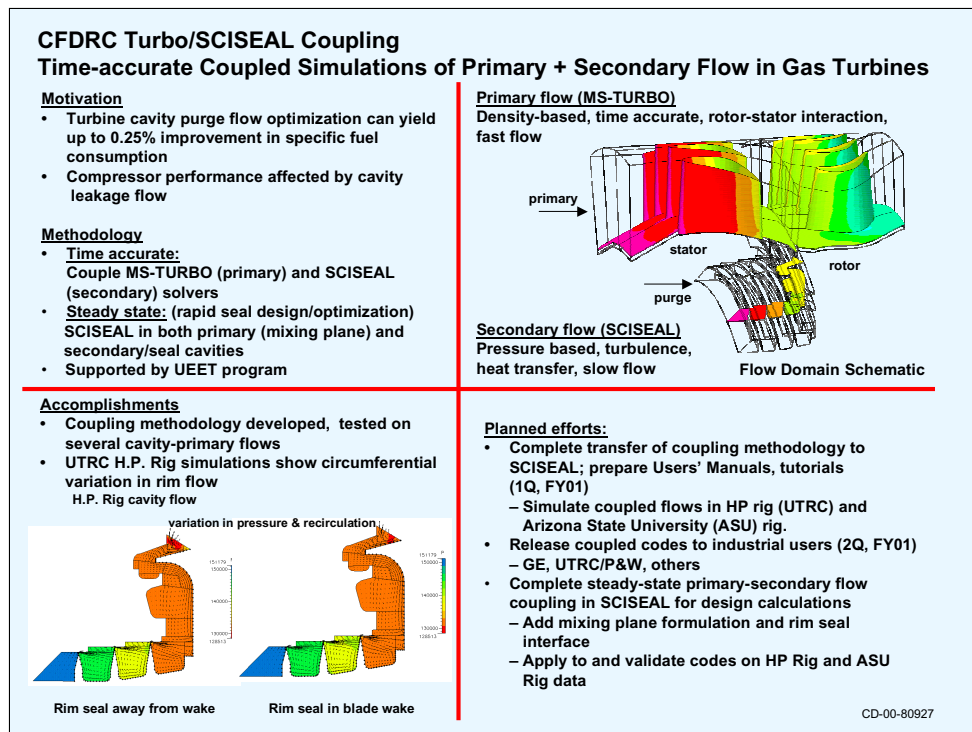
Schedule:

Task	FY00	FY01	FY02	FY03	FY04	
High misalignment seal						
High speed seal						
Large diameter seal						
Demo in core engine						

Partners: PW/Stein Seal/NASA GRC

CD-00-80927

Advanced engines may incorporate geared fans. In the fan location, large bending loads coupled with structural weight limits result in fan bearing compartment seal deflections much greater than conventional carbon face seal capabilities. P&W is under contract with NASA GRC to investigate candidate carbon face and annular seals capable of large angular and radial movements. Working with Stein Seal, P&W is investigating candidate concepts designed for large angular (0.5°) and radial (0.105") movements and testing them under laboratory conditions (see also Dobek et al, 2001 in this workshop proceedings for further details). Advancements made in this program could have immediate application to main shaft bearing compartment seals.



NASA contracted CFDRC to develop a coupled main flow path/ secondary air system solver to investigate complex main/turbine cavity/rim seal flow phenomenon.

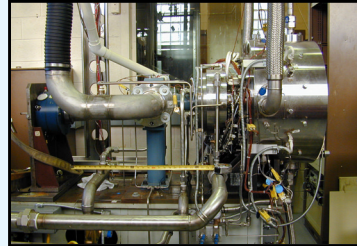
CFD- Research Corporation has completed the coupling of TURBO and SCISEAL for analyzing the complex main stream (TURBO) and secondary air stream (SCISEAL) interactions, including the effects of vane/blade wake interactions. The package can analyze flows from the engine centerline through the turbine rim seal location and through main flow path.

NASA also contracted with UTRC to measure the steady/unsteady turbine rim seal/cavity flows to assess the performance of baseline turbine rim seals. CFDRC has used this data set to validate the coupled TURBO/SCISEAL code. Beta release of the codes is expected in fall 2001.

NASA GRC High Temperature Turbomachinery Seal Test Rig

Goal: Test turbine seals at speeds and temperatures envisioned for next generation commercial and military turbine engines.

- **Temperature** Room Temperature thru 1500°F
- **Surface Speed** 1500 fps at 40,455 RPM, 1600 fps at 43,140 RPM
- **Seal Diameter** 8.5" design; other near sizes possible
- **Seal Type** Air Seals: brush, finger, labyrinth, film riding rim seal
- **Seal Pressure** 100 psi at 1500°F: Current
(Higher pressures at lower temperatures)
- **Motor Drive** 60 HP (60,000 RPM) Barbour Stockwell Air Turbine with advanced digital control for high accuracy/control
- **Financial Support:** TCT, HSR, UEET, Air Force, Other



Test rig is one-of-a-kind. More capable than any known test rig in existence.

CD-00-80927

NASA GRC has finished mechanical installation of the new high speed (1500 fps), high temperature (1500°F) turbine seal test rig. This test rig is capable of evaluating turbine seals (e.g. brush, finger, labyrinth) at all speeds and temperatures envisioned for next generation commercial and military turbine engines.

As of October 2000, the following tasks must be completed before testing will commence: complete programmable logic controller programming, complete internal rig heater functional check-out, complete lubrication system checkout, and perform overall rig functional checkout tests. Recently, the high temperature air heater passed a re-certification hydro-test enabling us to reach higher pressures (up to 100 psi) at 1500°F.

Demonstrated Preliminary Feasibility of Compliant Foil Seal

- **Objective**

Develop non-contacting high speed compliant foil seals for next generation turbine engines and assess scalability

- **Background**

NASA's oil free turbomachinery/bearing program basis for foil seal development:

- Mohawk innovative foil bearing designs
- GRC's advanced solid film lubricant: enables > 100,000 stop-start cycles (0–70,000 rpm); 1200 °F with virtually no wear

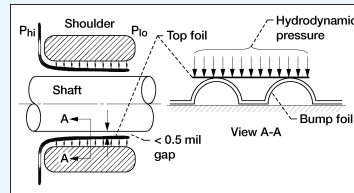
- **Development Program**

- **SBIR Phase 1 (FY 00):** Demo preliminary feasibility of foil seal in subscale test (complete)
- **SBIR Phase 2 (FY 01-02)**
- Evaluate manufacturing processes for larger seals
- Design, fabricate, test 3 seals (2.8, 6, 8.5 in.)

- **Partners**

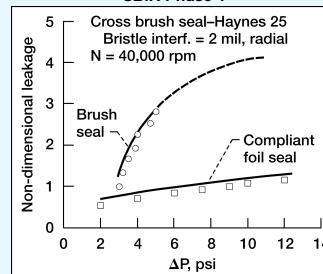
- Mohawk Innovative/NASA GRC

Compliant Foil Seal (CFS) Schematic



Foil Seal and Brush Seal Leakage Data

2.84 in. Dia. Journal; 68 °F
SBIR Phase 1



CD-00-80927

NASA has awarded to Mohawk Innovative Technology an SBIR Phase II to investigate film-riding compliant foil seals (see presentation by Walton et al, 2001 in this workshop proceedings for further details). Compliant foil seals (CFS) are derived from foil bearing technology and block flow between high and low pressure cavities through very narrow gaps between the shaft and the foil. The hydrodynamic lift between the seal and the shaft prevents rotor-seal contact during operation. High temperature solid film lubricants applied to the shaft prevent wear during start-up and shut-down when limited contact occurs (DellaCorte, 2000).

As shown in the figure, leakage is very low due to the small (<0.0005 in.) clearance between the top foil and shaft. The compliant foil seal leakage is about 1/3rd that of a comparably sized brush seal at 10 psi. Because of the non-contacting, non-wearing nature of the CFS, this very low leakage characteristic should remain with cycling. Brush seal leakage, however, increases with cycling as the brush seal bristles wear to an operating clearance.

Scope of Activities: Structural Seals



Objective:

Develop unique structural seals for extreme temperature engine, re-entry vehicle, and rocket applications.

Specific Goals:

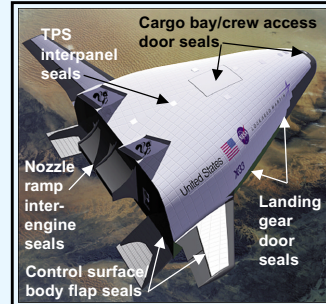
- Develop advanced structural seals capable of extreme (1500 – 5500 °F) temperatures.
- Exploit novel design techniques to meet leakage, durability, and resiliency (spring-back) goals across operating temperature range.
- Evaluate seal performance through compression, flow and extreme thermal tests.
- Develop/validate analytical models to predict leakage and resiliency performance.
- Demonstrate seal performance through prototype system tests.

Key Facilities:

- In House:
- High temperature (1500 °F) rope seal flow and compression test rigs.
 - Engine components lab (>2000 °F) & C-22 Rocket Facility (5130)
 - Planned: 2200+ °F compression test rig, Ames arc jet control surface seal fixture.

Partners:

Thiokol, Albany-Techniweave; Rocketdyne; Boeing; Air Force; Williams;
Other Industrial Partners.



CD-00-80927

NASA GRC is also developing unique structural seals for extreme temperature engine (air breathing hypersonic and other), re-entry vehicle, and rocket applications. Challenges in these areas are extreme temperatures (1500-5500°F), large (up to 3”) deflections, and pressures (100 - 1000 psi). Novel concepts are being developed that can satisfy these conditions while retaining their ability to follow adjacent wall movement. Seals are being constructed using advanced manufacturing techniques (e.g. braiding/weaving, other) from a range of high temperature carbon and ceramic materials.

NASA has unique facilities to evaluate the flow and durability performance of these seals at temperatures up to 1500°F (existing) and up to 3000°F (planned). NASA GRC also possesses a high heat flux H₂/O₂ rocket engine for subjecting materials and components to the extreme conditions anticipated in next generation Reusable Launch Vehicle (RLV) propulsion systems.

NASA GRC Seal Development for Space Transportation Programs

Current:

Shuttle RSRM Thermal Barrier Development

- Developed thermal barrier for Thiokol to block hot (5500°F) gases from damaging RSRM Viton O-rings.

GRC 5500°F Flame Test



X-38 Emergency Crew Return Vehicle Control Surface Seal Testing

- Evaluating control surface seals for JSC for X-38 (C.R.V. demonstrator)
- Goal: Determine if seal flow rates are low enough to prevent hot, re-entry gas ingestion/damage of control surface hardware. Assist in advanced concept development

X-38 Control Surface Seal Development



RLV Inter-engine Seal Development:

- Performed for Rocketdyne conceptual design of inter-engine seal showing promise of accommodating large 1-3" deflections in hot 3000+°F flow environment between aero-spike engine modules. Program discussions continuing.



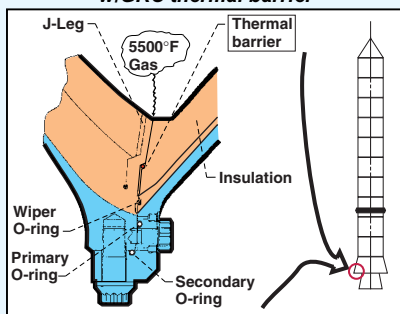
CD-00-80927

NASA GRC is contributing seal technology to the Space Shuttle, X-38, and RLV/X-33 programs. NASA GRC has developed a thermal barrier for Thiokol (supplier of solid-rocket-motors for the space shuttle) to block the hot (5500°F), pressurized (1000 psi) gases from damaging the solid-rocket-motor nozzle joint Viton O-rings (see detail next slide). For NASA Johnson, GRC is assisting with measuring seal flow rates and resiliency to assist in determining if Shuttle-derived thermal barriers will meet the X-38 rudder-fin flow-blocking requirement (see detail two slides forward). GRC has also performed a conceptual design of an inter-engine nozzle-ramp seal showing promise of accommodating the anticipated large (1-3") deflections in the hot (3000°F) nozzle flow environment.

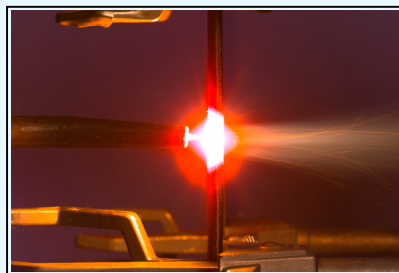
Thiokol Selects NASA GRC Thermal Barrier for RSRM Joint Redesign

- Thiokol experiences periodic hot gas effects on RSRM nozzle-joint Viton O-rings leading to extensive reviews before flight.
- Glenn thermal barrier braided of carbon fiber has shown outstanding ability to prevent hot (5500°F) gas from effecting downstream O-rings in multiple 1/5th scale MNASA RSRM tests.

Redesigned RSRM Nozzle-to-Case Joint w/GRC thermal barrier



GRC 5500°F Flame Test



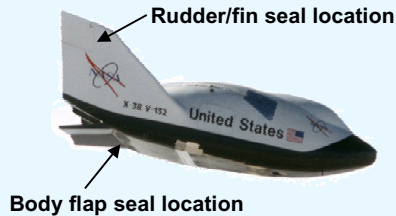
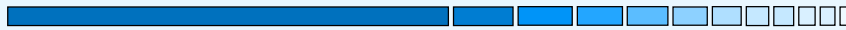
Thiokol has selected GRC thermal barrier for Nozzle-to-Case Joint redesign and strongly considering for Joint Numbers 1–5 redesign.

CD-00-80927

The NASA Glenn developed braided carbon fiber thermal barrier is the primary candidate being considered by NASA and Thiokol for the redesign of the space shuttle re-usable solid-rocket-motor (RSRM) nozzle-to-case joint and for nozzle joint 2. Incorporation of the NASA Glenn developed braided carbon fiber thermal barrier into the nozzle joints of the space shuttle RSRMs would eliminate hot gas penetration to nozzle joint Viton O-rings and prevent extensive reviews that delay shuttle launches.

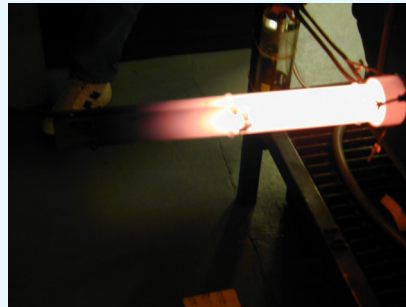
On August 10, 2000, a NASA Glenn developed braided carbon fiber thermal barrier was successfully evaluated in an MNASA reusable solid rocket motor (RSRM) at NASA Marshall (see also Bauer 2001, in this workshop proceedings for further details). The MNASA RSRM is a 1/5th-scale version of the full-scale RSRMs used to launch the space shuttle. Tested in a redesigned nozzle-to-case joint, an intentional flaw in the nozzle insulation allowed hot combustion gases to reach the thermal barrier. Soot was observed on hardware upstream of the thermal barrier, but none was seen on the downstream side. Post-test inspection revealed no damage or erosion to either the thermal barrier or to downstream O-rings that the thermal barrier is designed to protect. (see also Steinetz and Dunlap, 2000, for further details). Full scale static motor tests are planned for the Spring (nominal joint) and Fall (flawed joint) of 2001 in preparation for certification for space shuttle flight in 2003/2004.

X-38 Control Surface Seal Exposure Testing at GRC



JSC predicts that temperatures for Rudder/Fin seal will likely reach 1900+ °F

GRC performs furnace exposure tests on X-38 seal in compressed state at 1900°F and pre-and post-exposure flow tests



CD-00-80927

The X-38 vehicle is being developed as a precursor to a future Crew Return Vehicle to demonstrate necessary re-entry vehicle technologies including controls surface seals. For cost considerations, JSC is interested in using space shuttle thermal barrier/seals as control surface seals. NASA Johnson asked GRC to assist them in assessing sealing performance of the rudder/fin seal being considered for the X-38 vehicle.

NASA GRC has performed a range of compression (e.g. spring-back) and flow tests on thermal barriers in both their as-received and post- high temperature exposure (1900°F) conditions (see Dunlap and Steinetz, 2001 in this workshop proceedings for further details). The GRC tests showed that most of the thermal barrier/seal's resiliency - was lost after the 1900°F exposure test. These tests aided JSC in setting limits on acceptable gap openings in the rudder-fin location to prevent possible gap opening during re-entry due to seal permanent set. The flow tests also provided much needed permeability data for the JSC seal/gap thermal modeling effort.

Spaceliner-100/TPS-20 Control Surface Seal Development

Objective

- Develop and evaluate control surface seals for next generation re-entry vehicles

Approach

- Select candidate Shuttle-derived and current-technology seals
- Evaluate flow and thermal performance in relevant test fixtures
- Carefully measure aero-thermal heat loads under arc jet heating rates with
 - multiple seal gap conditions
 - control surface deflection into flow
- Use database to validate aero-thermo models to enable prediction of seal performance under actual re-entry conditions.

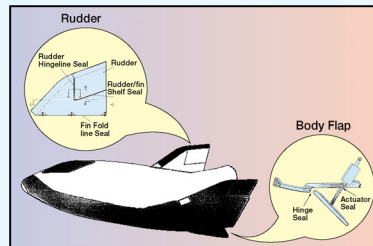
Schedule

- Complete arc jet tests 1Q FY01
- Validate aero-thermal models 2Q FY01
- Document results 2Q FY01

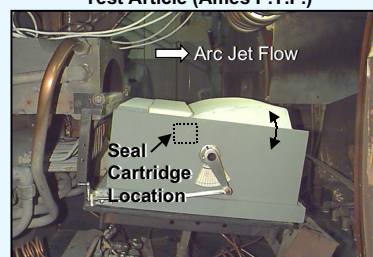
Partners

- Boeing Phantom Works/NASA GRC/NASA JSC/
NASA Ames/ HiTemp

Reference Vehicles: X-38, X-37



Arc Jet Control Surface Seal Test Article (Ames P.T.F.)



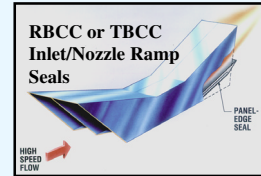
CD-00-80927

This joint NASA/Boeing effort addresses the development of high temperature structural seals for control surfaces for future highly-reusable launch vehicles. Successful development will contribute significantly to the mission goal of increasing re-use by 10 to 100 times that of the current shuttle fleet. This effort provides for the analysis, design, fabrication and testing of advanced structural control surface seal concepts. At the completion of the program, a matrix of seals and seal material combinations will have been tested for a range of aerothermal environments for a variety of advanced control surface applications (X-38, X-37, etc). See also presentation by Verzemnieks and Newquist, 2001, in this workshop proceedings for further details.

During the spring of 2001, the candidate control surface seals will be tested in the Ames 20 MW arc jet test facility under re-entry level heating rates using the arc jet test fixture model shown in figure. During arc jet operation the control surface is rotated into flow stream at angles up to 16 degrees (including 6 degree table angle) while pressures and temperatures are measured both upstream and downstream of the hinge-line gap seal. These measurements will also be used to validate an aero-thermal-structural model to be used to predict seal performance for other related programs.

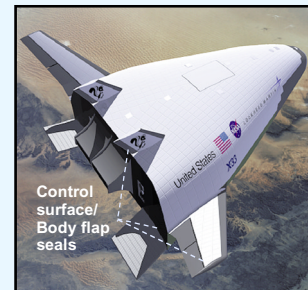
NASA GRC Seal Development for 3rd Generation Space Transportation Programs: FY01 Start

- Develop hot (2500+°F), flexible, dynamic structural seals for ram/scramjet propulsion systems (RBCC, TBCC, GTX)



- Develop reusable re-entry vehicle control surface seals to prevent ingestion of hot (6000 °F) boundary layer flow

Hot, dynamic seals critical to meeting 3rd generation program life, safety, and cost goals



CD-00-80927

NASA is currently funding efforts to conduct research on advanced technologies that could greatly increase the reusability, safety, and performance of future Reusable Launch Vehicles (RLV). Research work is being performed under NASA's 3rd Generation RLV program on both high specific impulse ram/scramjet engines and advanced re-entry vehicles.

Hypersonic engines attain higher specific impulse and save weight by burning high energy fuels and using air from the environment rather than from a liquid oxygen tank. Optimizing engine performance over the wide speed range (Mach 3-10+) requires movable inlet and nozzle ramps to tailor engine flow area. High temperature (2500+°F), flexible structural seals are required to prevent leakage of combustion gas into backside engine cavities.

Future RLV vehicles will be expected to operate at more aggressive re-entry conditions. High temperature seals are required to prevent ingestion of hot boundary layer gases into the control surface hinge-line locations.

NASA GRC is developing advanced structural seals for both of these needs by applying advanced design concepts made from emerging high temperature ceramic materials and testing them in advanced test rigs that are under development.

Summary

- **Seals technology recognized as critical in meeting next generation aero- and space propulsion and space vehicle system goals**
 - Performance
 - Efficiency
 - Reusability
 - Safety
 - Cost
- **NASA Glenn is developing seal technology and/or providing technical consultation for the Agency's key aero- and space advanced technology development programs.**

CD-00-80927

NASA Glenn is currently performing seal research supporting both advanced turbine engine development and advanced space vehicle/propulsion system development. Studies have shown that decreasing parasitic leakage through applying advanced seals will increase turbine engine performance and decrease operating costs.

Studies have also shown that higher temperature, long life seals are critical in meeting next generation space vehicle and propulsion system goals in the areas of performance, reusability, safety, and cost goals.

NASA Glenn is developing seal technology and providing technical consultation for the Agency's key aero- and space technology development programs.

NASA Seals Web Sites

- **Turbine Seal Development**

- + <http://www.grc.nasa.gov/WWW/TurbineSeal/TurbineSeal.html>

- NASA Technical Papers**

- Workshop Proceedings**

- **Structural Seal Development**

- + <http://www.grc.nasa.gov/WWW/structuralseal/>

- + http://www.lerc.nasa.gov/WWW/TU/InventYr/1996Inv_Yr.htm

- NASA Technical Papers**

- Discussion**

CD-00-80927

The Seal Team maintains three web pages to disseminate publicly available information in the areas of turbine engine and structural seal development. People interested in these web sites can visit them at the addresses indicated above.



References

References:

- Altshuller, G., 1996, "And Suddenly the Inventor Appeared: TRIZ, the Theory of Inventive Problem Solving," Translated by Lev Shulyak. Worcester, MA, Technical Innovation Center.
- DellaCorte, C., 2000, "High Temperature Solid Lubrication Developments for Seal Applications," 1999 NASA Seal/Secondary Air System Workshop Proceedings, CP-2000-210472 VOL1.
- Munson, J. and Steinetz, B.M., 1994, "Specific Fuel Consumption and Increased Thrust Performance Benefits Possible with Advanced Seal Technology," AIAA-94-2700.
- Steinetz, B.M., Hendricks, R.C., and Munson, J.H., 1998 "Advanced Seal Technology Role in Meeting Next Generation Turbine Engine Goals," NASA TM-1998-206961.
- Steinetz, B.M., and Dunlap, P.H., 2000, "Development of Thermal Barriers for Solid Rocket Motor Nozzle Joints," 1999 NASA Seal/Secondary Air System Workshop Proceedings, CP-2000-210472 VOL1.

WELCOME TO THE AIRLINE INDUSTRY

Sherry Soditus
United Airlines
San Francisco, California



Welcome to the Airline Industry

- **United has largest Engineering Staff**
 - Approximately 120 Engine Engineers
 - Approximately 700 total Engineers
- **Annual Maintenance Budget for Engines**
Alone is \$500,000,000
 - Looking for Best Bang for the Maintenance \$ Without Compromising Safety

• United has one of the largest technical departments in the airline industry. Overall UAL employs approximately 700 engineers, 120 alone in the jet engine overhaul shop in San Francisco. These engineers are responsible for overseeing the maintenance programs for both the engines and the aircraft.

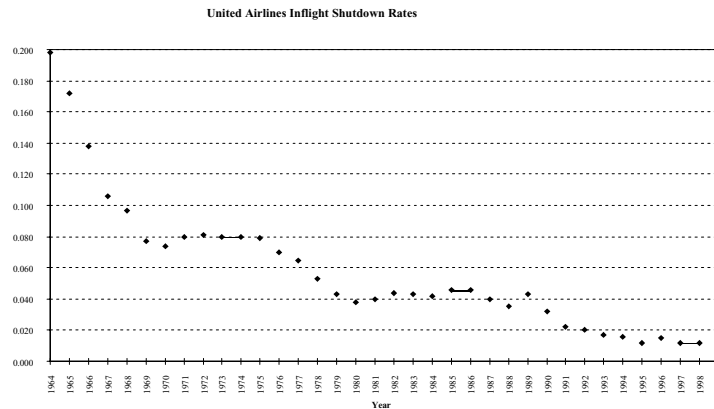
• United overhaul facilities are very capable. UAL can repair their own parts, develop their own repairs and in certain cases, manufacture their own parts. If a part cannot be repaired inhouse, it is sent out to an outside vendor (OSV). A good example of the repair capability is the ability to repair and create new knife edge seals in the flame spray shop.

• The annual maintenance budget for the jet engine overhaul shop alone is \$500,000,000 (this is only for the cost of new and repaired parts). With this money, approximately 650 engines are overhauled yearly. The primary mission for the United engineer is to develop and fine tune maintenance programs in order to increase reliability at minimal cost without sacrificing safety. In other words, to get the biggest bang for the maintenance buck.

• UAL engineer is constantly analyzing the maintenance programs to make sure that whatever amount of money is spend is recouped in increase efficiency and reliability. Particularly when it comes to seals and secondary flow systems. Just by increasing the efficiency of a system, engine or aircraft by a 0.1 to 0.5% means incredible savings to the airline.



IFSD Rate Today!



Example of the good results from some of the hard work. UAL has one of the best safety record and best IFSD record in the industry today.

Here is a chart of the In Flight Shut Down (IFSD) rate starting in 1964 when jet engines were first introduced through 1999. As you can see, we are constantly working to increase the safety and reliability of the fleet.

NOTE: This chart only reflects the IFSD rate of jet engines only.



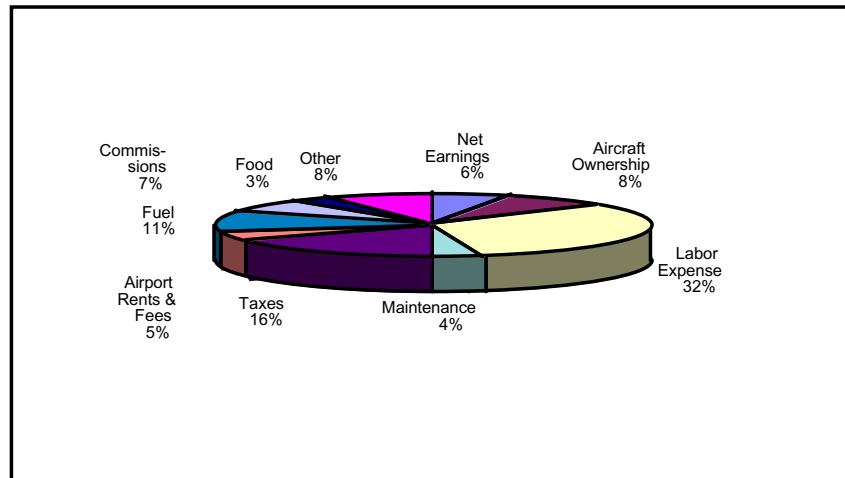
The Bottom Line

• \$\$\$

Why would United employ such a large engineering group in the first place. After all UAL could just follow the maintenance programs set out by the OEM's. Admittedly corporate headquarters does look at the engineering department as a money pit or black hole. But they do understand that engineering has a large effect on the bottom line. How do we do this? This is accomplished by actively reducing IFSD, by reducing delays and cancellations on the line and by implementing smart performance improvements which all save money.



Distribution of One U.S. Passenger Dollar



This pie chart represents how your travel dollar is spent. Engineering cannot effect commissions, airport rents and fees, taxes, aircraft ownership or food. But engineering can have a large effect on labor costs, fuel costs and maintenance costs.

Examples:

1) If a more reliable engine gearbox carbon seal is introduced, parts and labor savings can be realized by not having to replace the part on line. Also could save the cost of possible IFSD due to oil loss or the cost of a delay or cancellation due to replacement on the line.

2) Implementing a more durable and efficient engine brush seal would ensure the secondary flow system flows the proper amount of air. There would be no excess leakage and waste of expensive (compressor) air. And reduced premature deterioration of downstream parts.

3) Implementing a more durable engine bleed valve carbon seal again saves money by reducing the leakage and waste of expensive muscle pressure air.



The Need For Effective And Durable Designs

- **Increase η By 1.5% = 1 Cent Reduction In Fuel**
- **1 Cent Reduction In Fuel = \$30 Million In Savings / Year**
- **Increase Durability = Reduction In Premature Removals And Reduced Maintenance Cost**

Let's talk numbers.

If the efficiency of an engine can be increased by 1.5%, that would be equivalent to reducing the price of fuel by \$0.01. Based on the PW4000 engine fleet usage alone, 3 billion gallons of fuel are burned a year. Thus a 1.5% improvement in engine efficiency (PW4000) means a savings of \$30 Million a year. That is over 0.5% of the annual jet overhaul shop maintenance budget. Thus very, very small improvements in performance equals large savings for airlines. We struggle hard to make our fleets 0.5 to 1% better.

Additionally, we can measure improvements in premature removals and reduced maintenance costs by the implementation of more durable designs.



Goals

- **Opportunity To Examine Real Life Experience And To Understand The Overall Picture**
- **Opportunity To Make Large Impact On Airline Operating Cost By Reducing**
 - TSFC Deterioration
 - Premature Overhauls
 - Reduced Line Maintenance
 - Reduced Delays and Cancellations
 - Increase in Safety and Reliability

The seals and secondary air system workshop presents many opportunities. First, it gives an opportunity to examine real life experiences and to understand how new designs can make an impact on the overall picture.

The opportunities exist to make a large impact on the airline industry and reducing operating costs by reducing TSFC deterioration, premature overhauls, line maintenance costs, delays and cancellations and increase safety and reliability.

Last thought for the day. Airline travel is expected to double in the next 20 years. Although statistically speaking it is the safest mode of transportation, at the level of safety we are at today the number of incidents will double. This is not acceptable. An additional goal is to make future designs even safer and more reliable than they are today. Together we can make that happen.

DESIGN OF CRITICAL COMPONENTS

Robert C. Hendricks and Erwin V. Zaretsky
National Aeronautics and Space Administration
Glenn Research Center
Cleveland, Ohio

Critical component design is based on minimizing product failures that results in loss of life. Potential catastrophic failures are reduced to secondary failures where components removed for cause or operating time in the system. Issues of liability and cost of component removal become of paramount importance.

Deterministic design with factors of safety and probabilistic design address but lack the essential characteristics for the design of critical components. Each methodology considers the best available information regarding the materials and structural loadings and designs are required to meet codes or standards.

In deterministic design and fabrication there are heuristic rules and safety factors developed over time for large sets of structural/material components. Deterministic designs to code presume no failures will occur over the life of the component in the system. Buildings, weapons and tribological applications all possess a rich history of successful products. With safety factors, the designer presumes to know the perturbations to be placed on the product by the customer. In many instances, the customer does not know or understand the limitation of the product and abuse occurs. Under most factors of safety, the abuse must be extraordinary before the component will fail; sometimes catastrophically. Some buildings have survived excessive loads and abuse because the designer and the builder provided the know how and foresight to make it happen.

These factors did not come without cost. Many designs failed and many rules (codes) have standing committees to oversee their proper usage and enforcement. So the concept is to prevent catastrophic failures; failures will still occur; yet no one knows when or how.

In probabilistic design, not only are failures a given, the failures are calculated; an element of risk is assumed based on empirical failure data for large classes of component operations. Failure of a class of components can be predicted, yet one can not predict when a specific component will fail. The analogy is to the life insurance industry where very careful statistics are book-kept on classes of individuals. For a specific class, life span can be predicted within statistical limits, yet life-span of a specific element of that class can not be predicted. Also there is no relation between accepted deterministic safety factors and the assigned risk, which further complicates the matter. What this all means is that failures are acceptable in the computation/analysis of the product and testing verifies or validates these design criteria.

Both methods are unacceptable for the design of critical components. Each presumes apriori an acceptable level or given mortality for the design. As such, the customer system mortality is much higher, being proportional to the product of all subcomponent mortalities.

In critical component/product design probabilistic and deterministic designs can still be employed yet testing is imperative as the goal is component removal prior to failure. In turbomachines, a critical component such as a turbine disc represents an infinite source of energy to a mobile product such as an airplane, ship, submarine, automobile and a catastrophic source of energy to a stationary powerplant. One can not afford to have a component failure; it must be removed before it fails. This represents a different mind set. It says, no failures are the only acceptable mode. There is no acceptable or fixed level of risk.

Now on the Weibull plot, figure 1, a vertical line is the goal; every component fails at the same time or number of cycles. In reality these plots have fitted slopes not much different unity (Weibull Slope=1 ->exponential; 2->Rayleigh;3.57->normal distributions). As such, the dispersion is large; a few failures at time t_1 with progressive number of failures over a very large range with time. While this is acceptable practice to the community, there is no differentiation between graceful/benign and catastrophic failures.

Still looking more carefully at the data on the Weibull plot there seems to exist a region of no failures followed by a rapid rise or jump (vertical line) in failures. Design of critical components must be within this incubation region and the component removed prior to the “jump”. This jump point will be related to the initial crack from a fault in the material, yet unless the component characteristic length is very small or the material ultra fracture sensitive, the effect of this crack will not be detectable. However with time these defects progress, become measurable and continued loading leads to the jump seen in the Weibull plot.

Tallian (1962) delineated such a Weibull locus for bearings and a summary of efforts to define this “jump point” are shown in figure 2, taken from Takata et al. (1985) and found in Zaretsky (1992). For Weibull statistics of bearings, the jump point is related to the L_{10} life by a reliability factor.

$$L_n = a_1 L_{10}$$

where $a_1 = 0.053$ for reliabilities greater than 99.9%, p 70, table 10.2 (Zaretsky (1997)).

In reality, the data present a series of jumps as noted in figure 1. Extrapolating these data to the equivalent 99.9% reliability provides a higher than predicted life. This is good and bad. Good to have more life and bad because you have to test to determine the “incipient jump.”

In practice a conservative design could substitute for lack of knowing the jump point. For example, for bearings Zaretsky et al. (2000) found the Lundberg and Palmgren theory is the most conservative and maybe even the least accurate of several lifing theories e.g. Zaretsky , Harris. Still that conservative theory may be the best available for deterministic critical component (bearing) design.

Design of critical components will also require good probabilistic materials data as well as design methods coupled with that test data and engineering know how to delineate the “jump”.

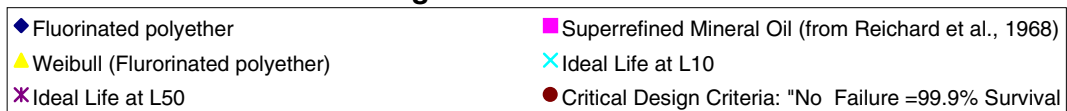
Conclusions

Critical components must be removed from service prior to the initial jump seen on the Weibull plot. Effective critical component design will require probabilistic data bases and validated probabilistic design codes. To date neither are available.

References:

1. Ioannides, E. and Harris, T.A. (1985) A New Fatigue Life Model for Rolling Bearings. *Journal of Tribology* 107, 3, pp 367-378
2. Takata, H., Suzuki, S., and Maeda, E. (1985) Experimental Study of the Life Adjustment Factor for Reliability of Rolling Element Bearings, *Proceedings of the JSLE International Tribology Conference*, Elsevier Science Publisher, New York, pp. 603-608.
3. Tallian, T., Chiu, Y.P., Huttenlocher, D.F., Kamenshine, J.A., Sibley, L.B. and Sindlinger, N.E. (1964) Lubrication Films in Rolling Contact of Rough Surfaces, *ASLE Transactions*, Vol. 7, No. 2, pp. 109-126.
4. Zaretsky, E.V., Poplawski, J.V., Miller, C.R. (2000) Rolling Bearing Life Prediction – Past, Present and Future. *International Tribology Conference ITC-Nagasaki-2000*, Japan Society of Tribology Oct 29- Nov 2, Nagasaki, Japan.
5. Zaretsky, E.V. (1992) STLE Life Factors for Rolling Element Bearings. STLE Publication SP-34.
6. *Tribology for Aerospace Applications*, Erwin V. Zaretsky, Editor (1997), STLE Publication SP-37.

◆ Fluorinated polyether	■ Superrefined Mineral Oil (from Reichard et al., 1968)
▲ Weibull (Fluorinated polyether)	✕ Ideal Life at L10
✕ Ideal Life at L50	● Critical Design Criteria: "No Failure =99.9% Survival"



OVERVIEW OF ULTRA-EFFICIENT ENGINE TECHNOLOGY (UEET) PROGRAM

Joe Shaw
National Aeronautics and Space Administration
Glenn Research Center
Cleveland, Ohio

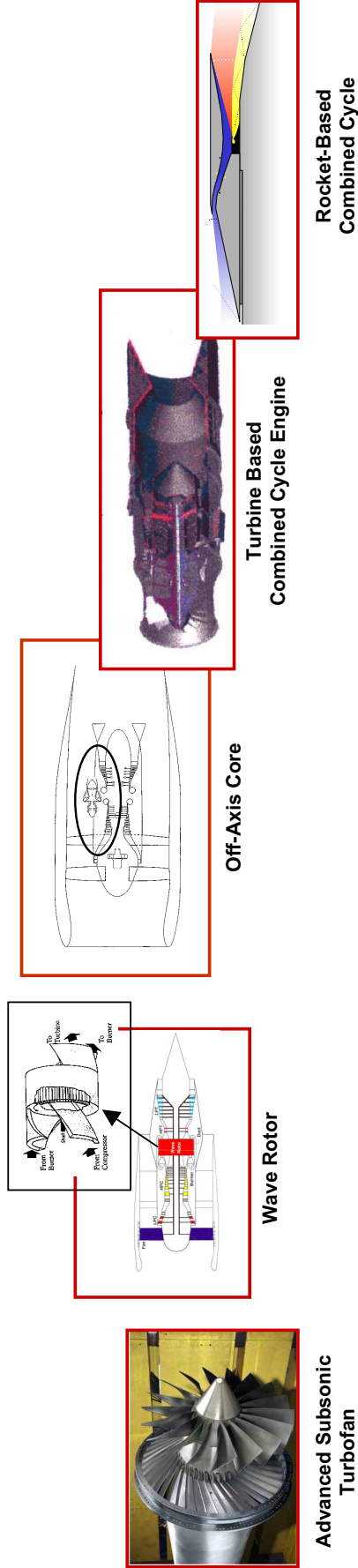
UEET

***Overview of
Ultra-Efficient Engine Technology (UEET) Program***

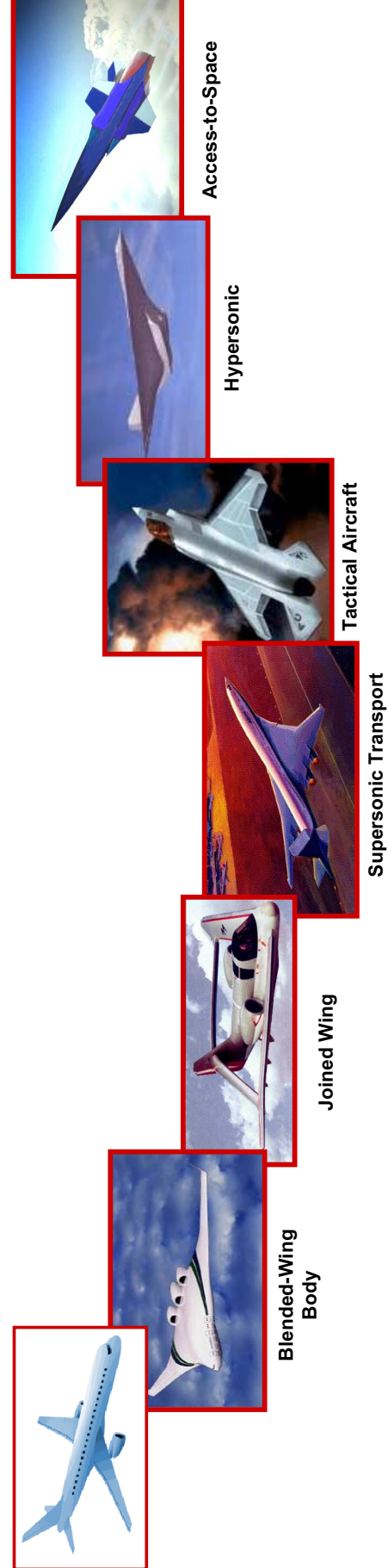
***Joe Shaw
Chief, UEET Program Office
NASA Glenn Research Center
Cleveland, OH 44135***

Administrator's November 20, 1998 charge to NASA Glenn.....

Plan a 5 yr. engine technology program that will enable next generation engines for both commercial and military applications. Emphasize revolutionary technologies that will enable future subsonic and high-speed applications. Actively seek collaboration with the DOD.



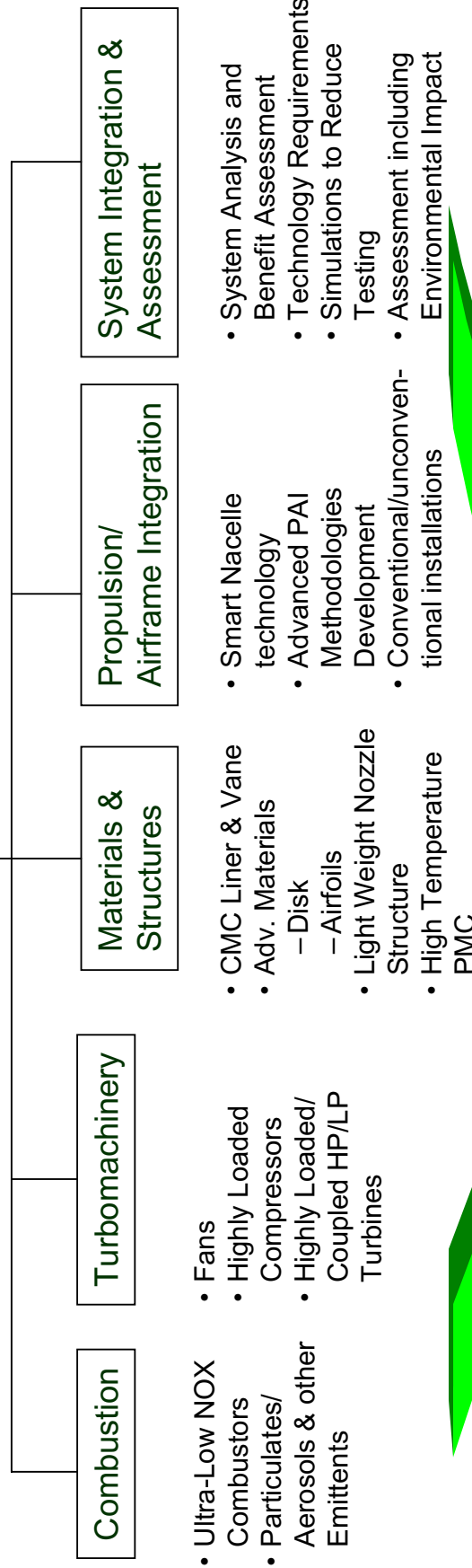
Develop and transfer revolutionary propulsion technologies that will enable future generation vehicles over a wide range of flight speeds.



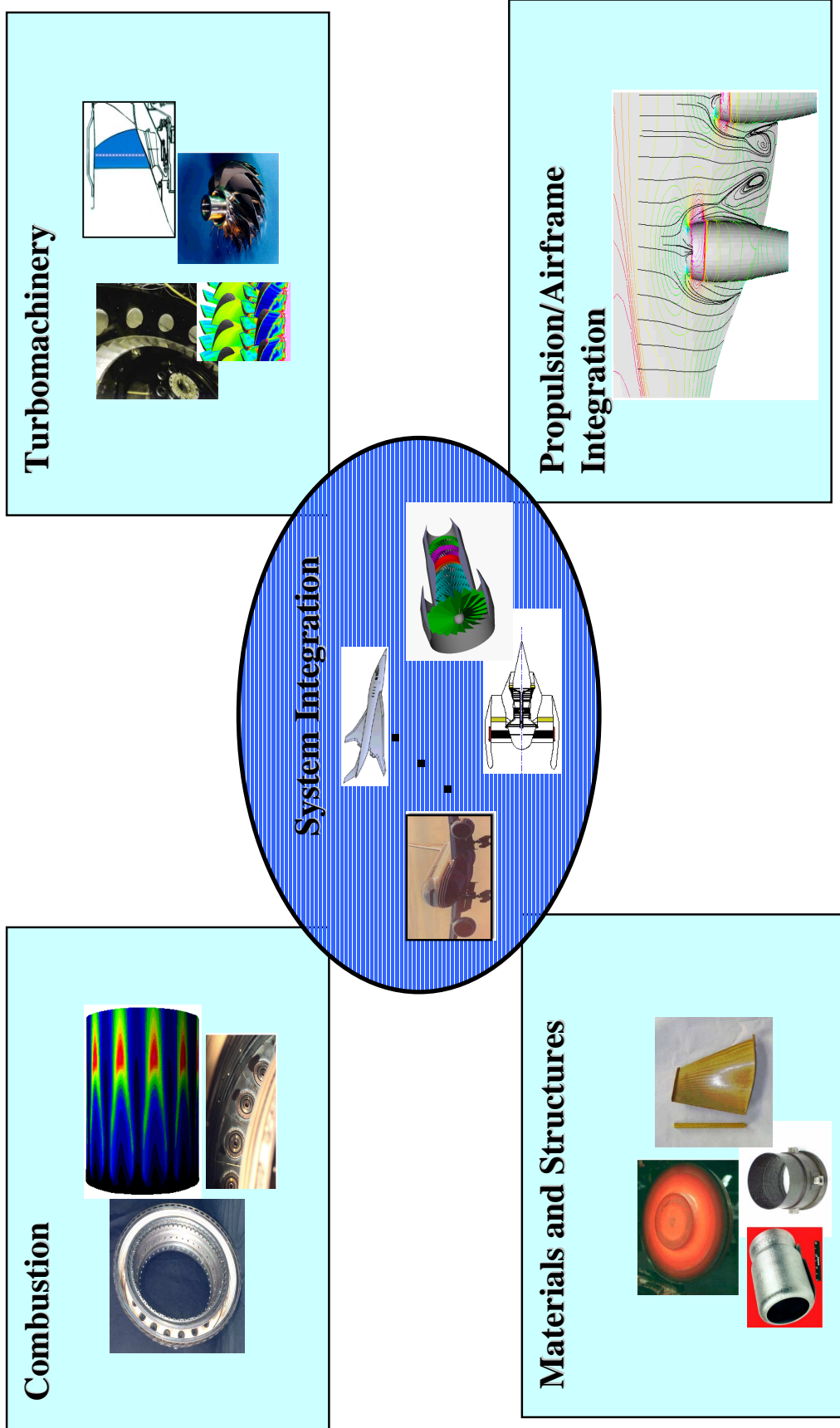
Develop and transfer revolutionary propulsion technologies that will enable future generation vehicles over a wide range of flight speeds.

- **Address long term aviation growth potential without impact on climate by providing technology for dramatic increases in efficiency to enable reductions in CO₂ based on an overall fuel savings goal of up to 15%.**
- **Address local air quality concerns as well as addressing potential ozone depletion by developing technology for 70% NOx emissions reduction at take-off and landing conditions, and also technology to enable aircraft to not impact the ozone layer during cruise operation.**
- **Technology Readiness to the Component Level (TRL 4-5).**

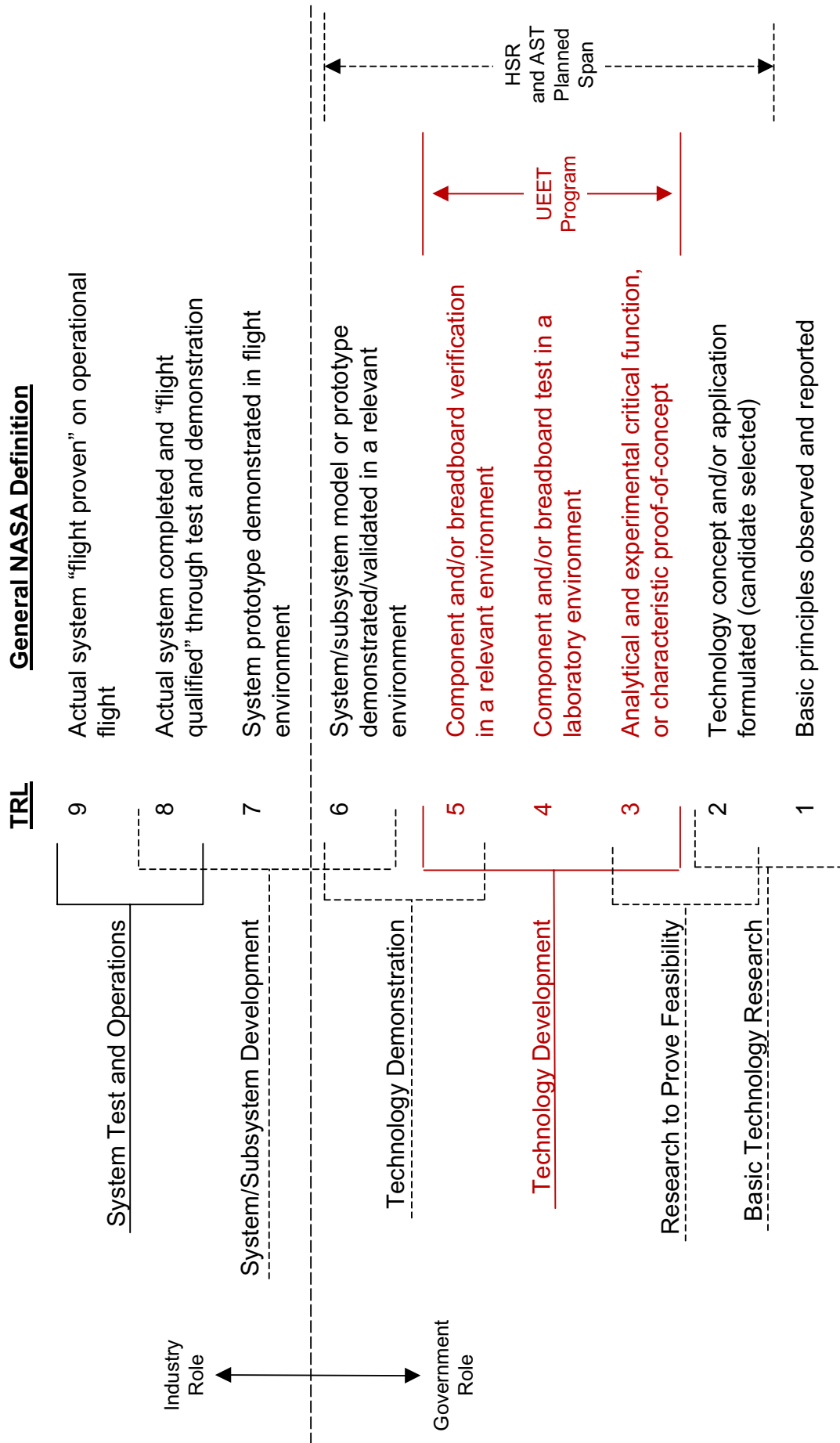
Ultra-Efficient Engine Technology



A Portfolio of Enabling Technologies for Future Generations of High Performance Engines (Commercial and Military)

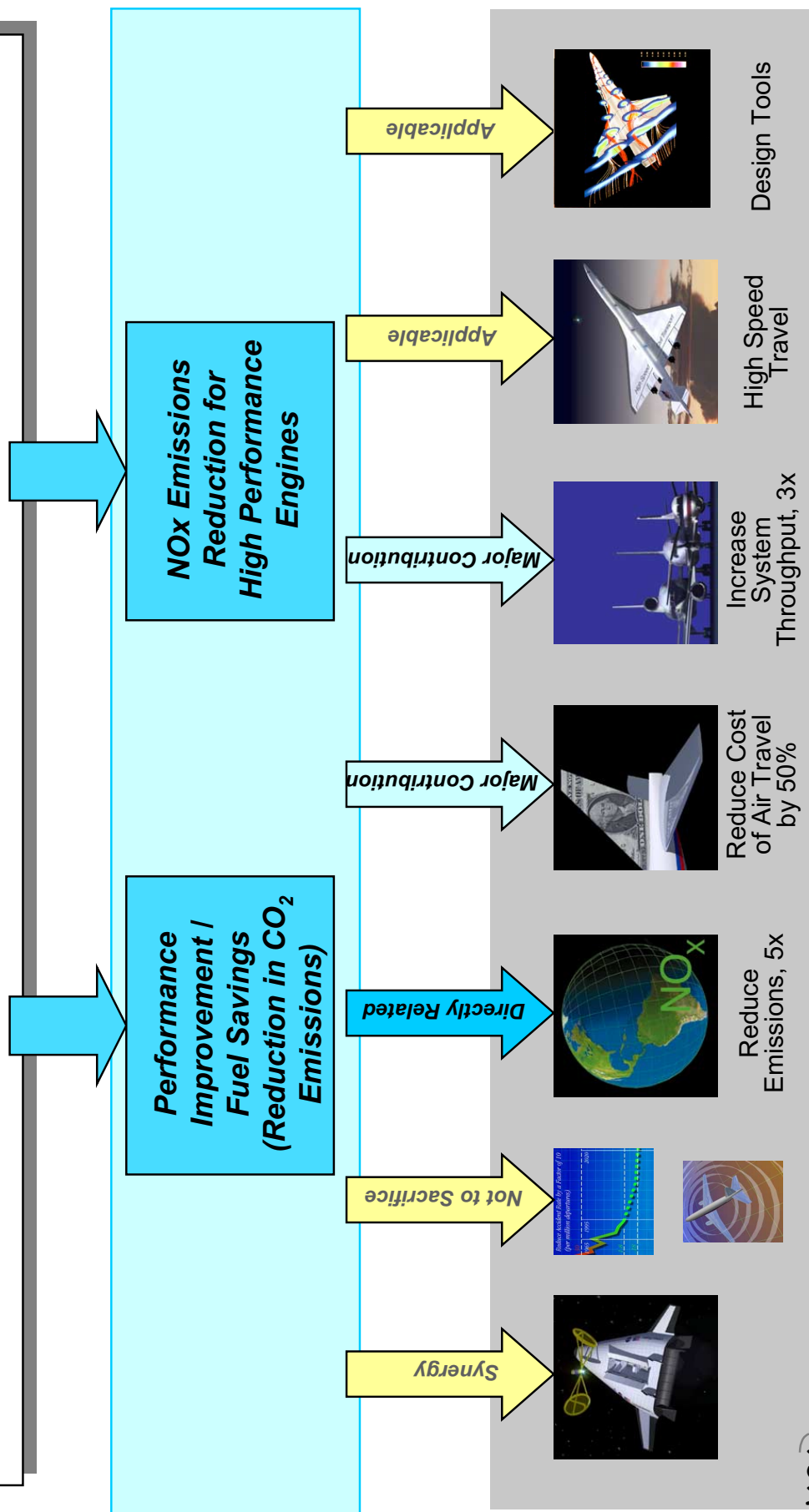


NASA's Technology Readiness Level (TRL) Scale Applied to UEET Program



Ultra-Efficient Engine Technology Program

Increased engine performance to enable and enhance a wide range of revolutionary aircraft from small to large, and over a wide range of flight speeds



NASA
Three
Pillars
Goal

9, 10

1

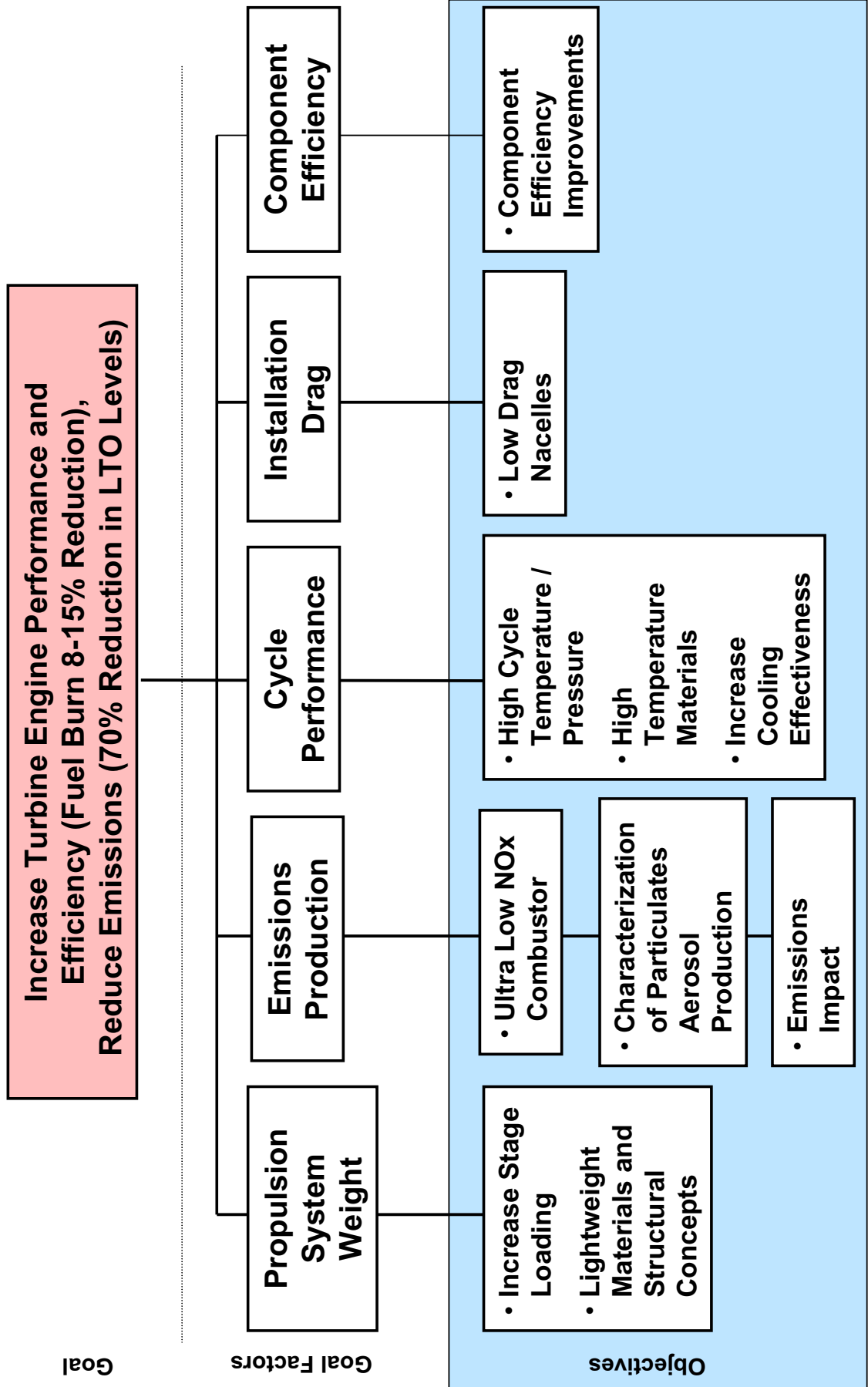
2

5

4

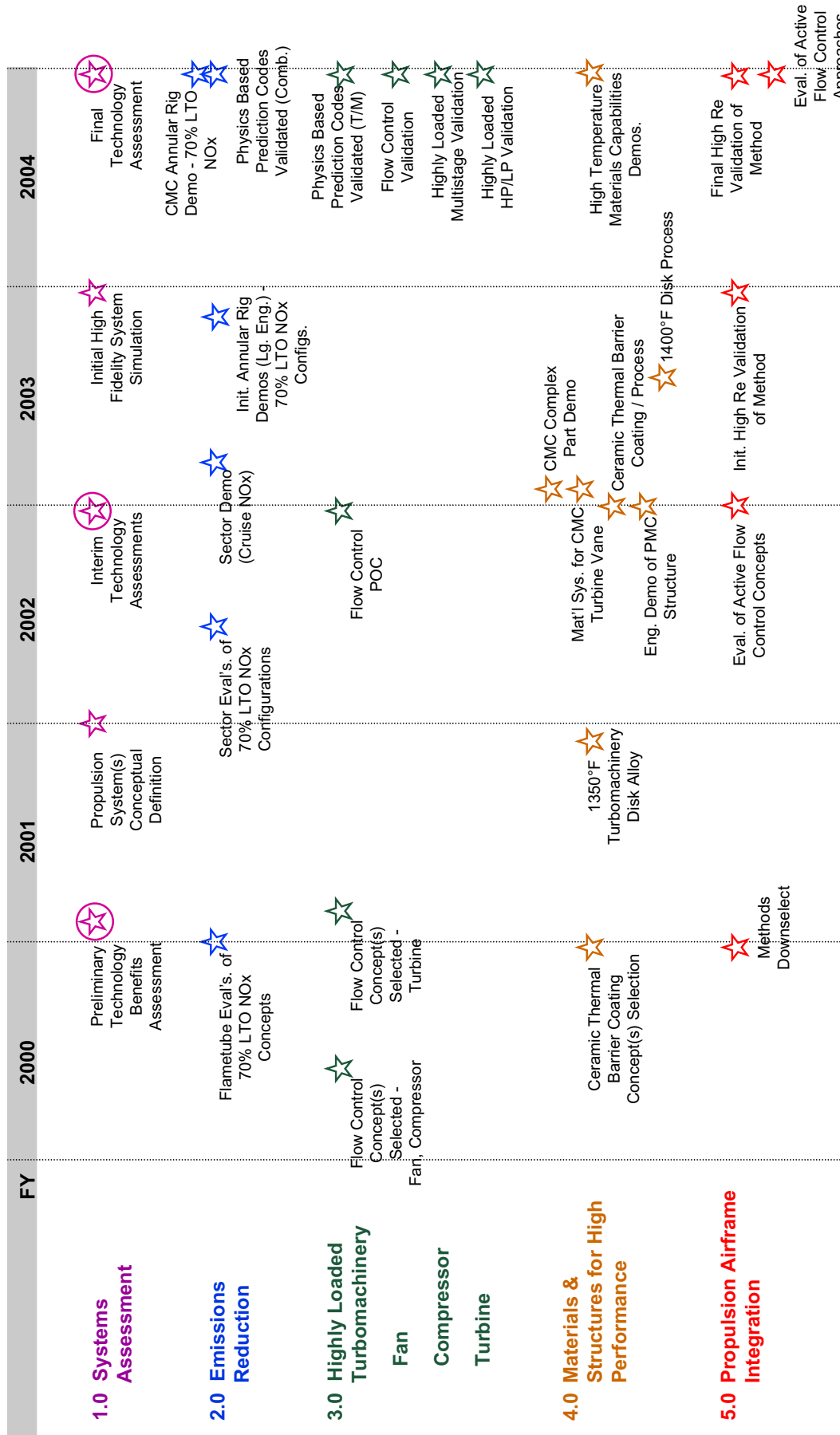
6

3



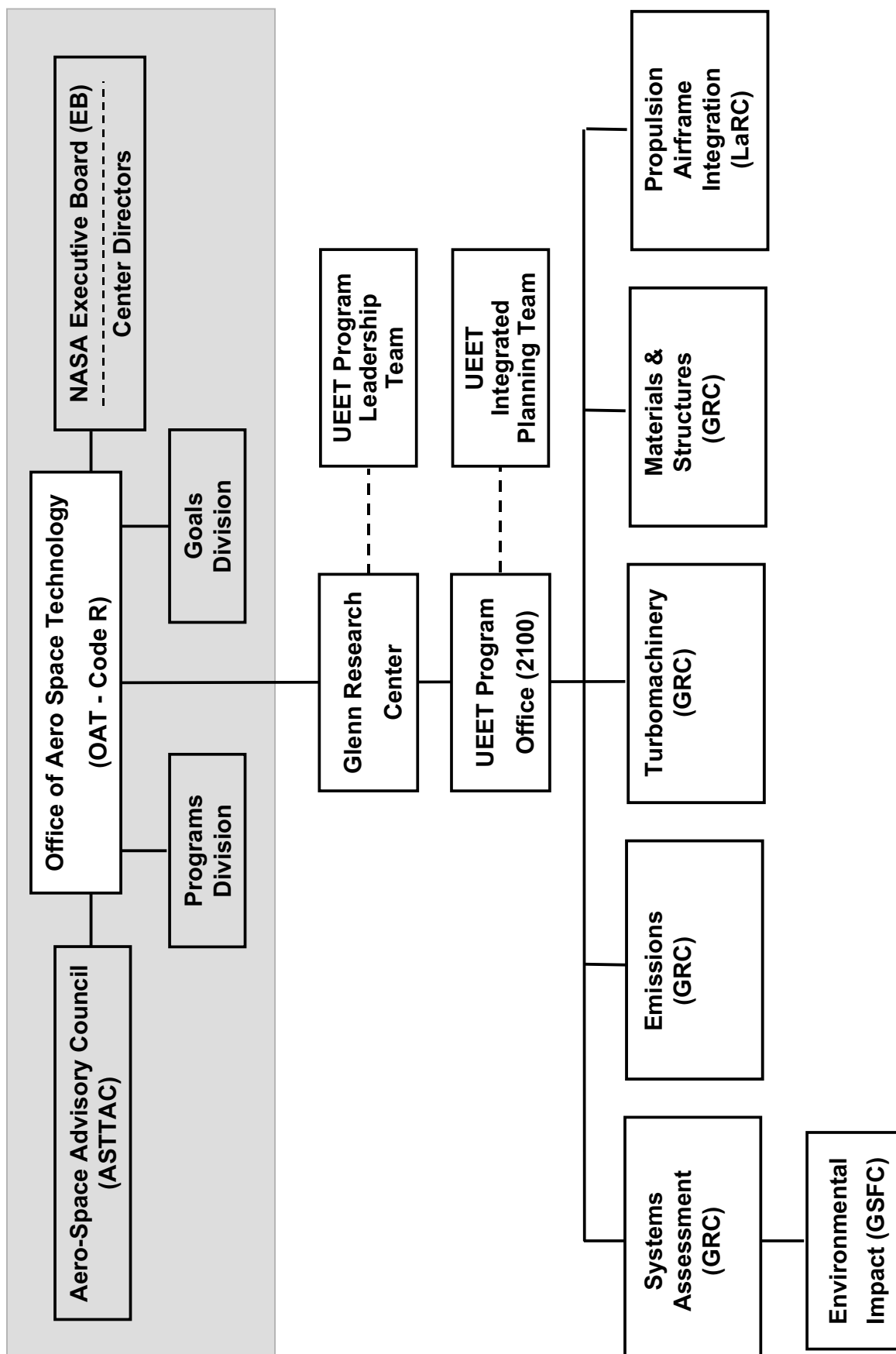
- 1.0 Systems Assessment**
- 2.0 Emissions Reduction**
- 3.0 Highly Loaded Turbomachinery**
- 4.0 Materials and Structures for High Performance**
- 5.0 Propulsion Airframe Integration**
- 6.0 Program Management**

Level I Milestone Schedule



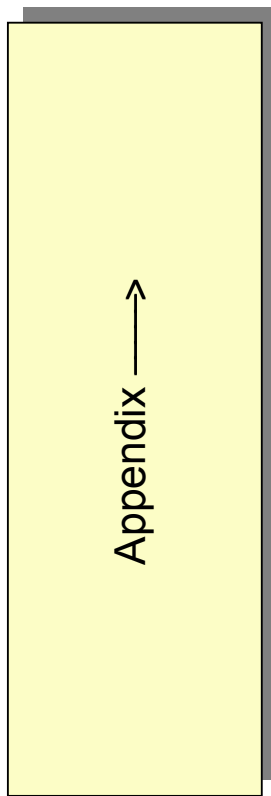
Notes: 1) All level I milestones are GPRA.

2) PCA milestones are denoted by

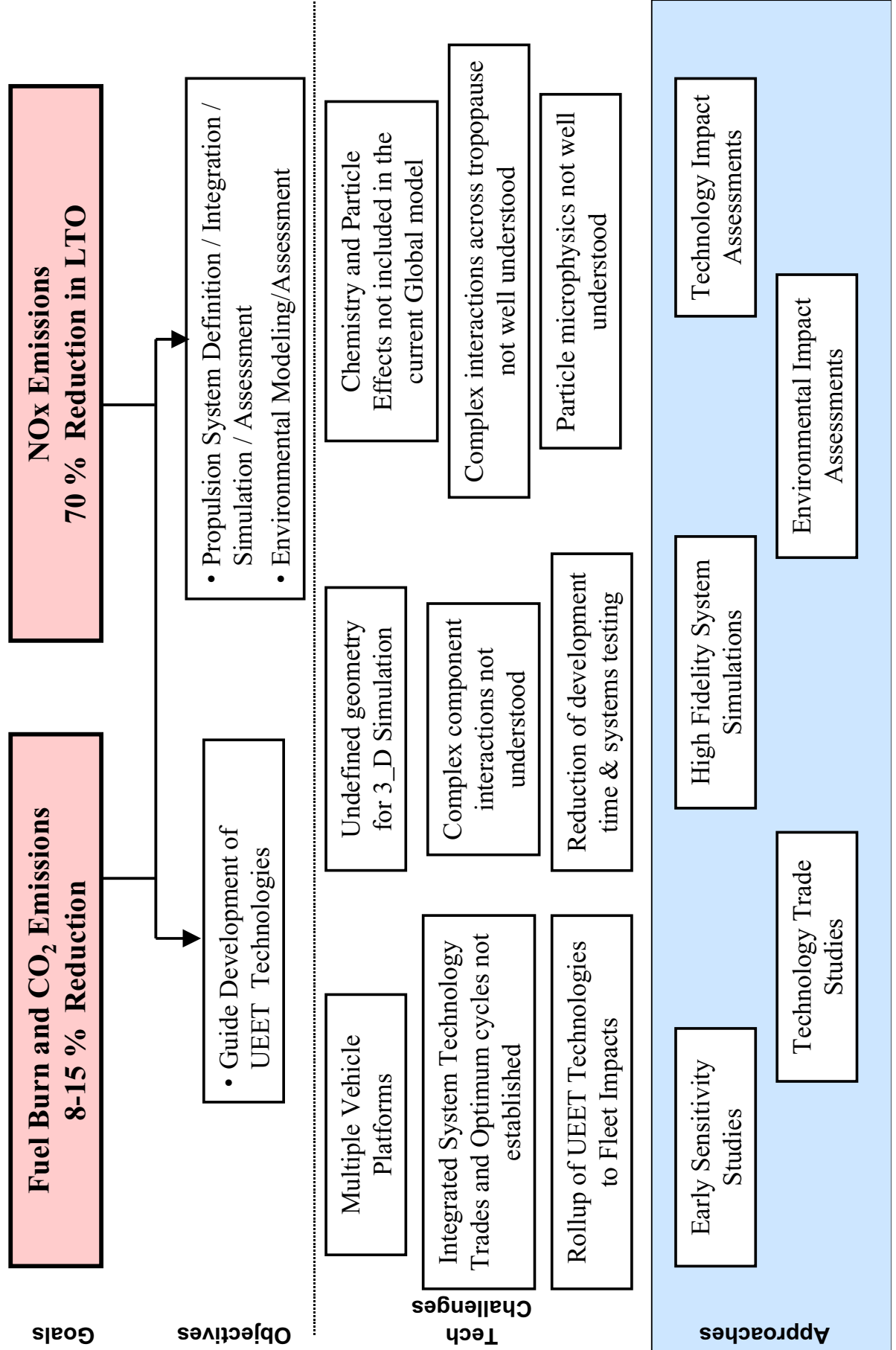


<u>Name</u>	<u>Organization</u>
Joe Shaw	NASA Glenn
Steve Jones	P&W
Fred Krause	GE
Vinod Nangia	Allied Signal
Scott Cruzen	Williams International
Gerry Brines	Allison
Jeff Lewis	Boeing
Don Williams	Lockheed-Martin

<u>Name</u>	<u>Organization</u>	<u>Responsibility</u>
Joe Shaw	UEET Program Office	Program Manager
Bob Plencner	High-Speed Systems Office	Systems Assessment Project Manager (1.0)
John Rohde	Subsonic Systems Office	Emissions Project Manager (2.0)
Kaz Civinskis	Subsonic Systems Office	Turbomachinery Project Manager (3.0)
Ajay Misra	High-Speed Systems Office	Materials and Structures Project Manager (4.0)
Jim Pittman	Aero Performing Center Management Office	Propulsion Airframe Project Manager (5.0)



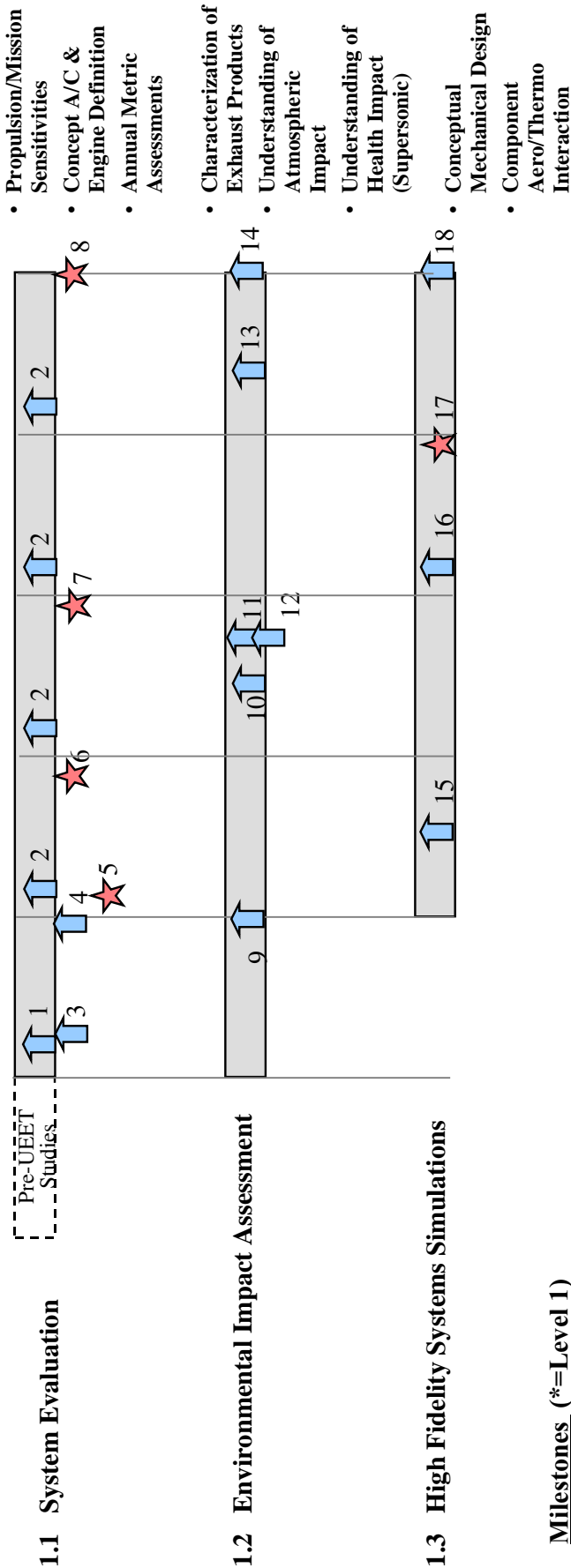
Overview Systems Integration & Assessment (1.0)



- ◆ Decision Point
- ★ Level I Milestone
- ↑ Level II Milestone

Systems Integration & Assessment (1.0)

Level II WBS

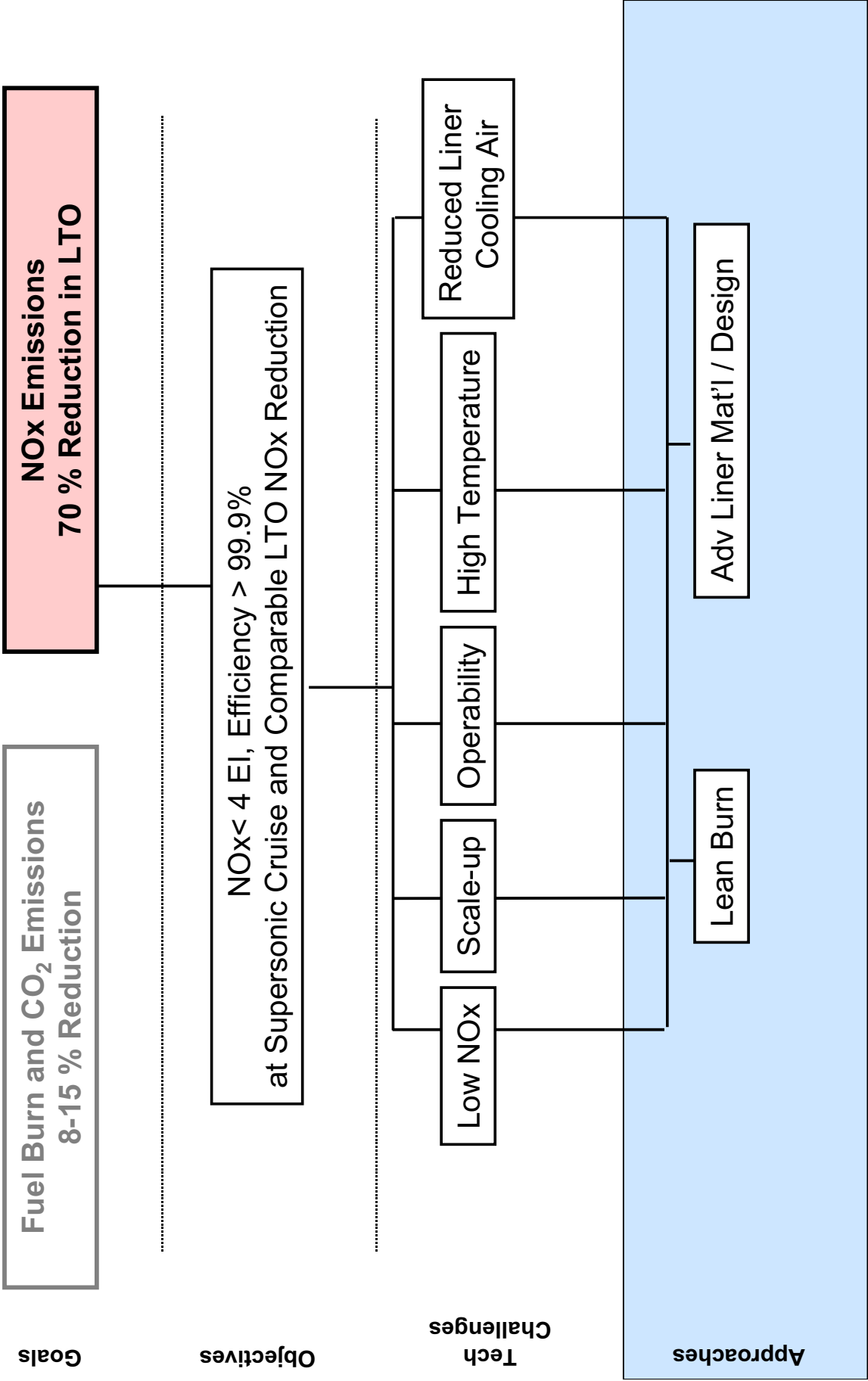


Milestones (*=Level 1)

- | | |
|---|--|
| 1. Metric Assessment Process Defined | 10. Mid-point Emissions Assessment |
| 2. Annual Metrics Assessments | 11. Mid-point Atmospheric Assessment |
| 3. Baseline propulsion and airframe tech configs with supporting gross sensitivities (including NOx/CO ₂) | 12. EPA Health Risk Assessment Framework |
| 4. Preliminary technology trade studies complete | 13. Final Emissions Assessment |
| *5. Preliminary Technology Benefits Assessment complete | 14. Final Atmospheric Assessment |
| *6. Propulsion Conceptual Definition | 15. Selection of system(s) for detailed simulation |
| *7. Interim Tech Assessment | 16. Conceptual Mechanical Aerodynamic and Thermal Designs |
| *8. Final Technology Assessment | *17. Initial High Fidelity System Simulation (Numeric test cell) |
| 9. Baseline Environmental Impact Assessment | 18. Assessment of Numeric Test Cell on Development Time |

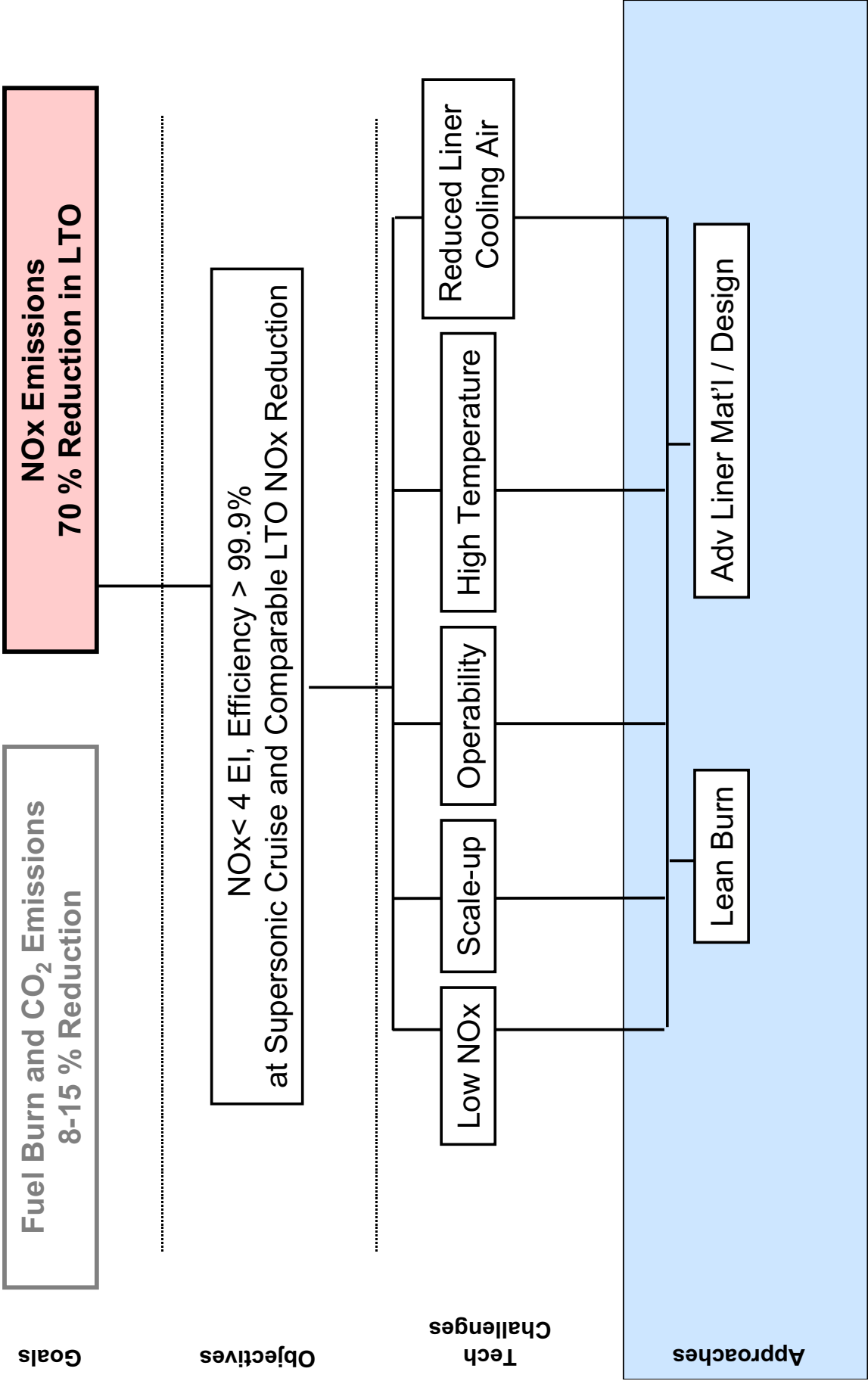
Overview Supersonic

Emissions Reduction (2.0)



Overview Supersonic

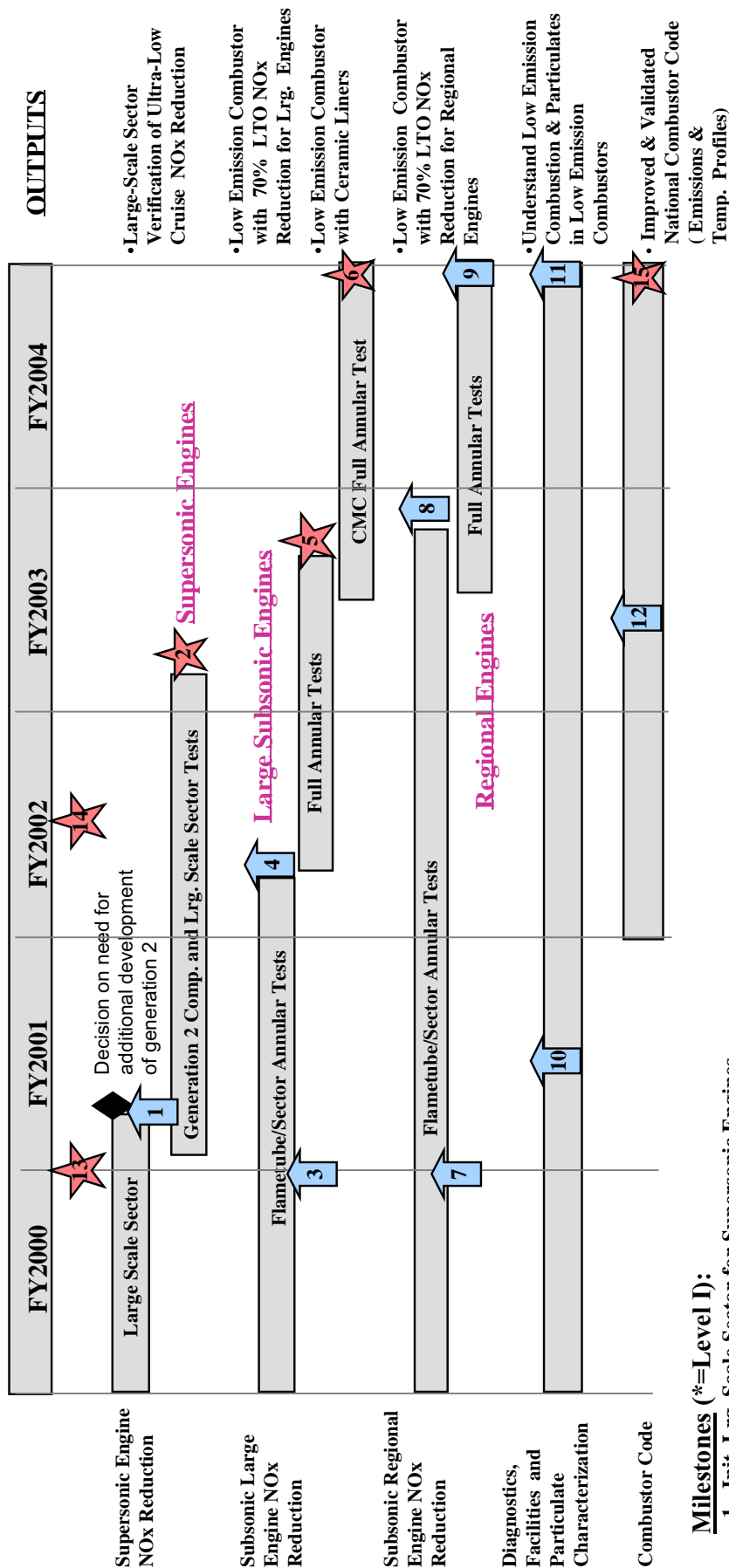
Emissions Reduction (2.0)



Level I and II Milestone Schedule

- ◆ Decision Point
★ Level I Milestone
⬆ Level II Milestone

Emissions Reduction (2.0)



Milestones (*=Level I):

- *1 - Init. Lrg. Scale Sector for Supersonic Engines
- *2 - Lrg. Scale Sector Verification of Ultra-Low Cruise NOx Combustor
- *3 - Demo. of 70% LTO NOx Reduction in Flametube for Large Engines
- *4 - Demo. of 70% LTO NOx Reduction in a Sector Rig for Large Engines
- *5 - Demo. of 70% LTO NOx Reduction in a Full Annular Combustor Rig for Large Engines
- *6 - Demo. of 2400°F Ceramic Liner in Full Annular Low Emission Combustor
- *7 - Demo. of 70% LTO NOx Reduction in Flametube for Regional Engines
- *8 - Demo. of 70% LTO NOx Reduction in Sector for Regional Engines
- *9 - Demo. of 70% LTO NOx Reduction in a Full Annular Combustor Rig for Regional Engines
- *10 - Complete Second Leg of Advanced Subsonic Combustion Rig
- *11 - Establish Understanding of Particulate with Advanced PAGEMS
- *12 - Init. Assessment of Subsonic Combustor Concepts with the National Combustor Code.
- *13 - 70% LTO NOx Reduction Demonstrated in Flametube
- *14 - 70% LTO NOx Reduction Demonstrated in Sector Rig
- *15 - Physics Based Prediction Codes Validated (Combustors)

Highly-Loaded Turbomachinery (3.0)

**Fuel Burn and CO₂ Emissions
8-15 % Reduction**

**NOx Emissions
70 % Reduction in LTO**

Goals

Objectives

**Reduce Component
Weight -20%, Engine
Weight -5%**

**Increase
Efficiency
by 1% to 2%**

**Increase
Average Stage
Loading
+50%**

**Increase Turbine
Inlet Temperature
+400°F at
Commercial Life**

**Reduce
Cooling Flow
by 25%**

Tech Challenges

- Large fan stage rotor-stator spacing dictated by noise
- High risk for structural integrity of blades
- Flow through blades limited by thickness
- Aero design needs to satisfy all operating conditions
- Minimize cost/complexity of new technology
- Minimize fan/stator interaction noise with reduced spacing
- Execute flow control concepts in 3D design

- Strong interaction of shock and viscous layers
- Increased diffusion in blade rows leads to higher losses without flow control
- Goals require turbomachinery performance beyond current "design space"
- Current design rules lead to low aspect ratios which will tend to increase weight & losses
- Higher aspect ratio at high loading levels susceptible to aeromechanical problems
- Higher loading limited by flow breakdown near endwalls and on blading
- Stability impacted by strong interaction between leakage flows and shocks

- Higher coolant temperature at 55:1 OPR
- Accurate prediction of internal and external heat loads
- Prediction of localized heat transfer effects particularly at edges & tips
- Unsteady effects on film-cooling effectiveness
- High Mach effects between HP and LP turbine stages (shock & mixing losses)
- Adverse flow impact of high-flare interstage duct & LP geometries

Approaches

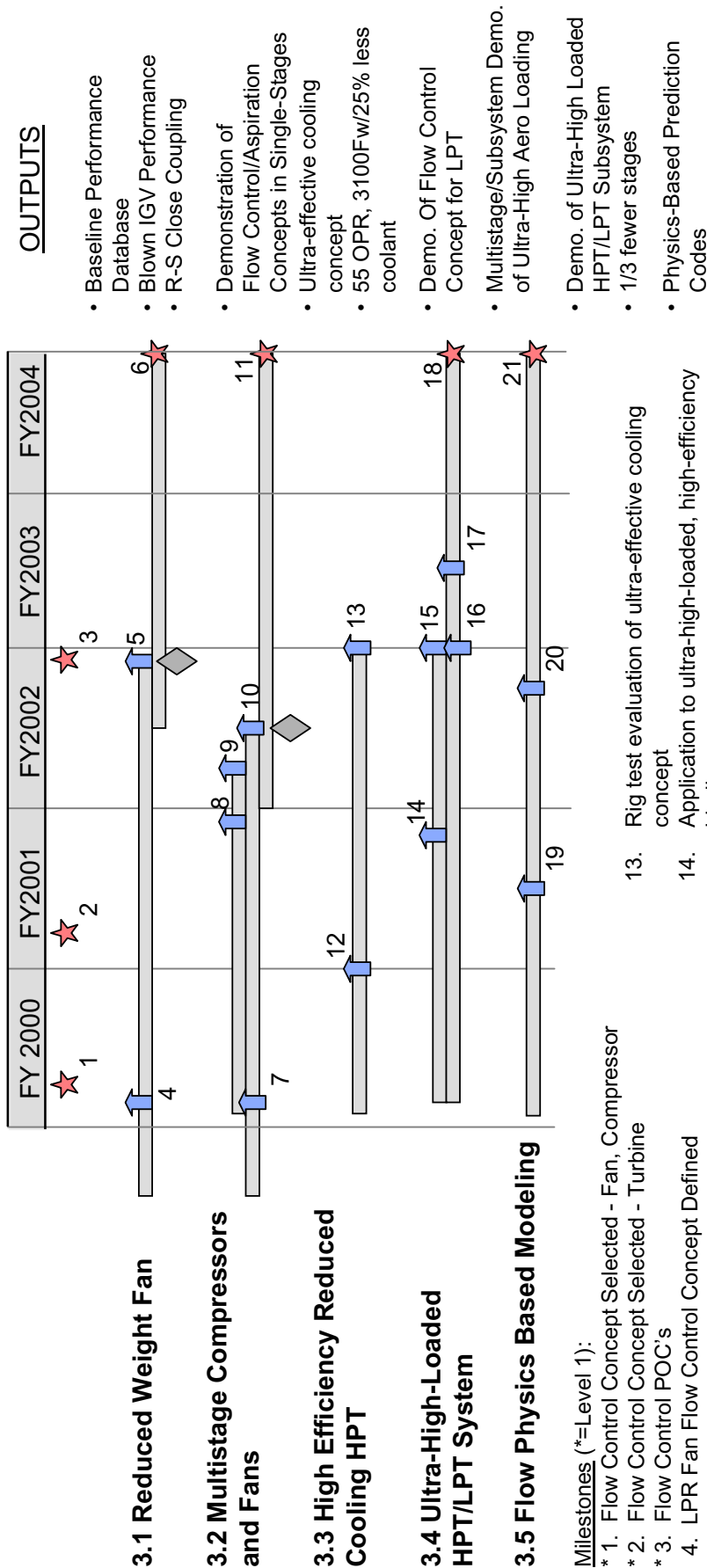
- Trailing edge blowing to fill wakes and allow close coupling
- Flow management through self-pumping within blade (Aspirated airfoils)
- Endwall and tip leakage flow management
- 3D viscous inverse design

- Physics-based modeling of flow control concepts
- 3D blading (sweep, lean, scallop, etc)
- Multistage 3D viscous CFD (steady & unsteady)
- Active/passive stability control
- Rig tests of flow control concepts in single-stage, multistage, and subsystem configurations

- Physics-based fluid/structural modeling for 3D heat transfer analysis of advanced cooling
- Aspirated LP airfoils
- Flow control for HP/LP turbine interstage ducting
- Rig test of close coupled HP/LP turbine system in dual-spool facility

Level II Milestone Schedule

Highly-Loaded Turbomachinery (3.0)

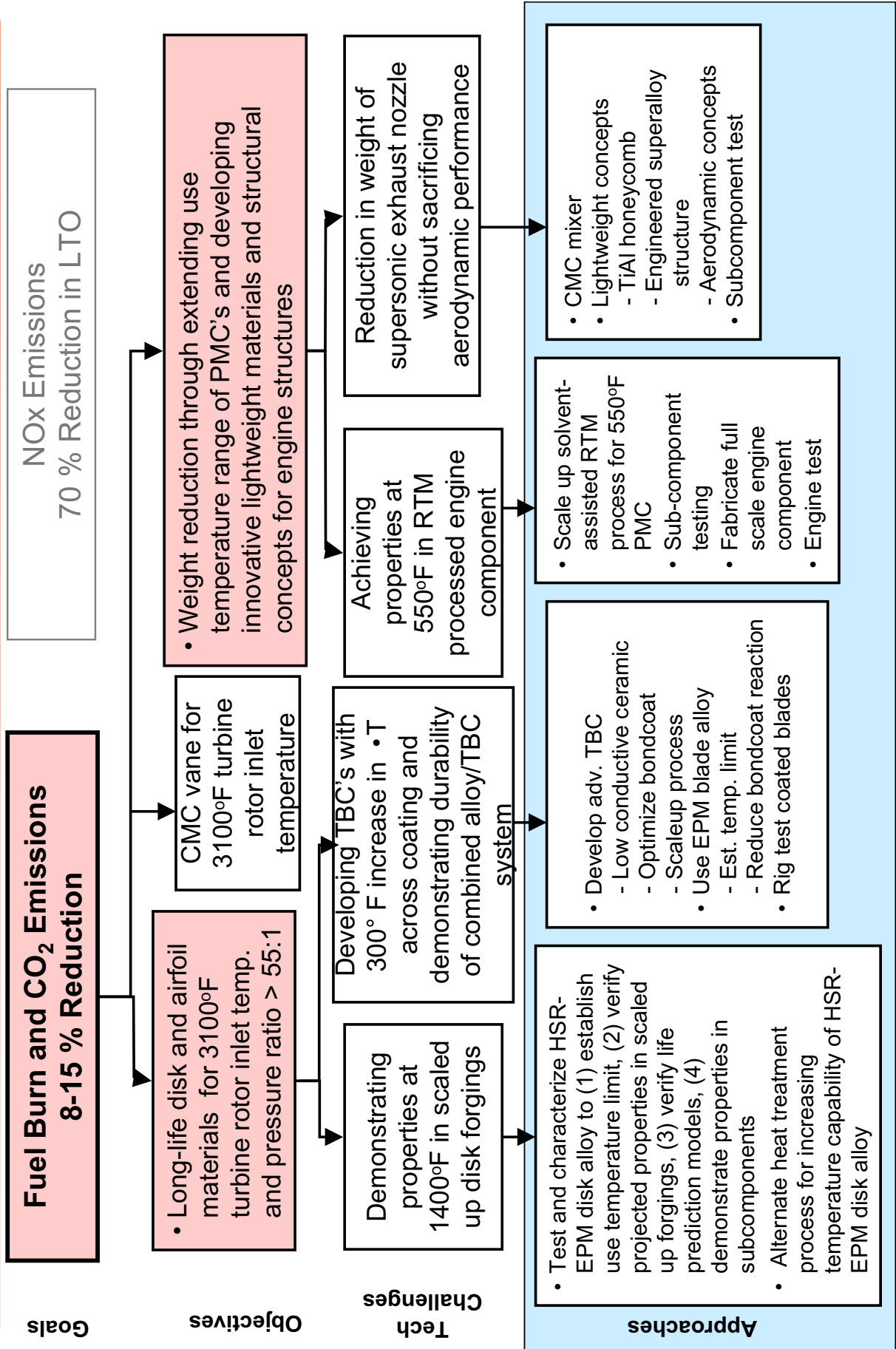


Milestones (*=Level 1):

- * 1. Flow Control Concept Selected - Fan, Compressor
- * 2. Flow Control Concept Selected - Turbine
- * 3. Flow Control POC's
4. LPR Fan Flow Control Concept Defined
5. LPR T.E. Ejection Concept Rig Test (Low Tip Speed Fan)
- * 6. Flow Control Validation Test
7. Compressor Flow Control/Aspiration Concept Defined
8. High-Loaded Multistage Performance Baseline Established (HSR 2-Stage)
9. Performance w/Blown IGV T.E. (HSR 2-Stage)
10. Highly-Loaded Flow-Controlled/Aspirated Single-Stage Compressor Test
- *11. Multistage Highly-Loaded Rig Test
12. Cooling concept design(s)
13. Rig test evaluation of ultra-effective cooling concept
14. Application to ultra-high-loaded, high-efficiency blading
15. Rig test of ultra-high-loaded stage
16. Counter-rotating dual-spool rig operational
17. Transition duct flow control concept selected
- *18. Rig test of highly-loaded, closely-coupled HP/LP turbine stages
19. Flow control models for design developed
20. Completed validated simplified model for particulates
21. Validated Physics-Based Prediction Capability for Design of Ultra-High Loaded Turbomachinery

Overview (1 of 2)

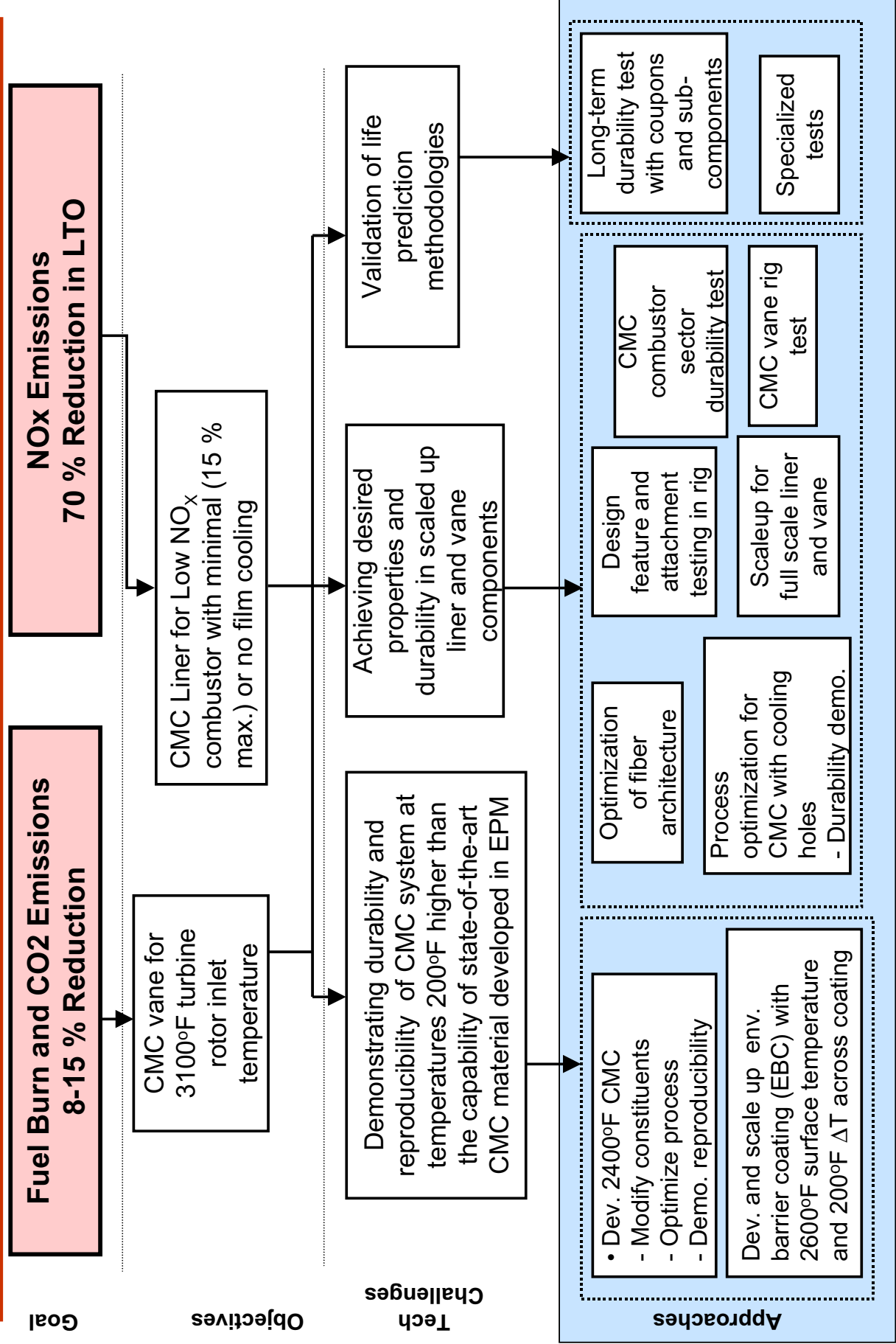
Materials & Structures for High Performance (4.0)



Overview (2 of 2)

Materials & Structures for High Performance (4.0)

UEET



Level II Milestone Schedule

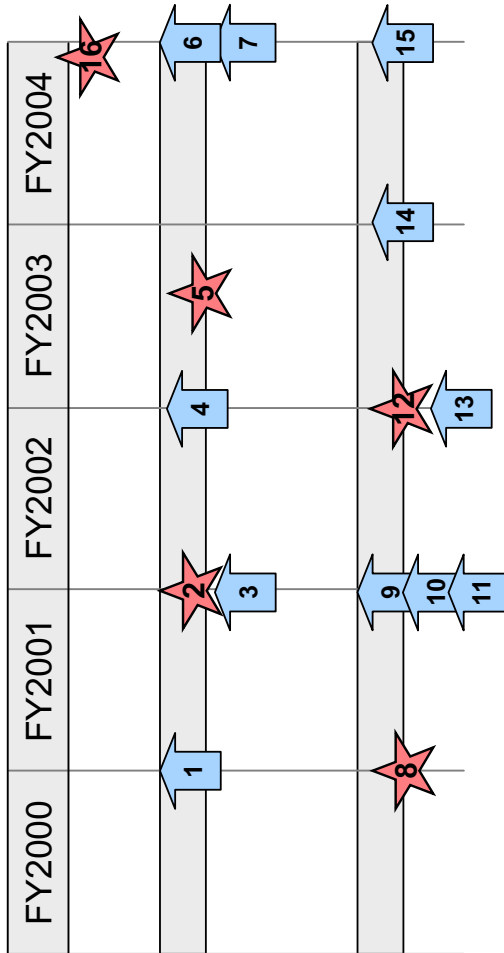
Materials & Structures for High Performance (4.0)

- ◆ Decision Point
- ★ Level I Milestone
- ↑ Level II Milestone

Outputs

- Demo'd properties in scaled-up HSR-EPM disk alloy at 1350°F
- Processing capability for achieving properties at 1400°F
- Verified probabilistic life prediction model
- Low conductive ceramic TBC composition & process for coating blades
- Optimized alloy/TBC system for 3100°F turbine inlet temperature
- Alloy/TBC combination demo'd in rig tests

Disk Alloy



Turbine Airfoil System

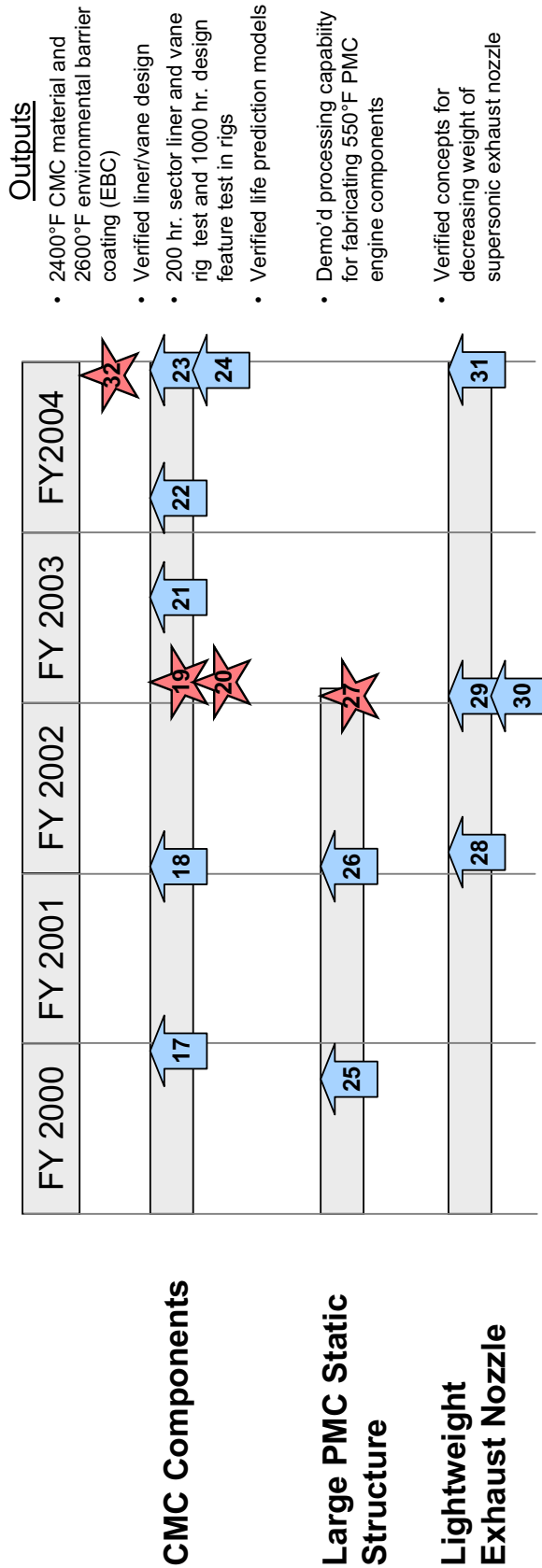
Milestones (*=Level I)

1. Alloy selected for regional engines
- * 2. Properties demonstrated in scaled-up forgings for HSR-EPM disk alloy in temperature range of 1350°F
3. Feasibility established for increasing temperature capability of HSR-EPM disk alloy
4. Properties demonstrated in scaled up disk alloy for regional engines
- * 5. Process selected for 1400°F disk
6. Properties demonstrated in 1400°F disk
7. Probabilistic disk life prediction model validated
- * 8. Low conductive ceramic TBC concepts selected
9. Feasibility of low conductive ceramic TBC established
10. Upper temperature limit established for HSR-EPM blade alloy
11. Bondcoat composition and process optimized
- * 12. Low conductive ceramic TBC system and process selected
13. Process optimized for preventing alloy-bondcoat interaction
14. Low conductive ceramic TBC process scaled up
15. Rig testing of coated blades complete
16. High Temp. Materials Capabilities Demo. (same as 32 on next chart)

Level II Milestone Schedule

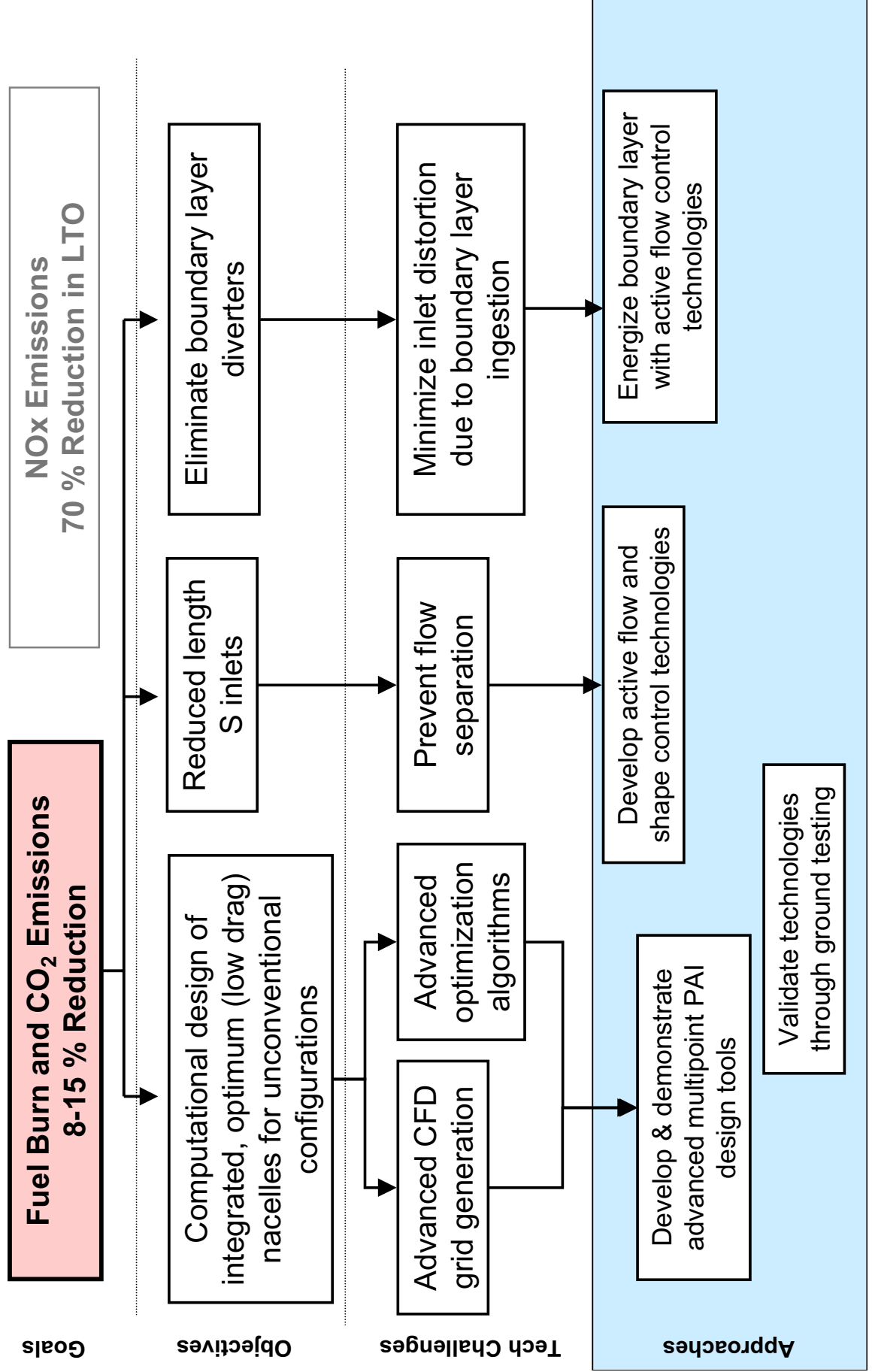
Materials & Structures for High Performance (4.0)

- ◆ Decision Point
- ★ Level I Milestone
- ↑ Level II Milestone



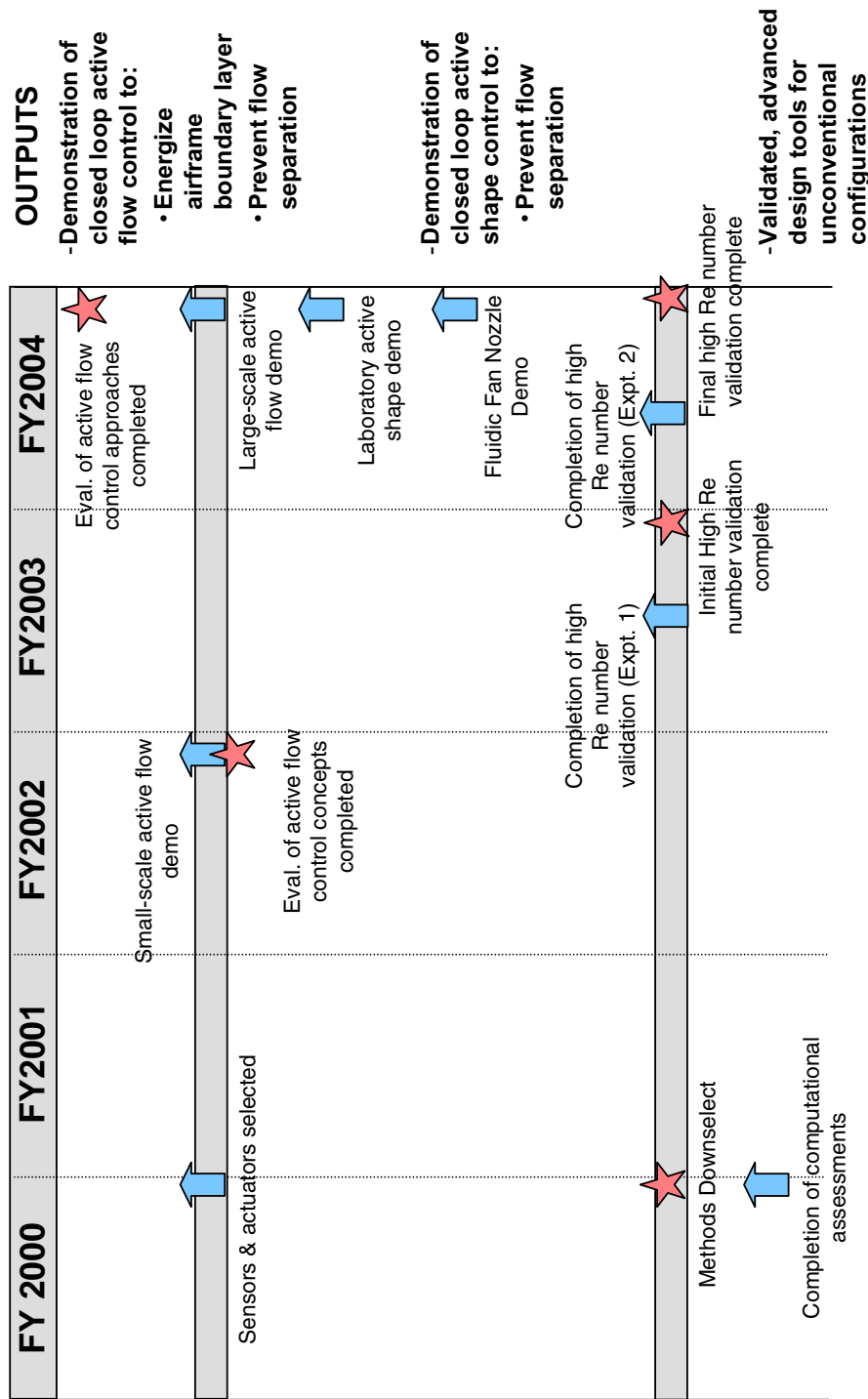
Milestones (*=Level I)

- | | |
|--|---|
| 17. Upper temperature limit of HSR-EPM CMC established | 25. PMC resin and process selected for engine component fabrication |
| 18. CMC system developed for combustor liner | 26. Engine test ready 550 °F PMC fabrication complete |
| *19. CMC combustor liner subcomponent/sector durability demonstrated in rig test for 200 hr. | *27. Engine test complete with 550 °F PMC structure |
| *20. CMC system developed for turbine vane | 28. CMC mixer fabrication demonstrated |
| 21. CMC process scaled up for full scale annular rig test | 29. CMC mixer test complete |
| 22. Design features demonstrated for turbine vane | 30. Lightweight materials/structural/aerodynamic concept selected |
| 23. CMC vane rig test complete | 31. Subcomponent test with adv. lightweight concept complete |
| 24. CMC liner subcomponent durability demonstrated for 1000 hr. in rig test | 32. High Temp. Materials Capabilities Demo (same as 16 on previous chart) |



Level 2 Milestone Schedule

- ◆ Decision Point
- ★ Level I Milestone
- ↑ Level II Milestone



Smart Nacelle Technologies

- Active Flow Control Inlet
- Active Shape Control Inlet
- Fluidic Nozzle Area Control
- Research methods

Advanced PAI Concepts

- Advanced methods
- Unconventional Configurations
- Wind tunnel validation

DEVELOPMENT OF AN ENHANCED THERMAL BARRIER FOR RSRM NOZZLE JOINTS

Paul H. Bauer
Thiokol Corporation
Brigham City, Utah

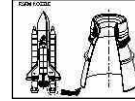
***Development of an Enhanced
Thermal Barrier for RSRM Nozzle
Joints***

P. H. Bauer

NASA Seal/Secondary Air System Workshop
25 October 2000



RSRM Nozzle



- **Reusable Solid Rocket Motor Joints**

- * Evaluation
- ** Qualification

Joint 1 *

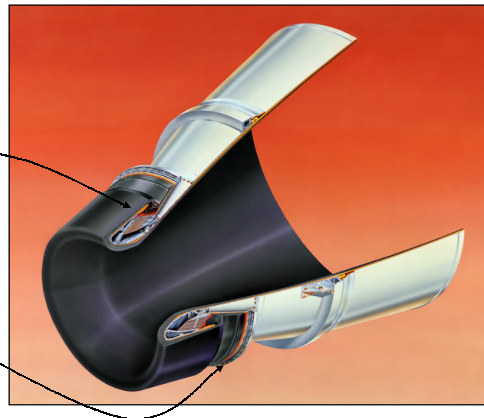
Joint 2 **

Joint 3 *

Joint 4 *

Joint 5 *

Joint 6 **

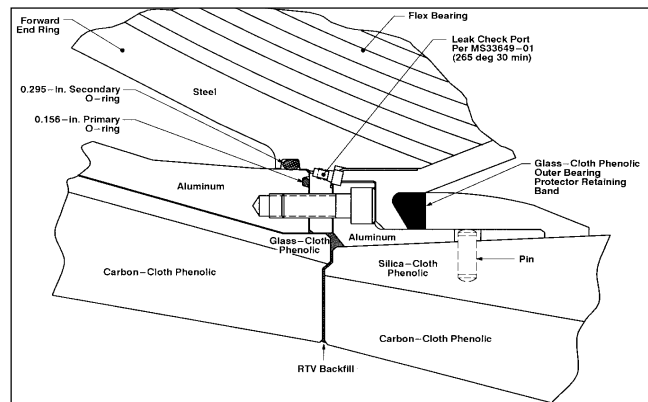


RSRM Nozzle is composed of 6 sections and has 6 sealed joints.

- 1) Exit cone joint
- 2) Nose cap to cowl
- 3) Nose cap to throat
- 4) Throat to exit cone
- 5) Bearing to fixed housing
- 6) Fixed housing to case

RSRM Nozzle Joint 2

- Joint 2 current design with RTV backfill



Current joint design uses an RTV backfill material as a thermal barrier and also is meant to function as a redundant seal. In joint 2 it does not function as designed. Joint motion fractures the backfill on most flights and allows pressurization of the o ring seals. In some cases, distinct gas paths may form and can heat-affect paint or even metal nozzle components.

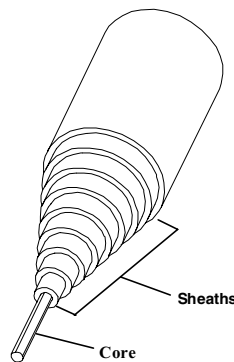
Design Requirements

- **Cool propellant gases.**
- **Filter slag and particulate.**
- **Conform to various joint assembly conditions as well as dynamic flight motion.**
- **Maintain positive margins of safety for all affected components.**
- **Provide barrier redundancy to ensure fault-tolerance.**

A re-design effort is underway by Thiokol to eliminate this risk. The redundant seal capability of the current thermal barrier/backfill material will be eliminated. New design will allow by design the pressurization of the o-rings, but ensure that the gasses are benign.

Albany International Techniweave

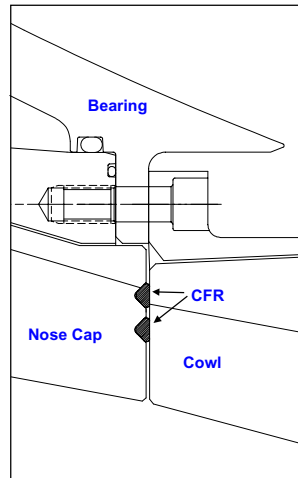
General Details	Rope Diameter	0.260 inches
	Fiber Material	Thornel T-300
	Fiber Diameter	2.76 x 10 ⁻⁴ inches
Core Details	Fiber Count	12 K
Sheath Details	Number of Sheaths	10
	Number of Carriers per Sheath	8 (sheath 1-5) 12 (sheath 6,7) 16 (sheath 8-10)
	Fiber Count per Carrier	1K (sheath 1-3) 3K (sheath 4-10)
	Braid Angle	0° (Core) 17° (sheath 1) 45° (sheaths 2-10)



Replacement material developed and produced by Albany International Techniweave proved to be highly thermally resistant, permeable and easy to handle.

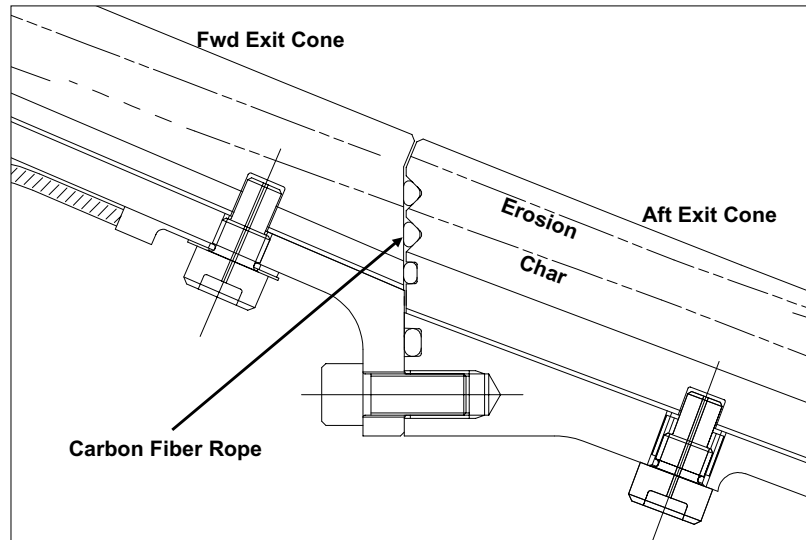
Joint 2 CFR Design

- Fault tolerant.
- Redundant 2-CFR design.
- Accommodates worst case joint tolerances.
- Straightforward to manufacture.
- Trouble-free assembly.



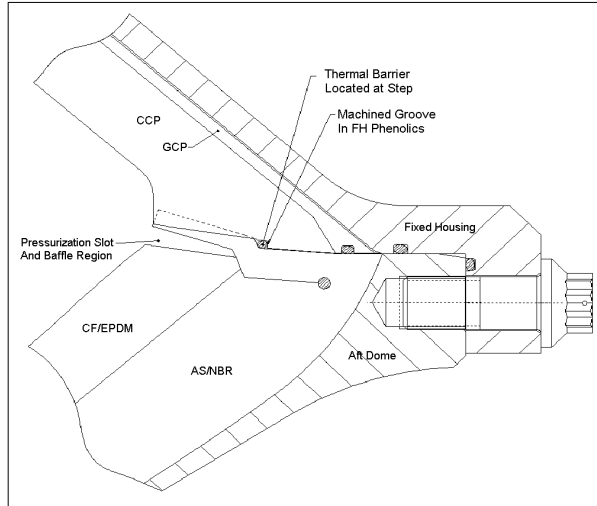
New design is fault tolerant, two barrier design. Each thermal barrier has the capability to cool and filter propellant gasses. Two barriers provides additional factor of safety. Design also accounted for manufacturing and assembly concerns. New barrier design will be much easier and cheaper to build.

Joint 1 CFR Design



Joint 1 is also being considered for redesign. Current concept is similar in most respects to joint 2.

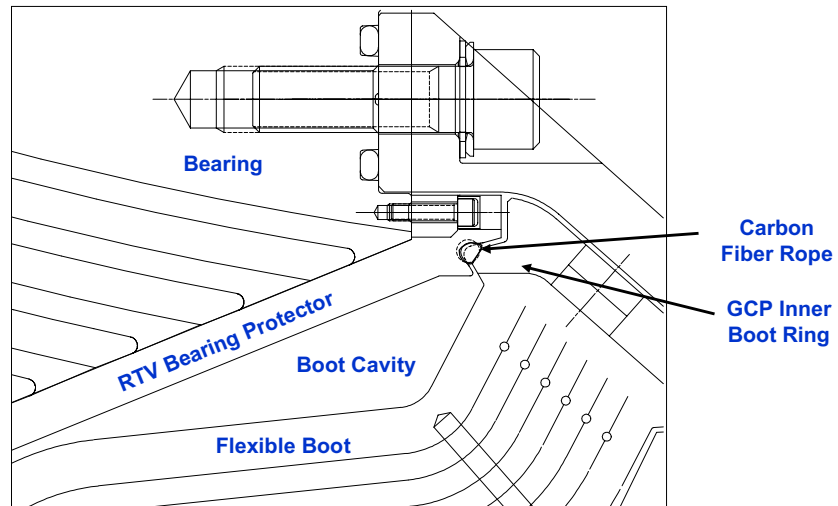
Joint 6 CFR Design



- **Fault tolerant**
- **Accommodates worst-case joint tolerances**
- **Straightforward to manufacture**
- **Trouble-free assembly**

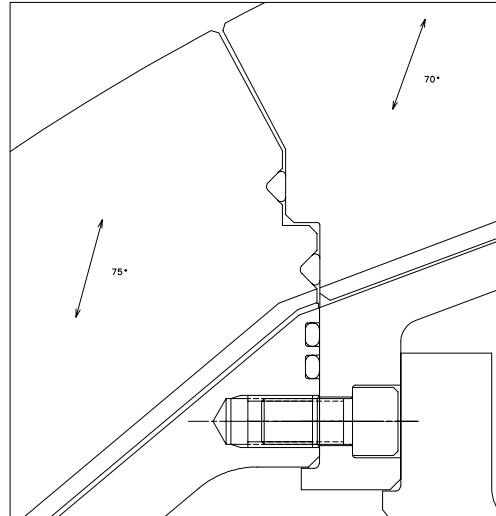
Joint 6 (or nozzle-to-case joint) is also being evaluated for flight. CFR has been located between NBR and CCP phenolic as a backup to the J-leg seal.

Joint 5 CFR Design



Joint 5 concept incorporates a single CFR barrier separating the boot cavity from the primary o-ring. Since boot cavity temperatures are already quite low, a single CFR barrier is being considered.

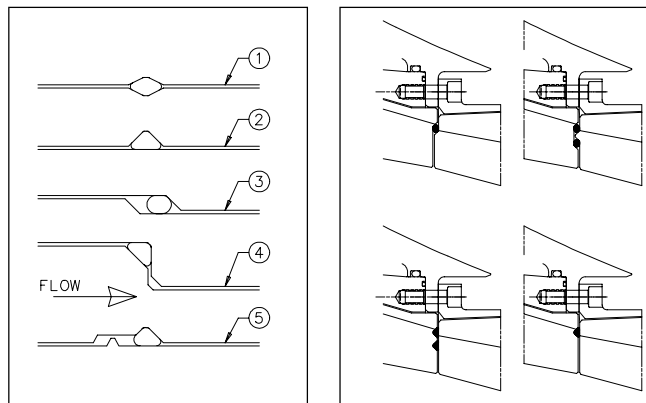
Joint 3 Preliminary Design Concept



Joints 3 and 4 are being considered for redesign but are behind joints 1, 2, 5, and 6 as far as development.

Design Concepts

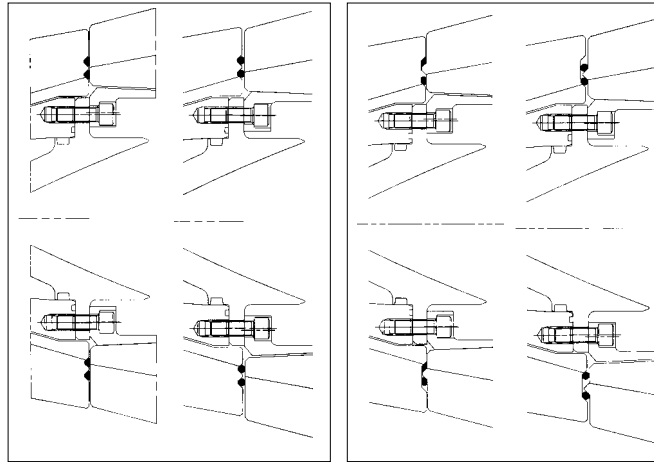
- General design concepts and final four design candidates for joint 2



Initial design concepts use a variety gland shapes, some better than others for accommodating tolerance stackup, joint dynamics, manufacturing and installation. The four designs on the left were evaluated for thermal performance.

Tolerance Study

- Tolerance extremes for face and dogleg gland designs



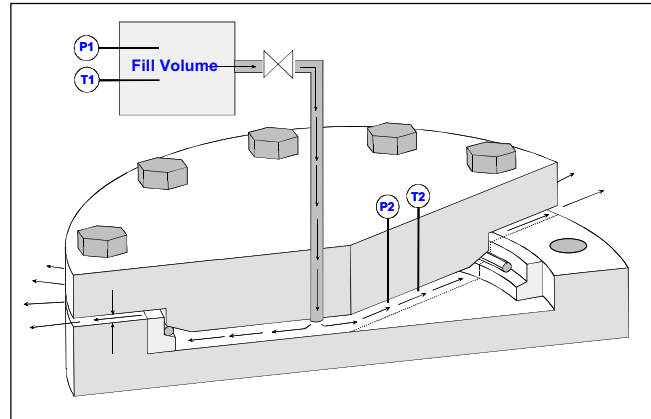
Tolerance study determines the final dimensions of the glands.

Test Program

- Tolerance Stackup Analysis
- JES 1 – Face preferred over dogleg.
- JES 2 – Double-CFR preferred over single.
- JES 3 – Confirm face preference.
- JES 4 – Confirm double-CFR preference.
- JES 5 – Confirm JES 1 results and demonstrate no-rope results.
- JES 6 – Test additional fill volume. (not fired yet)
- Cold Flow Testing
- MNASA-11 – Single-CFR dogleg.
- MNASA-12 – Double-CFR face.
- MNASA-13 – Single-CFR face (not fired yet).
- Circumferential Flow
- Full-scale Assemblies

Outline of test program.

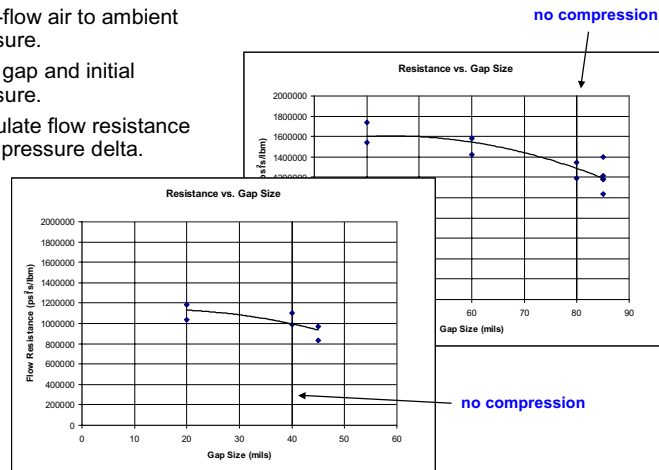
Cold Flow Fixture



Initial pressure tests show little difference between selected designs.

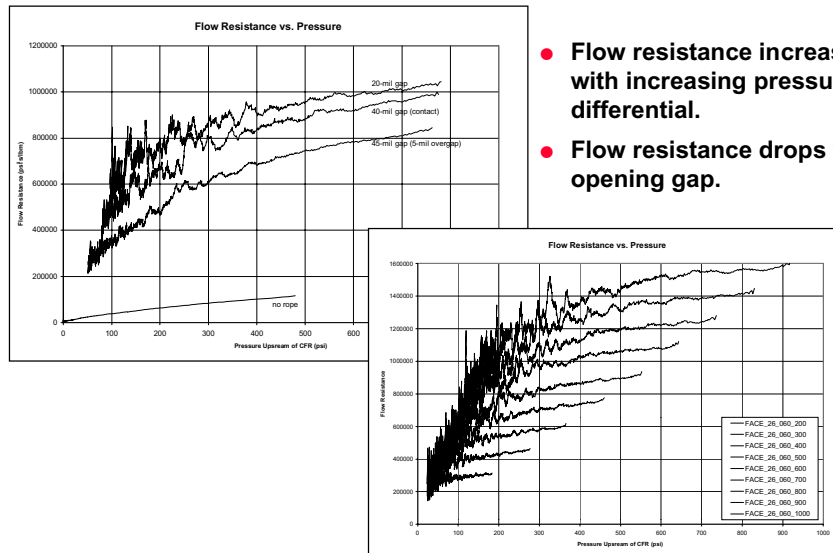
Preliminary Cold Flow Data

- **Seating**
 - Cold-flow air to ambient pressure.
 - Vary gap and initial pressure.
 - Calculate flow resistance from pressure delta.



Data shows good flow resistance for a variety of tolerance conditions. Testing covered extreme tolerance conditions where the barrier was no longer in compression. This gave us confidence that the CFR would perform in the dynamic (gap-opening) joint conditions.

Preliminary Cold Flow Data

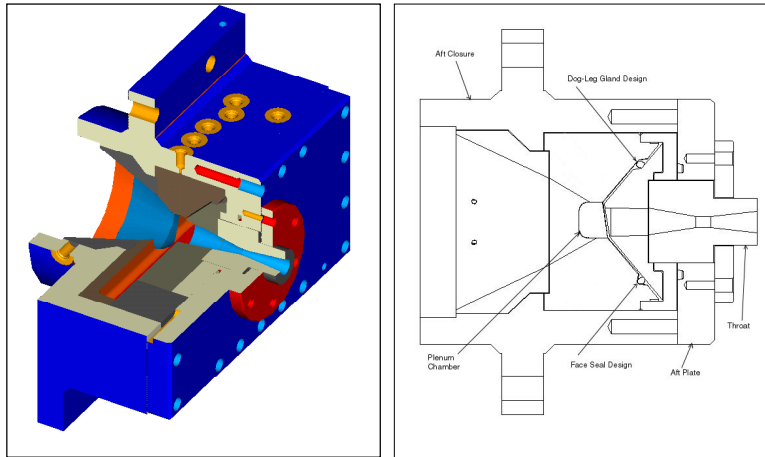


- Flow resistance increases with increasing pressure differential.
- Flow resistance drops with opening gap.

Flow resistance is not constant with initial pressure. This gave us more evidence that the barrier does react to the pressurization event and should equally distribute the flow circumferentially.

Sub-scale Nozzle JES Testing

- Cutaway view of plenum and test section.

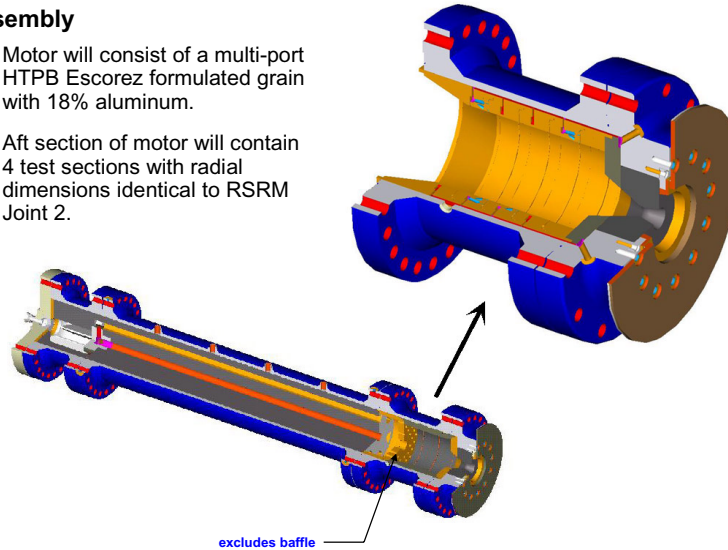


First hot fire test of the CFR in a Joint 2 environment. This motor tests a 5 inch section of CFR and is instrumented to record pressures and temperatures upstream and down stream of one or two CFR barriers.

24-inch Hybrid Motor Configuration

- **Assembly**

- Motor will consist of a multi-port HTPB Escorez formulated grain with 18% aluminum.
- Aft section of motor will contain 4 test sections with radial dimensions identical to RSRM Joint 2.

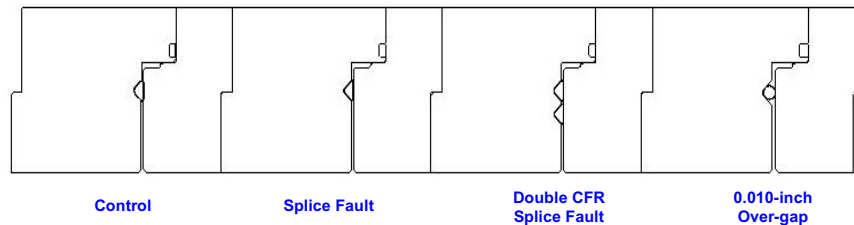


Larger sub-scale motor was recently fired to evaluate the fault-tolerance of the CFR thermal barrier. Results were encouraging, but did bring into question the hot durability of the CFR. High tensile strength material is being evaluated.

Test Sections

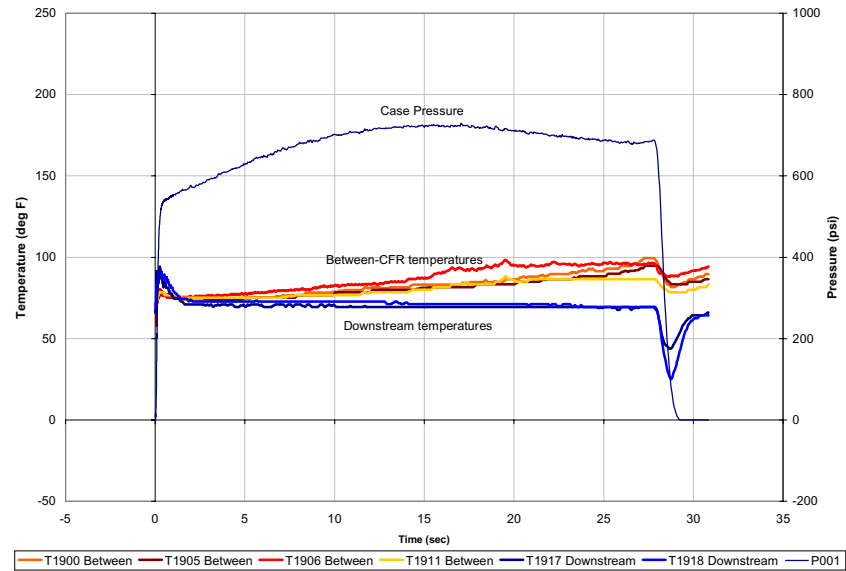
● Test Sections Description

- Control – Nominal gap, no flaw.
- Single CFR– Single Flaw, CFR cut through with 0.050-inch gap.
- Double CFR – Two Flaws, Clocked 180°
- Overgap Test – Zero CFR compression, 0.010-inch blow-by path.



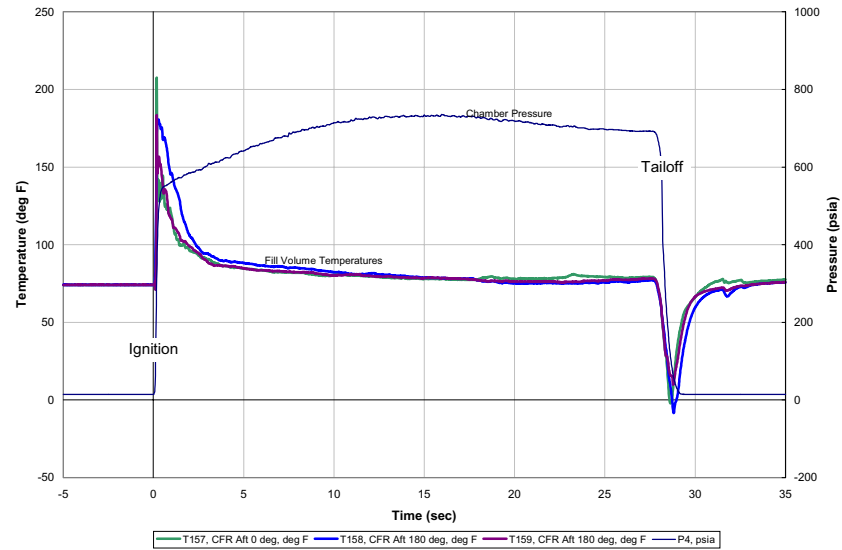
Details of the fault-tolerance test sections. Temperature profiles behind all four barriers were acceptable and no heat affects on any o-rings were noted. All CFR test sections had unexpected broken fibers, but did not affect the performance of the barriers.

MNASA-12 Test Data



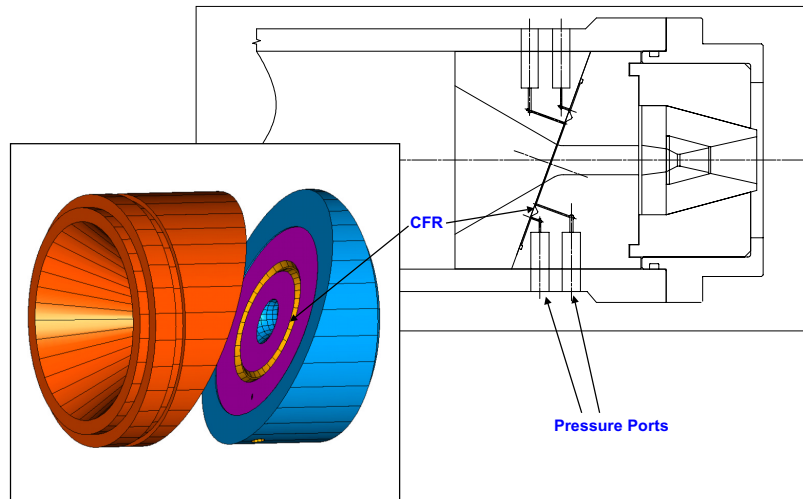
Several subscale RSRM motors were fired with nominal CFR barriers in place. This is test data from one of those motors. Note that the greatest temperature deltas are caused by gas compression and expansion. Heat passed from the combustion process to the thermocouples downstream of the second barrier is not measurable.

MNASA-11 Test Data



Single-barrier test on a subscale MNASA motor shows similar results.

Circumferential Flow Test Section



Circumferential flow is a concern in vented system. This test creates circumferential flow in a non-vectored motor with use of a canted test section. Designed to produce a 4-5 psi differential across several inches of CFR, the test is conservative. Actual expected differential pressure is 4-5 psi across 12 feet of CFR. Differential pressure and temperature was recorded both upstream and downstream of the CFR.

Differential Pressure Instrumentation

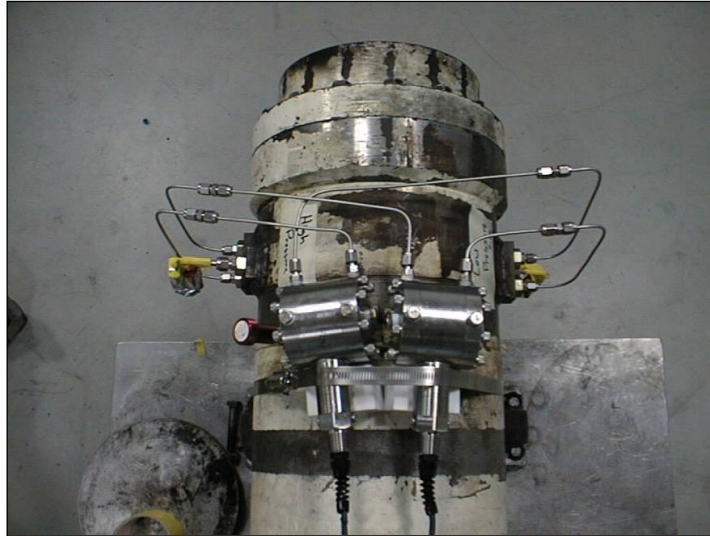
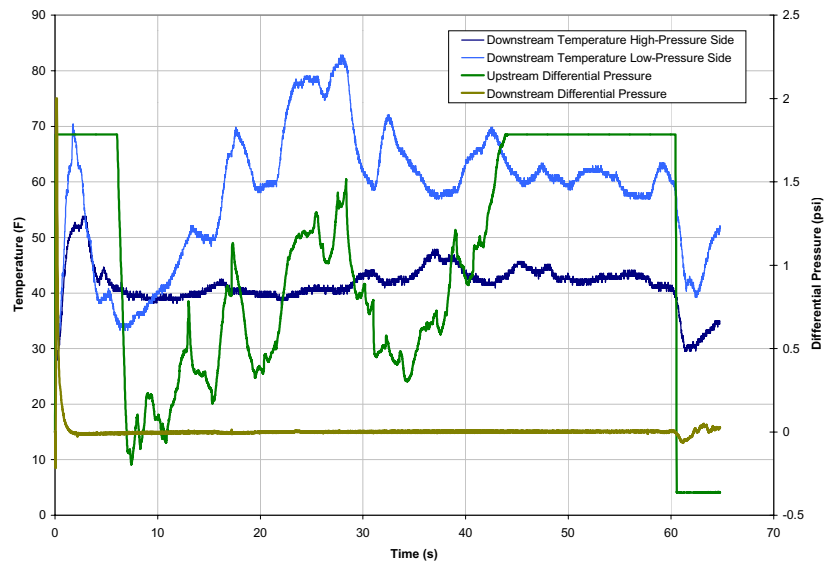


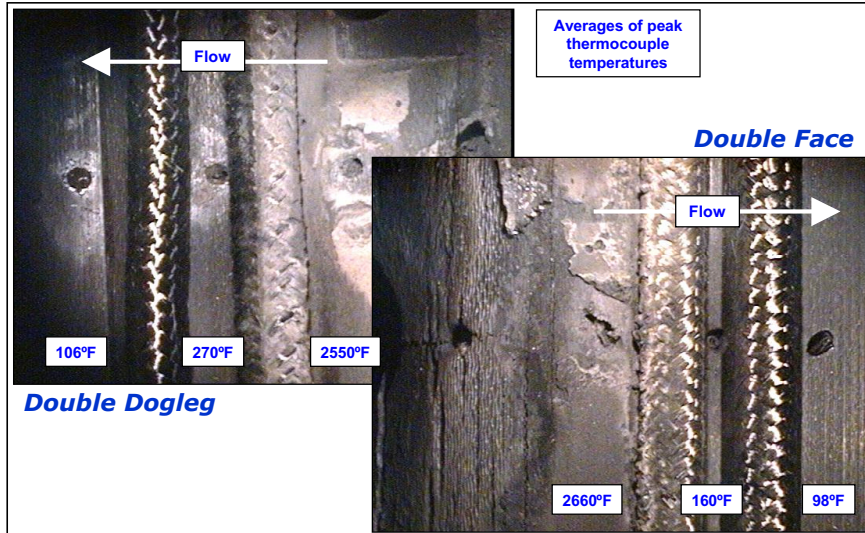
Photo of the actual test setup. Differential pressure gages are external.

Downstream Temperatures



Data shows excellent downstream temperatures. Differential pressure downstream of the barrier is not measurable.

Performance

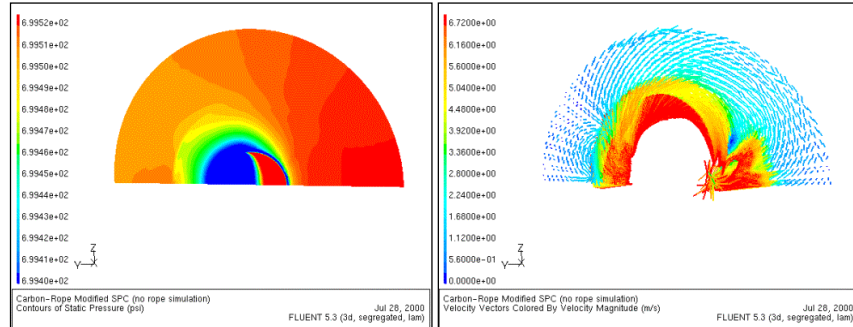


Typical post fire photos and peak temperatures. Note the large temperature change across the first barrier.

Thermal Analysis

SPC - Canted Test Section

No-CFR Pressure and Velocity Distributions



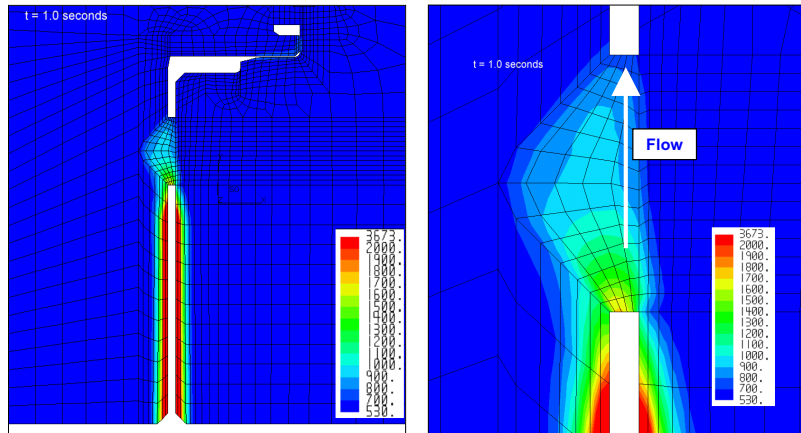
- Gap alone (no CFR) creates significant resistance to circumferential flow.
- Adding CFR flow resistance results in uniform pressure distribution downstream of CFR.

Circumferential Flow was modeled without CFR.

Thermal Analysis

- No Circumferential Flow

Temperature Contours at 1.0 Seconds

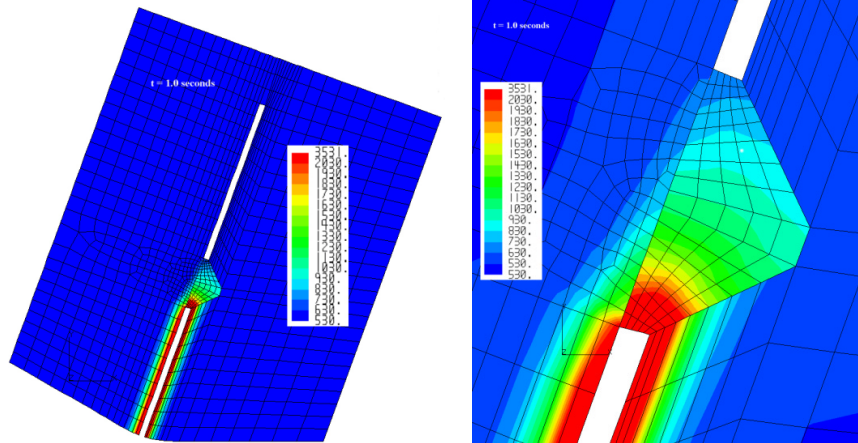


Predicted thermal performance of CFR without circumferential flow. Model is still under development but does match measured results well.

Thermal Analysis

● Circumferential Flow

Temperature Contours at 1.0 Seconds



Predictions with circumferential flow show a slight increase in temperature upstream of CFR, but no significant change to the downstream environment.



Summary

- Tolerance study and cold-flow tests provided good basis for project funding.
- All hot-fire tests demonstrated excellent capability. Provides incentive to evaluate all nozzle joints.
- Full-scale testing to be conducted in April 2001.
- More full-scale tests planned.
- Flight implementation for joints 2 and 6 may happen as soon as 2002.
- First flight would then be in fall of 2003.

ADVANCED SEALS AT GE RESEARCH AND DEVELOPMENT CENTER

Ray Chupp and Norm Turnquist
General Electric Corporate Research and Development
Niskayuna, New York

Research & Development Center - Advanced Seals


Advanced Seals at GE Research & Development Center

Objective:
Development of Advanced
Seals for Turbomachinery

Overview:
Briefly GE - CRD
Sealing Types
Application Areas
Experimental Facilities
Static Seals
Dynamic Seals

GE CRD Advanced Seals Team

- Saim Dinc
- Ray Chupp
- Norman Turnquist
- Mahmut Aksit
- Wei Ming Chi
- Hong Dai
- Farshad Ghasriipoor
- Jason Mortzheim
- Hamid Sarshar
- Chuck Golden
- Chuck Wolfe



Objective of CRD Seals Team is to develop advanced seals for turbomachinery applications

Presentation Overview - Who are the members, What seals we are developing, Where they are being applied, and What testing capabilities we have at CRD

CRD Seals Team Members - There is some flux in and out of the team; there are generally around 8 full time team members at any given time.

Advanced Seals at GE - Research & Development Center

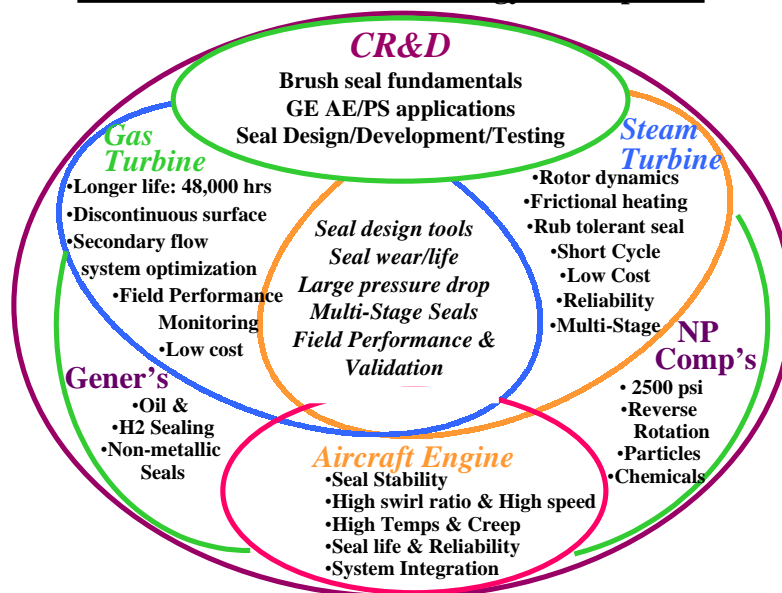
<u>Seal Types</u>	<u>Testing Capability</u>	<u>Applications</u>
Static Seals	Static Seal Testing	
• Cloth Seals	Brush & Cloth Seals	• Gas Turbines
• Piston Rings	1000 psi	• Compressor &
	1000F	
Dynamic Seals	36"/50" Dynamic Seal Testing	• Turbine Seals
	Brush, Aspirating, HC Seals	
• Brush Seals	36 & 50 in. Dia.	• Steam Turbines
• Aspirating Seals	800 ft/sec	
• Labyrinth Seals	120 psi	• Generators
• Honeycomb Seals	100 F	
• Abradable Seals	5" Dynamic Seal Testing	• Compressors
	Brush, Labyrinth Seals	
	1200 psi	
	1000 F	
	Air & Steam	• Aircraft Engines
	800 ft/sec	

Types of Seals being developed at GE CRD (Static and Dynamic).

Summary of Test Rigs at CRD and their capabilities (Shoebox, 36", 5.1").

Areas of Application for CRD-Developed Advanced Seals (GT, ST, Generators, Compressors, AE's)

GE - CRD Brush Seal Technology Development



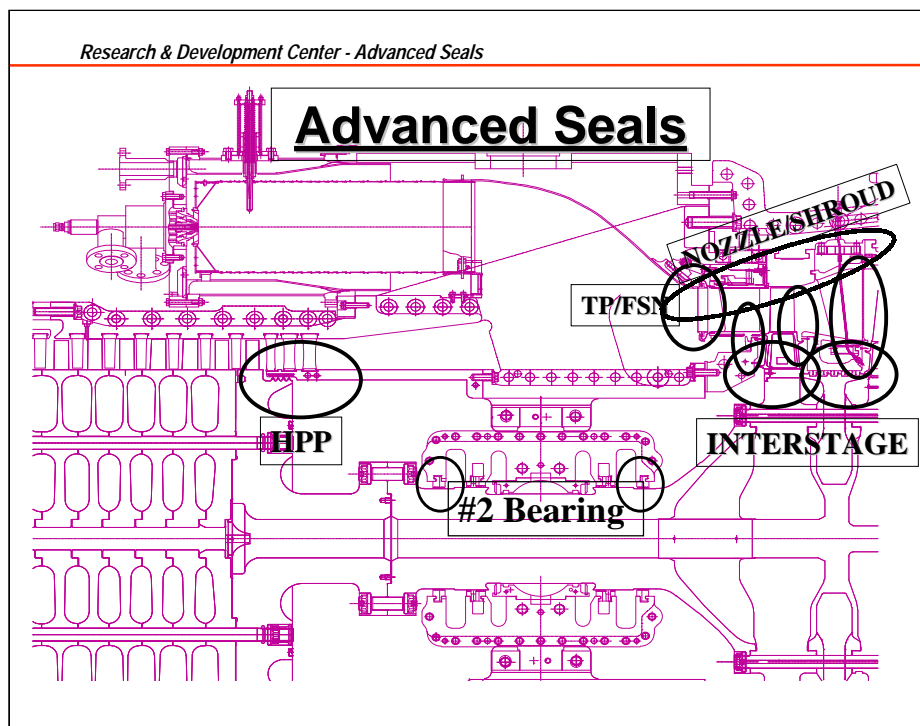
Synergy Chart

CRD develops seal fundamentals/design tools that are shared across GE businesses.

Many seal applications share common design challenges (where areas overlap).

Each application also has its own unique challenges.

CRD uses analytical tools (FEA, CFD, fundamental equations, statistical methods, etc.) as well as test data to develop Transfer Functions that can be used to design brush seals for new applications.



Example of areas where CRD-Developed Advanced Seals are being applied.

7EA GT has brush seals at HPP, #2 Bearing, and Interstage locations;
Cloth seals at Transition Piece/First Stage Nozzle (TP/FSN) and Nozzle
Shroud locations.

Advanced Seal Test Rigs at CRD

	<u>"Shoebox" Rig</u>	<u>5.1" Rotary Rig</u>	<u>36" Rotary Rig</u>
Working Fluid	Air	Air or Steam	Air
Total Flow Rate (lbm/s)	2.0	1.5 Steam/2.0 Air	12
Inlet Pressure (psig)	430	1200 Steam/450 Air	125
Exhaust Pressure (psig)	430	300	125
Temperature (°F)	1000*	750 Steam/1000 Air*	100
Speed (RPM)	N/A	36000	2400
Surface Speed (ft/s)	N/A	800	375
Axial Motion (in.)	N/A	+/- 0.75	N/A
Seal Configuration	12" max. linear strip (1 seal strip)	5.1" diameter brush, labyrinth, etc. (2 seals req'd)	36" dia. brush, aspirating, etc. (2 seals req'd)

Note: Temperature limits depend on test pressures. Limits given are absolute maximum.

Advanced seal testing capabilities at CRD

3 test rigs:

"Shoebox" (Static testing, Air only)

Used for static seal characterization and basic leakage testing of labyrinth, honeycomb, and brush seals.

5.1" Rotary Rig (Dynamic testing, Air or Steam, up to 1200 psia)

Used for testing subscale seals at approximately full scale conditions (speed, pressure, temperature)

36" Rotary Rig (can be reconfigured to 50") (Dynamic testing, Air only)

Used for testing full scale seals at subscale conditions.



CRD 5.1" Rotary Seals Test Rig

Used for dynamic leakage testing of labyrinth and brush seals.

Used for static leakage testing of piston rings, thermal rings.

Capable of testing in Air or Steam.

1200 psia maximum upstream pressure; can be backpressured to 300 psia.

Up to 800 ft/s surface speed.

GE CRD 5.1" Seals Test Rig



Side view of the CRD 5.1" Rotary Seals Test Rig

Air or Steam enters through center ring.

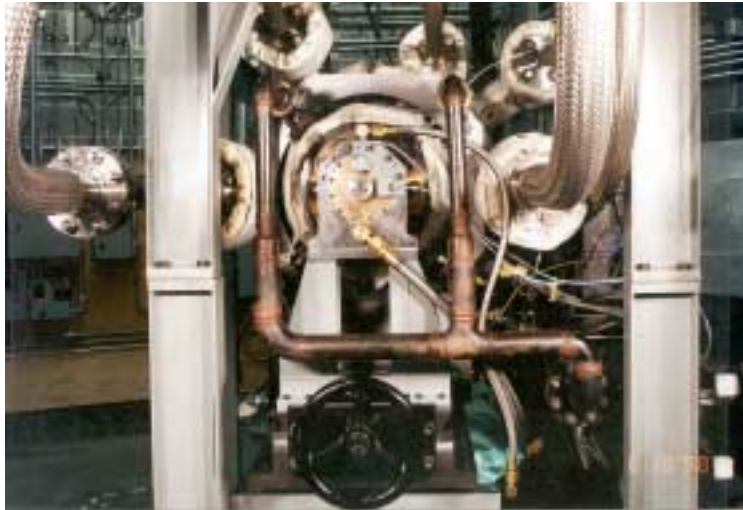
Flow splits between two sets of test seals.

Independent control of inlet and both exhaust pressures.

Pressure vessel mounted on slider for axial movement (for hysteresis testing).

Rig is used for leakage, wear, and hysteresis testing.

GE CRD 5.1" Seals Test Rig



End view of CRD 5.1" Rotary Seals Test Rig

Solid shaft mounted on hydrodynamic bearings.

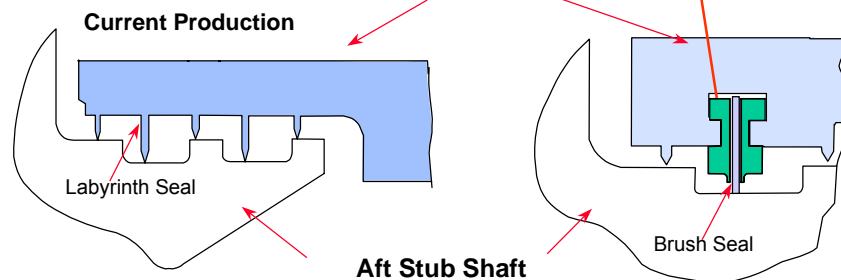
Variable-speed rotor up to 36,000 RPM.

Bentley-Nevada vibration data acquisition system to study seals' effect on rotor dynamics.

High-Pressure Packing / Inner Barrel

- **Brush Seals**

- Minimize Air Leakage
- Tolerant of Misalignments
- More Durable than Labyrinth Seals
- Retrofittable



10

- The seal between the Compressor Discharge Casing Inner Barrel and the compressor Aft Stub Shaft is known as the High-Pressure Packing.
- The HPP regulates flow of compressor discharge air between the stationary inner barrel and the compressor rotor aft stub shaft into the first forward wheel space.
- With conventional labyrinth tooth/land seal packings, the minimum clearance that can be tolerated is dictated by expected rotor displacements during transients, differential thermal growth, and by wheel space cooling requirements.
- When rubs do occur, labyrinth teeth can be damaged, which can result in excessive leakage through the packing. A 20 mil rub (not uncommon) translates into a loss in performance of up to 1%.
- The new brush seal replaces one of the existing labyrinth tooth/land seal with a rub tolerant brush seal element.
- HPP Brush seals consist of a pack of fine wires held in a frame mounted on the inner barrel. The inherent flexibility of the brush seal material allows it to bend under transient conditions which would damage the standard design labyrinth packing. The sealing efficiency of a single brush is approximately 10 times that of a labyrinth seal under similar conditions.
- Brush seals offer better than new performance and will enable the unit to sustain initial performance levels over extended periods of time because the inevitable rubs will not increase the leakage past the seals.



Example of a GT brush seal in the field

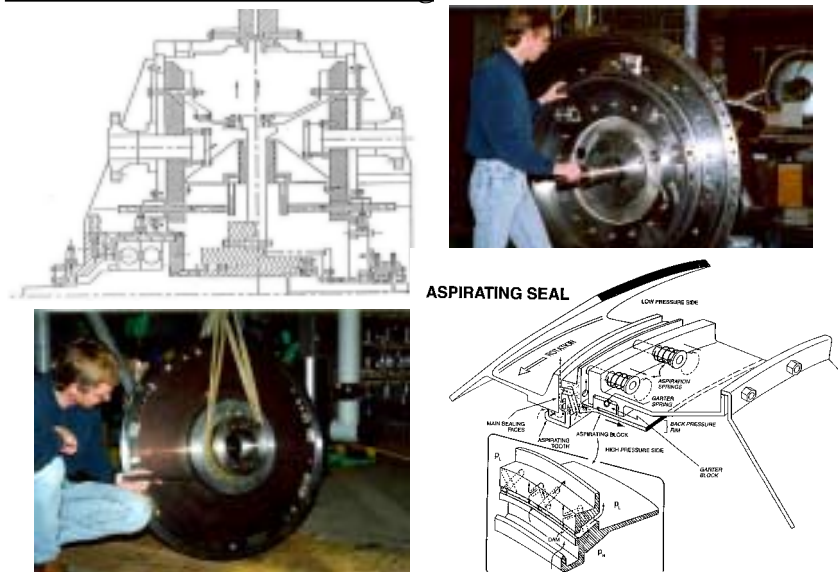
7EA HPP Brush Seal after 21,000 hours of service.

Minimal seal and rotor wear observed.

Seal was reinstalled for an additional 24,000 hours.

Commercial offering; GE has hundreds of these seals currently in service.

GE CRD 36"- 50" Seals Test Rig



CRD 36"/50" Rotary Seals Test Rig in 36" Aspirating Seal configuration

Cross section of the rig showing disk with Aspirating Seal on left side and Brush seal on right side.

In this configuration, air enters rig from both sides and exhausts through center plenum.

Both inlet pressures and the exhaust pressure are controlled independently.

Top right photograph shows pivot location (near 12:00 position) for tilt mechanism to simulate angular misalignment of seal to rotor.

Test results from Aspirating Seal development program presented at 1997, 1998, and 1999 NASA Seals Workshops by N.A. Turnquist.

New CRD Abradable Rub Rig



Rig and dedicated computer data acquisition system during operation

Rig variables:

- Max. blade surface speed
- Max. shroud surface temperature
- Incursion rate
- Incursion depth



Rig with cover open--sample is mounted below rotor and moves vertically

Parameter measured:

- Shroud location vs. time
- Shroud X & Y accelerations vs. time
- Backside temperature vs. time (via. T/C)
- Relative blade vs. shroud wear depth
- Surface conditions before/after rub

GE CRD's new Abradable Rub Rig

Rig being used to evaluate Abradable Seal materials/designs for various engine and turbomachinery applications.

Rig is currently located off-site; will be moved to CRD by end of 2000.

GE90 DEMONSTRATION OF ASPIRATING SEAL

Thomas W. Tseng
General Electric Aircraft Engines
Cincinnati, Ohio

GE90 Demonstration of Aspirating Seal

October 25 and 26, 2000

Presented at:

**NASA Glenn Research Center
Seal/Secondary Air System Workshop
Cleveland, OH**

Presented by:

**T.W. Tseng
GE Aircraft Engines
Cincinnati, OH 45215**

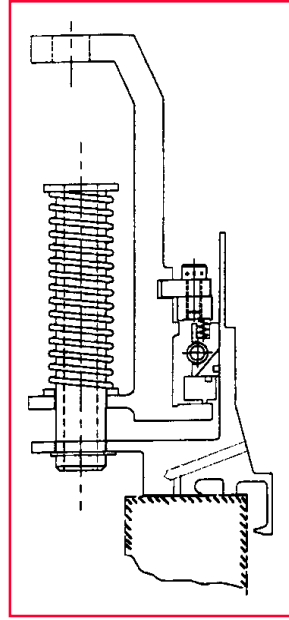
AT(PC)–001009/1–10/02/2001

Topics

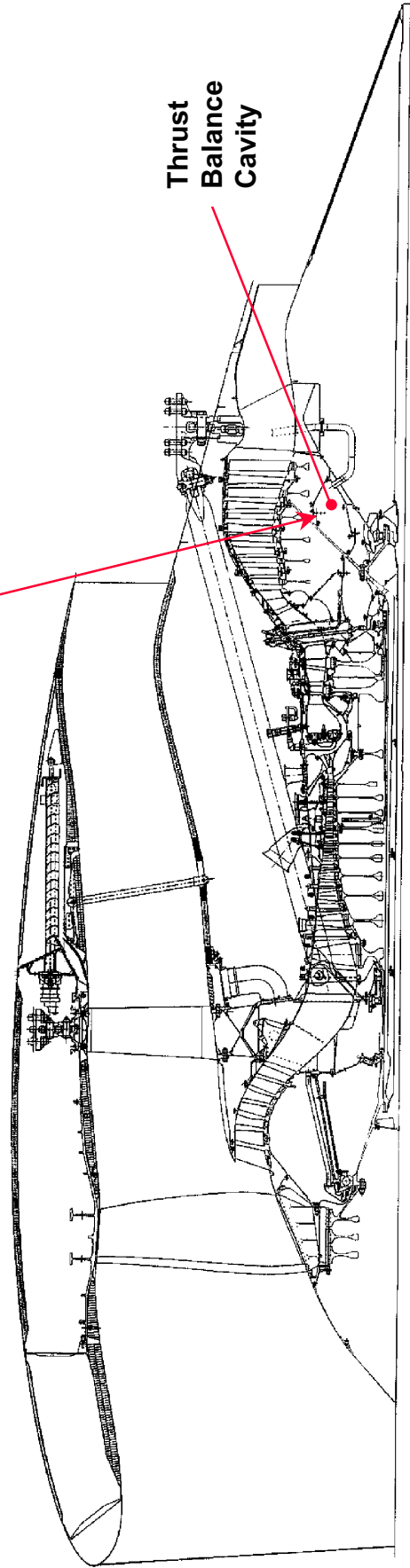
- Objective
- Aspirating seal location in GE90
- List of accomplished rig verifications tests
- Seal performance comparison
- Status of GE90 demo

Objective: Complete the development of aspirating seal for engine applications by demonstrating the seal in the GE90 engine after rig verification

36" Dia. Aspirating Seal

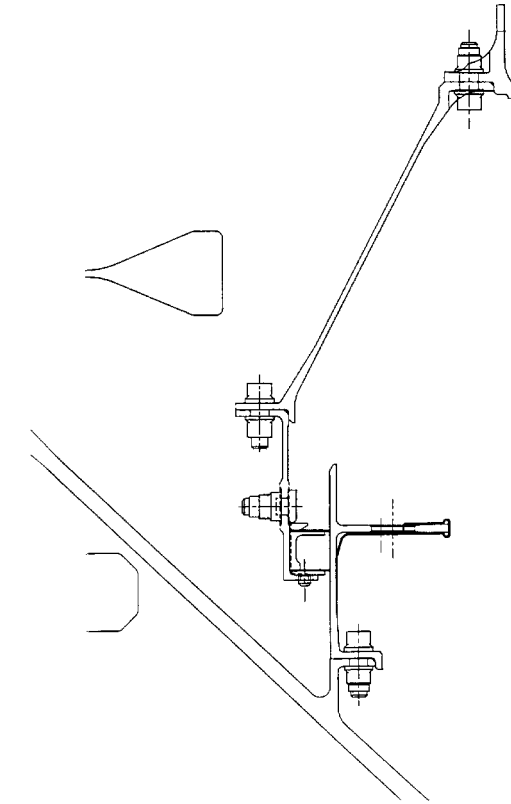


GE90 Engine
Cross Section

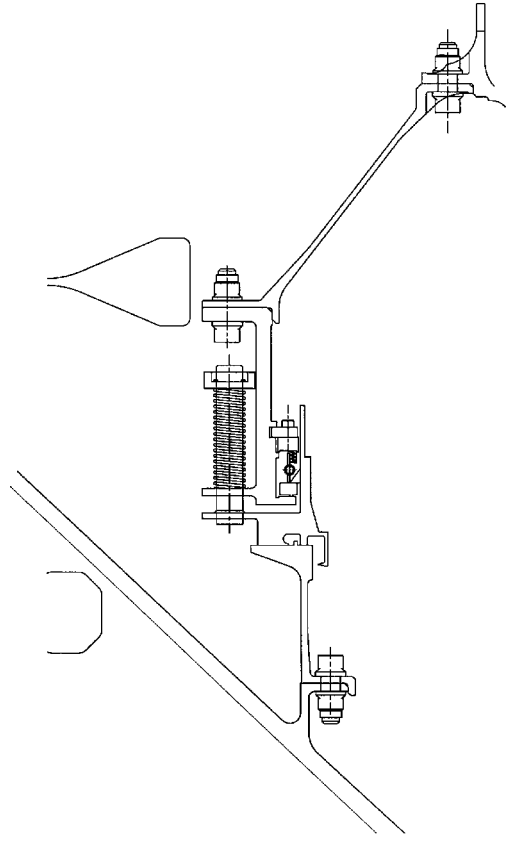


Thrust
Balance
Cavity

Seal Position



Production

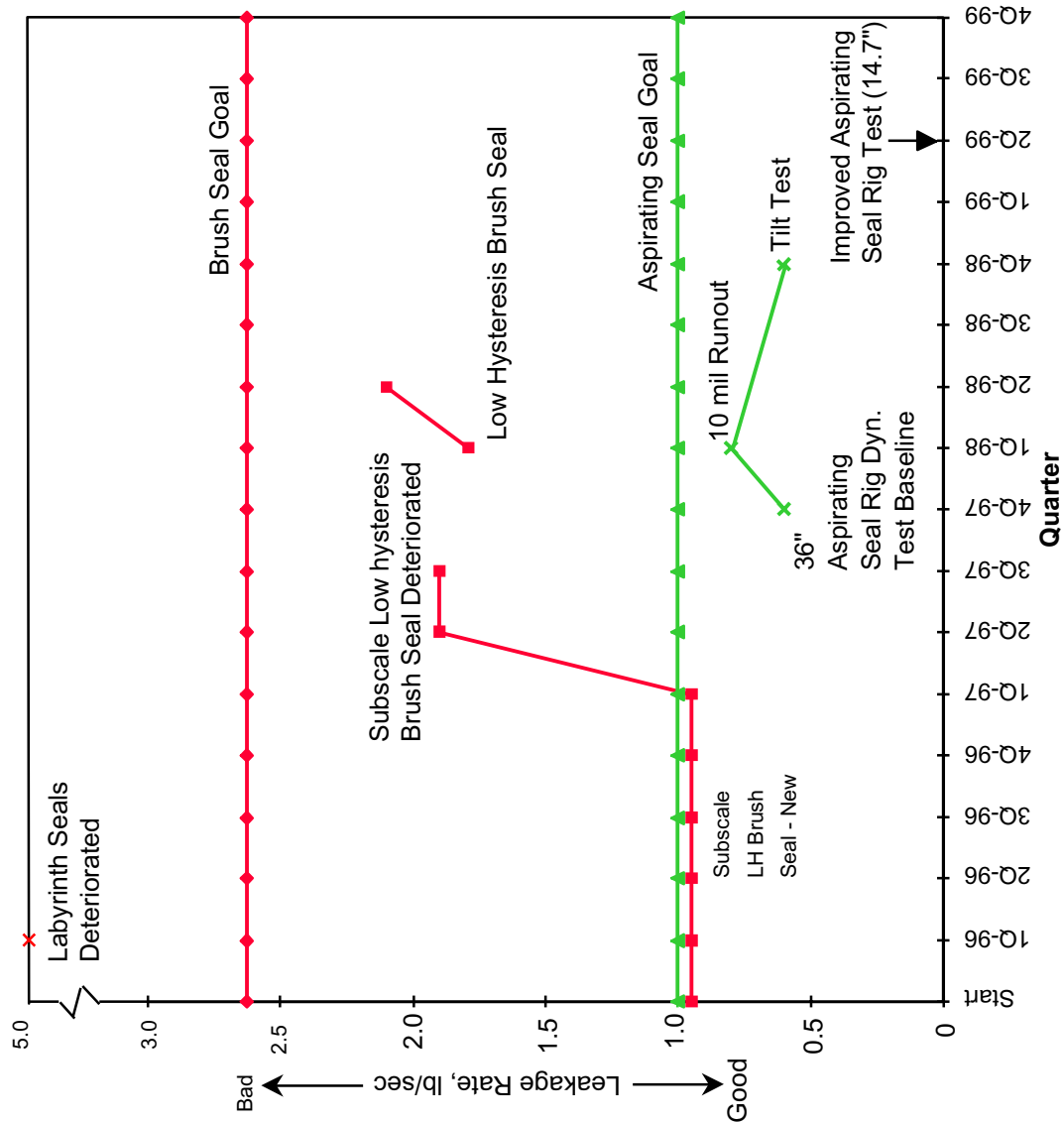


Aspirating Seal

List of Accomplished Aspirating Rig Verification Tests

- 15" Dia. Subscale Tests
 - 1000 hours endurance test (760 fps, 1000°F. 99 psid)
 - Dust Ingestion Test (400 fps, R.T., 100 psid)
- 36" Dia. Fullscale Rig Tests (400 fps, R.T., 100 psid)
 - Start/Stop Cycles
 - Runner Axial Face Runout: 5 & 10 mils
 - Simulated Maneuver Tilt

Seal Performance Comparison



Aspiring Seal:

- Lowest leakage
- No deterioration

Leakage Rate-Goals and Status for Brush Seals (Red) and Aspiring Seals (Green).

Status

<u>Status</u>	
• Seal, Runner and Support Designs	Complete
• Hardware Fabrications	In Progress
• Engine Demo	December, 2001

ADVANCED ASPIRATING SEAL

Alan D. McNickle
Stein Seal Company
Kulpsville, Pennsylvania

ADVANCED ASPIRATING SEAL

2000 NASA Seal/Secondary Air Delivery Workshop
NASA - Glenn Research Center, Cleveland, OH

Stein Seal Company, Kulpsville, PA
Alan D. McNickle, P.E.

October 25 - 26, 2000



Stein Seal Company
ISO-9001 Certified

NASA Seal Workshop - October 2000

Stein Seal Company developed a 14.7" and 36" advanced aspirating seal for GE Aircraft Engines. The seal is developed for a thrust balance application in gas turbine secondary flow path. Stein built and tested the 14.7" advanced seal. Tests included static tests, dynamic tests with rotor runouts up to .010" (TIR), and sand ingestion tests. All test were conducted at room temperature.

The advanced aspirating seal provides hydrostatic operation with low leakage and high gas film stiffness at high differential pressures and high temperatures. The all metal seal has the ability to operate at high temperature with large rotor runout. The design process and comparison to the original aspirating seal will be discussed along with recent test data.

The advanced aspirating seal performed successfully during extreme rotor runout tests up to .010" (TIR), whereas the original aspirating seal could not tolerate a rotor runout above .005".

Agenda / Goals

Agenda

- Design Goals & Operating Conditions
- Seal Operation
- Analysis - Original & Advanced Seal Design
- Rig Test Results
- Performance Attained

Goals

- Develop 14.7" & 36" Advanced Aspirating Seal
- Meet Leakage and Performance Goals
- Increase Gas Film Stiffness
- Increase Seal's Ability to Follow Extreme Rotor Runouts
- Build & Test 14.7" Seal



Stein Seal Company
ISO-9001 Certified

NASA Seal Workshop - October 2000

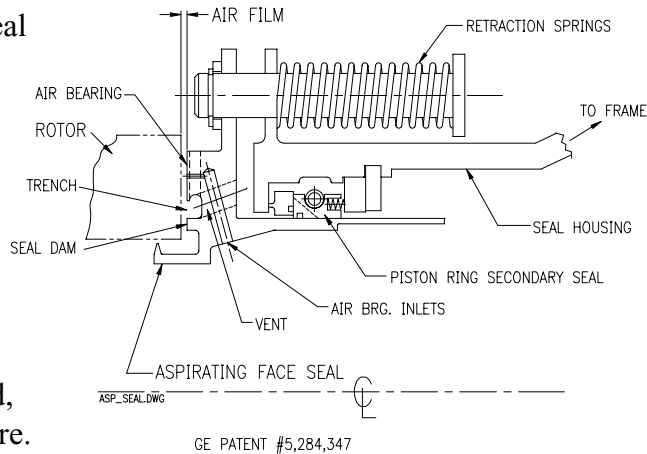
The advanced aspirating seal is developed by Stein Seal Company in conjunction with GE Aircraft Engine Company. The advanced seal offers improvements beyond the original aspirating seal design built several years ago.

Two seal sizes were studied and include a 14.7" seal and a 36" seal. The 14.7" seal was built and tested. The 36" seal was designed but not built.

The topics for discussion and program goals/objectives are included above.

What is an Aspirating Seal?

- A Hydrostatic Face Seal
 - Rides on a film of air
 - » 1.5 to 2.5 mils
- Provides controlled leakage throughout all operating conditions.
- Performance does not degrade over time.
 - non-contacting seal
- Operates at high speed, temperature, & pressure.
- Designed to replace labyrinth and brush seals



Stein Seal Company
ISO-9001 Certified

NASA Seal Workshop - October 2000

This slide shows the aspirating seal's major parts and features. The aspirating seal is a replacement for labyrinth and brush seal applications.

GE patent #5,284,347

Requirements / Challenges / Application

Operating Conditions:

Shaft Speed: 392 ft./sec.
 ΔP .: 100 psid
Air Temp.: 750 °F
Leakage: ~ 2.0 scfm/psid
Seal Life: Unlimited
(non-contacting)

Applications:

- Gas Turbines (Aviation & Land)
 - Thrust Balance
 - Compressor Discharge
 - LPT
- Labyrinth & Brush Seal Replacement

Challenges:

- Improve gas film stiffness
- Maintain uniform gas film clearance during all conditions
- Maintain low leakage performance
- Provide infinite seal life
 - Non-contacting, all metal design

Funding:

- Provided by GE Aircraft Engine
 - Developed under NASA's AST program (Glenn Research Center)
 - » IHPTET initiative

Target Engines:

- GE-90, UEET



Stein Seal Company
ISO-9001 Certified

NASA Seal Workshop - October 2000

The operating conditions are shown and are representative for the 36" seal.

The seal is developed under NASA's AST program and funded by GE Aircraft Engine Company.

The advanced seal requires an improvement to the gas film stiffness as compared to the original seal. Low leakage and uniform gas film clearance are requirements for the all metal non-contacting seal design.

The advanced aspirating seal is targeted for gas turbine secondary flow applications (I.E.: compressor discharge, LP turbine). The GE-90 and UEET engines are targets for seal integration. The aspirating seal is a replacement for brush seals and has significant leakage improvement as compared to brush seals. The aspirating seal leakage is approximately 20% of a brush seal.

Two Seal Sizes Developed:

Sub-Scale Seal

- 14.7" Seal (Rig Seal)
 - Optimized design
 - For rig testing at Stein
 - Utilizes highest gas film stiffness and fits GE-90 rotor envelope

Full Size Seal

- 36" Seal (Paper study)
 - Seal targeted for GE CRD test rig
 - Utilizes existing rig rotor with minor changes
 - High gas film stiffness not realized due to rig rotor constraints



Stein Seal Company
ISO-9001 Certified

NASA Seal Workshop - October 2000

14.7" seal

This seal has the widest face configuration that fits the GE-90 rotor envelope. The gas film stiffness is greatly improved compared to the original aspirating seal. This seal configuration was chosen for rig tests due to the performance increase.

The flow diverted is not required on the rotor.

36" seal

This seal has a radial face configuration that fits the existing rig rotor face on the GE CRD rig. This seal was developed to demonstrate that an improved aspirating seal could be developed to fit an existing test rig. This seal, to date, has not been built.

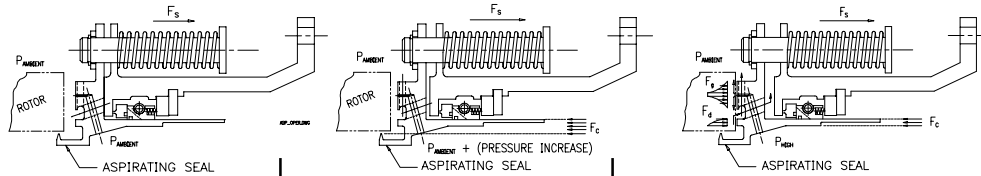
Rotor flow diverter

The rotor diverter is a metal protrusion on the rotor face that projects into the seal's trench (annulus) between the seal dam and air bearing. The rotor flow diverter is required of the 36" seal. The 14.7" seal does not require the rotor flow diverter.

The function of the flow diverter (when required) is to direct the seal dam gas flow into the radial and axial vent slots on the seal. Without the diverter, the gas path may tend to go radially outward, across the air bearing, and disrupt the flow and performance of the air bearing. It may be possible for the seal not to close without the flow diverter.

Seal Operation

$$\text{Force Balance Equation, } F_c = F_g + F_d + F_s + \text{Inertia} + \text{Friction}$$



START-UP / SHUT-DOWN:

(0 PSID)

- Springs retract seal open
- Large gap exists between seal and rotor face

AT PRESSURE INCREASE:

(< 3 PSID)

- Pressure builds and seal starts to close towards rotor.
 - Pressure drop occurs across balance dia. and laby tooth
 - Closing force overcomes retraction spring and friction forces
- Gap between rotor and seal face decreases

WITH PRESSURE DIFFERENTIAL:

(> 3 PSID)

- Pressure builds and seal closes toward rotor
 - Retraction spring force, friction force, and inertia forces are overcome
- As seal approaches rotor
 - Pressure drop occurs across seal dam
 - Air bearing force is established
- Laby tooth is no longer the primary pressure breakdown mechanism
- Seal is in equilibrium (1.5 to 2.0 mils gap)
 - Closing forces = Opening forces



Stein Seal Company
ISO-9001 Certified

NASA Seal Workshop - October 2000

The seal operation is characterized by non-contacting operation.

Start up / Shut down:

At rest, the seal is retracted open by springs. This pulls the seal away from the rotor. At this position the seal has no pressure drop across the seal.

At pressure build up:

As pressure builds, the closing force starts to increase, overcoming the retraction spring forces and the friction and inertia forces. The pressure force is established by the area created by the balance diameter and the laby tooth (located beneath the rotor.)

At full pressure:

The seal is in equilibrium at 1.5 to 2.0 mils. The closing force equals the opening force. The closing force is established by the area created by the balance diameter and the seal dam ID. The opening force is created by the air bearing force. This force tends to open the seal.

Tasks Performed

1. Parametric Study
 - Varied seal features to yield best performance gain:
 - » Seal dam, gas bearing, & trench geometry
2. Gas Bearing Analysis & Rig Tests
 - Analysis performed by Wilbur Shapiro, Inc.
 - » NASA GFACE Code
 - Rig tests validated analysis
3. CFD Analysis (CFDRC Corp.) performed on 14.7” & 36” seals
 - 14.7” Seal: Rotor flow diverter not required
 - 36” Seal: Rotor flow diverter is required
 - Operating Gap: .0015” to .0020”
4. Optimized Seal Features:
 - 36” Seal: .550” gas bearing, .050” dam, .180” trench
 - 14.7” Seal: 1.250” gas bearing, .250” dam, .450” trench
5. Rig Tests (Sub-Scale seal)



Stein Seal Company
ISO-9001 Certified

NASA Seal Workshop - October 2000

Parametric design studies looked at all possible seal configurations that would show improved seal performance as compared to the original aspirating seal. Features that affect seal performance include:

Size and placement of the seal dam and air bearing

Number of air bearing holes, hole diameter, and number of rows of holes, and hole spacing

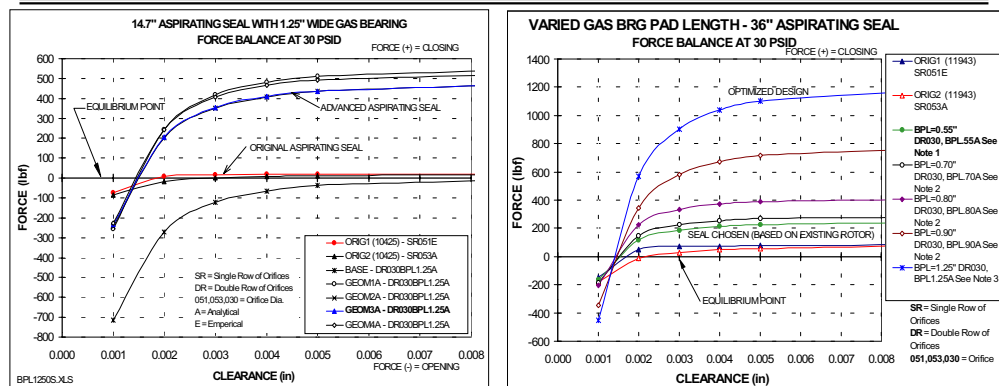
Seal aspirator tooth placement

Gas bearing analysis and static rig tests were performed to determine the gas bearing performance. Wilbur Shapiro, Inc. performed the gas bearing analysis. The static gas bearing rig tests were used to correlate the NASA GFACE seal code and Coefficient of Discharge, Cd.

The optimized seal configurations for both seal sizes are shown. The 14.7” seal has the widest radial face as it has the optimum gas bearing stiffness per unit length. The 36” seal fits the existing rig rotor at GE CRD.

Computational Fluid Dynamics (CFD) was performed on both seal sizes. CFDRC of Huntsville, Alabama, performed these studies. Conclusions showed that the rotor flow diverter was required on the 36” seal but not required on the 14.7’ seal. The seals operate properly with a gas film of 1.5 to 2 mils.

Analytical Summary - Force vs. Clearance at 30 psid 14.7" & 36" Seals



Advanced Seal has:

- Higher Gas Film Stiffness vs. Original Seal
- Improved load capacity
- Steep "Force vs. Clearance" slope at Seal Equilibrium point yields:
 - Small change in clearance = Large Restoring Force
 - High stiffness permits seal following during high rotor runouts



Stein Seal Company
ISO-9001 Certified

NASA Seal Workshop - October 2000

The aspirating seal operates at an equilibrium point where the gas film is maintained at 1.5 to 2.5 mils.

Seal equilibrium point is where Force = 0 lbf. on the Y-axis. The operating gas film clearance is determined where the curve line cross the equilibrium point.

Steep line slopes are desirable since any change in clearance is a correspondingly high change in force.

The original aspirating seal configuration (solid circle) has a less steep slope as compared to the improved aspirating seal configuration (open triangle).

Gas bearing face width comparison:

.440" Original aspirating seal

1.250" Advanced aspirating seal

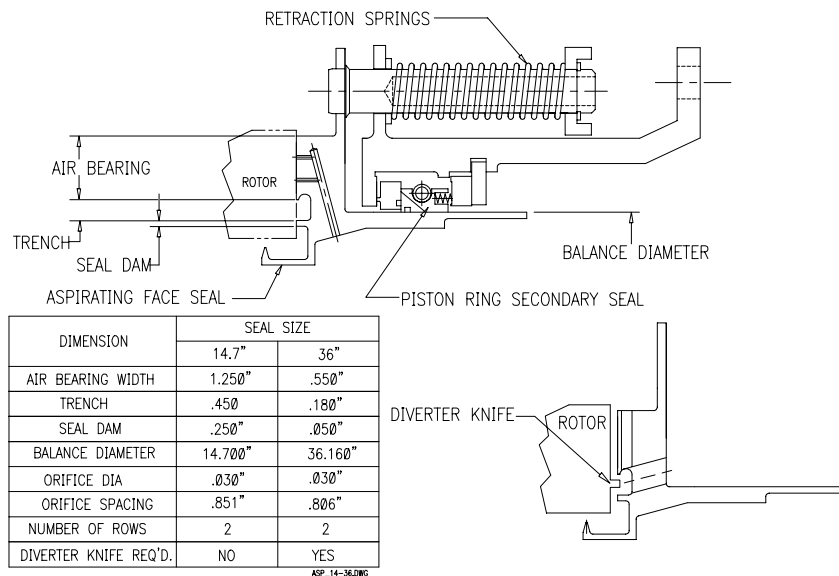
Gas film stiffness improvements are gained compared to the original seal design:

14.7" seal: 5.5 : 1 greater stiffness vs. original seal

36" seal: 1.7 : 1 greater stiffness vs. original seal (dictated by rotor size)

36" seal (optimized design): 6 : 1 greater stiffness vs. original seal

Seal Dimensions – 14.7” & 36” Seals



Stein Seal Company
ISO-9001 Certified

NASA Seal Workshop - October 2000

Dimensional comparison between the 14.7” and 36” advanced aspirating seals.

The balance diameter defines the nominal seal size.

The gas bearing for the 14.7” seal offers the best gas film stiffness improvement as compared to the original aspirating seal. This is due to the wide gas bearing face and placement of the seal dam and air bearing relative to the seal balance diameter.

The gas bearing for the 36” seal is the best size that fits the existing test rig rotor at the GE CRD facility. If space permitted a larger rotor, then a wider gas bearing face would be utilized. A wider gas bearing would improve the gas film stiffness.

Each seal has a double row of gas bearing orifices for optimum gas film stiffness for the space permitted.

It is important to note that the 14.7” seal does not require the rotor diverter knife, whereas the 36” seal does require the rotor diverter knife. CFD analysis dictated the rotor diverter knife requirements.

Analysis - Air Bearing Stiffness Comparison

- Improved Gas Film Stiffness (based on 30 psid)
 - 14.7” Advanced Seal Stiffness 5.5 > Original Seal
 - 36” Improved Seal Stiffness 1.7 > Original seal
 - » Seal fits existing rig rotor face
 - 36” Advanced Seal Stiffness 6.0 > Original seal
 - » Optimized design, fits GE-90 engine
- Improved Seal Stiffness Benefits:
 - Improves load support
 - Large servo force restores seal to equilibrium
 - Steep “Force vs. Clearance” slope at Seal Equilibrium point yields:
 - » Original seal has shallow “Force v. Clearance” slope
 - Seal tracks extreme rotor runout



Stein Seal Company
ISO-9001 Certified

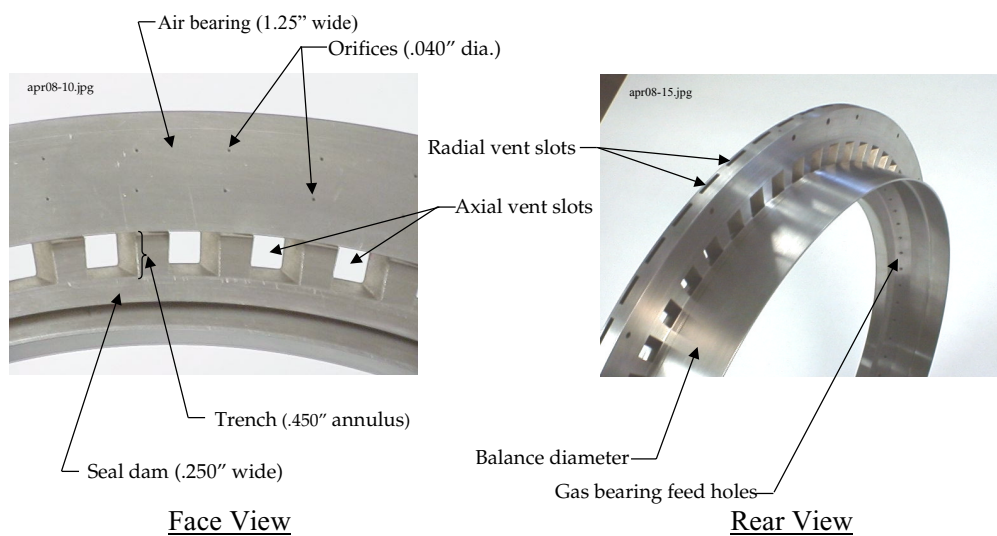
NASA Seal Workshop - October 2000

This slide shows the air bearing stiffness summary highlights.

Important points here are:

1. The advanced seal has high gas film stiffness compared to the original aspirating seal.
2. The 36” seal designed for the GE CRD rig has a slightly improved gas film stiffness due to the space limits of the existing rig rotor.
3. The 36” seal for GE-90 space envelope does have a significant gas film increase as compared to the original aspirating seal.
4. Steep slopes for “Force vs. Clearance” is desirable as this will provide the largest restoring force to keep the seal in equilibrium.
5. Large variations in rotor runouts can be accommodated if seals have high gas film stiffness.
6. Advanced aspirating seals have identical leakage and film gap characteristics compared to the original seal.

Seal Features - 14.7" Advanced Seal



Stein Seal Company
ISO-9001 Certified

NASA Seal Workshop - October 2000

The photographs show the 14.7" aspirating seal features
Material: 410 stainless steel

14.7" Aspirating Seal Comparisons



Seal Dam:	.250"	0.100"
Bearing pad:	1.250"	0.400"
Orifice dia.:	0.051"	0.053"
# Orifices/ Row:	60	60
# Row of Orifices:	Double row	Single Row
Trench width:	0.450"	0.150"



Stein Seal Company
ISO-9001 Certified

NASA Seal Workshop - October 2000

This slides shows the features of the advanced and original aspirating seals.

Rig Tests Performed

1. Gas Bearing Static Tests
2. Gas Film Calibration / Verification
 - Establish film clearance at operating pressure
3. Performance Mapping
 - Static/Dynamic tests
 - Speed and Pressure traverses
4. Rotor Runout Tests
 - 5 mil & 10 mil rotor (one per rev)
5. Flight Cycle Tests
 - GE-90 Conditions
6. Sand Ingestion (Original Seal)
 - 0 to 10 micron particle size, 1/3000 lb/sec flow rate



Stein Seal Company
ISO-9001 Certified

NASA Seal Workshop - October 2000

The rig test series is described in this slide.

The static gas bearing rig is a small sub-scale rig (~ 4" dia.) that is used solely for gas bearing testing. This affords quick part change-out that yields performance curves for various bearing configurations.

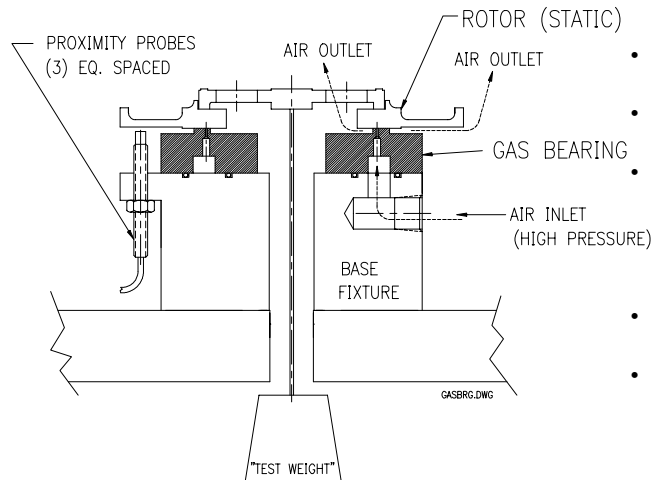
The dynamic rig is capable of testing the 14.7" aspirating seal to the conditions of the full size 36" seal parameters. Hot tests were not conducted on this rig.

Gas film calibration tests are used to assess the leakage performance with fixed film clearances between the rotor and seal face. Clearances are achieved by the use of shim stock material that is cemented to the rotor face at equidistant positions.

Rotor runout tests are performed to simulate gas turbine rotor whirl on a "one per rev" cycle.

Proximity probes measure the gas film clearance. Seal leakage is also measured on both static and dynamic test rigs.

Static Gas Bearing Rig



- Features the Gas Bearing portion of the seal (F_g)
- Test weight simulates the seal closing force (F_c)
- Tests provide data for Pressure vs.:
 - Leakage
 - Film clearance
 - Load capacity
- Data used to validate NASA GFACE code
- Sub-scale rig permits quick bearing change-outs for alternate bearing faces:
 - Multiple orifice rows
 - Orifice hole size and spacing



Stein Seal Company
ISO-9001 Certified

NASA Seal Workshop - October 2000

Static gas bearing test rig for sub-scale testing.

The rig is used to collect information such as:

Leakage vs. pressure

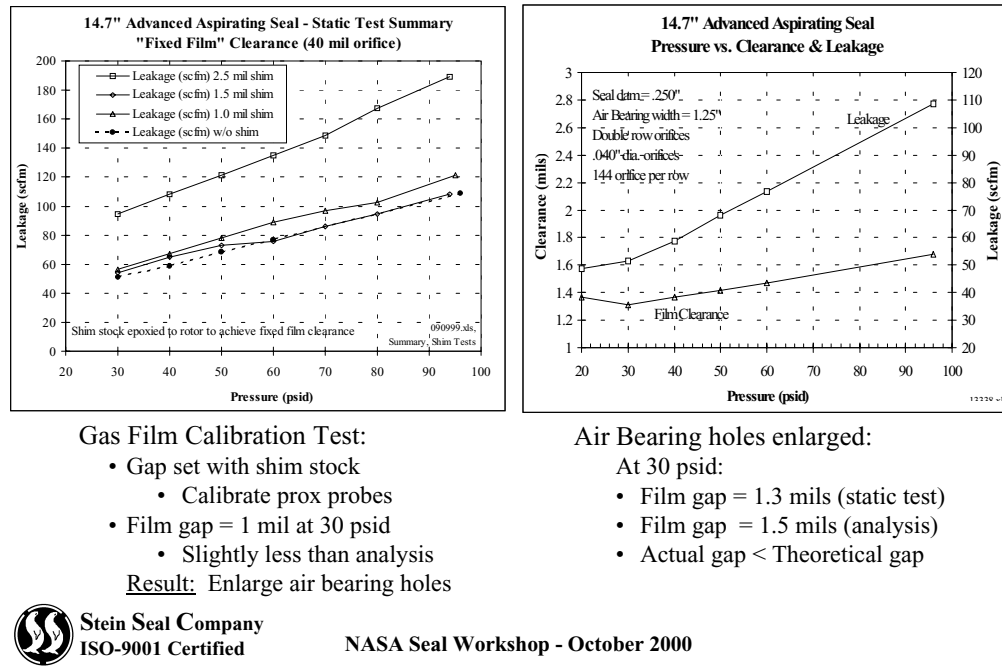
Film clearance vs. pressure

Proximity probes measure the gas film clearance.

Gas flows into the fixture and exhausts on either side of the gas bearing face. The test weight simulates the seal closing force at the rated pressure differential.

The data from this rig is used to correlate the NASA GFACE seal code.

Static Test Results – Advanced Seal



The two graphs represent the 14.7" seal performance on the dynamic test rig. Leakages include the primary face seal and the piston rig secondary seal.

Both graphs represent Pressure Differential vs. Seal leakage.

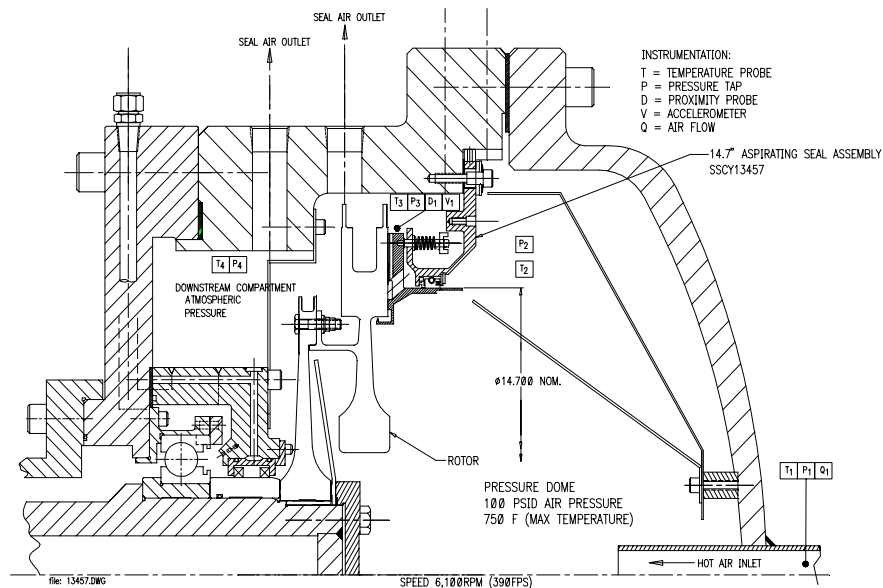
Left graph

This graph shows the seal leakage for the "fixed film" calibration tests. The solid lines represent the "fixed film" performance, while the dotted line represents the seal performance allowing the seal to float at its equilibrium point. In this graph, the film clearance is slightly less than 1 mil, running parallel to the 1 mil "fixed film" clearance test curve. The conclusion of this test shows that the actual film clearance is less than the theoretical film clearance for the same given pressure. The result of this test lead to an enlarged air bearing hole diameter, which will permit the seal to operate at a larger film clearance.

Right graph

This graph shows that the seal performance with enlarged air bearing holes (.040" dia.). The gas film clearance is approximately 1.3 mils at 30 psid. The analysis shows the gap is 1.5 mils at 30 psid, therefore, the analysis overstates the film clearance.

Dynamic Test Rig - 14.7" Aspirating Seal



Stein Seal Company
ISO-9001 Certified

NASA Seal Workshop - October 2000

During operation the high pressure air enters the rig pressure dome through the air inlet pipe at the far right side. At 0 psid the seal is retracted open by mechanical springs, pulling the seal away from the rotor leaving a .090" gap. As pressure builds to approximately 3 to 4 psid, the seal is aspirated closed towards the rotor, overcoming the retraction spring force and piston ring friction force. The gas film is established between the rotor and seal face: 1.5 to 2.5 mils.

Test conditions:

Shaft speed: 6,100 rpm (390 fps)

Pressure differential: 100 psid

Temperature: ambient

Instrumentation includes:

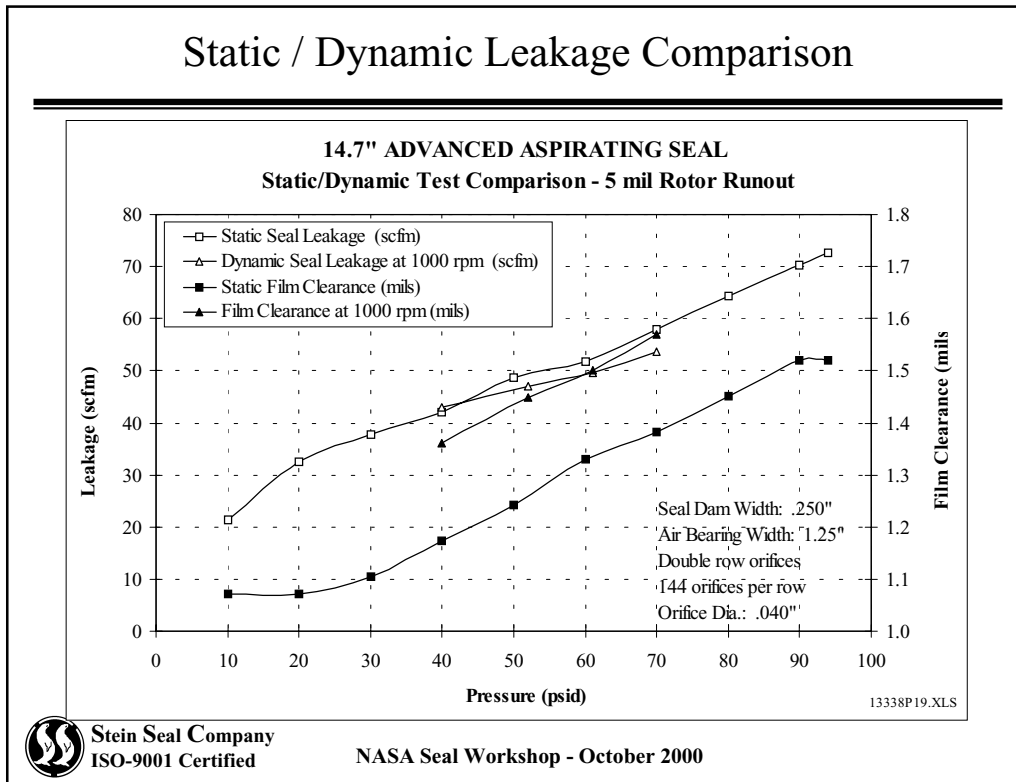
- (3) proximity probes (gas film measurement), mounted on the seal and aimed at the rotor tip face
- (1) Accelerometer (mounted on seal to measure axial displacement caused by rotor runout)
- (2) Accelerometers mounted on rig bearings for rig monitoring

Various thermocouples for dome temperature, surrounding rotor temperature, bearing oil sump temps., etc.

Various pressure taps for dome pressure, bearing oil pressure, etc.

Rotameter: seal leakage

Static / Dynamic Leakage Comparison



This graph depicts the static and dynamic seal performance for Pressure vs. Leakage and Film clearance. The shaft speed for the dynamic test was 1,000 rpm (65 ft./sec.)

Leakage and film clearance are closely matched for static and dynamic test conditions.

The rotor face runout during the dynamic test was 5 mils.

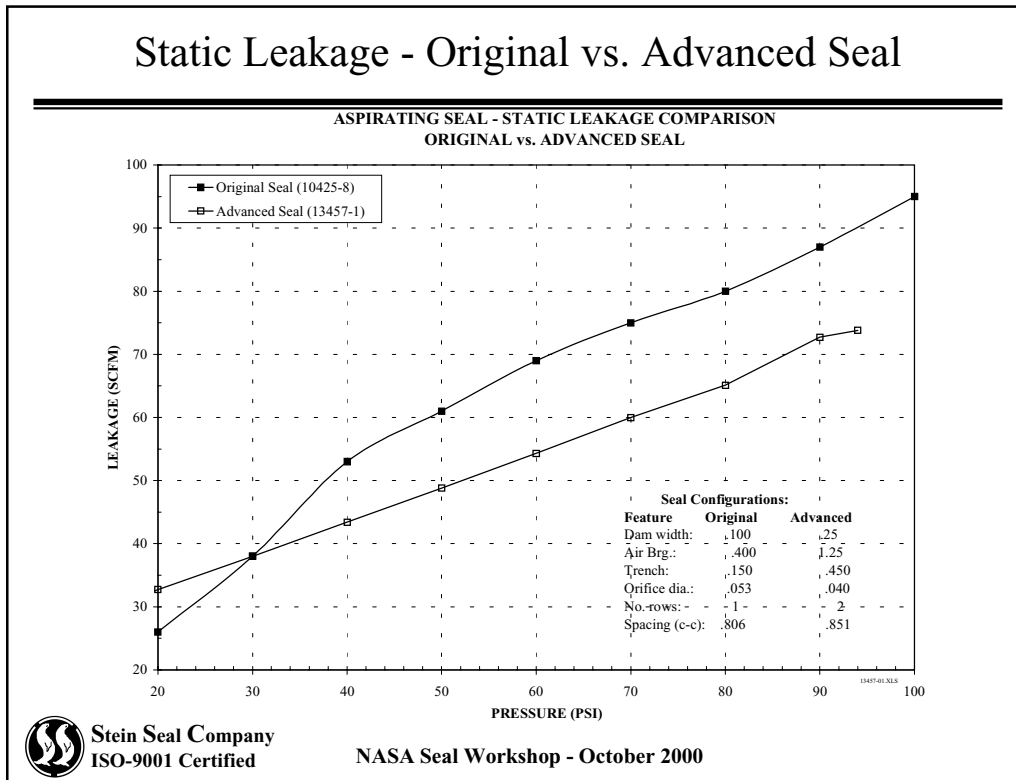
The results of the test demonstrate that the seal performance is very close to the analysis for film clearance measurements.

Test: 1.1 mils (static test @ 30 psid)

1.3 mils (dynamic @ 30 psid & 1,000 rpm, interpolated film clearance)

Analysis: ~ 1.5 mils (30 psid)

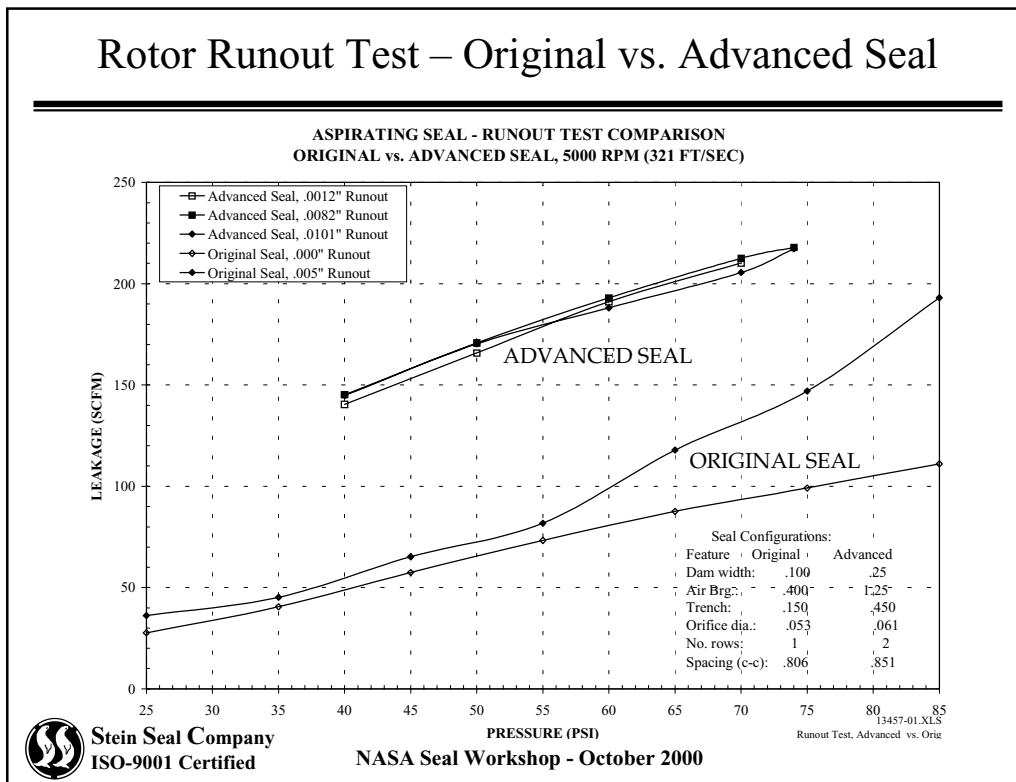
Static Leakage - Original vs. Advanced Seal



This graphs depicts the Pressure vs. Leakage for the Original and Advanced aspirating seals.

The significance of this graphs demonstrates that the improved gas film stiffness does not affect the seal leakage or gas film clearance performance. Yes, there is a seal leakage difference between the two curves shown above, however, enlarging the air bearing holes in the advanced seal will make the seal operate with a slightly higher film clearance, hence, increasing the leakage.

Rotor Runout Test – Original vs. Advanced Seal



This Pressure vs. Leakage graph depicts the dynamic seal performance with rotor runout for both the Original and Advanced seals. The shaft speed for the dynamic test was 5,000 rpm (321 ft./sec.)

Advanced Seal

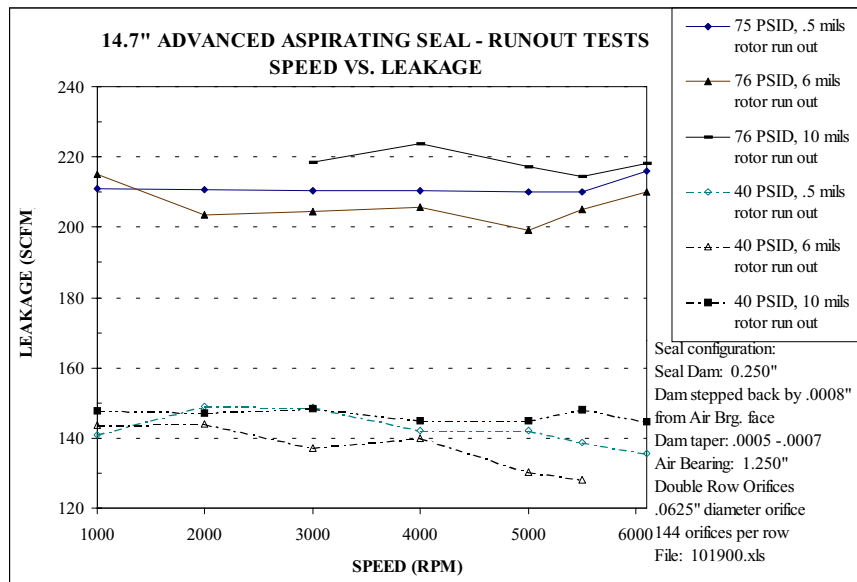
Leakage (and film clearance) are closely matched for the dynamic test conditions with all three runouts: 1 mil, 8 mil, and 10 mil. The seal performed successfully during all dynamic conditions. Follow-on tests included successful tests at the max 6100 rpm speed.

Original seal

The original seal has somewhat varied leakage rates for the 0 mil and 5 mil rotor runout tests. The 5 mil runout test is characterized by higher leakages as air pressure increases. The seal may not be fully tracking the rotor at the 5 mil runout case. Attempts to run 10 mil rotor runout was unsuccessful as the seal rubbed the rotor face.

The results of the test demonstrate that the Advanced seal with higher gas film stiffness permits higher rotor runouts as compared to the Original seal.

Rotor Runout Test - Advanced Seal



Stein Seal Company
ISO-9001 Certified

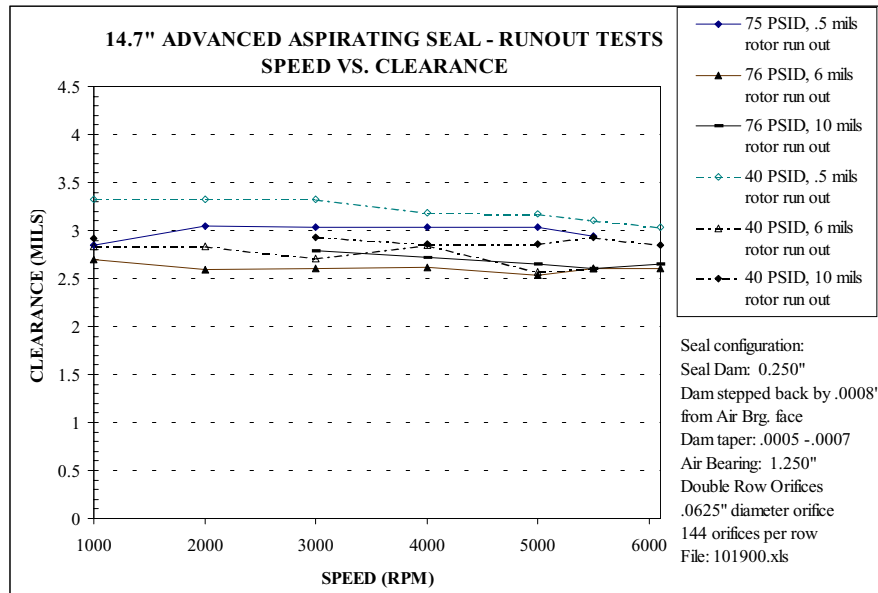
NASA Seal Workshop - October 2000

This graph depicts the rotor runout results for two pressure points: 40 psid and 76 psid. The leakage is plotted against increasing rotor speed.

Results show that seal leakage is slightly influenced by increasing rotor runouts.

The seal tracked the rotor successfully with 10 mil rotor runouts.

Rotor Runout Test - Advanced Seal



Stein Seal Company
ISO-9001 Certified

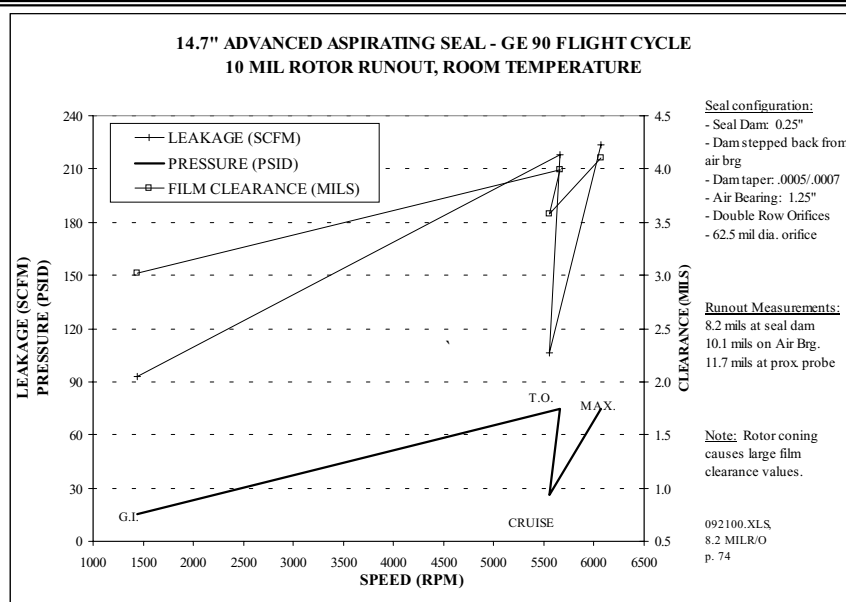
NASA Seal Workshop - October 2000

This graph depicts the rotor runout results for two pressure points: 40 psid and 76 psid. The gas film clearance is plotted against increasing rotor speed.

Results show that film clearance is slightly influenced by increasing rotor runouts.

The seal tracked the rotor successfully with 10 mil rotor runouts.

Flight Cycle Results

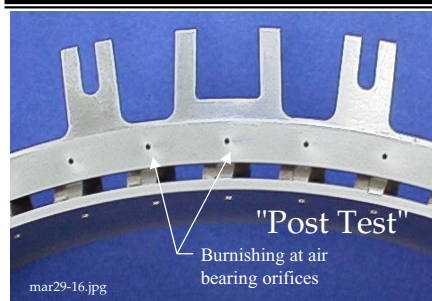


Stein Seal Company
 ISO-9001 Certified

NASA Seal Workshop - October 2000

This graph depicts seal performance during a GE-90 flight cycle (room temperature). Three cycles were performed successfully without any problems.

Sand Ingestion Test - Original Aspirating Seal



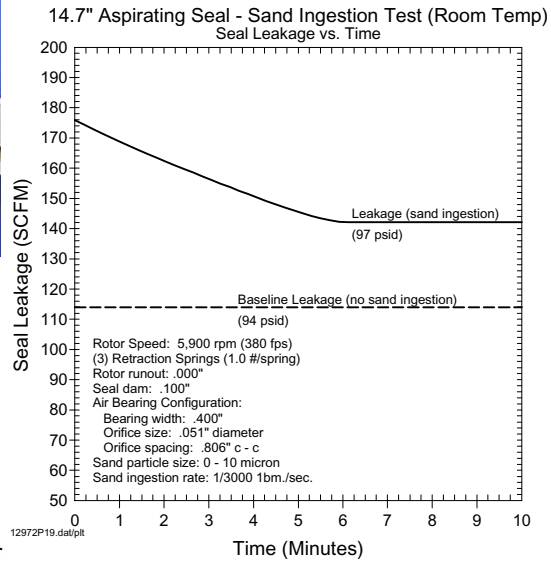
Test Conditions:

- Sand delivered at:
 - 1/3000 lb./sec.
 - 10 micron particle size
- 5,900 rpm (380 fpm)
- 97 psid
- No measurable damage to seal or rotor



Stein Seal Company
ISO-9001 Certified

NASA Seal Workshop - October 2000



The sand ingestion was performed on the Original Aspirating Seal with good results. (This test was performed in 1995)

The sand was delivered into the test head for ten minutes at 1/3000 lbm/sec at 97 psid pressure differential.

The leakage at the onset of sand was approximately 54% higher than the leakage for a test without sand ingestion. As time passed, the leakage settled lower to approximately 24% higher than a seal without sand ingestion.

No damage was noted to the seal faces or orifice holes. It is noted that burnishing did occur near the orifice holes and on the rotor face. Slight burnishing appeared on the seal dam.

Summary

- Seal performance is predictable
- Seal operated successfully to:
 - 392 ft/sec (goal: 392 ft/sec)
 - 96 psid* (goal: 100 psid) * compressor limit
 - 10.1 mil Runout (goal: 10 mil)
 - Room temp. (goal: 750 °F)
- Seal performed flawlessly during extreme conditions
 - Rotor Runouts (5 & 10 mil runout) and Rotor Coning
 - Sand Ingestion (1/3000th lbm/sec)
 - Engine Cyclic Tests (at max rotor runout condition)
- Seal is ready for engine test



Stein Seal Company
ISO-9001 Certified

NASA Seal Workshop - October 2000

Seal performance is predictable, uniform, and validates the seal codes employed in the aspirating seal design. CFD is a valuable tool in the design of the aspirating seal to determine if the rotor flow diverter is required. CFD correlated the Stein and NASA GFACE seal codes.

Successful dynamic tests proved the Advanced Seal can perform at extreme rotor runout (10 mils), engine flight cycles, and sand ingestion.

The aspirating seal is an ideal alternative to labyrinth or brush seal replacement in gas turbine secondary flow path. The seal operates in high pressure, high temperature, and high speed conditions.

The aspirating seal leakage is an order of magnitude less than the labyrinth or brush seals.

The aspirating seal life can be infinite due to its non-contacting performance.

Unlimited seal life will afford the engine manufacturers an extended time between overhauls and reduce costly engine teardowns as currently experienced with labyrinth and brush seals.

Engine integration is the next planned task and is targeted for the GE-90 engine.

DEVELOPMENT OF HIGH MISALIGNMENT CARBON SEALS: OVERVIEW

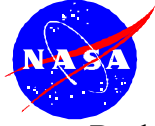
Lou Dobek
Pratt & Whitney
East Hartford, Connecticut



**2000 NASA Seal/Secondary Air System Workshop
October 25-26, 2000
NASA Glenn Research Center
Cleveland, OH 44135**

Development of High Misalignment Carbon Seals (UEET)

Lou Dobek



High Misalignment Carbon Seals

Background

Advanced Commercial Engines will be subjected to extreme conditions such as:

- High angular and radial seal misalignments
 - Gyroscopic loads - angular misalignment
 - Sun input gear orbiting - radial/eccentric misalignment
- Higher LPC shaft speed; ~10,000 RPM
- Large Diameter Fan Hub

Seals capable of accomodating high misalignment levels, high rubbing speeds, low pressure differentials and large diameters must be developed

Background information on principal causes of extreme conditions in Advanced Commercial Engines. Such conditions impose on seals high misalignment, high rubbing speed, large diameters and low pressure differentials.



High Misalignment Carbon Seals

FY 00 Objectives:

- Demonstrate feasibility of new seal designs for advanced engine environments
- Enabling technology for Geared Fan Engine

High Misalignment Seal - determine misalignment capabilities of existing circumferential segmented seals and develop design(s) to meet requirements.

Other industry applications

benefiting from new seal technology

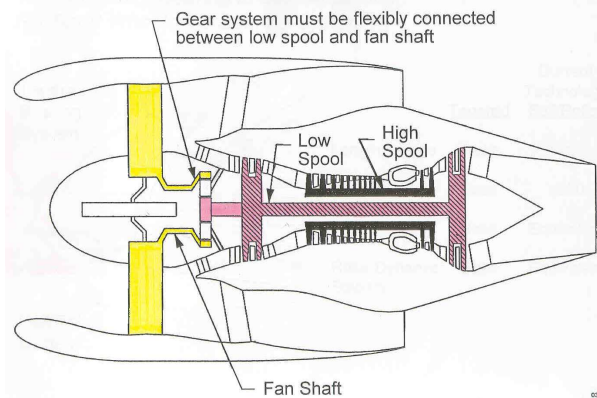
- F119 - Circumferential segmented seal employed
- Higher thrust GTF to use a 16" diameter seal
- High speed high misalignment seal applications
- Other aircraft engine manufacturers will see improved background in today's size, speed and misalignment seal capabilities

Overview of FY'00 objectives: start development of the high misalignment seal with baseline testing. Other possible industry beneficiaries of improved seal technology are also listed.



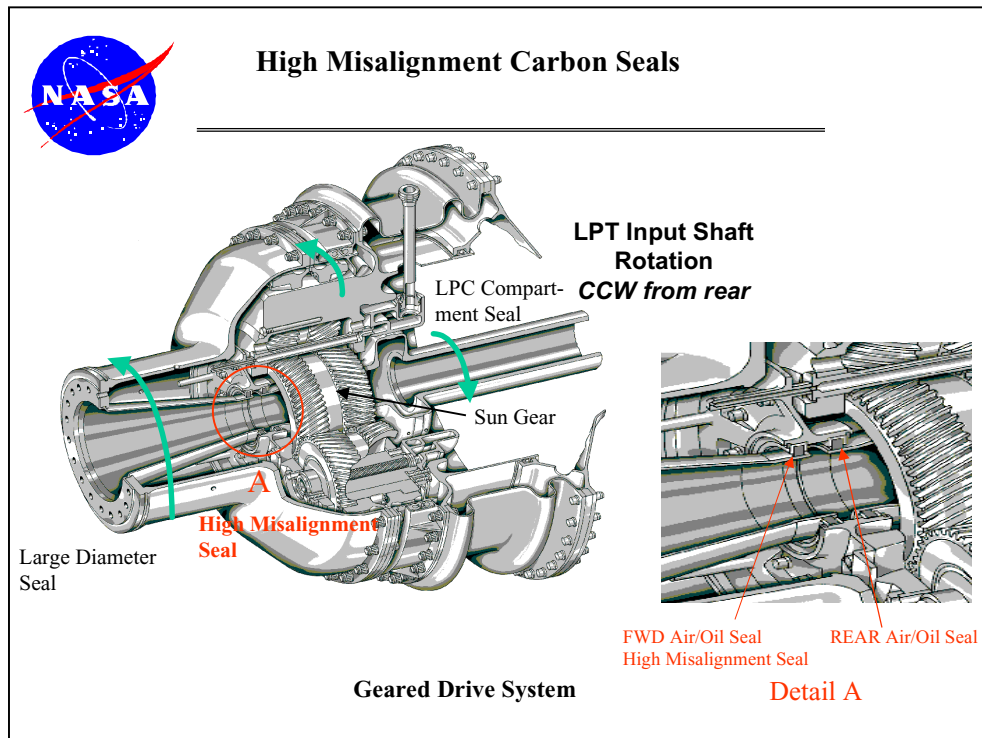
High Misalignment Carbon Seals

GTF



Geared Turbo Fan Schematic

Sketch of Geared Turbo Fan position and connection to the rest of the engine. Input shaft to GTF is connected to LPC shaft and the GTF output shaft is connected to the fan shaft.



Cutaway 3D sketch of the Geared Drive showing location of misalignment seal.

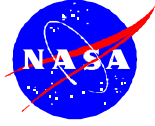


High Misalignment Carbon Seals

	FWD. AIR/OIL SEAL	REAR AIR/OIL SEAL	FDGS/LPC COMPARTMENT SEAL	FDGS COMP. FWD SEAL
Required Life (hours)	30,000	30,000	30,000	30,000
Delta P (psi)	<50	<50	40-50	~0
Surface Speed (ft/s)	50	129	380	200
Buffer Air Supply Temperature (deg. F)	350	350	415	
Angular Misalignment (deg)	0.5	0.2	0.1	
Eccentricity (inches)	0.005	0.02	0.005	
Sealing Diameter (inches)	2.95	2.95	8.7	16
Type	Segmented/ bellows/ other	Segmented/ other	Segmented/ ring/ other	Segmented/ Face/ Cartridge

Seal Operating Conditions

Seal operating conditions (required life, pressure differentials, speeds, misalignment levels and others). Critical requirements are highlighted.



High Misalignment Carbon Seals

Misalignment Seal Test Rig Program

Technical Approach

Pratt & Whitney selected Stein Seal as the seal vendor.

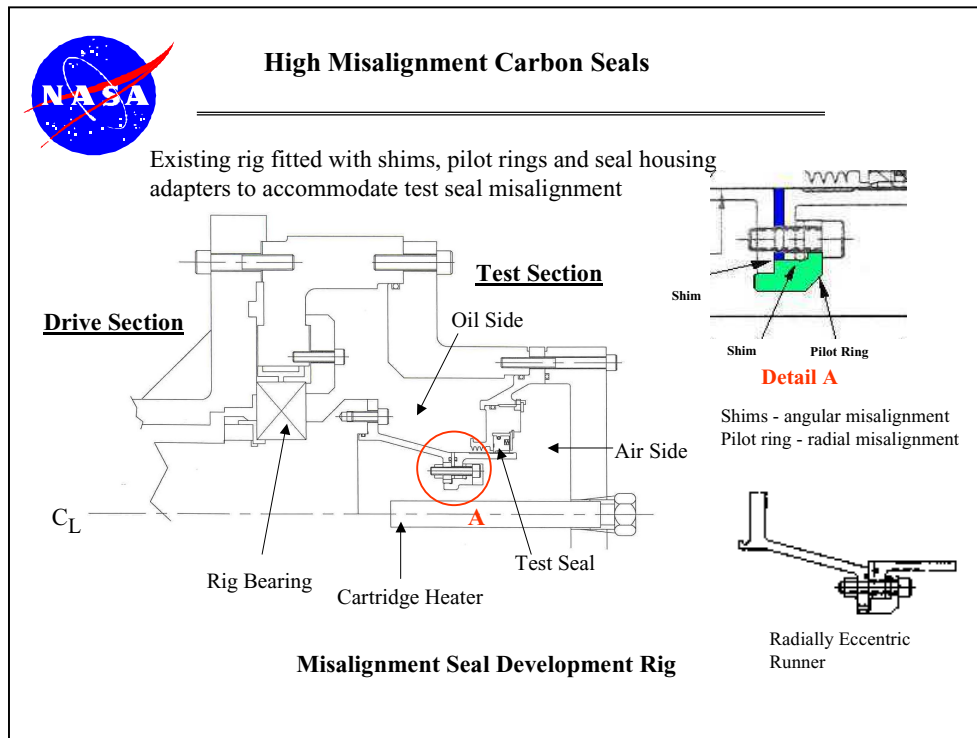
Testing at supplier's facilities.

- Step 1- Start with "baseline" seal with 0.020 in. shaft clearance.
Carbon grade: Carbone JP1000 - high strength, low modulus.
Testing in this phase will not include endurance.
Misalignment level increased in steps.
- Step 2 - Modify baseline seal to attain 0.040 in. shaft clearance.
- Step 3 - Increase shaft clearance to 0.060, 0.080, 0.1 in.

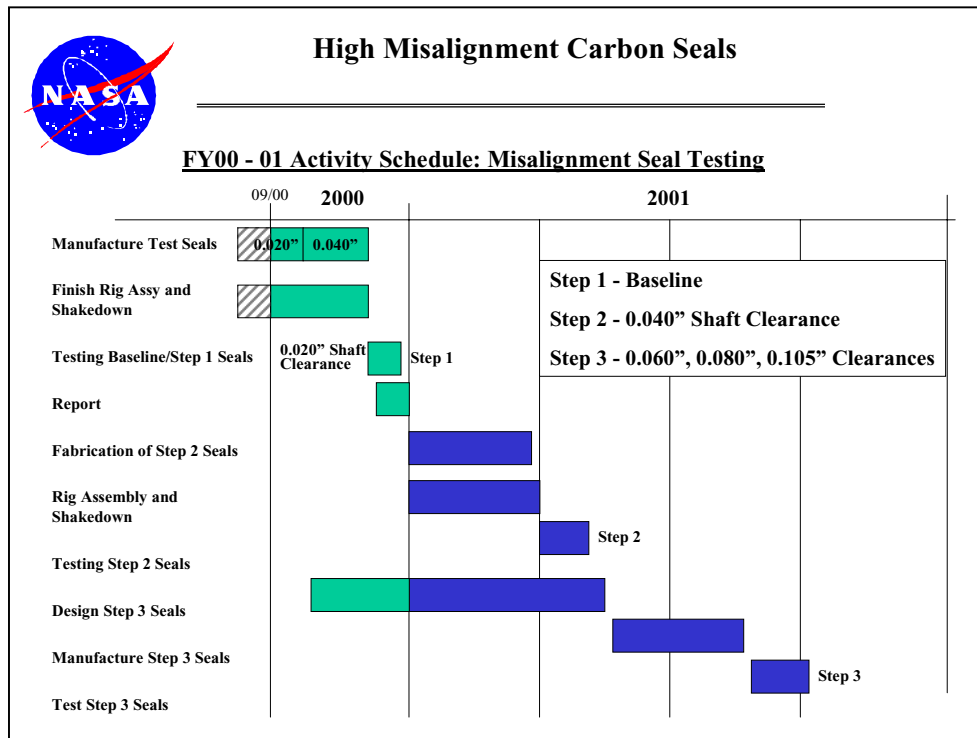
Backup plan in case carbon fails includes seal re-design and testing.

- Two backup design schemes being examined.
- Alternative carbon grade being considered.

Technical approach of misalignment seal development program. Three main steps will be followed starting from a "baseline" seal testing.



Sketch of misalignment seal rig. Simulation of angular and radial misalignment achieved by means of shims and pilot rings tilting and translating seal runner.



Activity schedule for FY'00 and FY'01. Three main steps needed to develop high misalignment carbon seals for the GTF application.

DEVELOPMENT OF HIGH MISALIGNMENT CARBON SEALS: DESIGNS

George Szymborski
Stein Seal Company
Kulpsville, Pennsylvania

Development of High Misalignment Carbon Seals (UEET)

George Szymborski



Stein Seal Company



Seal Selection

- TYPES CONSIDERED
 - Segmented circumferential seal
 - Face seal
- CONSIDERATIONS
 - Seal mass
 - Must operate with high inertia loads
 - Strength
 - Ability to survive potential high impact loads
 - Flexibility
 - Conformance to rotating surface



Stein Seal Company



This slide describes seal selection.
Only contact seals were considered.

Segmented Circumferential Seal Chosen

- Low seal mass
 - Small cross-section made of light weight carbon material
- Conformability to shaft
 - Segmented design allows better tracking
- Simple design
 - No secondary seal with this design



Stein Seal Company



This slide discusses selection of the segmented circumferential seal. Historically face seals have large sections, thus greater mass. A face type seal requires a secondary device which could complicate operation at high misalignment.

MATERIAL SELECTION

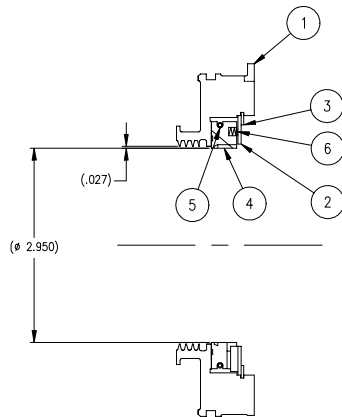
- DESIRED PROPERTIES
 - High strength
 - Low elastic modulus
- CARBONE JP1000 SELECTED
 - Of the materials considered, **CARBONE JP1000** has the combination of **high flexural strength** and **low elastic modulus**



Stein Seal Company



An alternative material is a carbon-carbon type with very high strength in one direction and low modulus. Stein has no experience with this material.



ITEM REQ'D	PART NO.	DESCRIPTION	MAT'L.	MAT'L. SPEC
6	12	SSCY2645CS	COMPRESSION SPRING	INCO X-750 AMS 5698
5	1	SSCY13804-17	GARTER SPRING	INCO X-750 AMS 5698
4	1	SSCY13804-11	CIRCUMFERENTIAL SEAL RING	C-GPH JF1000
3	1	SSCY81001-393	RETAINING RING	302 SST -
2	1	SSCY13804-27	BACKPLATE	17-4 PH AMS 5643
1	1	SSCY13804-21	SEAL HOUSING	17-4 PH AMS 5643

LIST OF MATERIALS

← SHAFT ROTATION TO BE
 CLOCKWISE
 WHEN VIEWED FROM THIS DIRECTION

NOTES:

1. THIS ASSEMBLY, WHEN ASSEMBLED ON A 2.950-2.949 DIA RUNNER, MUST NOT LEAK IN EXCESS OF 0.50 SCFM AT 35 ±1 PSIG AIR PRESSURE.



Stein Seal Company



NASA/UEET GTF Shaft Seal Considerations

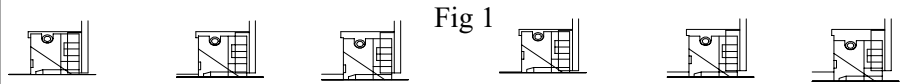


Fig 1

<ul style="list-style-type: none"> •Up to a .027 radial clearance between housing & shaft. •Max radial movement to be .022 <p>Normal design practice used for baseline testing</p>	<ul style="list-style-type: none"> •Up to a .047 radial clearance between housing & shaft. •Max radial movement to be .042 <p>Within normal design practice except face dam increased</p>
---	--

<u>ADVANTAGES</u>	<u>DISADVANTAGES</u>
<ul style="list-style-type: none"> •Simple design •Least costly •Requires less space than other designs 	<ul style="list-style-type: none"> •High garter spring load •Joint wear (at .047" radial clearance) •Larger face and bore dam widths •Lock slot and key wear •Higher heat generation •Higher bore wear

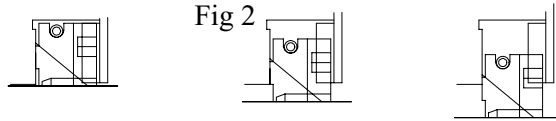


Stein Seal Company



This slide discusses the baseline seal for this program and lists its advantages and disadvantages. The seal has a longer than normal tongue and socket but is within current design practice.

NASA/UEET GTF Shaft Seal Considerations



- Up to a .110 radial clearance between housing & shaft.
- Max radial movement to be .105

Beyond normal design practice

Must look at:

1. Joint overlap must increase
2. Joint gap must be increased
3. Lock slot clearance must be increased
4. Bore and face dam must be increased
5. Undercut face dam in ID

Concerns

1. Joint wear
2. Lock slot wear
3. Extension spring movement
4. Compression spring

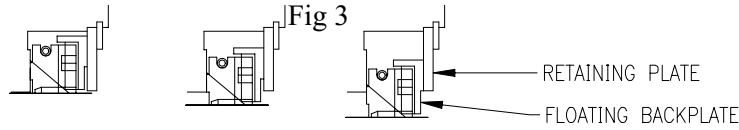


Stein Seal Company



This slide discusses the effect of trying to use current design practice for large shaft misalignments. There are too many concerns that are difficult to address and the configuration is not being considered.

NASA/UEET GTF Shaft Seal Considerations



New design concept – Floating (counter bored) backplate up to a .110 radial clearance between housing & shaft. Max radial movement to be .105
 •Eliminates joint, lock slot, spring movement concerns

Must look at:

- Anti rotation of floating backplate
- Friction between plates
- Face and bore dams must be increased
- Material for plates

ADVANTAGES

- Normal tongue and sockets to decrease breakage potential
- Normal tongue and socket gap
- Minimal joint wear
- Requires less space than Figure 4
- Minimal lock slot and key wear

DISADVANTAGES

- High garter spring load
- Complex, unproven backplate design
- More costly
- Larger face and bore dam widths
- Higher heat generation
- Higher bore wear

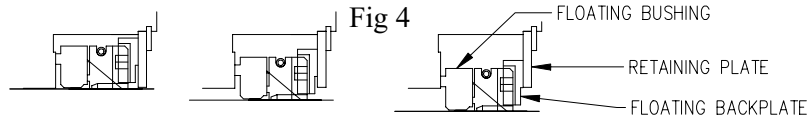


Stein Seal Company



This slide describes the design to be used for radial clearances above .040". To minimize inertia effects, light weight materials for the floating backplate will be evaluated. Hardenable material or hard coated surfaces will be considered to reduce friction between the floating backplate and retaining plate.

NASA/UEET GTF Shaft Seal Considerations



New design concept – Floating (counter bored) backplate and floating bushing up to a .110 radial clearance between housing & shaft.

- Max radial movement to be .105
- Allows for near normal segmented seal design
- Must look at:**
 - Anti rotation of floating backplate
 - Friction between plates
 - Material for bushing and plates

ADVANTAGES

- Normal circum. seal ring design
- Normal garter spring design
- Normal tongue and sockets to decrease breakage potential
- Normal tongue and socket gaps
- Minimal joint wear
- Normal size face and bore dam widths
- Less bore wear and heat generation
- Minimal lock slot and key wear

DISADVANTAGES

- Complex design
- Backplate design unproven
- More costly
- Ceramic floating bushing
- Floating bushing unproven in aerospace applications
- Requires more space than other designs



Stein Seal Company



This slide describes an alternative design for the large clearances in this application. Addition of the floating bushing allows the segmented seal to operate as a normal clearance device. Stein has used floating bushings in industrial applications.

FINGER SEAL DEVELOPMENT FOR A COMBUSTOR APPLICATION

Arun Kumar
Honeywell Engines & Systems
Phoenix, Arizona

Finger Seal Development for a Combustor Application

presented at

**NASA Seal/Secondary Air System Workshop
NASA Glenn Research Center
Cleveland, Ohio**

by

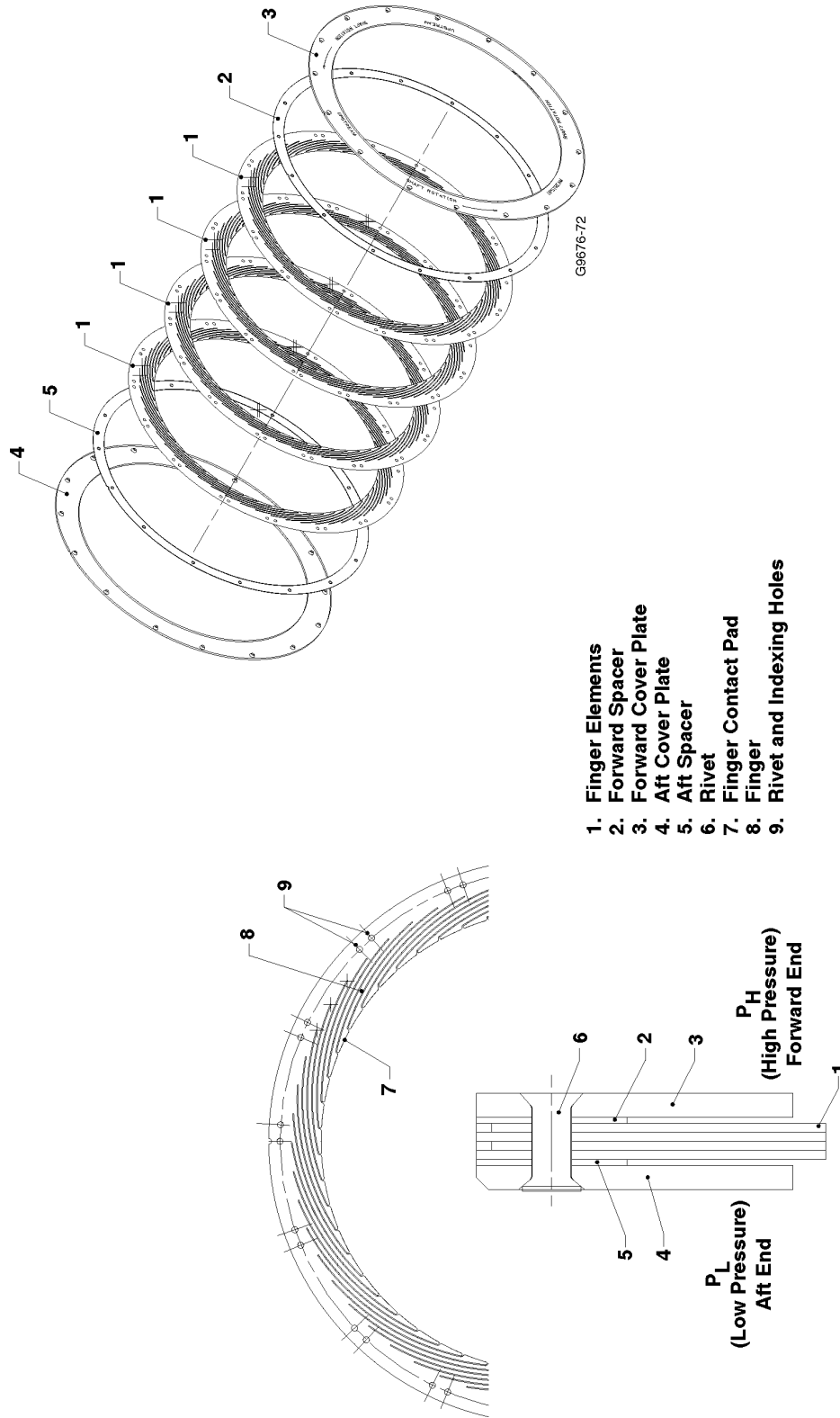
Arun Kumar
Honeywell Engines & Systems
Phoenix, Arizona

Work presented was partially supported by the Naval Air Warfare Center
under Contract No. N00421-97-C-1049

Honeywell

Seal/Secondary Air System Workshop, 25-26 Oct 2000,
NASA Glenn Research Center, Cleveland, Ohio.

Finger seal laminate stack design ...

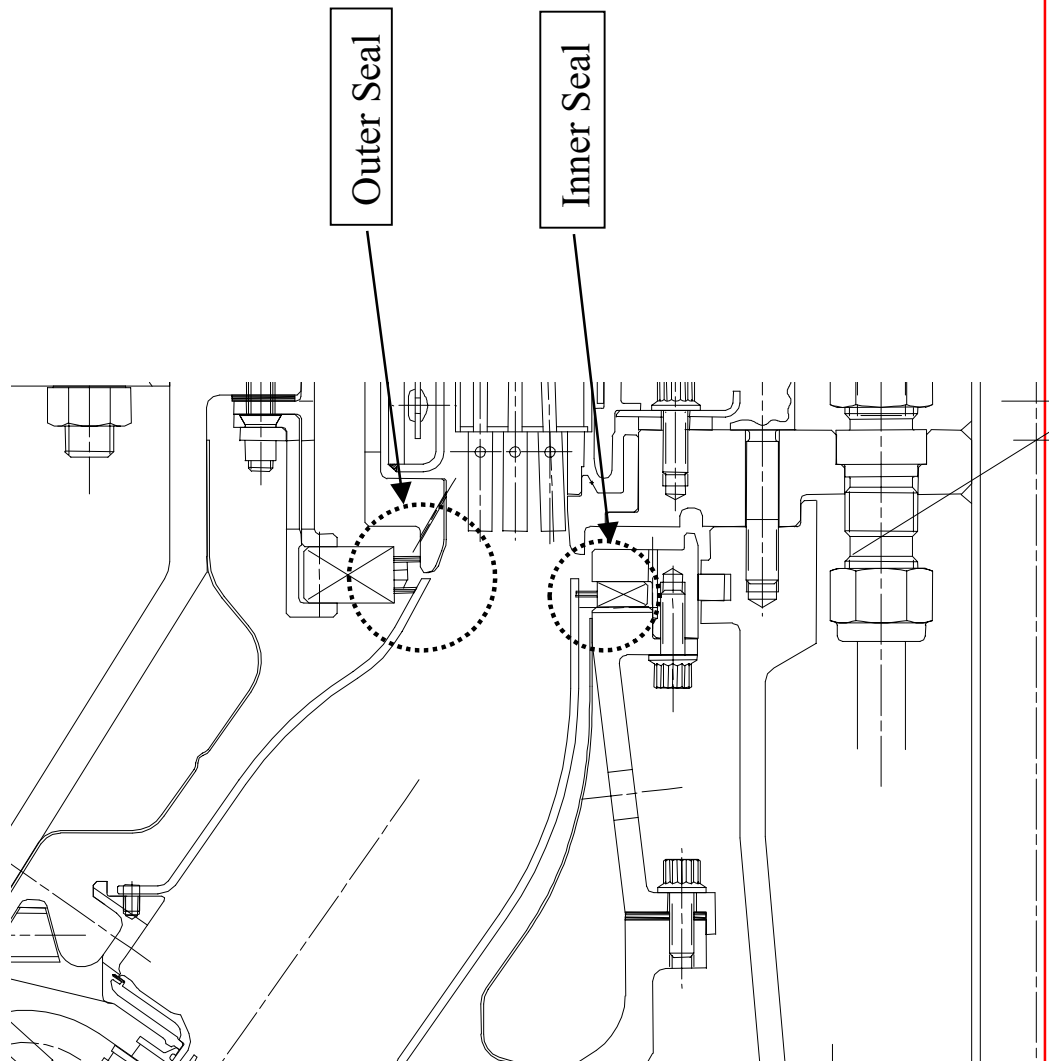


... leads to low manufacturing cost

Honeywell

Seal/Secondary Air System Workshop, 25-26 Oct 2000,
NASA Glenn Research Center, Cleveland, Ohio.

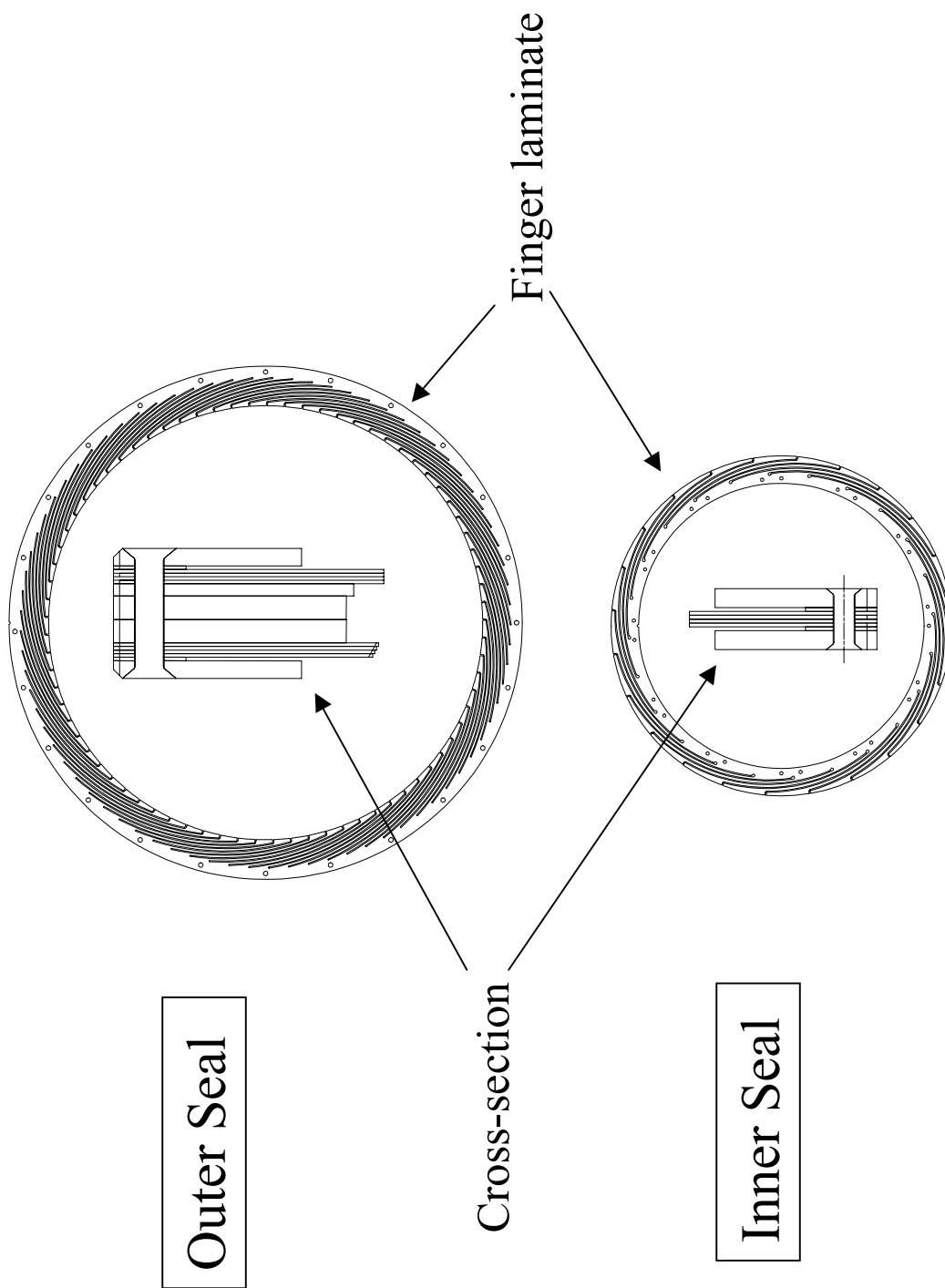
Engine Layout showing Seal Locations



Honeywell

Seal/Secondary Air System Workshop, 25-26 Oct 2000,
NASA Glenn Research Center, Cleveland, Ohio.

Seal cross-section and laminates



Honeywell

Seal/Secondary Air System Workshop, 25-26 Oct 2000,
NASA Glenn Research Center, Cleveland, Ohio.

Design Requirement

Engine Requirement

- 6,000 hours operational life
- 7,500 LCF cycles for hot parts

Finger Seal Requirement

- Low radial force applied on CMC combustor liner under all conditions
- Radial deflection capability as below :

	Radial Deflection		
	Build	Steady State	Max Transient
Outer seal (without combustor offset)	0.002"	0.032"	0.044"
Inner Seal (without combustor offset)	0.050"	0.028"	0.015"

Honeywell

Seal/Secondary Air System Workshop, 25-26 Oct 2000,
NASA Glenn Research Center, Cleveland, Ohio.

Finger seal material

Materials being considered

- AS800 mono-ceramic (Silicon Nitride)
- MA-956 (Fe based high temperature superalloy, high creep resistance,)
- Haynes-188 (Co based high temperature superalloy, good oxidation resistance)

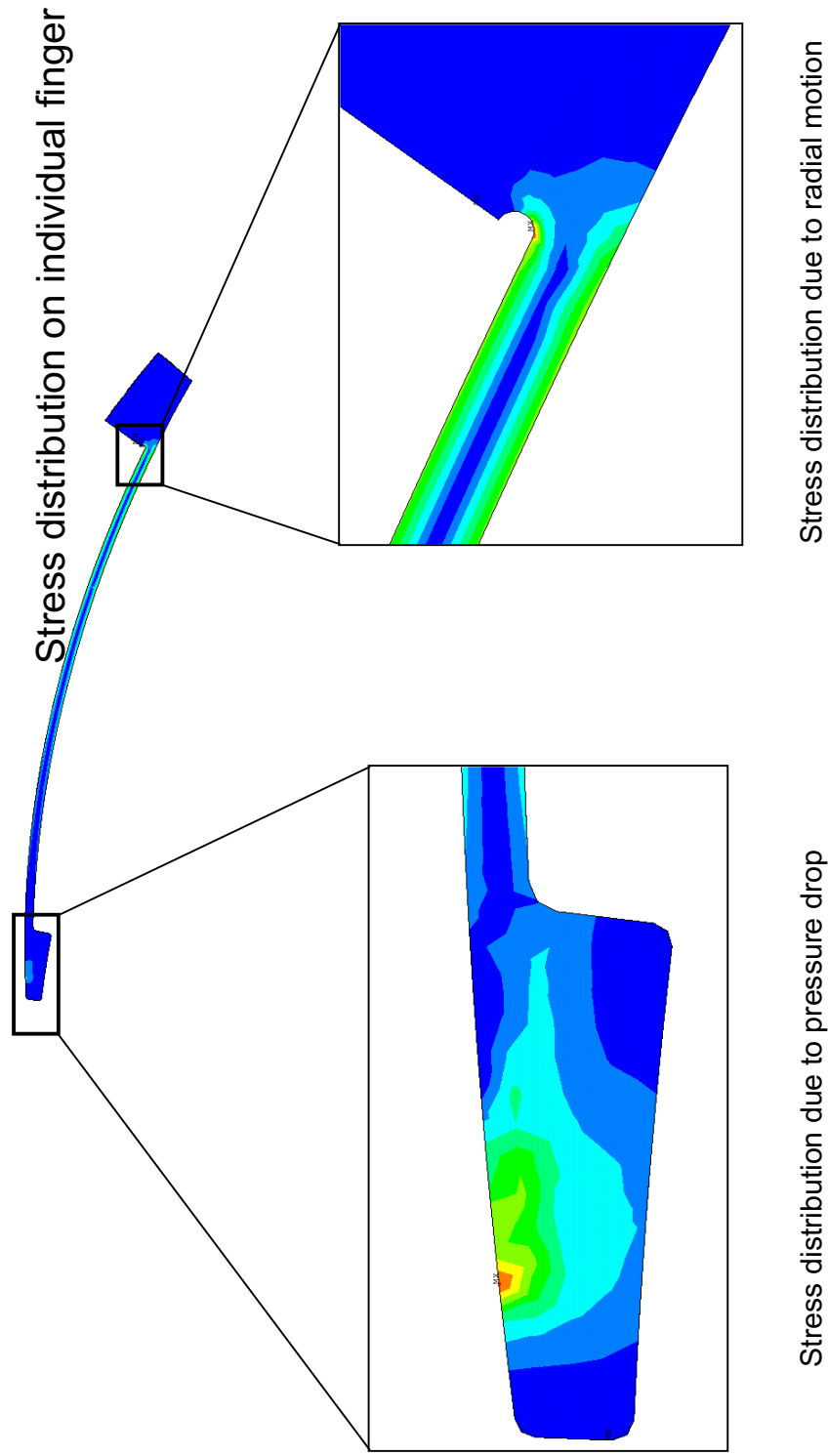
Materials used for the test

- MA-956 for inner seal
- Haynes-188 for outer seal

Honeywell

Seal/Secondary Air System Workshop, 25-26 Oct 2000,
NASA Glenn Research Center, Cleveland, Ohio.

Finite Element Analysis was used...

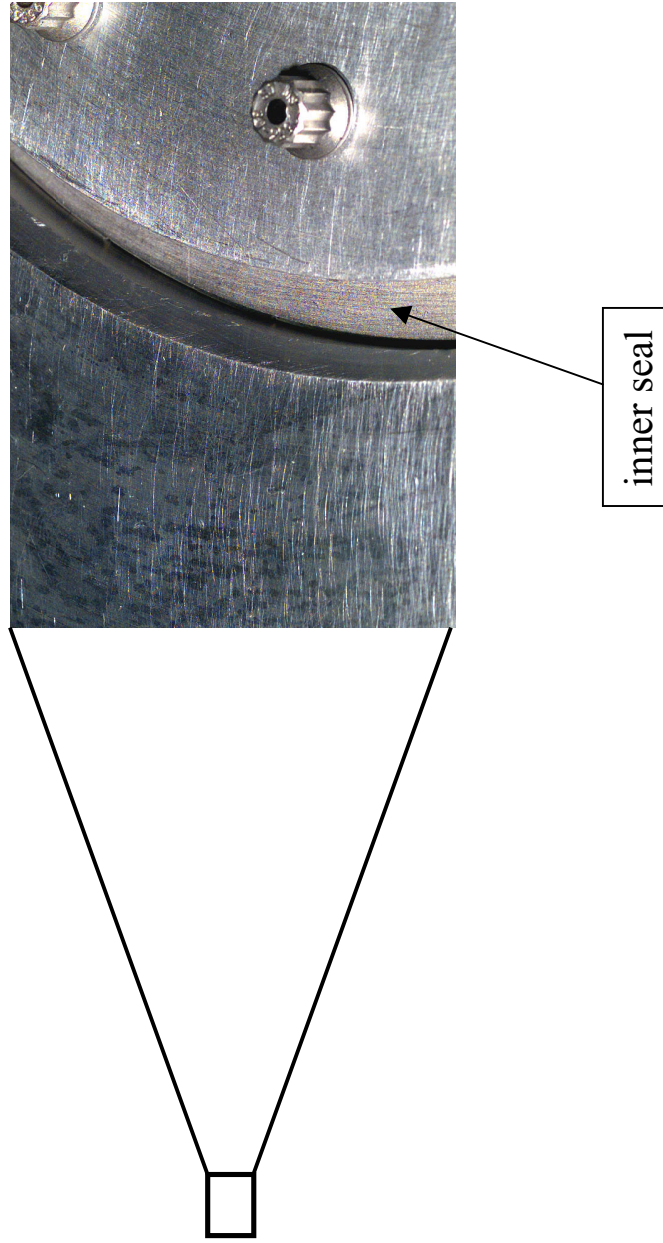


... to ensure meeting design requirements

Honeywell

Seal/Secondary Air System Workshop, 25-26 Oct 2000,
NASA Glenn Research Center, Cleveland, Ohio.

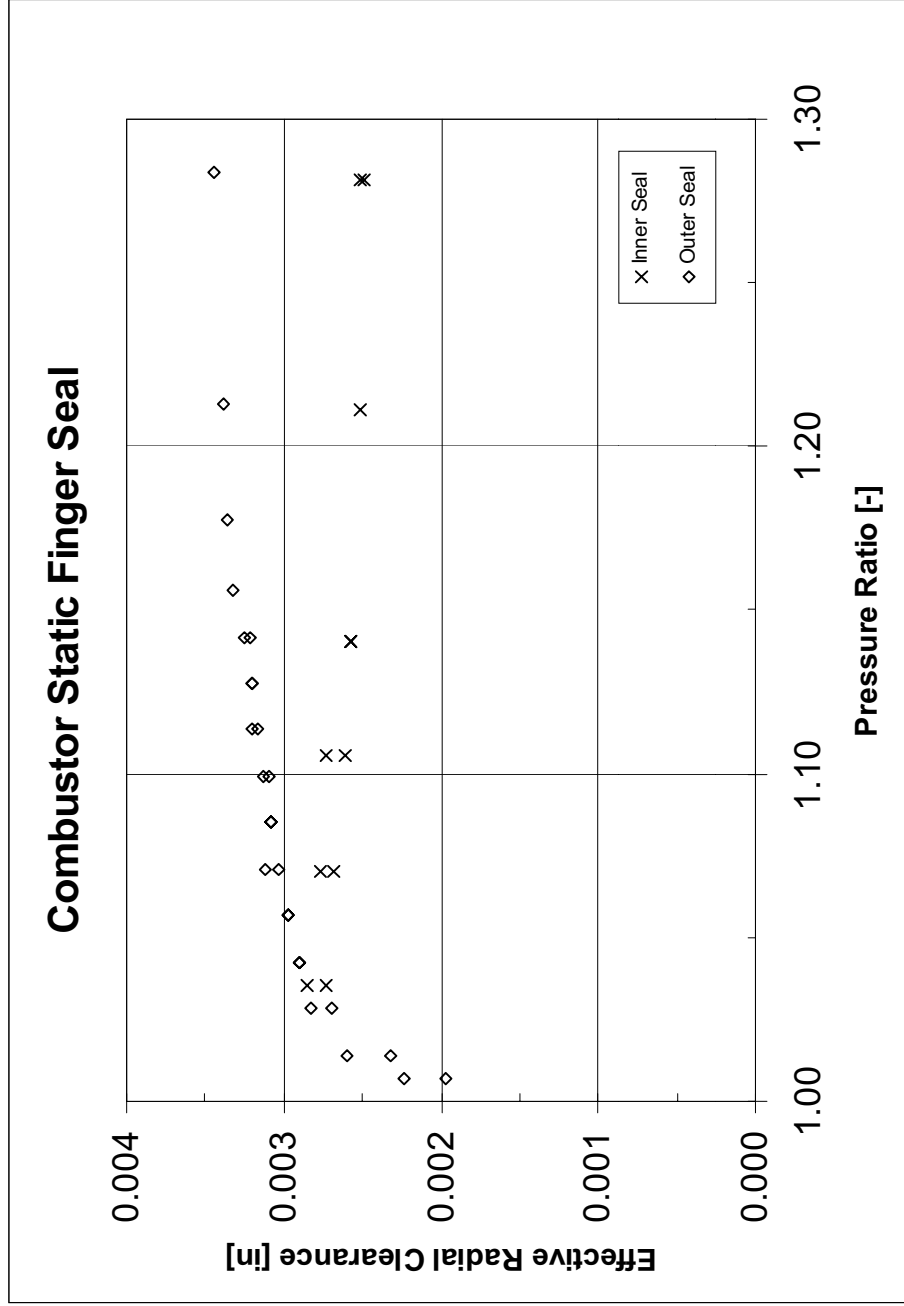
Cold flow testing at operating interference



Honeywell

Seal/Secondary Air System Workshop, 25-26 Oct 2000,
NASA Glenn Research Center, Cleveland, Ohio.

Cold flow testing data....



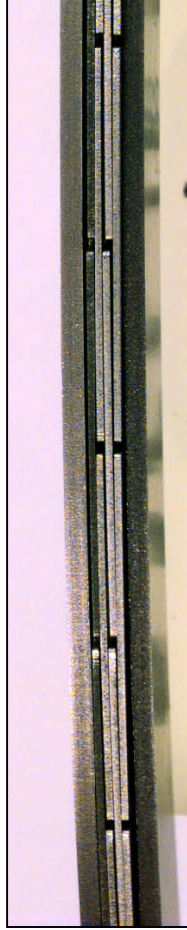
... validated design air leakage

Honeywell

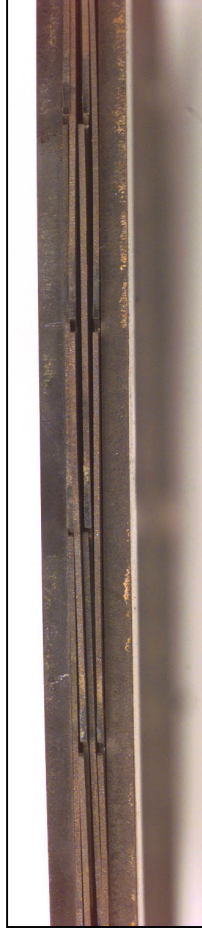
Seal/Secondary Air System Workshop, 25-26 Oct 2000,
NASA Glenn Research Center, Cleveland, Ohio.

Inner seal : pre- and post-test comparison....

Material: MA-956 (Fe based superalloy)



pre-test laminates



post-test laminates

... showed superficial oxidation but no distress

Honeywell

Seal/Secondary Air System Workshop, 25-26 Oct 2000,
NASA Glenn Research Center, Cleveland, Ohio.

Outer seal : post-test inspection....

Material: HA-188 (Co based superalloy)



post-test laminates

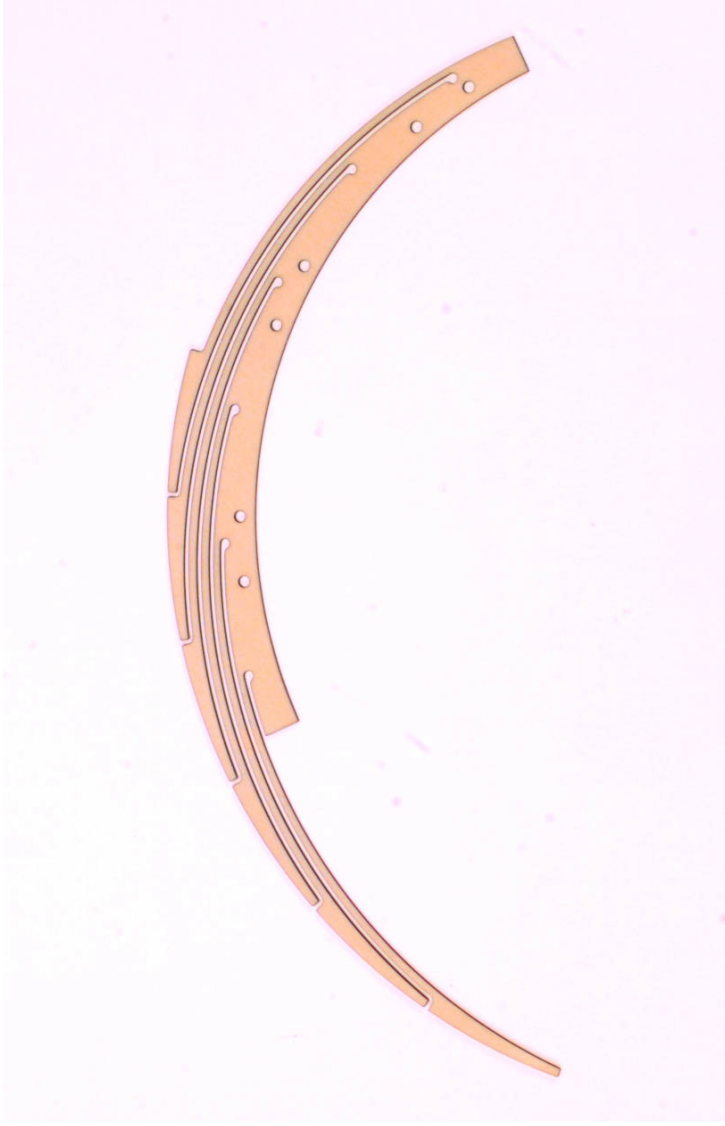


... showed slight handling damage but no distress

Honeywell

Seal/Secondary Air System Workshop, 25-26 Oct 2000,
NASA Glenn Research Center, Cleveland, Ohio.

Seal material: AS800 mono-ceramic



- **Ceramic Components, Honeywell**, has developed cost-effective manufacturing feasibility of AS800 mono-ceramic laminate segments.
- Full scale ceramic seal testing planned in 2001.

Honeywell

Seal/Secondary Air System Workshop, 25-26 Oct 2000,
NASA Glenn Research Center, Cleveland, Ohio.

Conclusions

- Finger seals met sealing requirements of a CMC (ceramic matrix composite) combustor
- Finger seals were found to be a cost effective option for CMC combustor sealing
- High temperature superalloys were investigated as potential finger seal materials
 - HA188, MA956 meet rig requirements
 - AS800 mono-ceramic being developed for engine

Honeywell

Seal/Secondary Air System Workshop, 25-26 Oct 2000,
NASA Glenn Research Center, Cleveland, Ohio.

HIGH TEMPERATURE PERFORMANCE EVALUATION OF A COMPLIANT FOIL SEAL

Mohsen Salehi, Ph.D., Hooshang Heshmat, Ph.D., and James F. Walton II
Mohawk Innovative Technology, Inc. (MiTi)
Albany, New York

**HIGH TEMPERATURE
PERFORMANCE EVALUATION OF
A COMPLIANT FOIL SEAL
NASA Seal/Secondary Air Flow System
Workshop
October 25-26, 2000**

**Mohsen Salehi, Ph.D.
Hooshang Heshmat, Ph.D.
James F. Walton II**

**Mohawk Innovative Technology, Inc.(MiTi)
1037 Watervliet-Shaker Rd
Albany, NY, 12205
MiTi.cc**

This presentation is a summary of work completed recently under two different contract activities and MiTi IR&D. The support of NASA/GRC is acknowledged.

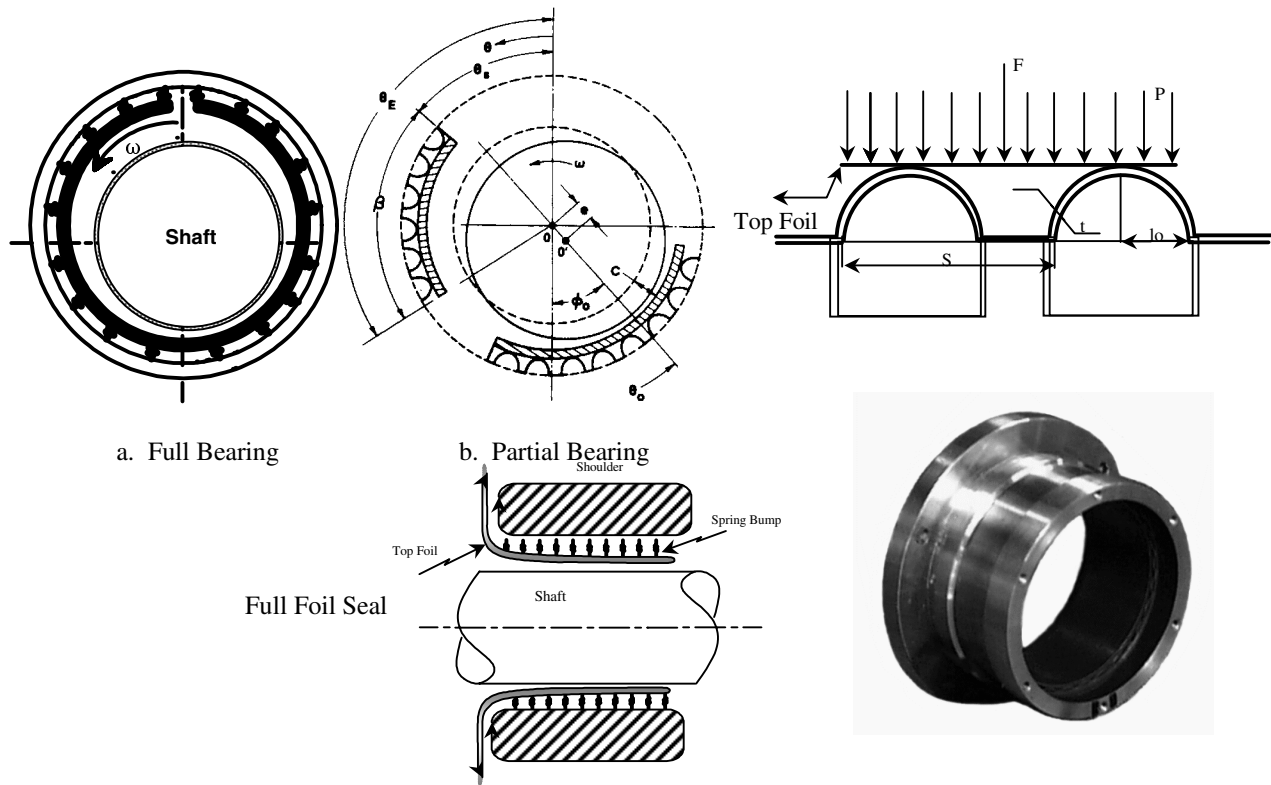
Outline

- Overview of Compliant Surface Foil Seal (CFS)
 - Configuration-Principles
- Experimental System
 - Bearing/Seal Simulator
 - Rotordynamics
- Test Results
 - Dynamic Response of Simulator
 - Compliant Foil Seal Performance
 - Tests with Brush and Labyrinth Seals
- Conclusions

During this presentation the basic configuration and operating principles of the compliant foil seal will be presented, followed by a brief discussion of the test rig facilities used to validate the seal performance; the test results and finally a summary of the material presented.

It should be noted that a portion of the presentation will focus on the rotor system dynamics with the seal. The reason for this emphasis will become evident as the test results are reviewed.

Compliant Foil Bearing and Seal Structure



This chart shows the basic concept for the compliant foil seal and its foil bearing heritage. The upper left two figures are end view cross sections showing the MiTi approach to foil bearing design, namely a single top smooth foil supported by compliant spring elements. The key spring elements design parameters are shown in the upper right portion of the figure. To achieve the desired structural stiffness the corrugated bump pitch (s), material thickness (t) and bump height and radius may be varied.

A segmented or multi-pad bearing/seal arrangement is also possible as shown in the middle of the figure.

Regardless of design, the corrugated bumps can be tailored to provide circumferential and axial variable stiffness. The variable stiffness accommodates the developed hydrodynamic pressures which in turn permit liftoff and separation of the top foil from the shaft at low speed.

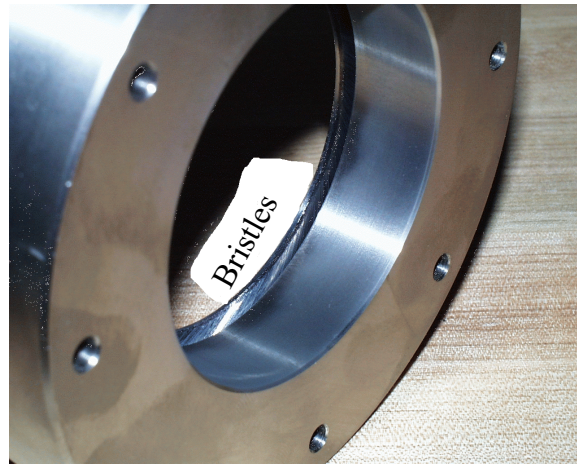
Since the corrugations run axially, an end flange is included to provide the sealing feature.

The figure in the lower right portion of the chart is the first prototype fabricated seal as tested.

Tested Seals



Compliant Foil Seal 99-0067

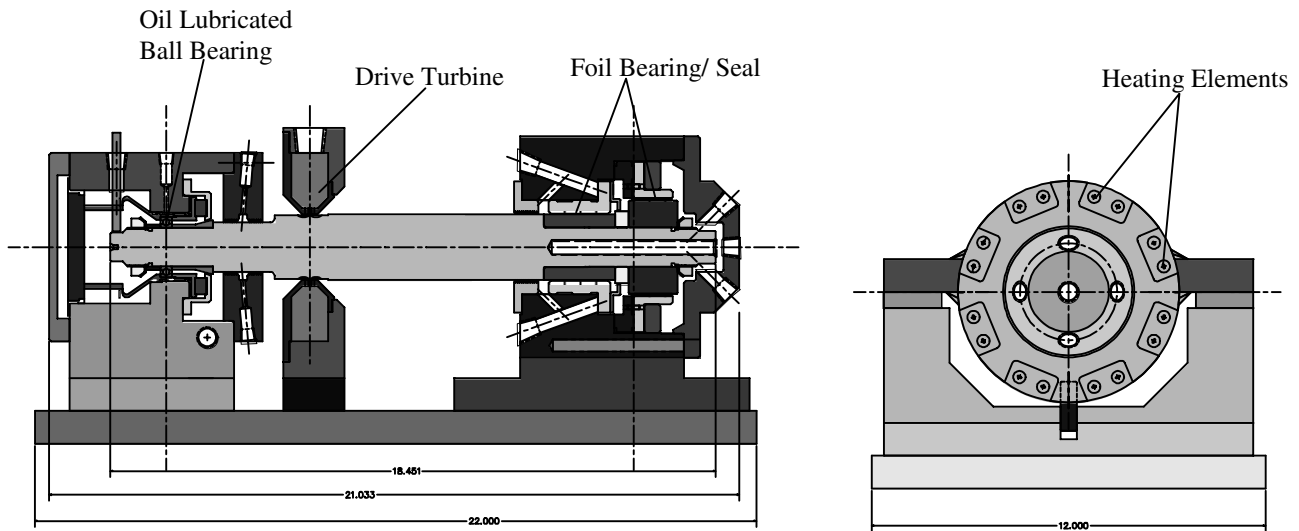


Brush Seal

Fabricated by Cross MFG CO. LTD

Shown here is the 72 mm diameter compliant foil seal and a comparable brush seal purchased from Cross for comparative tests. The foil seal is approximately 15 mm in length for an L/D ratio of approximately 0.2.

High Temperature Bearing/Seal Dynamic Simulator

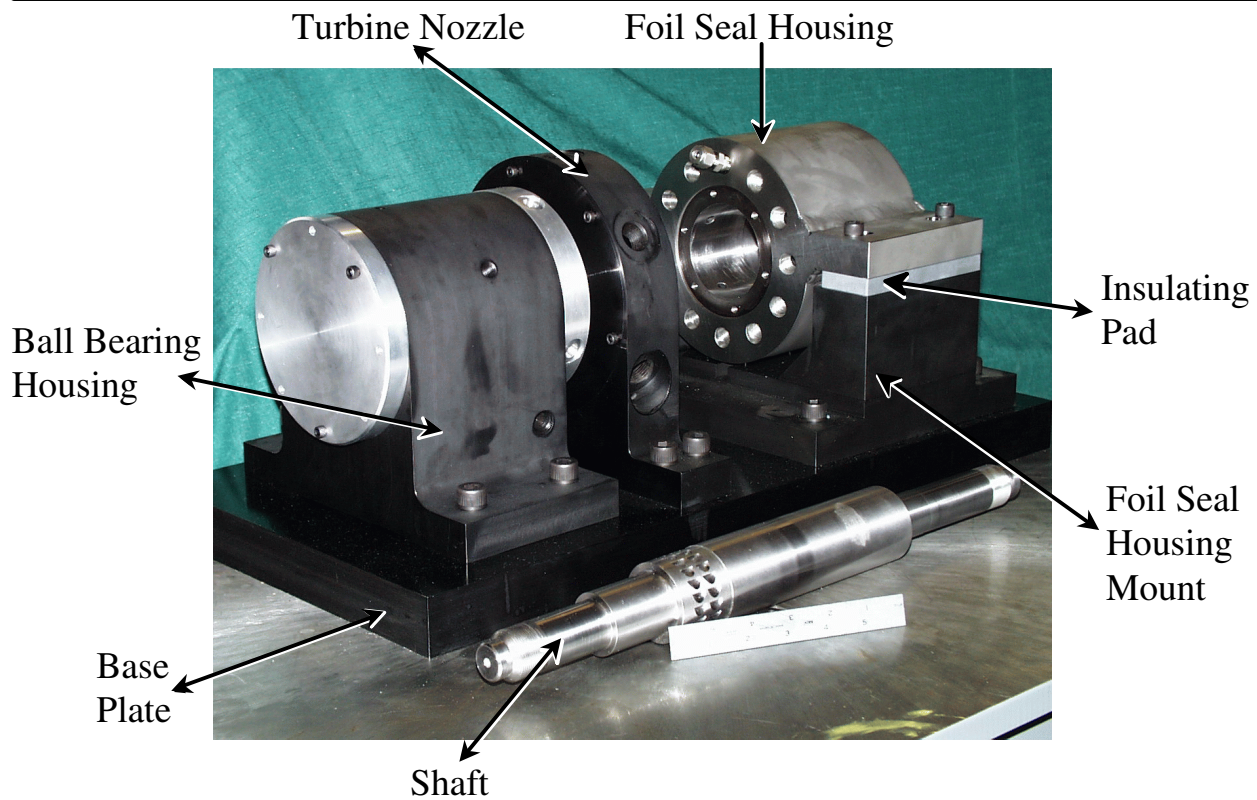


HSA - 404

The high temperature test rig used to evaluate the compliant foil seal is shown here. Working from left to right we have an oil lubricated damped angular contact ball bearing, an integral impulse drive air turbine and the foil bearing and seal housing. The oil-free foil bearing and seal aft housing incorporates 16 cartridge heaters to raise housing temperature to 1000 F and two series of holes which are used to introduce high pressure air into the seal compartment or to vent to ambient atmosphere. Pressurized air may also be heated to 1000 F.

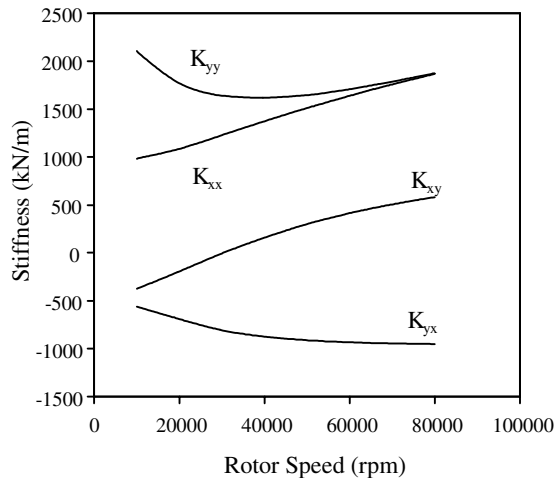
The rotor weight was approximately 8 Kg and operating speeds to almost 60,000 rpm are possible.

Test Rig Hardware

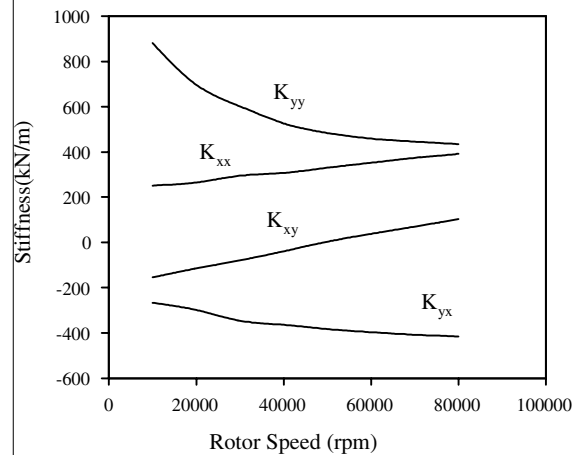


This photo shows the key test rig components as fabricated.

Foil Bearing & Seal Stiffness



**Foil
Bearing**

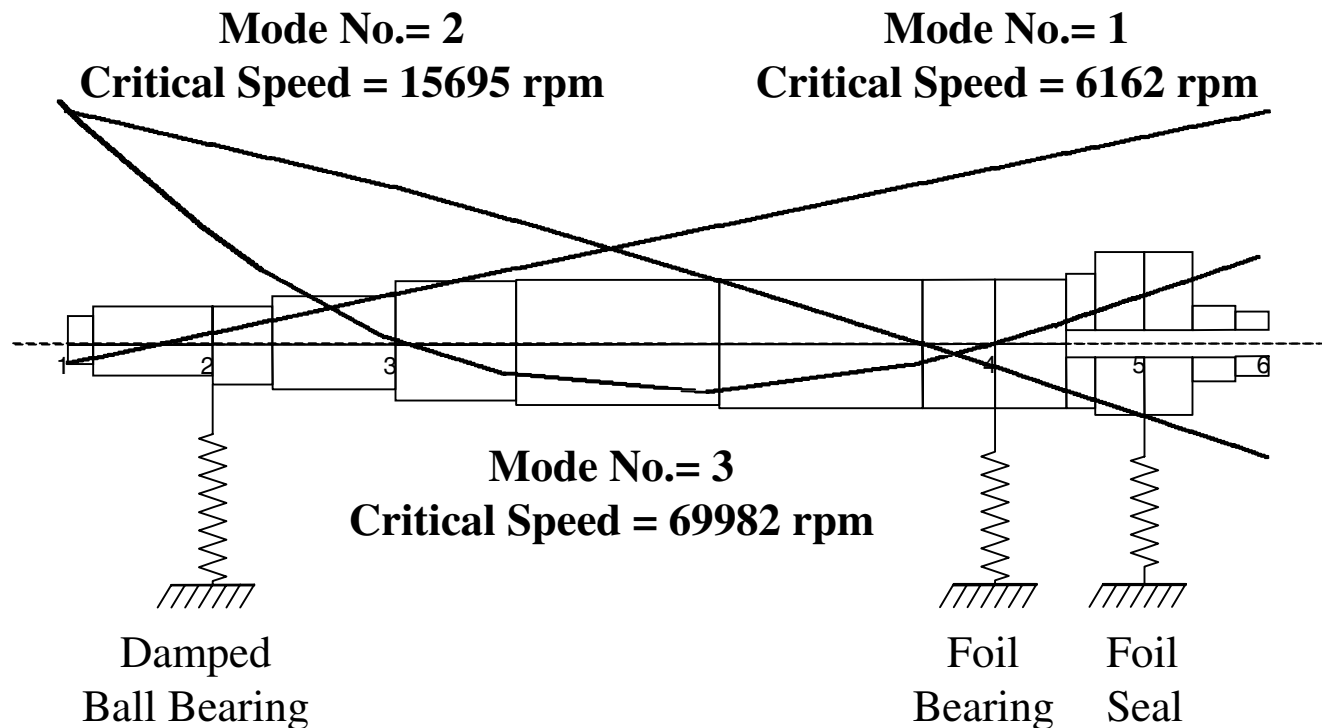


**Foil
Seal**

As stated earlier, the foil seal has many of the same characteristics of the foil bearing. This similarity is evident in the two stiffness vs speed curves. It should be noted that both the foil bearing and seal have both direct and cross coupled stiffness as is expected for a hydrodynamic bearing. However, with both the bearing and the seal it is possible to configure and design the compliant elements to minimize the magnitude of the cross coupled terms and hence the generation of any destabilizing forces (e.g. Alford).

It should be noted that while the characteristics of the bearing and seal are similar, that the magnitude of the foil seal stiffness terms is less than the bearing. None-the-less, this stiffness and likewise the corresponding damping of the foil seal can have a positive impact on rotor system dynamics.

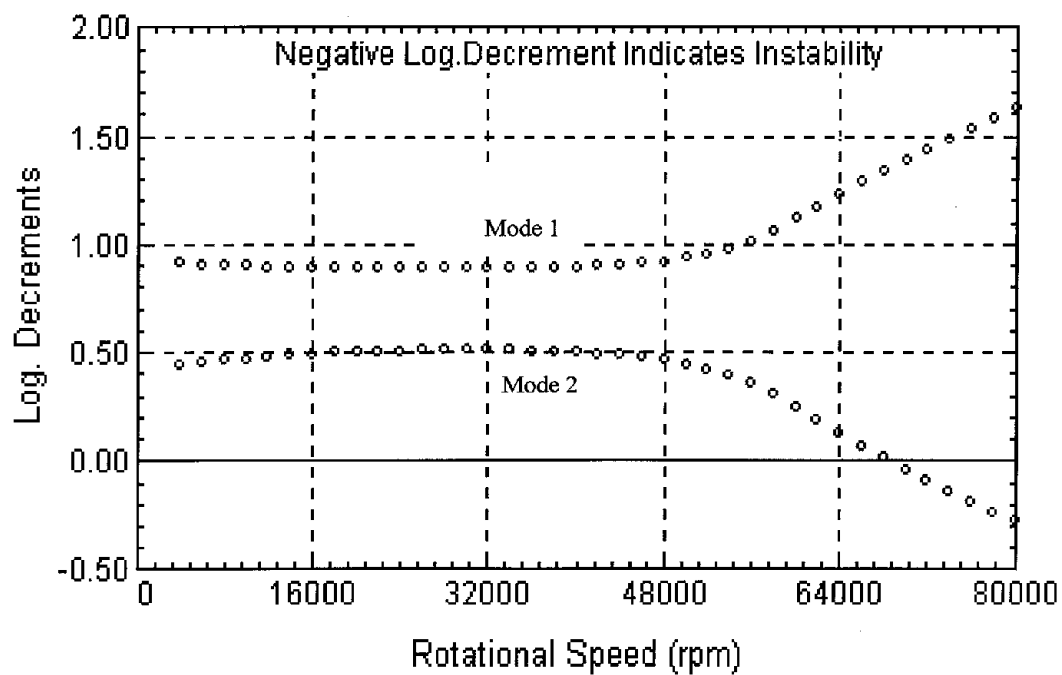
Critical Speed Analysis - Mode Shapes



Using estimated speed independent bearing coefficients the preliminary rotor critical speeds and mode shapes were determined as shown here. With a maximum operating speed of just under 60,000 rpm, the first bending critical speed is not expected to pose any limitation on system operation or testing.

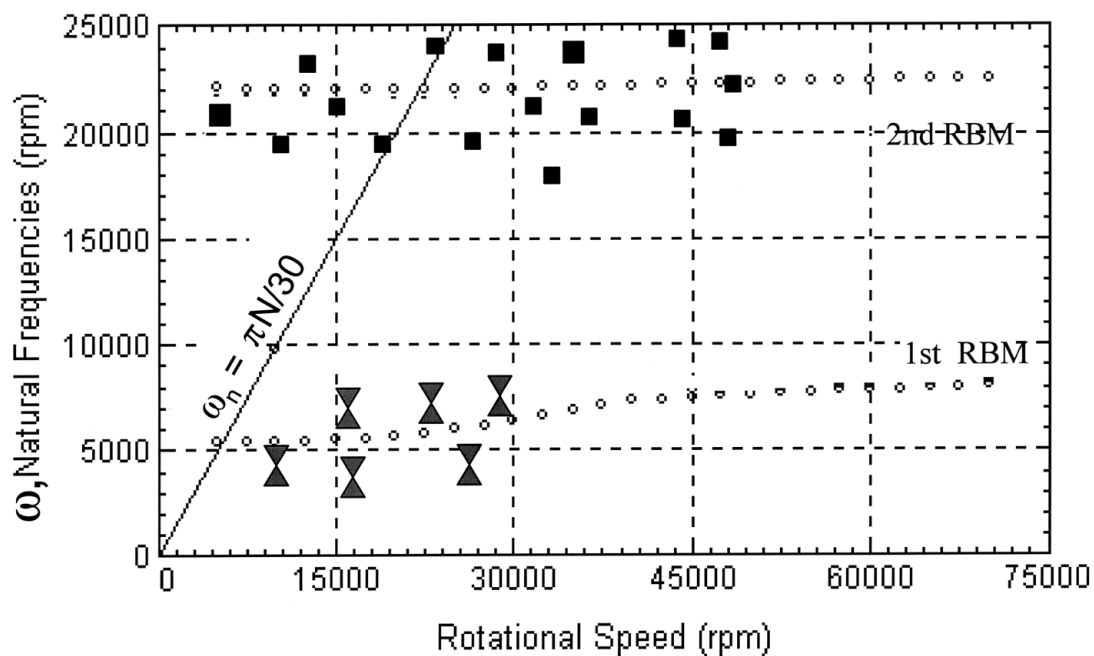
The first mode should be well controlled since there is motion at both the foil bearing and seal. Similarly, based on the amplitudes at the ball bearing and foil seal location the second mode should be well controlled.

Stability Map



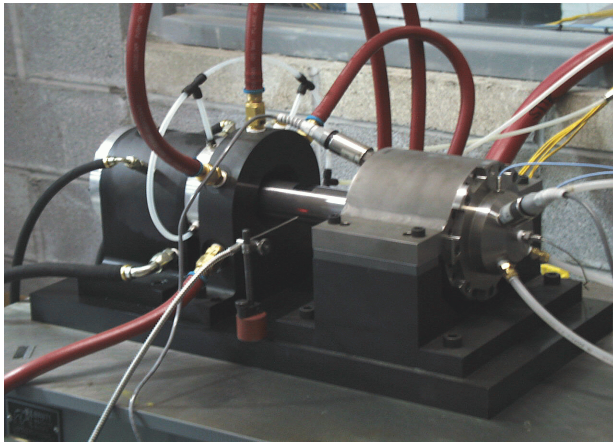
The stability map, which plots logarithmic decrement vs speed, shows that the rotor bearing system is expected to be stable at speeds in excess of 64,000 rpm.

Natural Frequencies - Foil/Seal Rotor System



One of the first things accomplished during checkout and initial operation of the test rig was to verify the analytically predicted rotor modes. This allows us a measure of validation of the bearing coefficients. As seen here, both the first and second measured modes correlate well with the predictions, giving confidence in the bearing and seal stiffness predictions as a function of speed.

Simulator & Instrumentation Setup



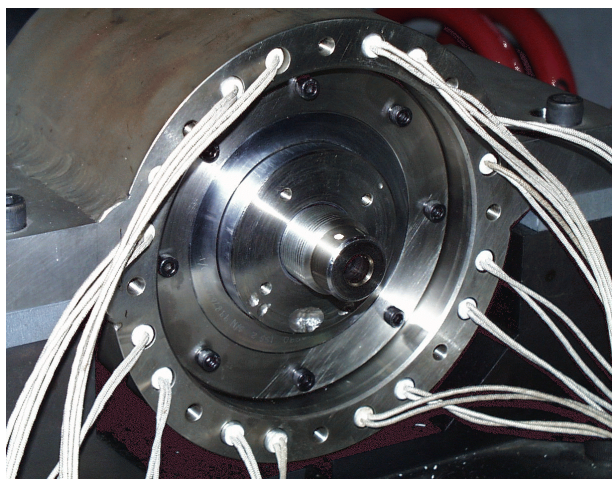
Hybrid Simulator

Instrumentations



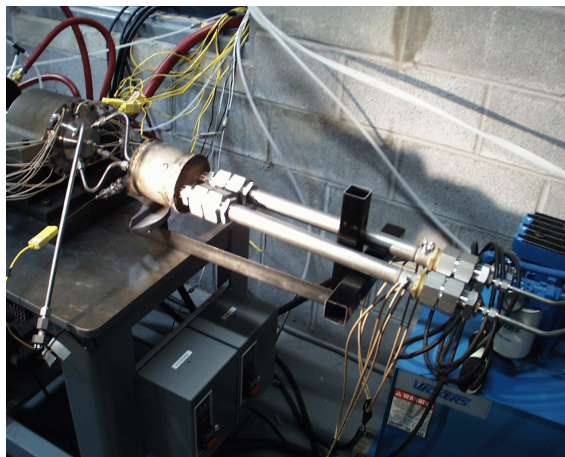
Shown here are the test rig installed in the test cell and the instrumentation set up including the PC based Labview data acquisition system, the dual channel FFT analyzer and the FM tape recorder.

Test Rig High Temperature Components



Cartridge Heaters

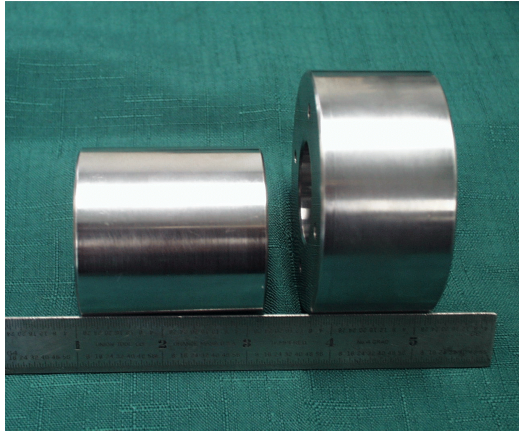
Shell & Tube Pre-Heaters



These two photos show the features incorporated for high temperature operation. The left figure shows the cartridge heaters installed in the bearing and seal housing. The aft view also shows the end of the foil seal.

The right figure shows the high temperature inline air heaters used to inject the high temperature pressurized air into the seal chamber.

Compliant Foil Seal/Bearing Journals



Low Temperature Journals

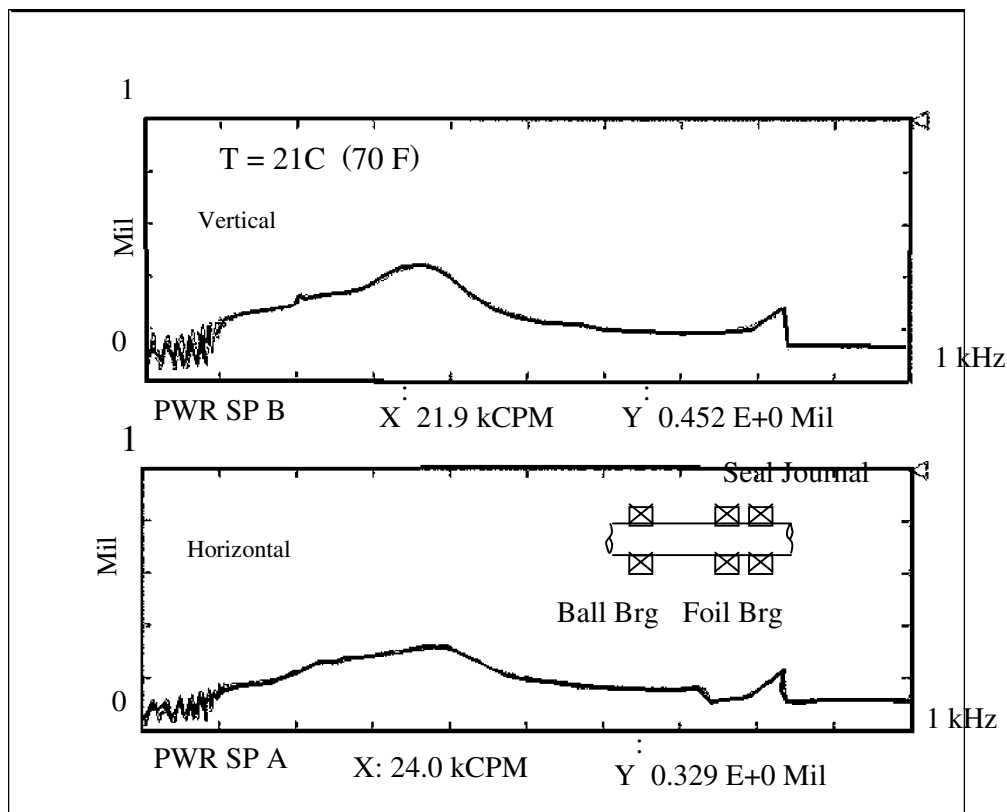


High Temperature Journals

These two figures show the foil bearing and journal seals. The left figure shows the electrolyze coated journals used for low temperature tests.

The right figure shows the journals coated with PS304 for high temperature testing.

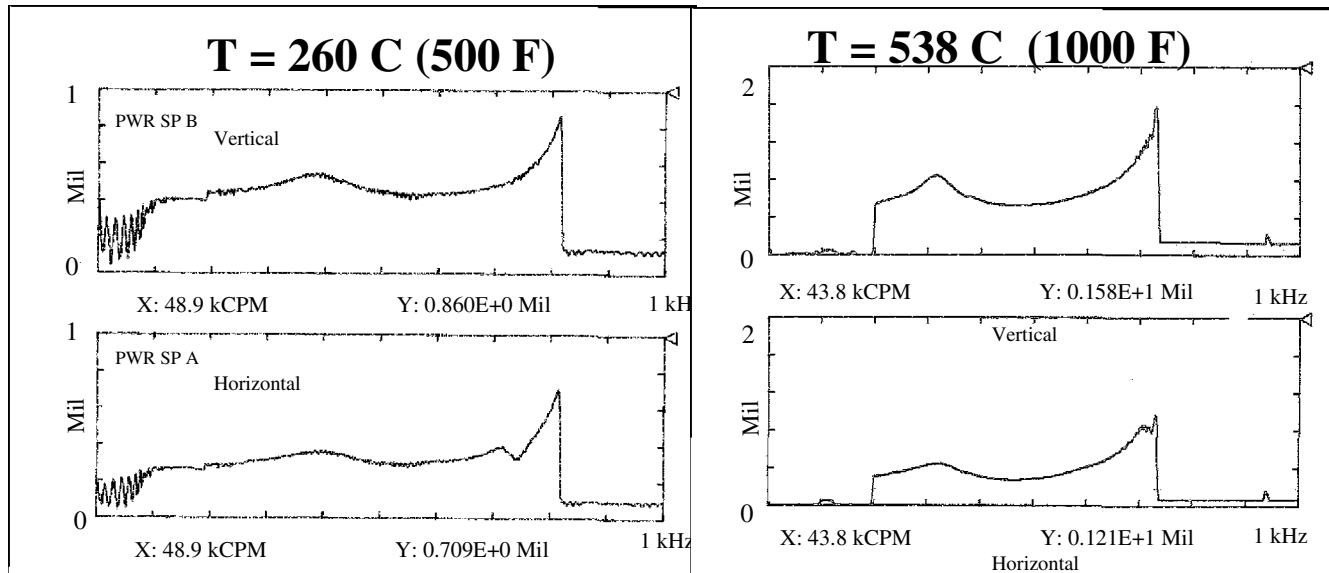
CFS Coast Down at Room Temperature



HSA - 419

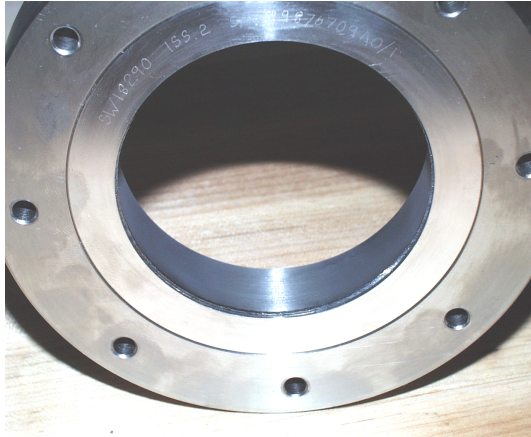
These peak hold synchronous vibration coast down plots show that the rotor system is well controlled throughout the entire expected operating speed range with both the foil bearing and seal installed.

Coast Down w/CFS at Two Temperatures



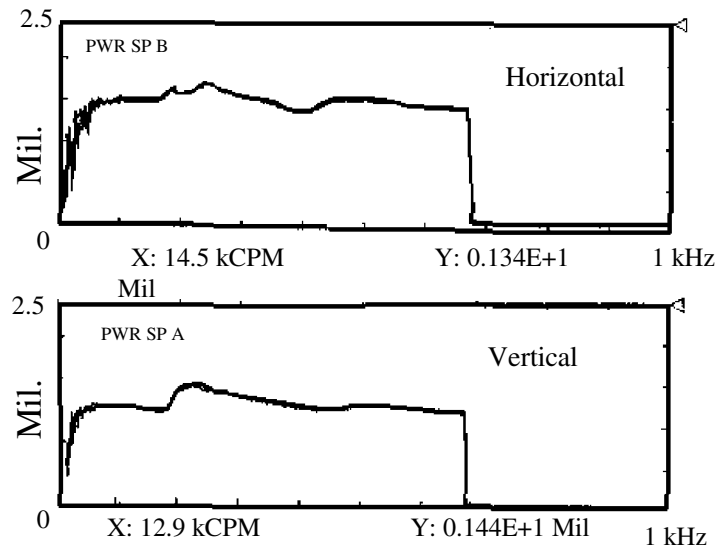
As temperature is increased first to 500F and then to 1000F rotor response is still well controlled. However, it should be noted that the response amplitude of rotor vibration increases over the room temperature baseline. This increase in vibration amplitude is most likely due to a reduction in material modulus and hence bearing stiffness as temperature increased.

Coast Down On Brush Seal at RT



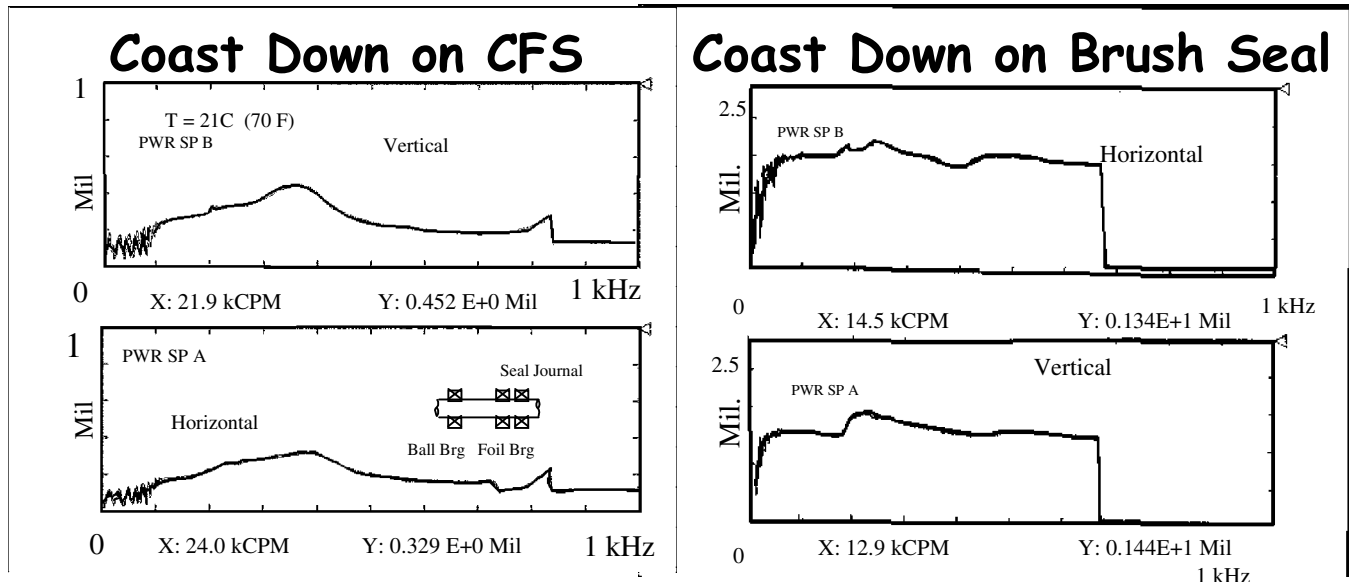
*Brush Seal By Cross
TM*

Coast Down on Brush Seal



This chart shows the brush seal as tested along with the resulting rotor response. The brush seal was installed with a 0.002 inch interference.

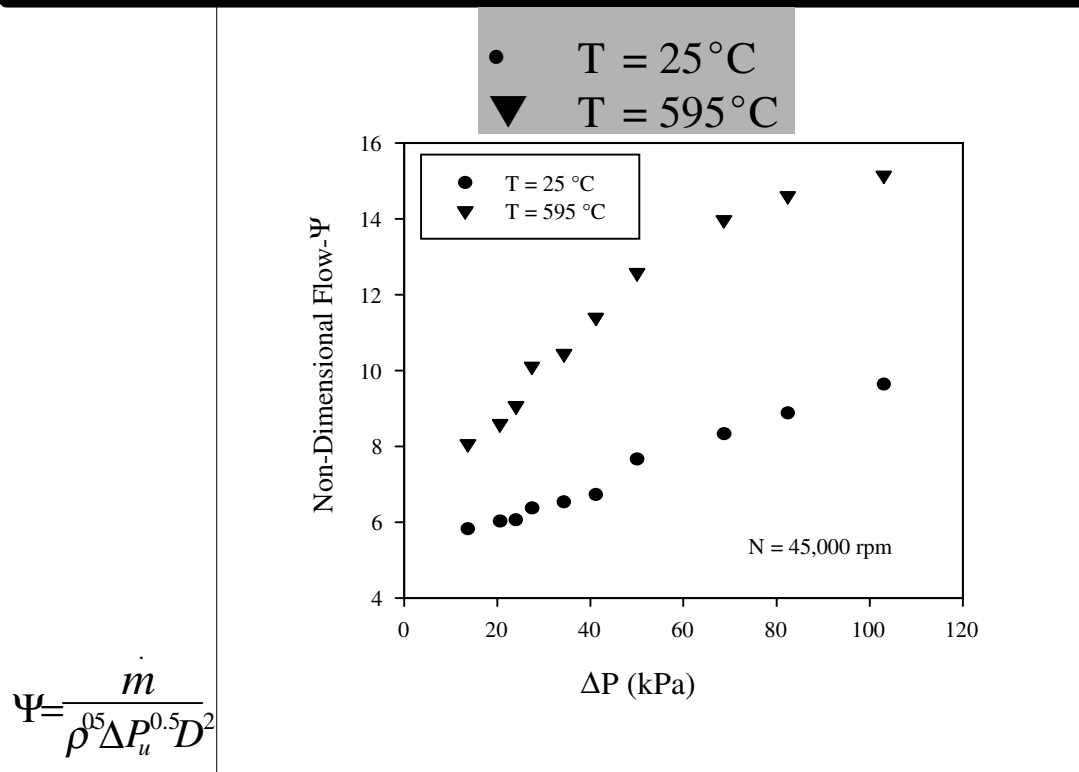
Compliant Foil Seal vs Cross™ Brush Seal Coastdown



HSA - 419

This chart compares the rotor response performance of both the compliant foil seal and the brush seal at room temperature. Note the vibration amplitude scales (ordinate) for the brush seal is 2.5 mils while the foil seal max scale is 1 mil and that peak vibration amplitude for the foil seal is less than 0.5 mils while the peak rotor vibration is 1.34 mils when the brush seal was installed. This vibration response shows that the stiffness and damping contribution from the foil seal has a positive impact on the rotor.

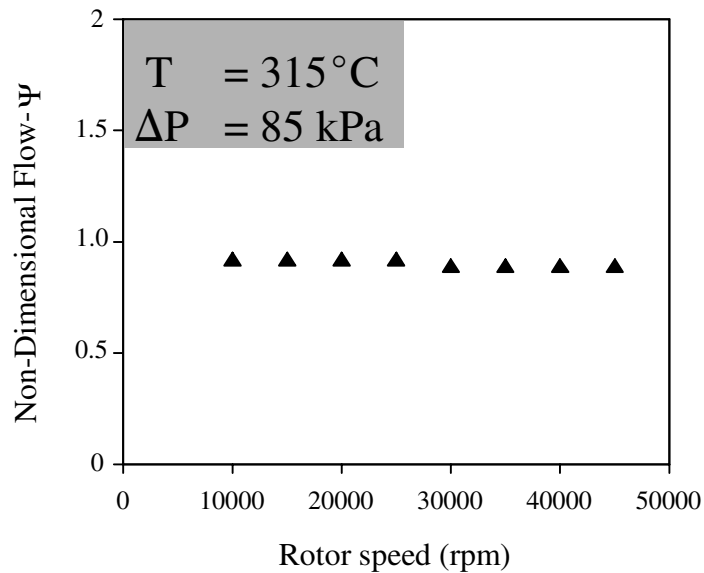
CFS Performance with Temperature



Once the rotor performance was deemed acceptable, evaluation of the compliant foil seal was performed. As seen here the foil seal performance does degrade slightly as differential pressure and temperature increases. In both cases however, the increased leakage is nearly linear over the range of pressures tested. The results presented here are for a spin speed of 45,000 rpm and at both room temperature and 595C.

CFS Performance with Rotor Speed

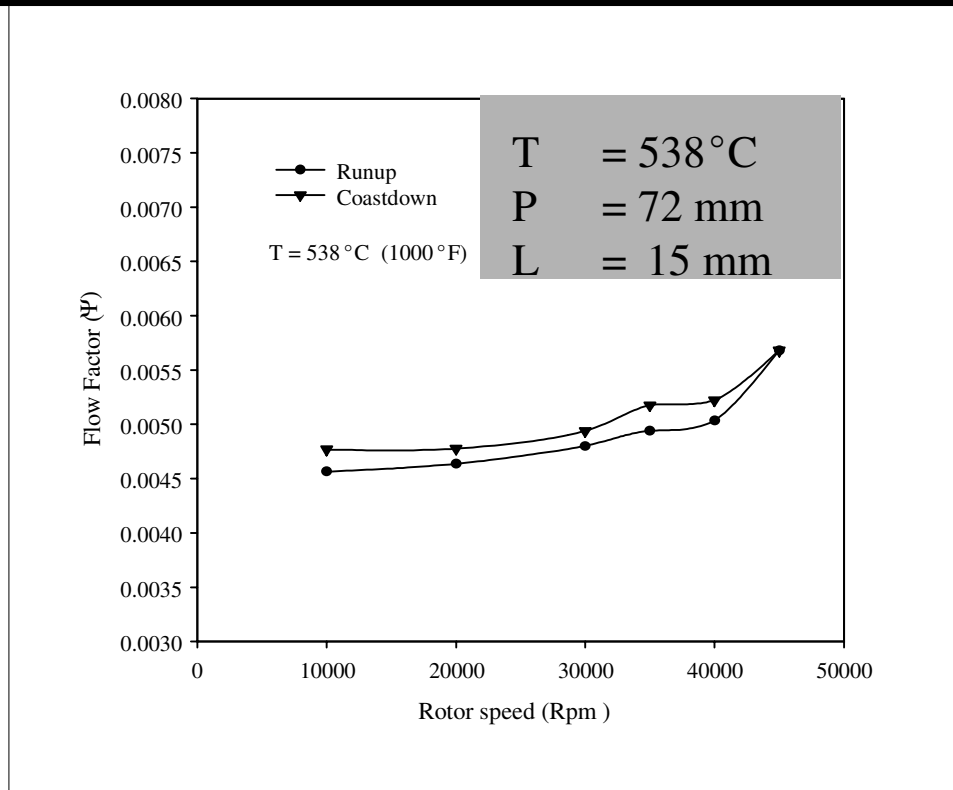
Diameter = 72 mm Length: = 15 mm



In this test, the differential pressure was held constant as speed was increased. As seen the flow or seal leakage remained constant over the entire speed range tested.

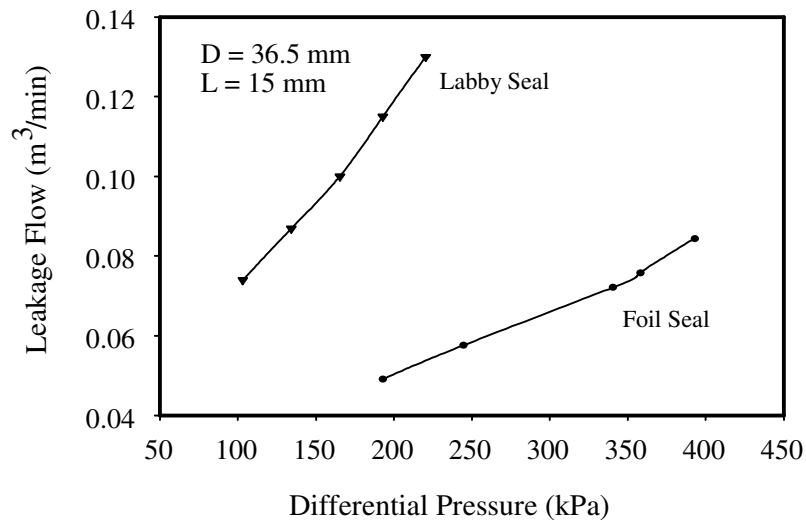
CFS Performance @ 1000 F

$$\Psi = \frac{m \sqrt{T}}{P_u D}$$



This chart, which plots flow factor as a function of spin speed for the 72 mm diameter seal shows that the leakage remains fairly constant for the entire speed range and that performance is fairly repeatable having taken data both during the acceleration and deceleration. Flow factor data for the CFS was plotted versus speed in this case since this is one measure used to assess brush seal performance.

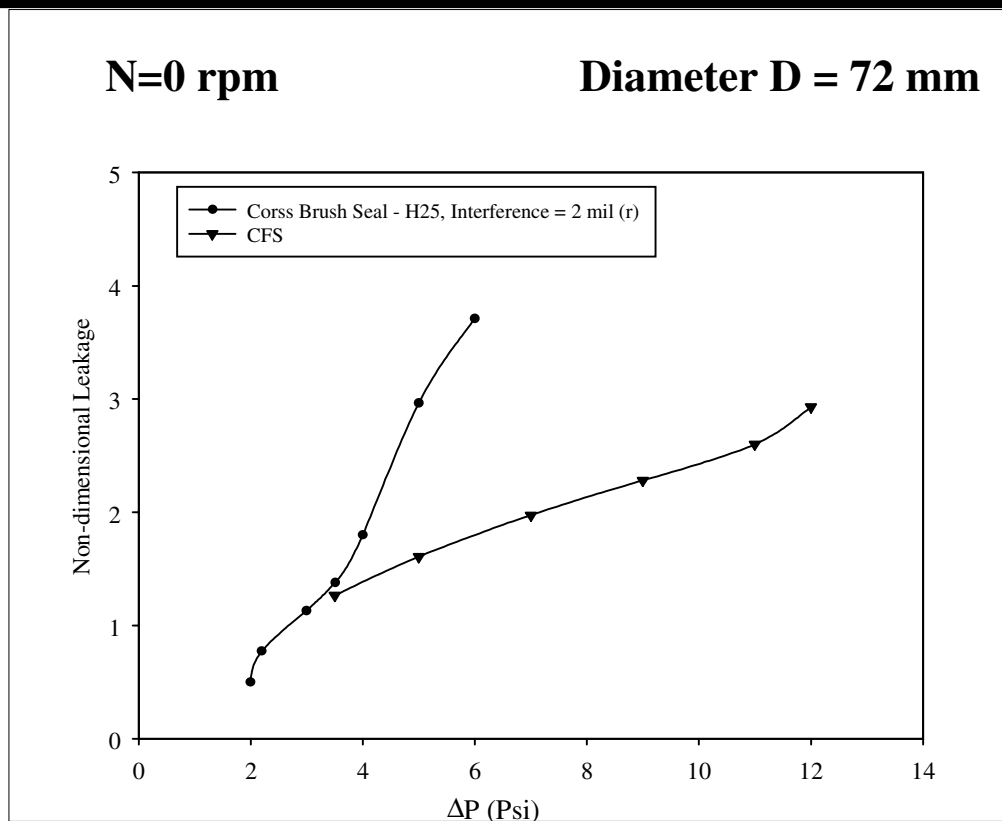
Static Test with Labyrinth Seal and CFS



Having demonstrated operation of the compliant foil seal, the next step was to demonstrate its superiority over a comparable labyrinth seal. The experimental data presented here is for a static or non-rotating condition. This testing with the 36 mm diameter foil seal vs a comparable labyrinth seal shows that the foil seal leakage increases nearly linearly with differential pressure and that the leakage is significantly lower than that for the labyrinth seal.

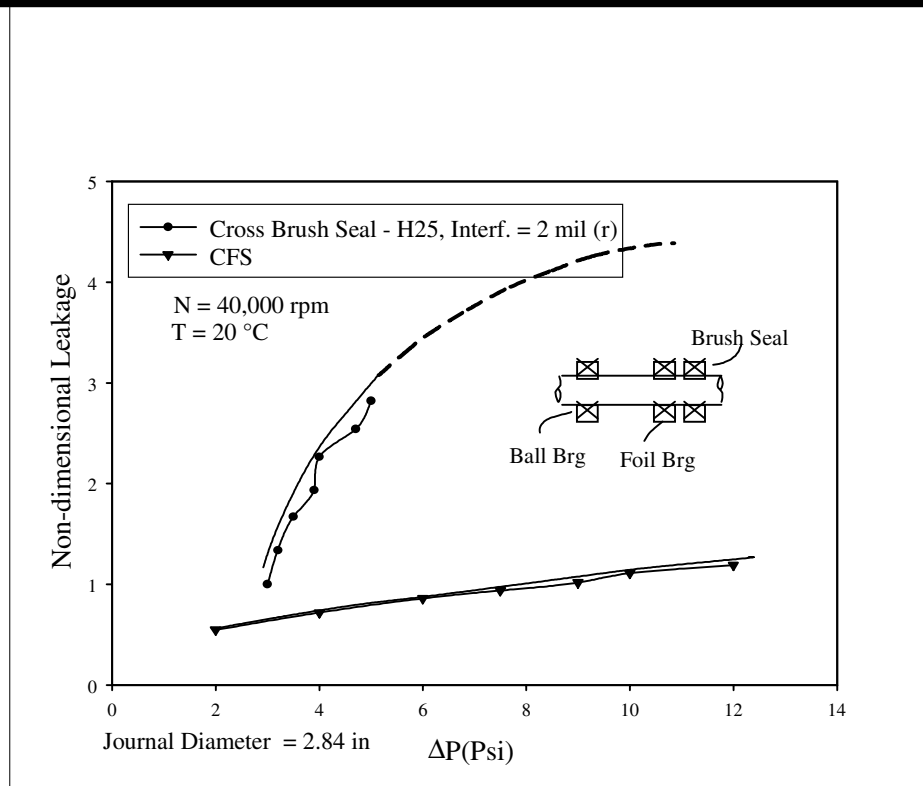
The performance of the compliant foil seal is to be expected since the nominal operating clearance is less than the labyrinth seal, being on the order of 0.5 mil as opposed to approximately 3-6 mils. Under dynamic conditions this same performance trend is expected.

Compliant Foil Seal vs Cross™ Brush Seal



This chart compares the compliant foil and brush seal non-dimensional leakage versus differential pressure under static non-rotating conditions. The experimental data shows that the foil seal leakage again increases nearly linearly with differential pressure and that the leakage is significantly lower than that for the brush seal. As a matter of fact, the brush seal which was made of Haynes 25 bristles and installed with a 0.002 inch interference fit could only sustain a 6 psi differential pressure. This low achieved differential pressure is likely due to fence height.

CFS and Brush Seal Comparison



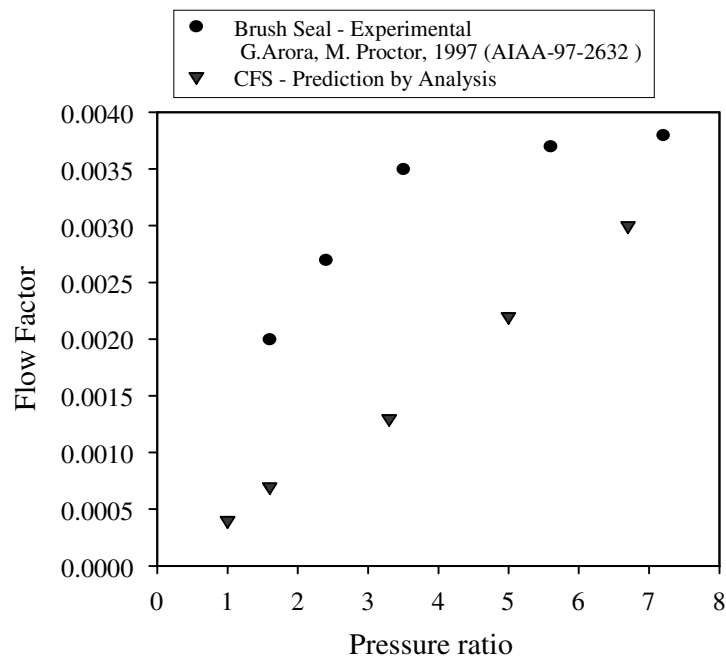
A dynamic room temperature, 40,000 rpm comparison of the 72 mm diameter foil and brush seals is shown here. As seen before the foil seal leakage increases linearly with a low slope while the brush seal leakage increases dramatically over the same range of pressures.

Brush Seal Wear Track on Journal



This figure shows the wear tracks evident on the rotor seal surface. Several wear tracks are evident. The two primary wear tracks resulted from flipping the brush seal around so that a new running surface could be used for different tests. A close examination of the shaft at the inboard wear track reveals it to be wider than the original bristle stack due most likely due axial flexing of the bristles under the axial pressure gradient.

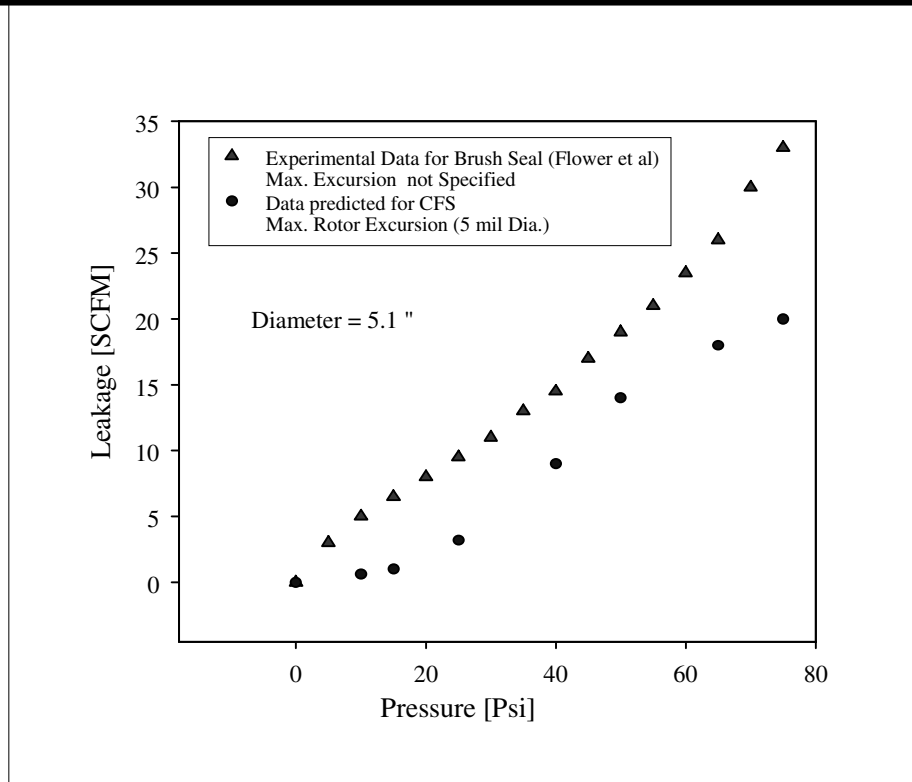
Brush Seal Test Results vs CFS by Analysis



To further validate the feasibility of the foil seal, published data for brush seals was used to assist in establishing comparable CFS designs that could then be analytically compared to the brush seal. As seen here predictions indicate that the CFS should out perform comparable brush seals even at pressure ratios as high as 7 to 8. The data used here was published by Arora and Proctor in 1997 in paper AIAA-97-2632.

While the differential sealing pressures evaluated under this effort were limited to less than 60 psi, it is recognized that higher pressure testing will be needed to validate the high pressure performance.

Brush Seal Test Results vs CFS by Analysis



Another comparison of the CFS against brush seal data published by Flowers et al is shown here. As shown previously, the comparable foil seal design is expected to have less leakage than the brush seal even at differential pressures of 80 psi.

Summary and Conclusions

- **A hybrid small gas turbine engine simulator was successfully designed and tested for a range of speeds and temperatures (0-56,000 rpm, 20-640 °C)**
- **Feasibility of the non-contact compliant foil seal (CFS) was demonstrated**
 - Hi-Temperature operation w/NASA PS304 coating & MiTi Bearing & Seal
 - Rotor vibrations reduced
 - CFS exceeded performance of Brush and Labyrinth seals w/o wear
- **The CFS has great potential for hi-speed, hi-temperature applications**
- **Further work**
 - Demonstrate rotor excursion capabilities
 - Demonstrate scaling

The key points to be gleaned from the effort reported herein are that the CFS has been demonstrated in conjunction with a foil bearing in a small gas turbine simulator at temperatures as high as 1000F and outperformed a comparable brush seal.

Having demonstrated the feasibility of the CFS, it would appear that this new seal design has application potential in a wide range of machines. What remains is to demonstrate performance at higher pressure ratios, consistent performance at large rotor excursions and the ability to manufacture the seal in much larger sizes exceeding by an order of magnitude that which has been tested to date.

LARGE-DIAMETER SPIRAL GROOVE FACE SEAL DEVELOPMENT

Xiaoqing Zheng and Gerald Berard
PerkinElmer Fluid Sciences
Beltsville, Maryland



This presentation reports our recent development of film-riding face seals for large diameter gas turbine engines.

A new design tool, incorporating a commercial finite element program ADINA, has been developed for advanced analysis of film-riding face seals. This code is capable to model transient fluid-structure interaction inside a general seal configuration, enable designer to predict seal responses to speed, temperature and pressure changes in a time-dependent manner. Therefore, through evaluation of influences of different seal parameters, the application envelopes of conventional spiral groove face seal can be extended to larger diameter, higher speed range.

For applications that seal surface coning due to high speed and large diameter is too much for a conventional spiral groove seal to handle, a new double spiral groove design has been developed with significantly increased angular film stiffness. Axial and angular stability are crucial for successful operation of large diameter seals. Like the original double spiral groove design, the seal face consists of a pair of spiral groove seal sections, but the new design features an outward pumping groove section in the outer region. Both inner and outer grooves are fed through one set of deep middle feeding grooves that are connected to high-pressure gas through restricted orifices. The new design simplifies the seal stator ring, while resulting in a more robust concept less dependent on the thermal properties of materials. The feeding holes that lead high pressure into the middle feeding grooves are designed to have restrictive effects on feeding groove pressure when film thickness is large. Additionally, this greatly improves the film stiffness in large film gap regions.

A computer program has been developed to analyze and design the new double-spiral groove seal. ADINA was used to analyze the orifice restriction factor of the feeding holes. Through calculating pressure drops at different mass flow rates in various sizes of feeding holes, an empiric formula is obtained from the computational results to relate the pressure drop ratio to flow parameters. The simple formula resulted from heavy, extensive computation is plugged into the seal design code to obtain fast solution.



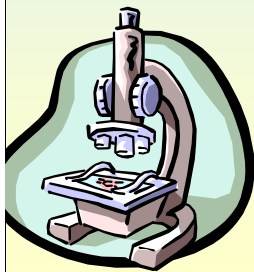
Introduction

- Non-contacting, film-riding face seals for large diameter gas turbine engines.
- Low leakage, low wear.
- High speed.
- High temperature.
- High angular deflection.

Non-contacting, film-riding face seals have been used successfully for industrial applications ever since their introduction in 1969. Extremely low leakage and wear characterize non-contacting face seals. Because of that, there have been continuous efforts made by investigators in aerospace to develop non-contacting face seals for large diameter gas turbine engines, where the potential payoff is very high. As it turns out, the application of non-contacting face seals in gas turbine engines is much more demanding than in industrial applications

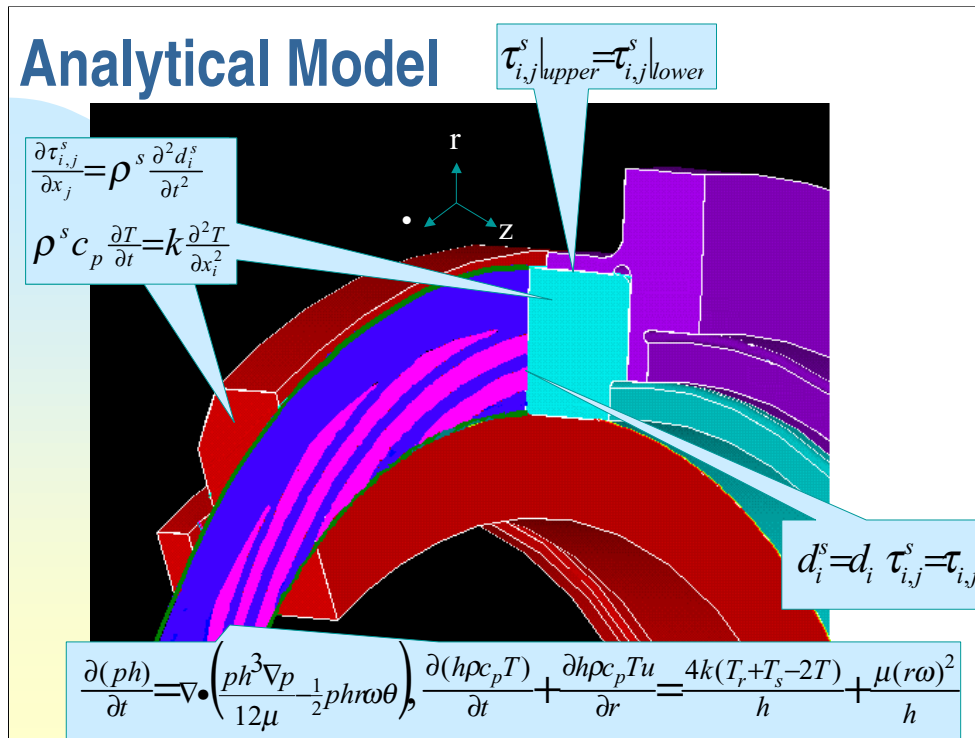
There are two major difficulties associated with using face seals for high rotational speed and large shaft diameter turbomachines. First, controlling the flatness of the seal faces is very difficult because of the size. Second the seal faces of both the rotor and stator can cone in either inward or outward direction due to the large thermal and pressure effects. A negative deflection causing a divergent flow path can be disastrous for a standard hydrodynamic face seal, since it tends to cut off the flow of gas into the region between the faces. With standard hydrodynamic face seals the deflection is expected to be much larger than the film thickness that the face seal runs on. Large positive coning can also result in failure for large diameter face seals because the resulting weak film stiffness increases the chance of face contact

Analytic Design Tools Development



- General seal configurations.
- Conjugate heat transfer analysis.
- Deflections by pressure and centrifugal loading.
- Face coning in composite design.
- Transient analysis of seal responses to the changes of operational conditions.

Tight R&D budget prevents systematic evaluation of large diameter spiral groove face seal designs in laboratory. More and more product development relies on theoretical analysis. Rig test is only a validation tool, other than a development vehicle as it used to be.



The seal equation, the Reynolds equation, is solved in the (r, \bullet) plane to obtain pressure and leakage. It is inserted into a commercial finite element program, ADINA, which is capable of transient dynamic analysis of structural deflections due to thermal stress, pressure, and centrifugal force in a full three-dimensional way. But in most cases, the energy equation and solid structural equations are solved in (r, z) plane as axisymmetrical problems. Therefore the whole system of equations is quasi-three dimensional. The pressures from seal equation are circumferentially averaged before they are passed to structural analysis.

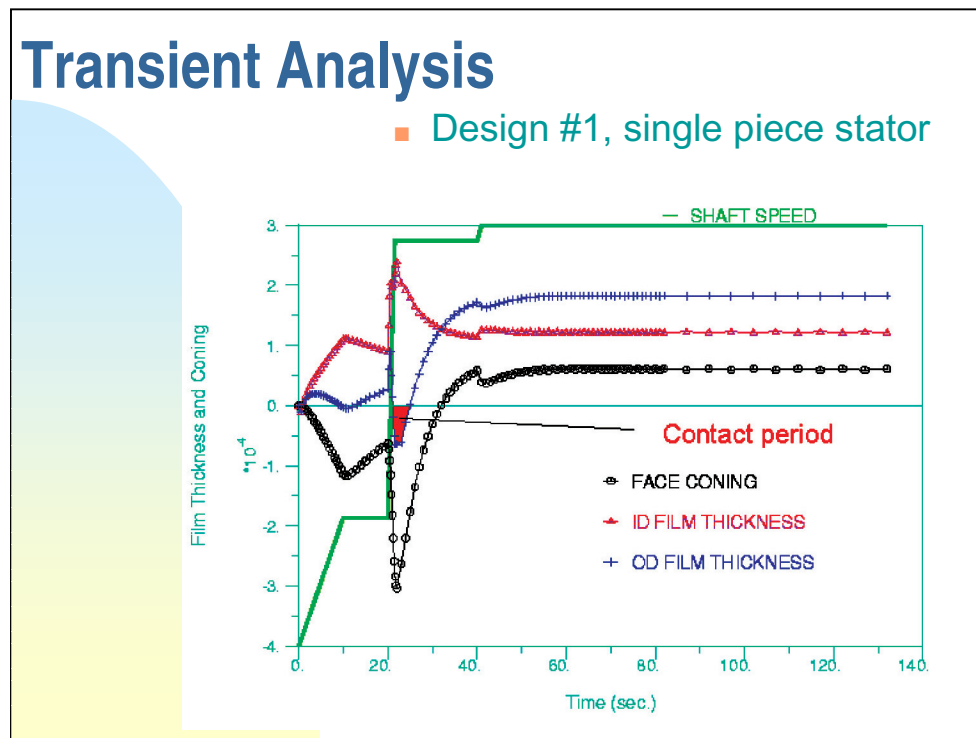


Application Examples

- 6" diameter, over 19,000 rpm
- 5" diameter, over 14,000 rpm

Transient Analysis

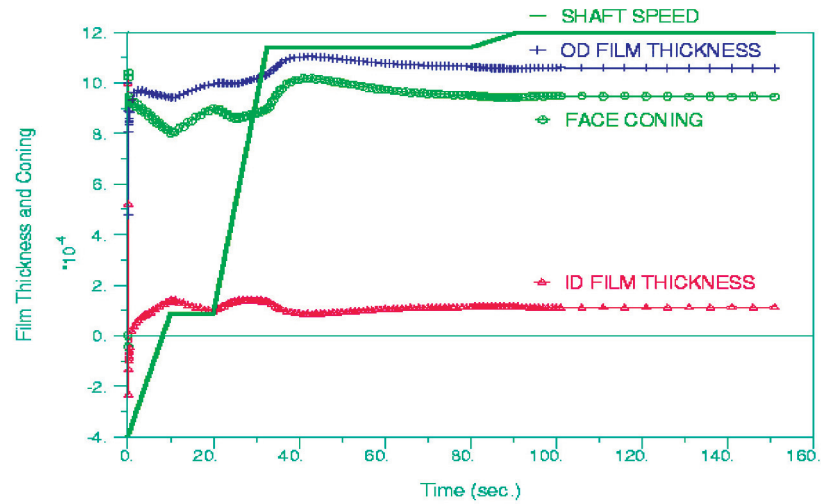
■ Design #1, single piece stator



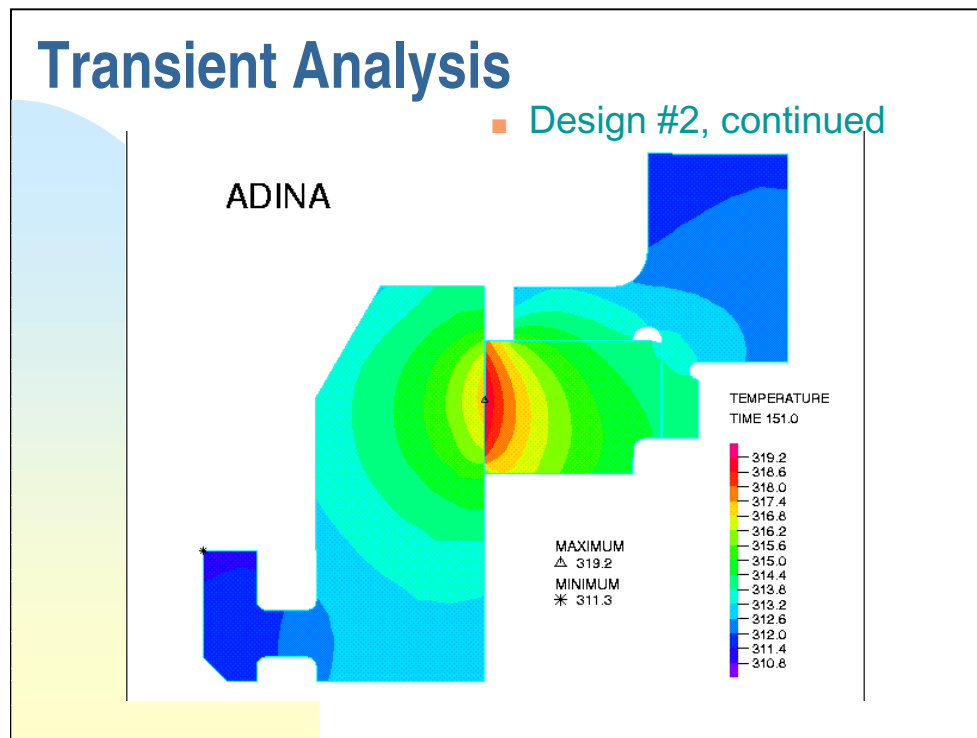
The seal is OD pressurized, with hot oil in the OD side and cold air in the ID side. The seal is designed to pump low-pressure air into high-pressure oil side. The above image shows the history of shaft speed, seal film thickness at ID and OD, as well as face coning. It is interesting to find out that the seal experiences momentary OD contact during the shaft acceleration, in contrast to usual ID contact for most seals in transient phase. Careful examination of results reveals that this phenomenon is due to the faster temperature increase in OD than that in the ID. As we know that the heating from the seal face rubbing makes the seal faces cone positively, leading to ID contact. But for this seal, the heating from oil in the OD overcomes the seal face heating and leads to OD contact.

Transient Analysis

■ Design #2, composite stator



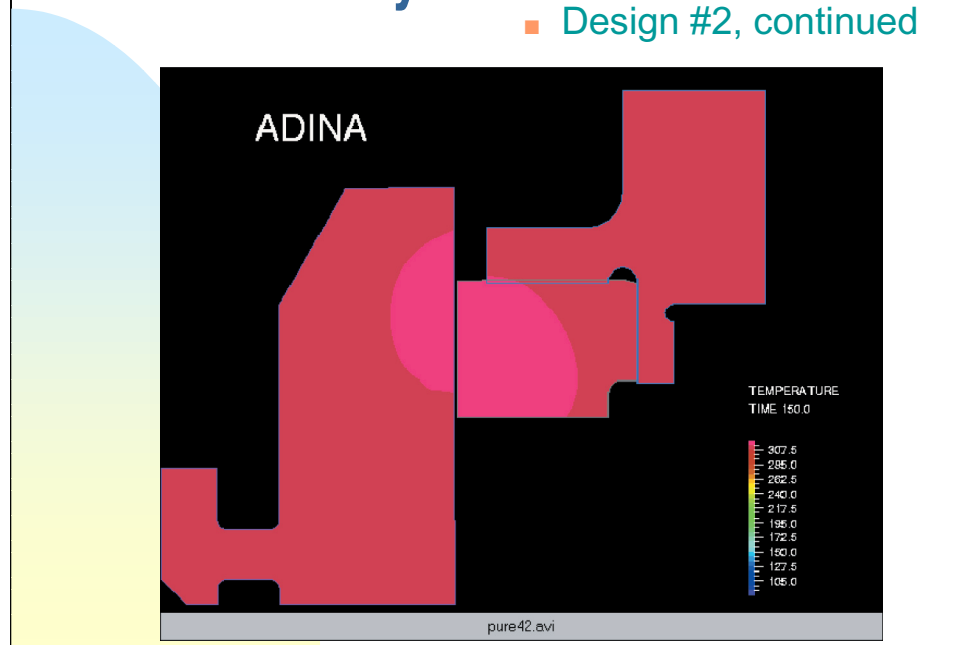
A revised composite stator design saves axial space and also provides favorable face coning for outward-pumping face seal



Temperature contours at final steady state

Transient Analysis

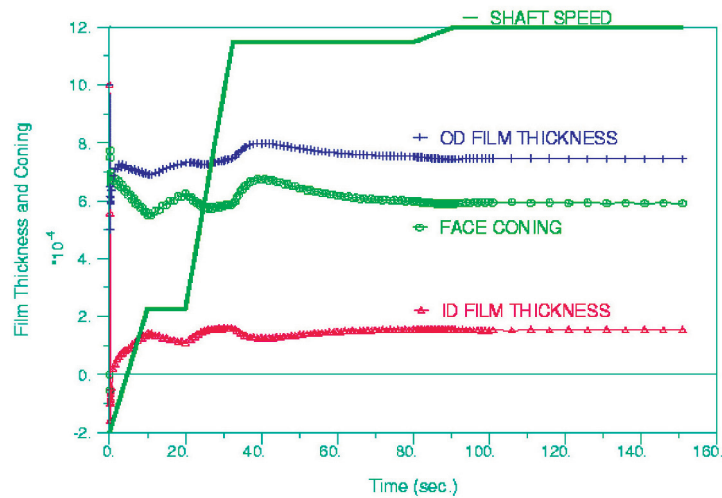
■ Design #2, continued



This animation shows a magnified view of seal deflection due to thermal and pressure effects. Colors are shown for temperature profiles.

Transient Analysis

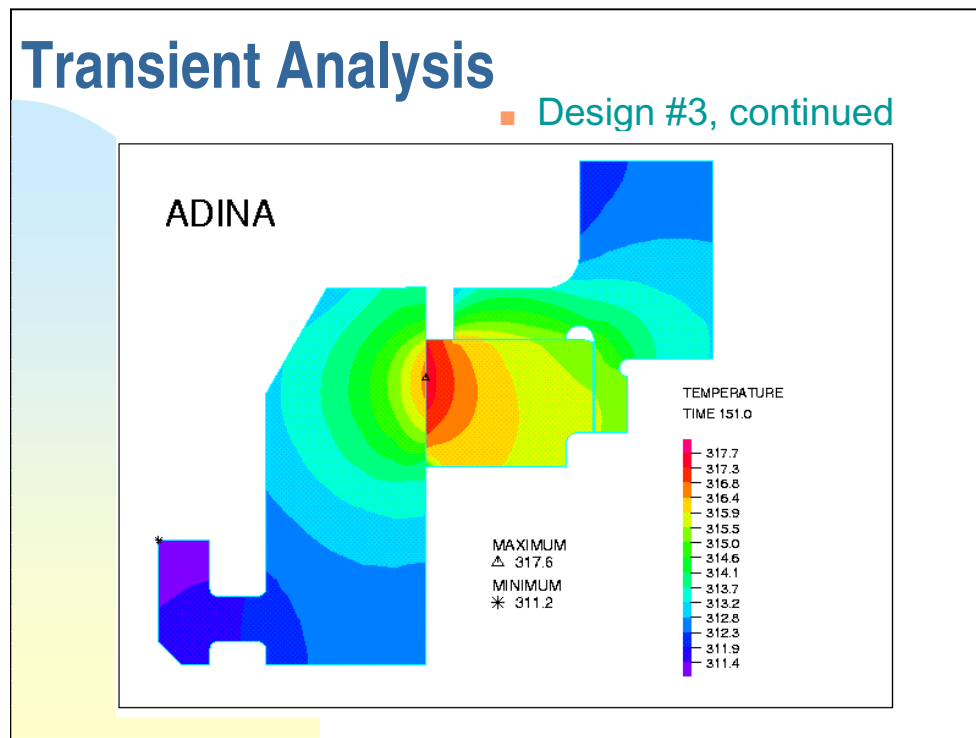
■ Design #3, composite stator



A further revised design reduces face coning provide more uniform gas film.

Transient Analysis

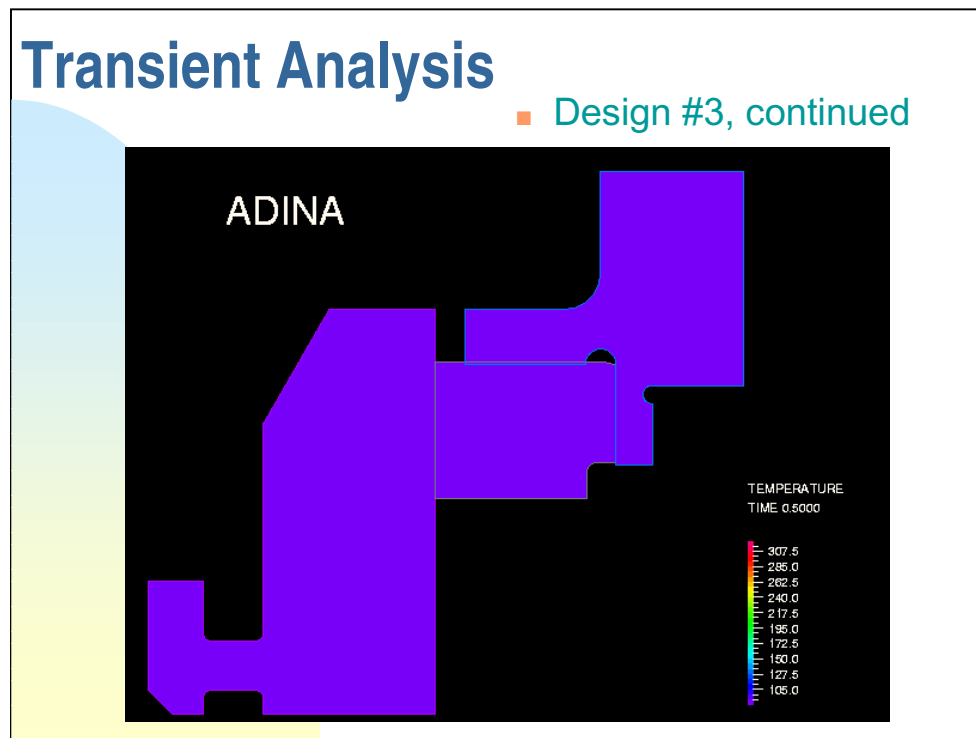
■ Design #3, continued



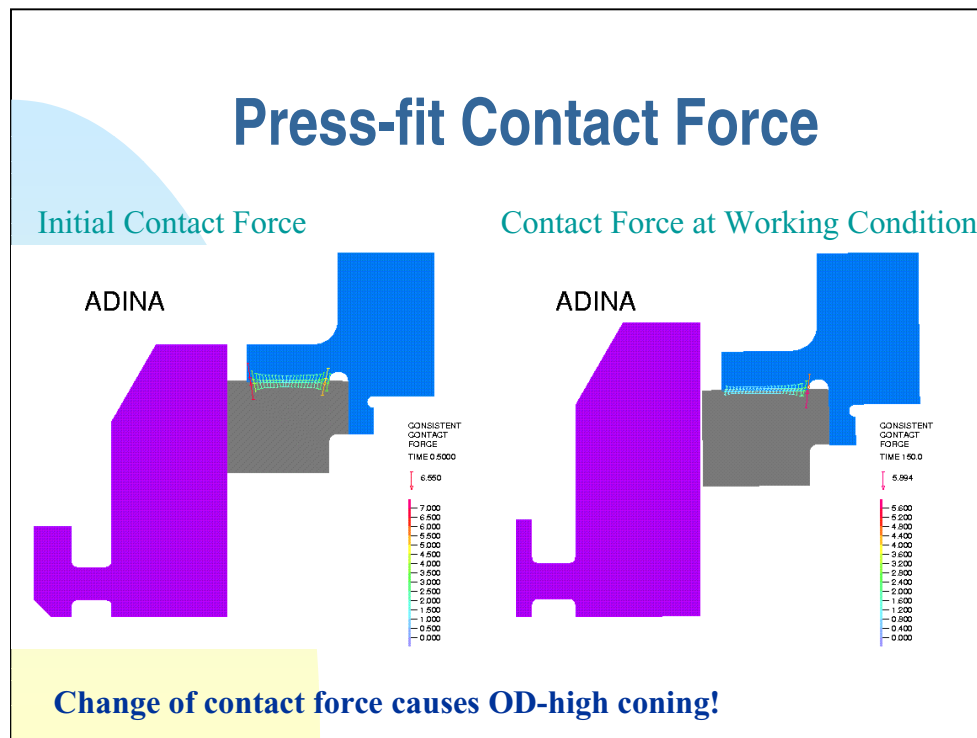
Final temperature contours at steady state.

Transient Analysis

■ Design #3, continued



Animation shows the magnified seal deflection during the transient. Colors are shown for temperature contours.



Thermal relief of contact stress in composite stator causes the stator face to cone in OD-high, which is opposite to usual thermal face coning. The amount of face coning is dependent on material differences and initial interferential fit. Those parameters can be used to achieve the desirable face coning.



Conclusion of Advance Analysis

- Link to general finite element package.
- Fully coupled FSI transient analysis
- High efficiency, 3D reduced to two 2-D problem
- High accuracy, real time boundary conditions can be imposed

The new design tool, incorporating a commercial finite element program ADINA, is capable to model transient fluid-structure interaction inside a general seal configuration, enabling designer to predict seal responses to speed, temperature and pressure changes in a time-dependent manner. Therefore, through evaluation of influences of different seal parameters, the application envelopes of conventional spiral groove face seal can be extended to larger diameter, higher speed range.

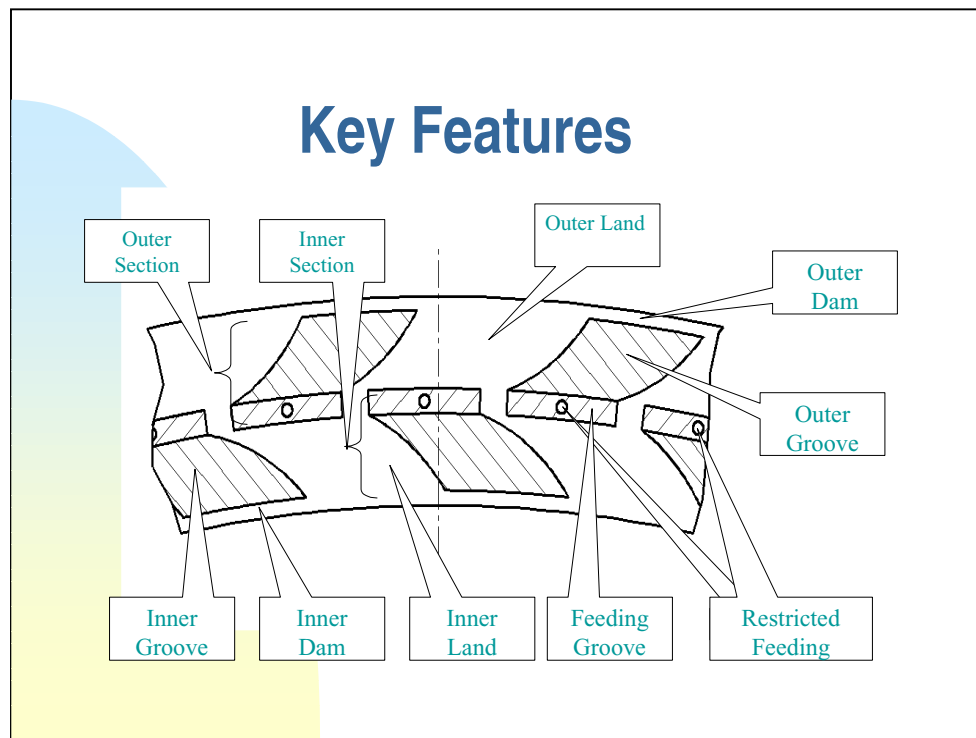


Double Spiral Groove Face Seal

--- Solution for high speed, large diameter apps.

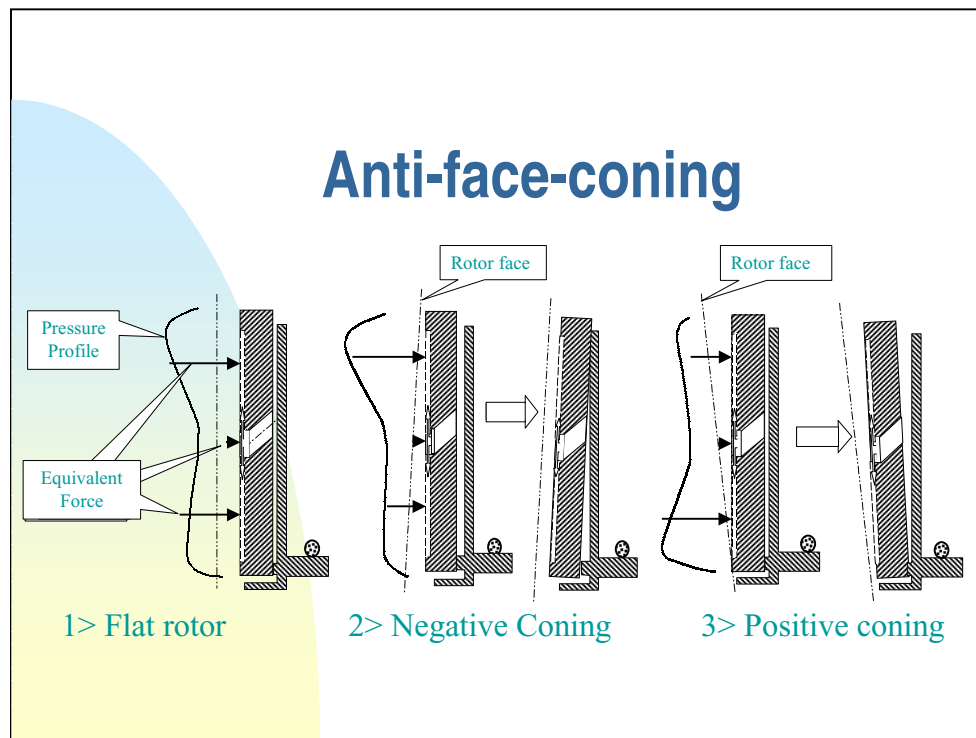
- **Strong anti-coning groove design.** (Divert double spiral grooves)
- **High film stiffness** (optimal groove shape and depth, combined hydrodynamic and hydrostatic effects)
- **Thick film** (reducing thermal deflection, tolerating face waviness)
- **Flexible stator ring** (adapt to rotor deflection)

In case that conventional spiral groove face seals cannot meet operational requirements in large turbine engines, a new double-spiral groove face seal has been designed. Two sets of seal sections and single center feed groove are used for the seal face. This configuration is able to provide higher film stiffness giving the stator more power to adapt to the deflection of the rotor.



Two basic strategies were used to achieve the high film stiffness, high coning restorability of the face seal. First, the seal face was redesigned to have strong anti-coning capability. A unique feature of the new seal is that the film will not be pinched under any condition. Secondly, orifice restrictive effects of the feeding holes are consciously used to enhance film stiffness whenever the film thickness in one or both seal sections is too large to render the hydrodynamic force effective.

The seal face consists of two sets of seal sections and a set of either segmented or connected deep grooves. Each seal section contains a hydrodynamic section, marked with an alternating groove and land pattern, and a dam section near the face edges. System fluid or gas, which is allowed to leak in a small amount, is fed into the middle feed grooves of the face seal through restricted feeding holes, and pumped inward and outward simultaneously by specially designed grooves on the stator and/or rotor face. This allows the seal to work through harsh conditions of severe face deflection. Since the fluid enters from the center, face coning will never cut off fluid from getting into the seal face.



When the rotor face deflection causes negative coning, the outer seal section is working in a convergent film (refer to the flow direction). That makes the groove work more effectively to create higher pressure in the hydrodynamic section. Therefore, the outer seal section generates more positive moment to open up the clearance at outer diameter. Meanwhile, the inner seal section is working at a divergent film. That reduces the hydrodynamic effects of the grooves. Less pressure, and therefore less negative moment, is generated by the inner seal section. The net increase of positive moment causes the stator ring to cone positively and form a uniform film thickness.

When the rotor face deflection causes positive coning effect, the outer seal section is working in a divergent film. That makes the groove work less effectively to create a high-pressure zone in the hydrodynamic section. Therefore, the outer seal section generates less positive moment. Meanwhile, the inner seal section is working at a convergent film, which increases the hydrodynamic effects of the grooves. Higher pressure, and therefore larger negative moment, is generated by the inner seal section to open up the clearance at inner diameter. The net increase of negative moment causes the stator ring to cone negatively and form a uniform film thickness.



Restrictive Orifice Design

Purposes:

- Control leakage

- Extend the range of high film stiffness

- Improve film stiffness

- Calculation of effectiveness

 - Empirical formula

 - Detailed CFD simulation

 - Integrated into double-spiral groove seal design code

The restricted orifice design is not only good at increasing coning film stiffness, but also effective to improve axial film stiffness. The pressure between seal faces is not only dependent on the hydrodynamic effects of spiral grooves, which is a function of film thickness, but is also affected by the hydrostatic effects of restricted orifices. The pressure in the feeding groove is strongly dependent on the flow amount through the feeding holes. As the film thickness increases, the pressure drop through the feeding hole increases. The opening force will drop as a result of lower pressure in the seal faces. At very thin film, the double-spiral grooves alone can generate enough film stiffness. The restricted feeding holes can be designed in such a way that it is most effective at relatively thick film, so that the seal has large film stiffness in a wide range of film thickness. In other words, once the seal faces open up, hydrodynamic effect from spiral groove diminishes gradually; the hydrostatic effect kicks in to continue the strong dependency of opening force on film thickness.

CFD Simulation

- Governing equations

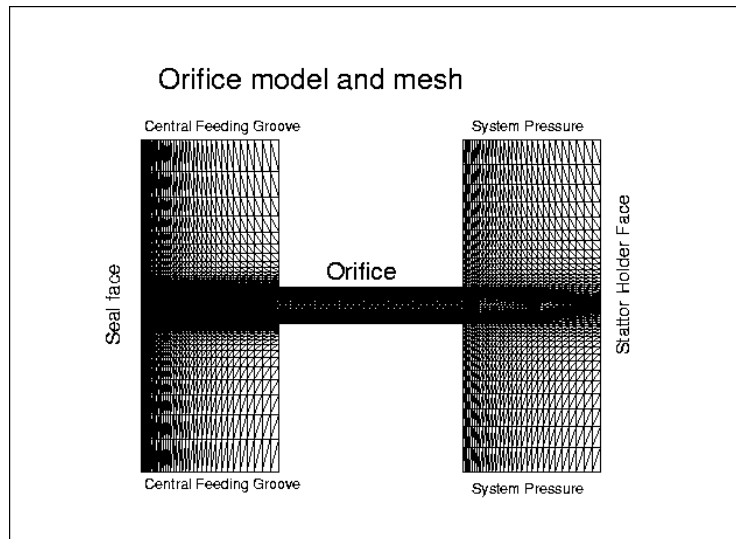
$$\frac{\partial U}{\partial t} + \nabla \bullet (F - G) - S = 0$$

Where:

$$U = \begin{bmatrix} \rho \\ \rho v \\ \rho e \end{bmatrix} \quad F = \begin{bmatrix} \rho v \\ \rho vv \\ \rho vh \end{bmatrix} \quad G = \begin{bmatrix} 0 \\ -pI + \tau \\ \tau \bullet v - q \end{bmatrix} \quad S = \begin{bmatrix} 0 \\ f \\ f \bullet v + q_s \end{bmatrix}$$

The orifice restrictive effects of the feeding holes play an important role in performance of the new seal. A simple formula for pressure drop over orifice can be found in current published literature, however a more accurate solution is required owing to the significance of pressure drop over the feeding hole at maximum operating condition. A CFD model was built to find the pressure drop as a function of flow rate.

Orifice Model



ADINA, a general fluid and solid finite element analysis program, is used to solve the problem. Because of the rotational surface at the flow exit, the flow is actually three-dimensional. Here each feeding hole and the feeding groove at the exit is modeled approximately as an axisymmetric case. Figure 6 shows the whole cut plane. But only half of the domain needs to be solved.

Orifice Results

Flow parameter:

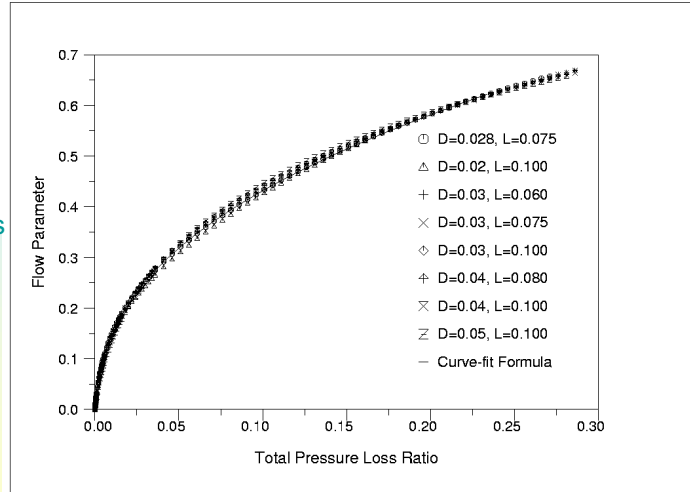
$$\phi = \frac{\dot{m}\sqrt{T^*}}{\frac{1}{4}\pi d^2 p_{Inlet}^* K}$$

Total pressure loss ratio

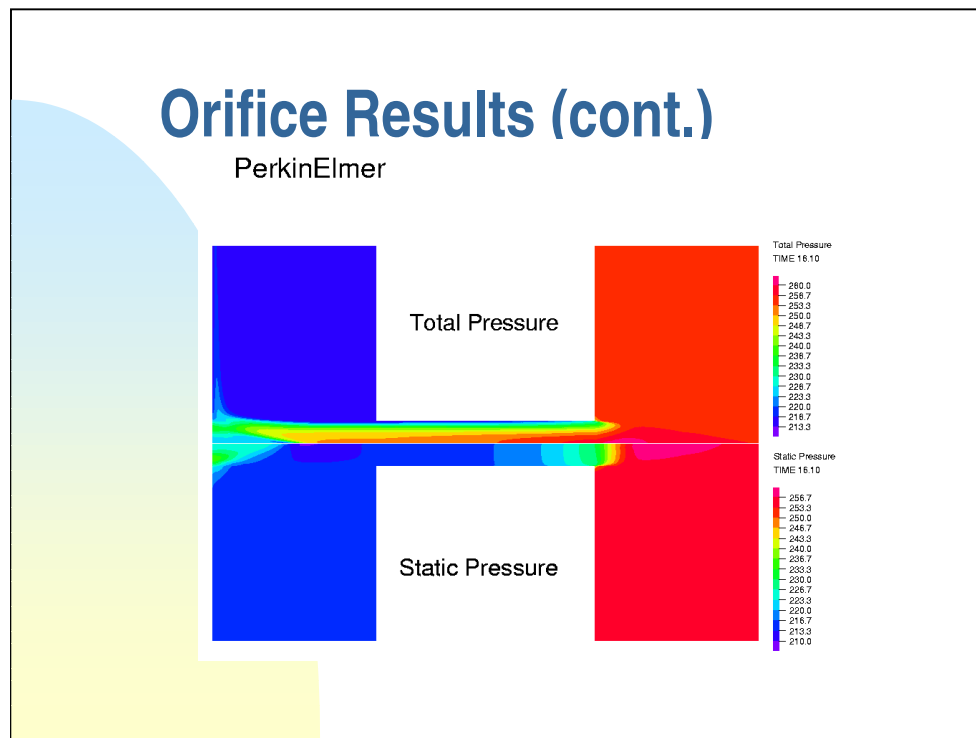
$$\eta = \frac{p_{Inlet}^* - p_{Exit}^*}{p_{Inlet}^*}$$

Empirical formula

$$\eta = 0.02756 \phi + 0.1637 \phi^2 + 0.8978 \phi^3 - 0.4184 \phi^4$$

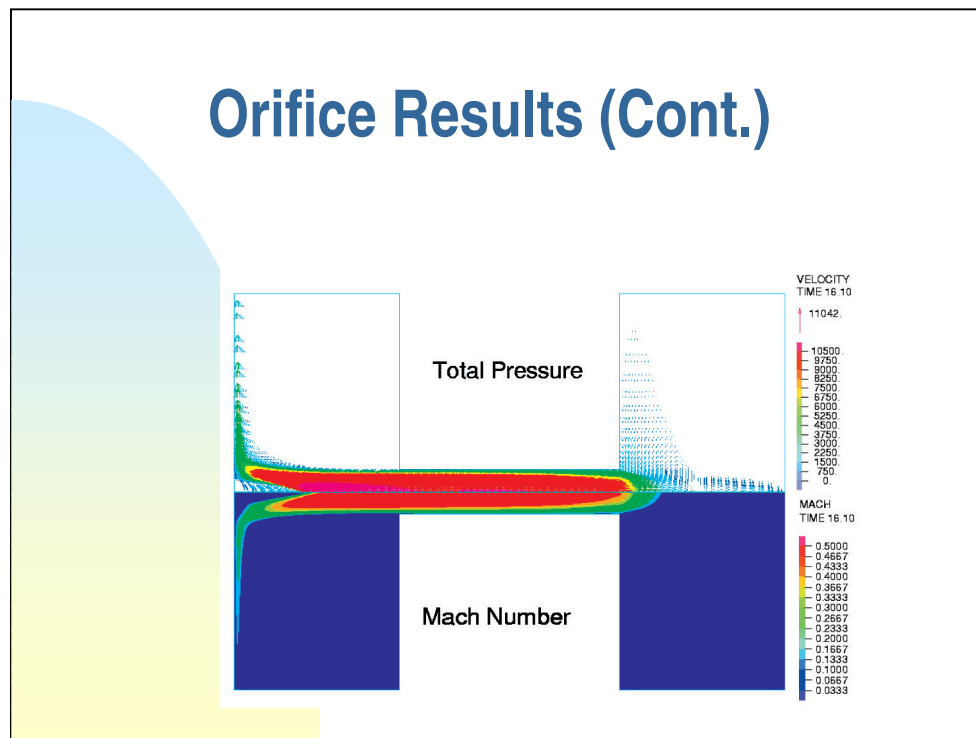


The purpose of this analysis is to find out the relationship between pressure drop and orifice flow rate for various orifice dimensions. Hopefully, their relationship can be expressed in a single formula and in terms of non-dimensional variables. Then the formula is plugged into the seal design code to obtain fast solutions. First, all the data for all possible choice of orifice dimensions are plotted together. In terms of flow parameter and pressure drop ratio, we found that they closely form a curve as shown in Figure 8. Therefore a curve-fitting program was used to approximate the data in a polynomial form.



This plot shows the total pressure contours on the upper half plane, and static pressure contours on the lower half plane for the orifice of current design at high pressure conditions. It easily can be seen that there are major total-pressure changes near the entrance and in the region of stagnation point on the rotor seal face. At large pressure difference conditions, the air stream speeds through the orifice and keeps straight ahead until it hits the rotor seal face. Because of high momentum of the flow, the sudden expansion at the orifice exit does not cause the air stream to spread sideward and slow down. The core flow is only slowed down when it hits the rotor seal face and spreads outward, causing great total-pressure loss due to large shear stresses.

Orifice Results (Cont.)



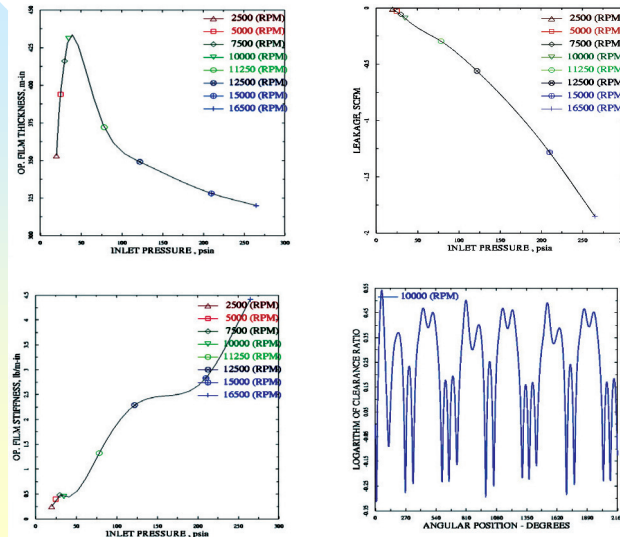


DSFS Design Code

- 2-D Reynolds equation
- 1-D Navier-Stokes equations
- Pressure deflection
- Thermal distortion
- Dynamic tracking
- Axisymmetric CFD orifice simulation
- Fully coupled fluid-structure solutions

The computer code for double-spiral groove face seal analysis and design is based on a well-calibrated gas seal design code for conventional spiral groove seals, which was developed by James Gardner a decade ago, and has been enhanced greatly by Prit Basu and Zack Williams. The first author added an integrated graphics package to it and built it into a web-based application program for ease of access within the local intranet. More advanced iterative solution methods are used to improve the efficiency and the ability to cope with the new geometric configuration was implemented by the first author.

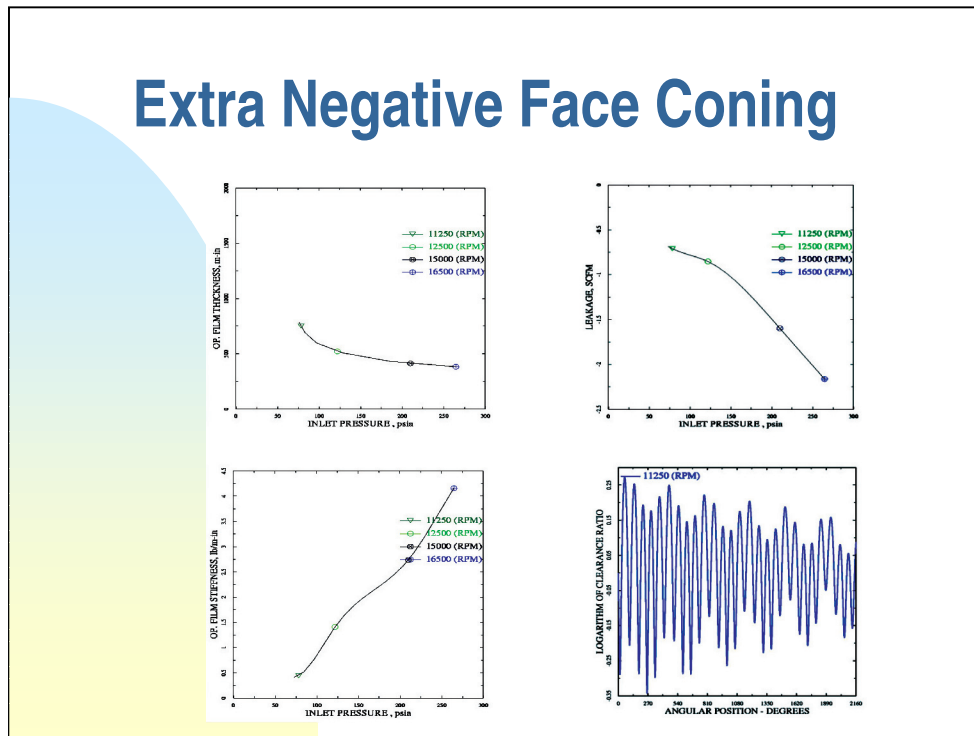
Seal Performance



With help of the design code developed for the new configurations, we are able to design the seal with outstanding performance at various rotor face coning conditions. First of all, the new seal was found quite insensitive to material properties. That is the most desirable characteristics since the choice of high temperature and tribological compatible materials is very limited. Second, the new seal works very well for all expected rotor face coning.

The strong capability of anti-coning of the new seal enables it to work under conditions of severe positive and negative rotor face coning. The seal can tolerate 0.010 inches of positive and 0.004 inches of negative face coning for all speeds higher than 2500 rpm. For high-pressure and high-speed conditions, the seal can deal with rotor face coning more than 0.010 inches of negative face coning. Negative face coning is usually deadly for single-spiral groove face seal. But for the divert double-spiral groove seal, it is no longer a problem.

Extra Negative Face Coning



If the rotor face has extra coning from either transient effects or some other unforeseen reasons, the seal is still able to work well.

If the rotor face has an extra negative coning of negative 0.010 inches (about 0.6 degrees), there exists OD contact for operating pressure difference of less than 50 psi. Extra rotor face coning of 0.010 inches is just too much for the stator ring to react at low speed and low pressure. But for higher pressure and speed, the seal works quite well.

Extra Positive Face Coning

The figure consists of four sub-graphs illustrating the effects of extra positive face coning on bearing performance at different rotational speeds (RPM).

- Top Left Graph:** Shows the relationship between Inlet Pressure (psi) on the x-axis (0 to 300) and Oil Film Thickness (mils) on the y-axis (0 to 150). The curves for various RPMs (2500, 5000, 7500, 10000, 11250, 12500, 15000, 16500) show a peak in film thickness around 100-150 psi, followed by a decline at higher pressures. The 11250 RPM curve shows the highest peak thickness, reaching approximately 145 mils.
- Top Right Graph:** Shows the relationship between Inlet Pressure (psi) on the x-axis (0 to 300) and Leakage (SCM) on the y-axis (0 to 17). The curves for various RPMs show a U-shaped relationship, with leakage reaching a minimum around 150-200 psi. The 11250 RPM curve shows the lowest minimum leakage, around 12 SCM.
- Bottom Left Graph:** Shows the relationship between Inlet Pressure (psi) on the x-axis (0 to 300) and Oil Film Stiffness (psi) on the y-axis (0 to 3.5). The curves for various RPMs show a generally increasing trend in stiffness with increasing inlet pressure. The 11250 RPM curve shows the highest stiffness, reaching approximately 3.4 psi at 300 psi inlet pressure.
- Bottom Right Graph:** Shows the relationship between Angular Position (Degrees) on the x-axis (0 to 180) and the Logarithm of Clearance Ratio on the y-axis (-0.15 to 0.05). The shaded area represents the range of clearance ratios, with the 11250 RPM curve showing the highest values, peaking around 0.04 at 0 degrees.

With sufficient margins, the seal can operate successfully under extra rotor face coning conditions ranging from -0.004 to 0.004 inches.



Summary for Double-spiral Groove Face Seal

- The seal:
 - Excellent face coning recovery capability.
 - Simple and the cost-effective.
 - High film stiffness, robust.
- The computer code.
 - Pressure deflection.
 - Thermal distortion.
 - Hydrodynamic effects of spiral grooves.
 - Restrictive orifice effects.

ABRADABLE SEAL DEVELOPMENTS AT TECHNETICS

Doug Chappel and Harold Howe
Technetics Corporation
Indianapolis, Indiana

Technetics
CORPORATION

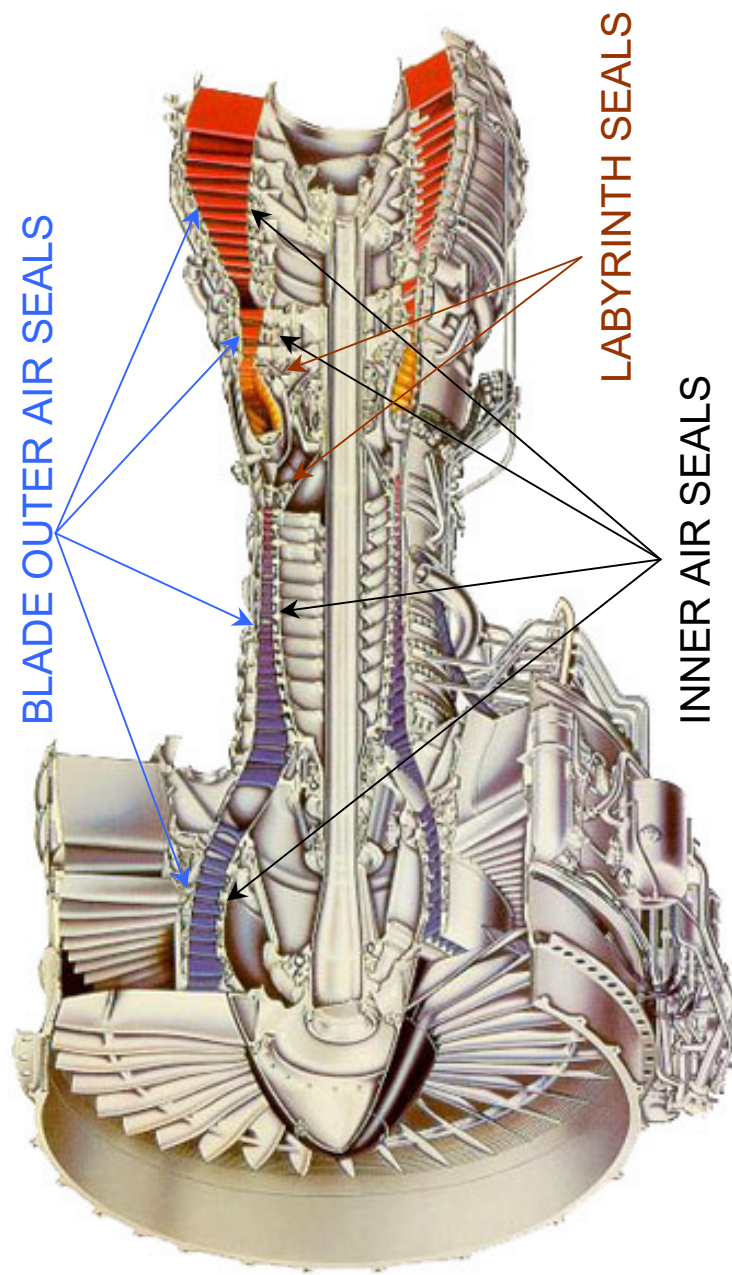


Abradable Seal Developments At Technetics

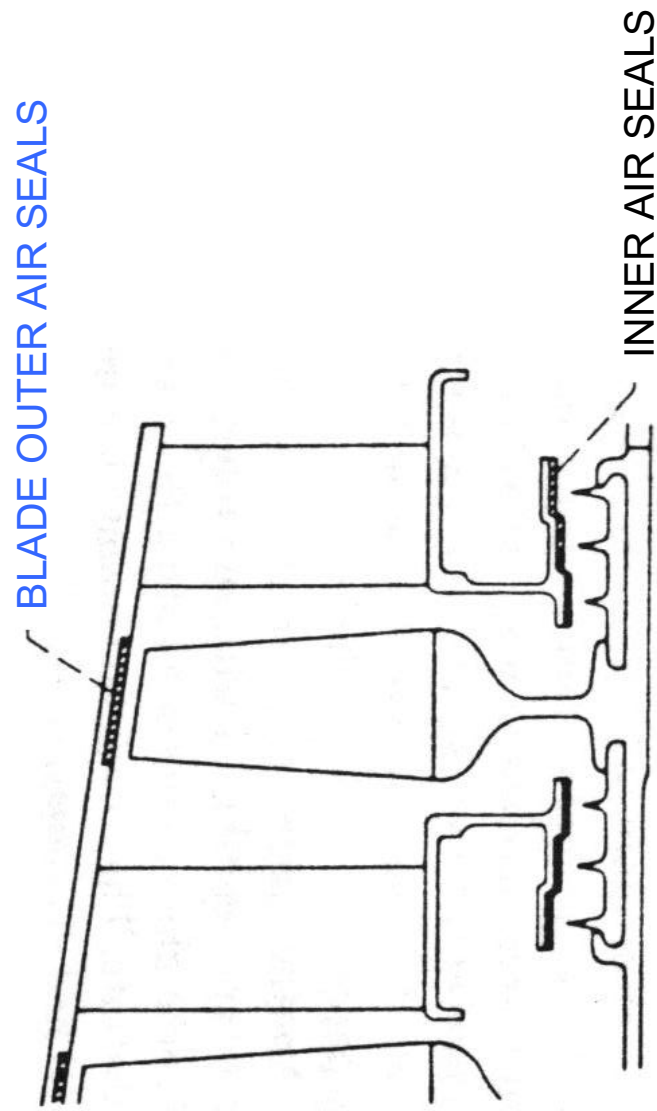
Doug Chappel
Harold Howe

NASA Seal / Secondary
Air System Workshop
October 25, 2000

Typical Abradable Seal Applications

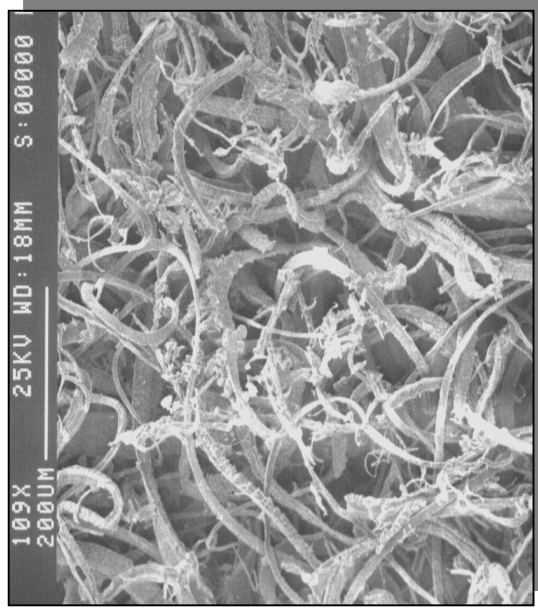


Typical Abradable Seal Applications

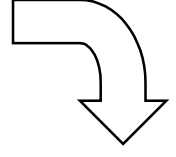
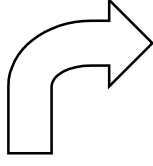


What Is Feltmetal®?

Micron Size Fiber Sinter Bonded Into A Continuous Felt



- Typically Hast-X or FeCrAlY
- Density Range 10 – 50%
- UTS Range 500 – 3000 psi



Key Requirements For Abradable Seal Materials

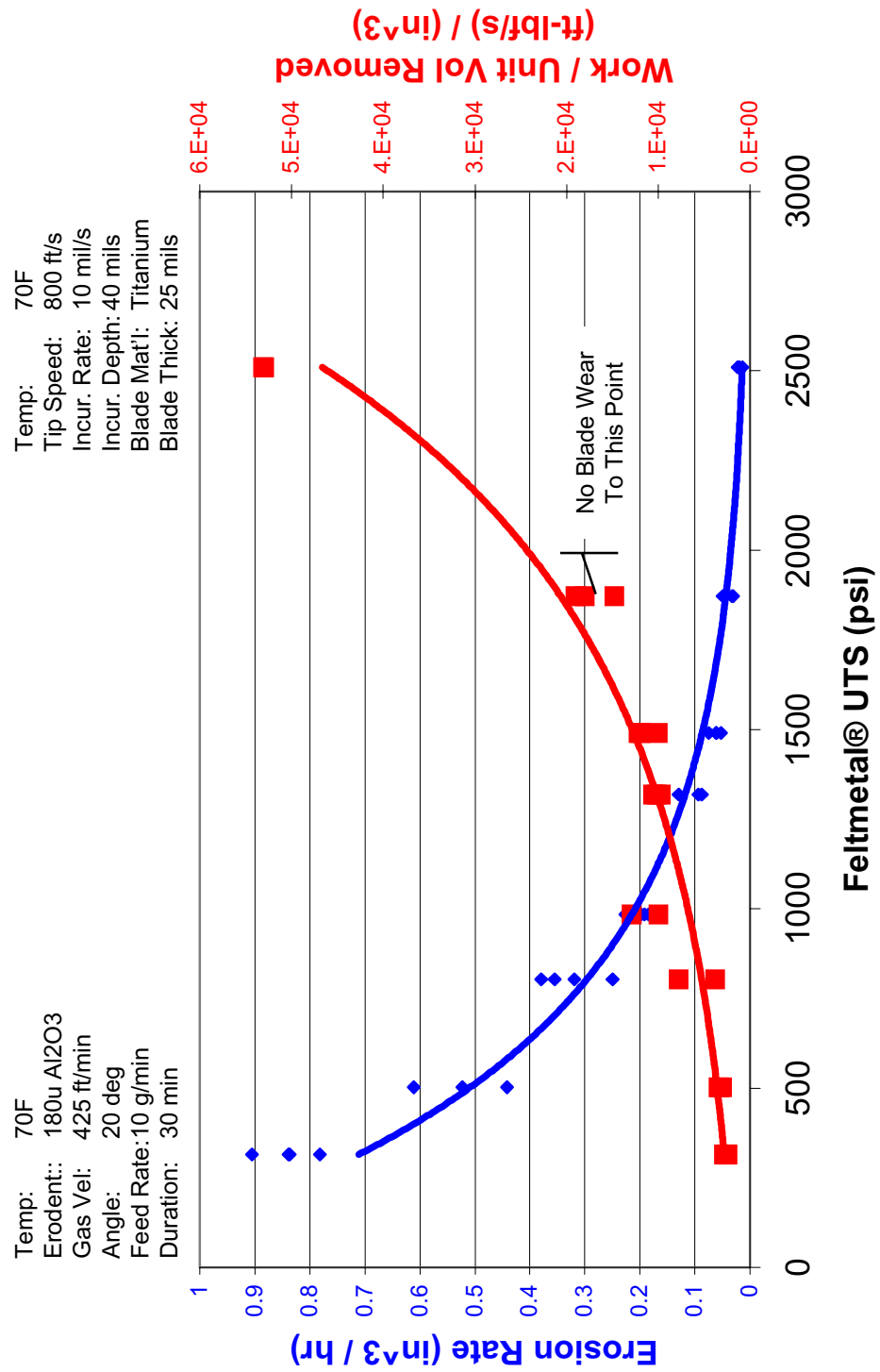
- Clean Cutting With Minimal Blade Wear
- Erosion Resistance
- Operating Life

Performance Is Application Specific

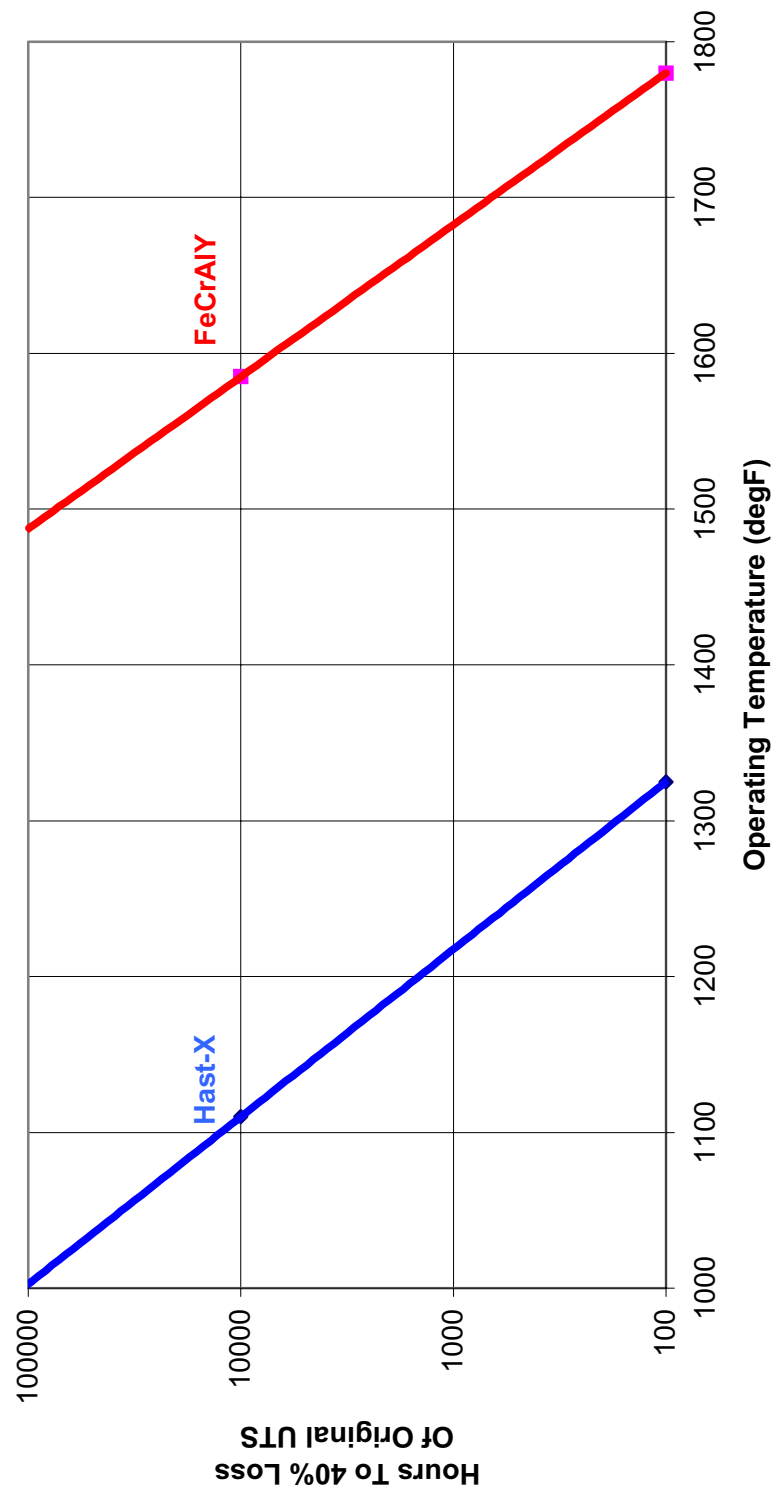
<i>Typical GT Compressor</i>	AERO	UTILITY
Max Tip Speed	1400 fps	1200 fps
Max Temp	1300 F	1200 F
Incursion Rate	10 mil/sec	0.1 mil / sec
Incursion Depth	20 mils	40+ mils
Blade Material	Ni, Ti	Steel
Blade Thickness	25 mils	Up to 300 mils

Erosion And Abradability Are Conflicting Properties

Felt Tensile Strength Is The Driving Material Property



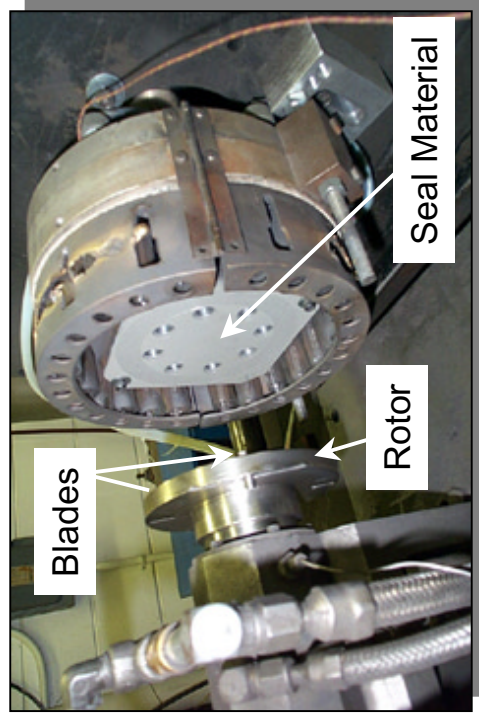
Material Selection Based On Operating Environment



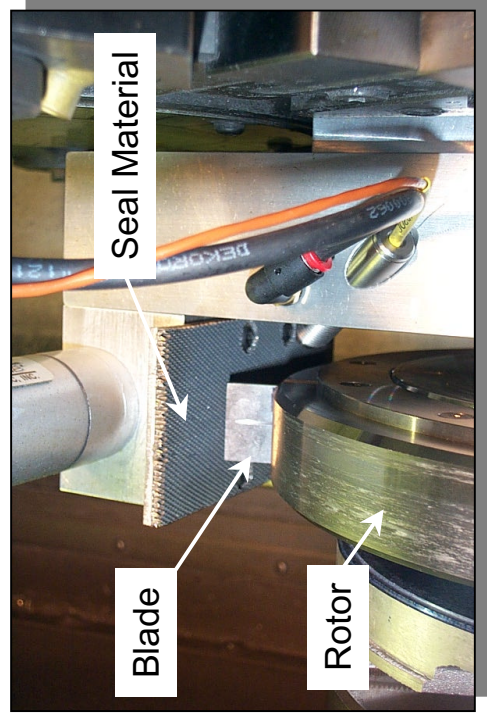
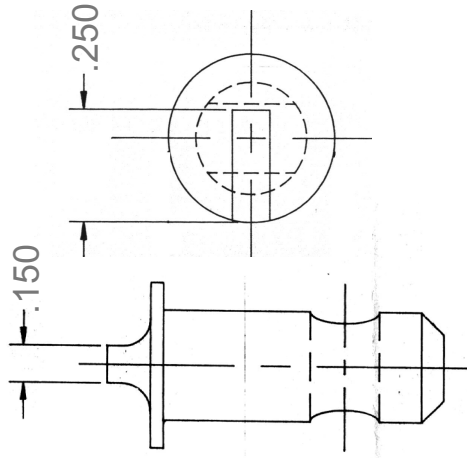
Majority Of Available Literature Has Aero Focus And Experimental Evaluations Run On Disparate Test Rigs

Title	Author(s)	Organization	Date
Advanced Seal Technology	Mahler	P&W	1972
Development Of Abradable Gas Path Seals	Shiembob	P&W	1974
Continued Development Of Abradable Gas Path Seals	Shiembob	P&W	1975
Aerodynamic Performance Of Conventional And Advanced Design Labyrinth Seals With Solid-Smooth Abradable And Honeycomb Lands	Stocker, Cox, Holle	Detriot Diesel Allison	1977
Friction And Wear Of Sintered Fibermetal Abradable Seal Materials	Bill, Shiembob	AVRADCOM, P&W	1977
Development Of Improved Abradable Compressor Gas Path Seals	Erickson, Jarvi	Technetics	1977
Friction And Wear Of Several Compressor Gas-Path Seal Materials	Bill, Wisander	AVRADCOM	1978
Some Cosideration Of The Performance Of Two Honeycomb Gas Path Seal	Bill, Shiembob	AVRADCOM, P&W	1980
Rub Energetics Of Compressor Blade Tip Seals	Lavery	P&W	1982
Improved Compressor Performance Using Recessed Clearance (Trenches) Over Rotor	Beacher, Wisler	GEAE	1986
NiCrAl / Bentonite Thermal Spray Powder For High Temperature Abradable Seals	Clegg, Mehta	-	1987
The Wear Mechanisms Occurring In Abradable Seals Of Gas Turbines	Borel, Nicell, Schlapfer, Schmid	Sulzer Plasma-Teknik	1989
Thermally Sprayed Coating Systems For Surface Protection And Clearance Control Applications In Aero Engines	Rhys-Jones	-	1990
The Selection And Performance Of Thermal Sprayed Abradable Seal Coatings For Gas Turbine Engines	Novinski	Metco	1990
Basic Characteristics Of Different Abradable Coatings	Oka, Nakahira, Noritoh	-	1990
A High Performance Alternative To NiCrAl / Bentonite For Gas Turbine Abradable Seals	Dorfman, Novinski, Kushner, Rotolico	-	1992
Advances In Abradable Coatings For Gas Turbine	Nicoll, Schmid	Sulzer Innotec	1994
A Review Of Clearance Control Wear Mechanisms For Low Temp Aluminum Silicon Alloys	Dorfman, Ghasripor, Russo, Schmid	Sulzer Metco/Innotec	1997
Abradables Improve Gas Turbine Efficiency	Ghasripor, Schmid, Dorfman	Sulzer Innotec	1997
Optimizing The Performance Of Plasma Sprayed Clearance Control Coatings Up To 850C	Ghasripor, Schmid, Dorfman, Wei, Correa, Tilikaran	Sulzer Metco/Innotec	1998
Abradable Coatings For Gas Path Seals In Turbine Engines	Pritchard, Rush, Kiela	VAC AERO	1998
CABC Family Of Sprayed Abradable Materials	Wolfla	Chromalloy	1999

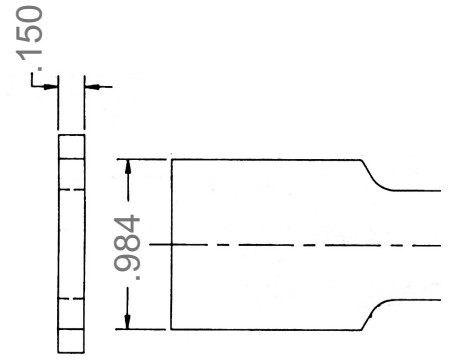
Initial Goal: Quantify Feltmetal® Performance For Utility Gas Turbine Type Applications



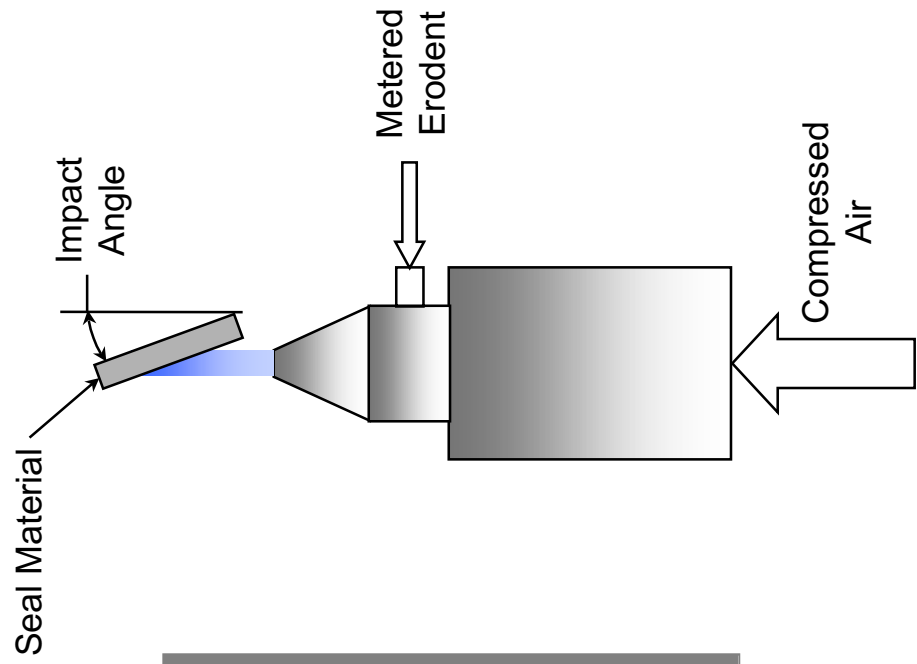
High Speed
Rub Rig



Low Speed
Rub Rig



Erosion Test Rig



High Speed Abradability Test Results

Temp: 70F

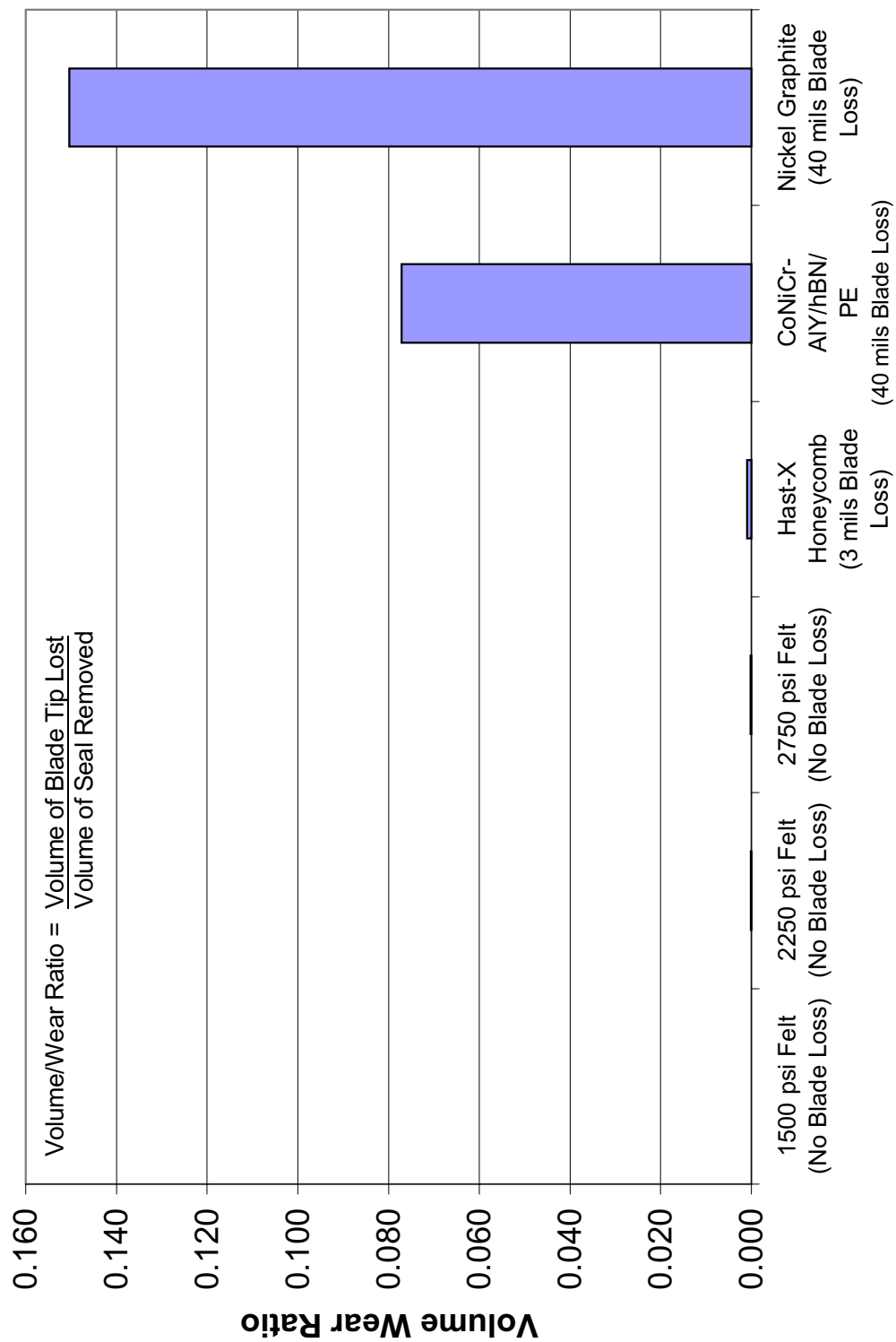
Tip Speed: 900 ft/s

Incur. Rate: 0.11 mil/s

Incur. Depth: 40 mils

Blade Mat'l: 403 SS

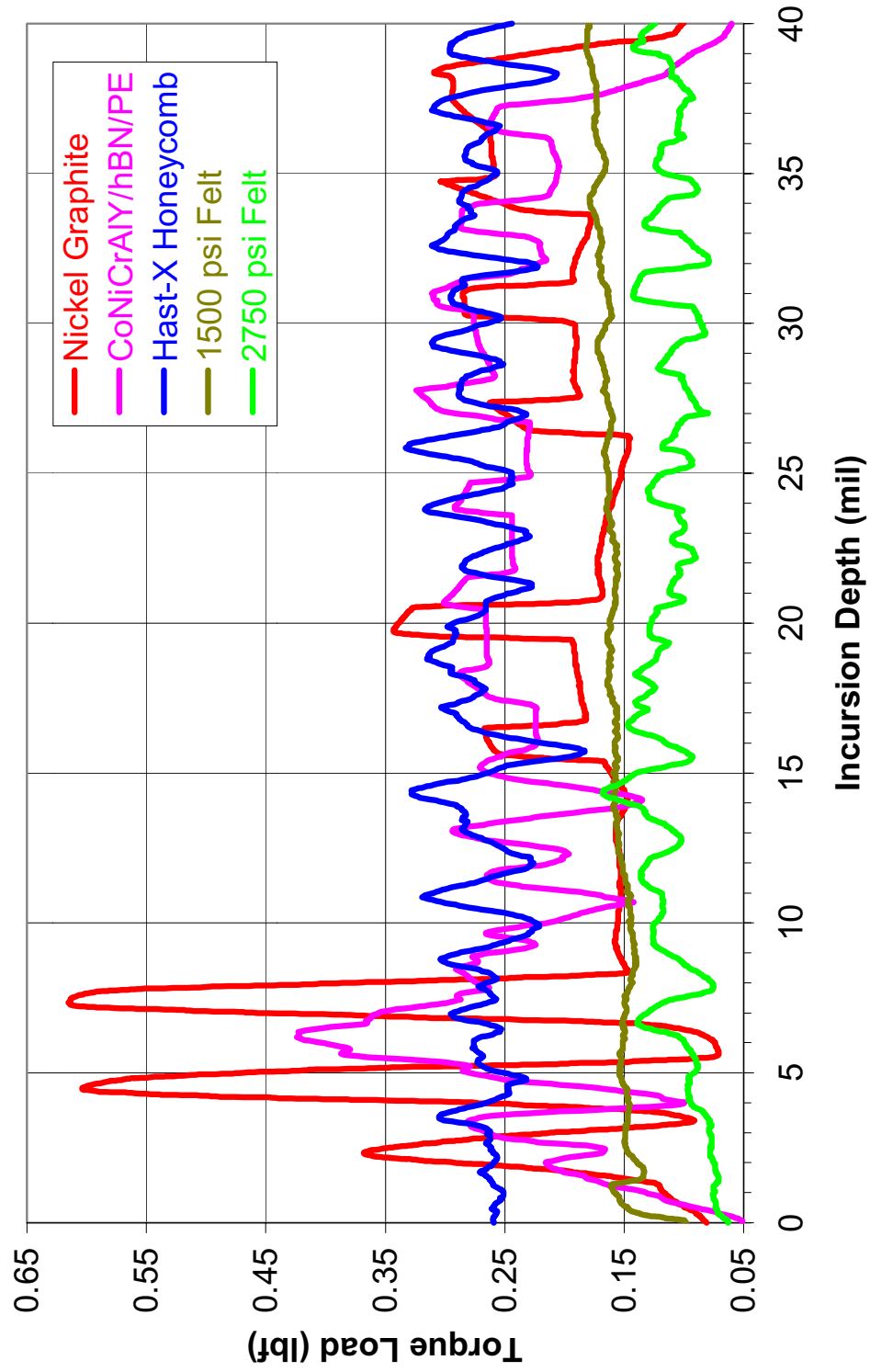
Blade Thick: 150 mils



High Speed Abradability Test Results

Temp: 70F
Tip Speed: 900 ft/s
Incur. Rate: 0.11 mil/s
Incur. Depth: 40 mils
Blade Mat'l: 403 SS
Blade Thick: 150 mils

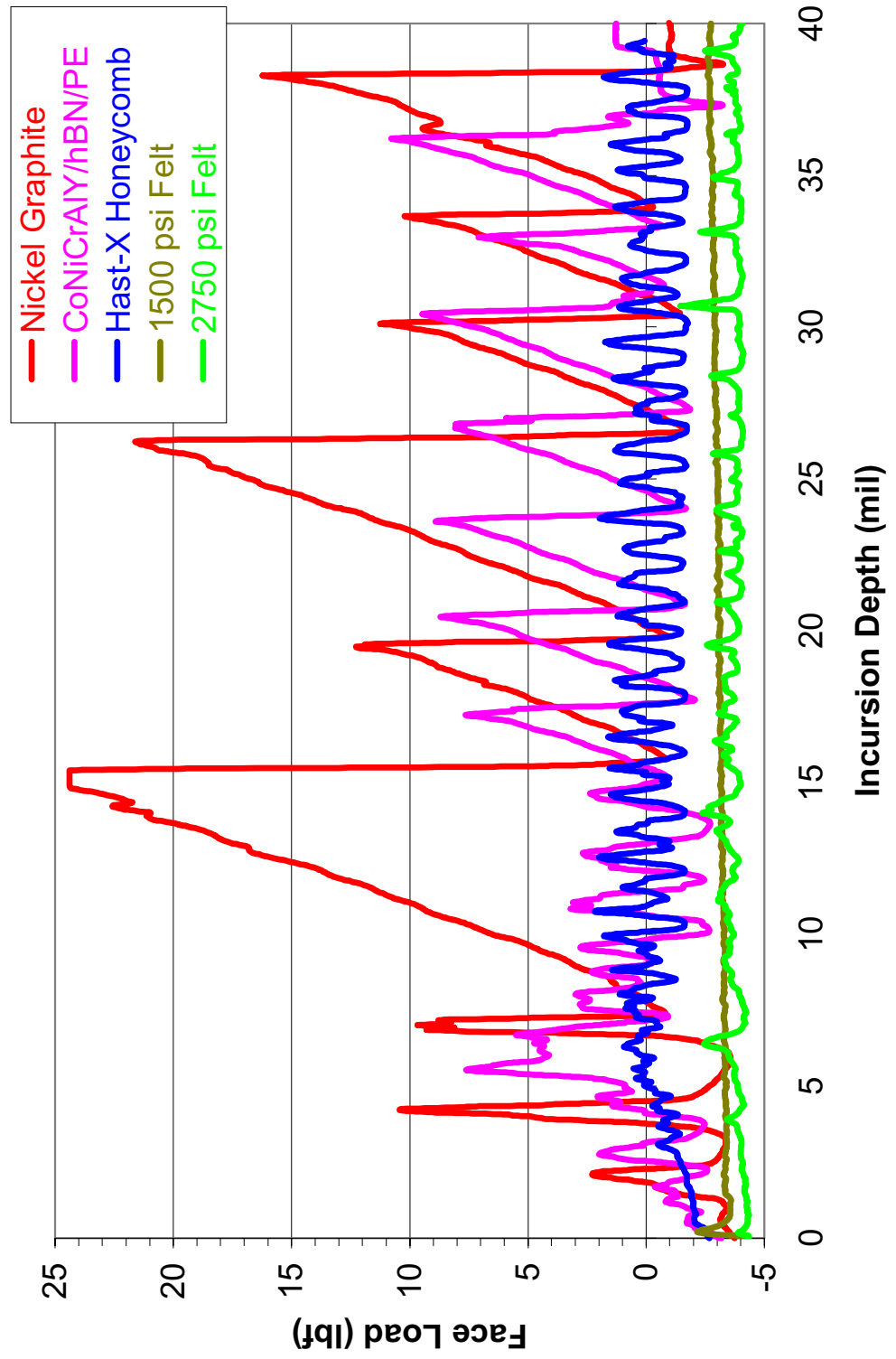
Circumferential Torque Imparted To Seal Material



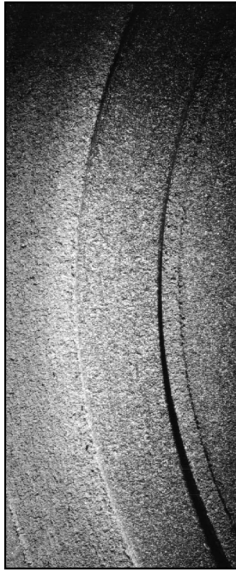
High Speed Abradability Test Results

Temp: 70F
Tip Speed: 900 ft/s
Incur. Rate: 0.11 mil/s
Incur. Depth: 40 mils
Blade Mat'l: 403 SS
Blade Thick: 150 mils

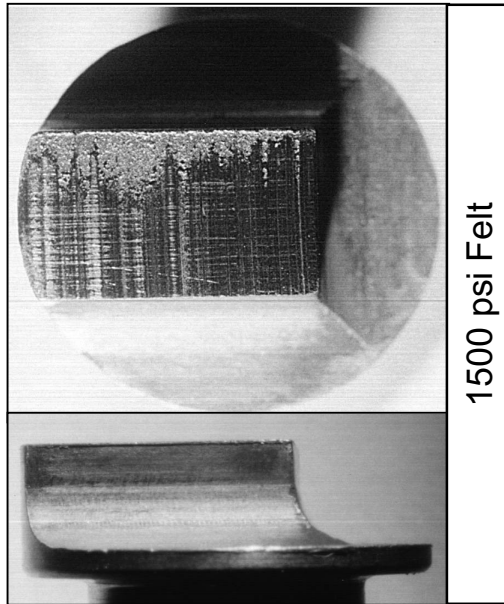
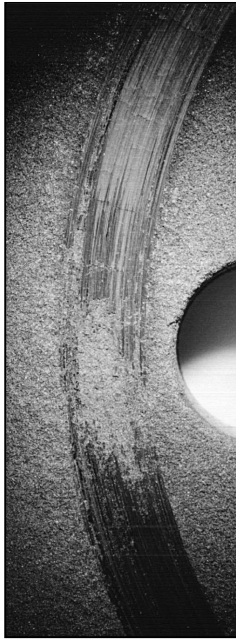
Axial Face Load Imparted To Seal Material



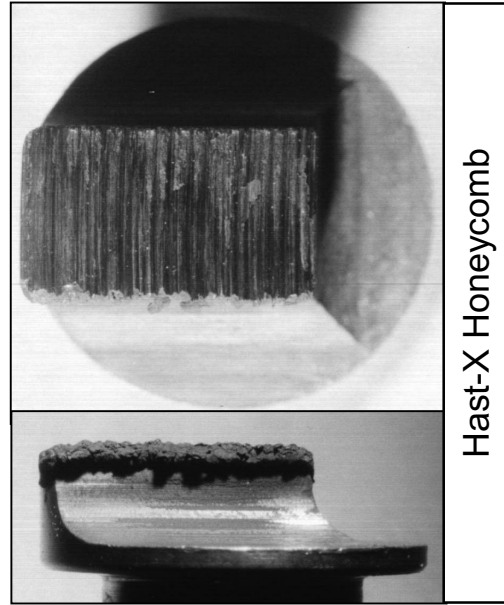
1500 psi Felt
Rub Track



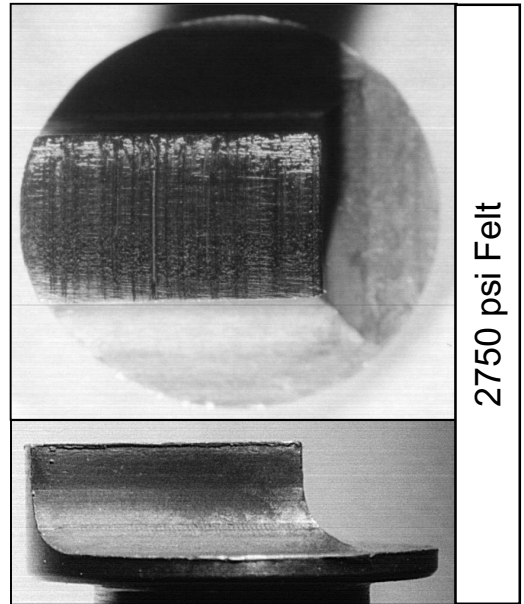
NiGr
Rub Track



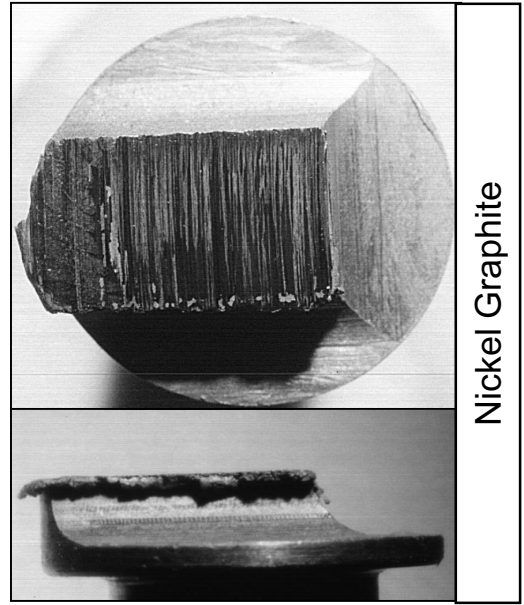
1500 psi Felt



Hast-X Honeycomb



2750 psi Felt

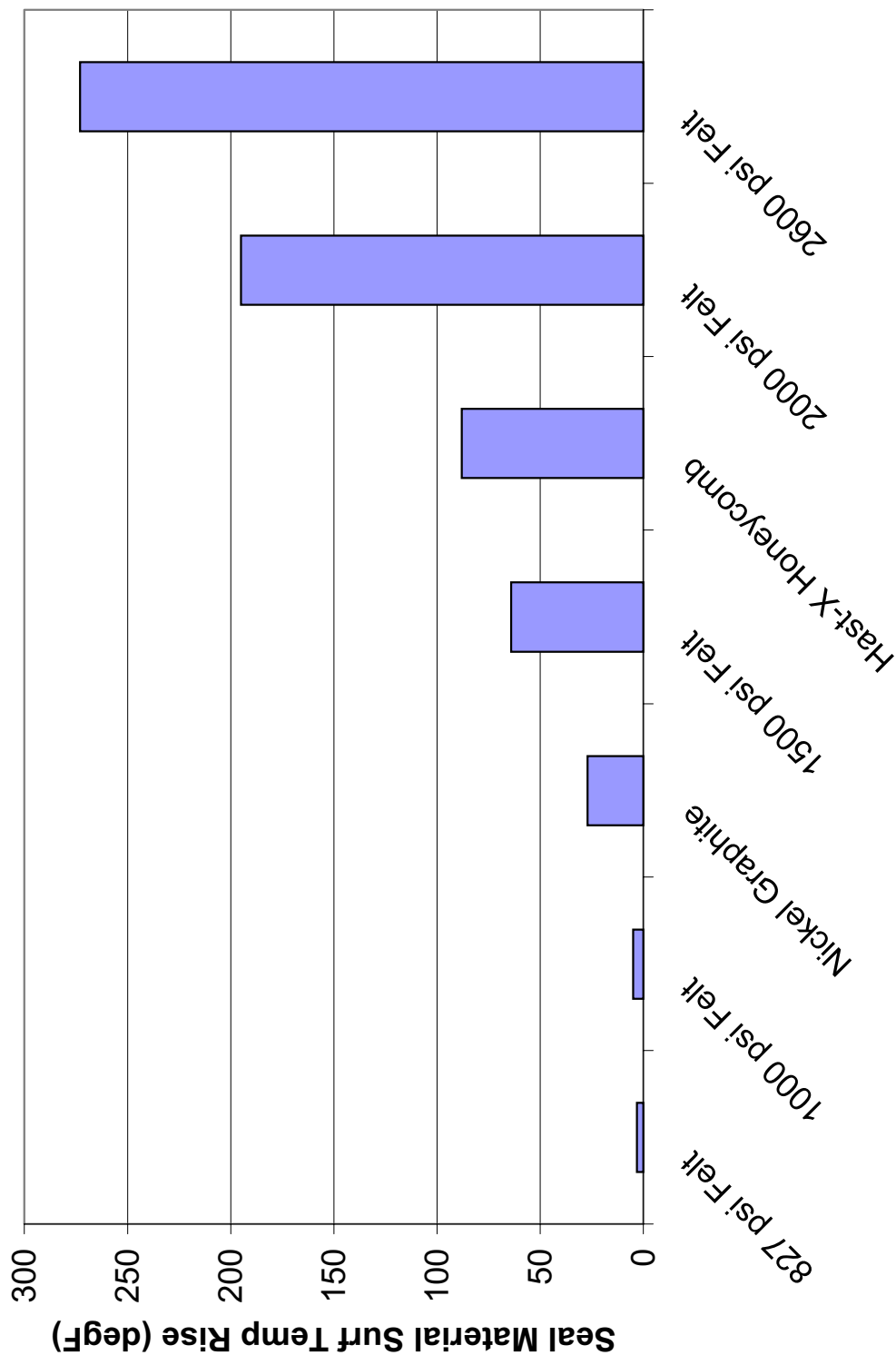


Nickel Graphite

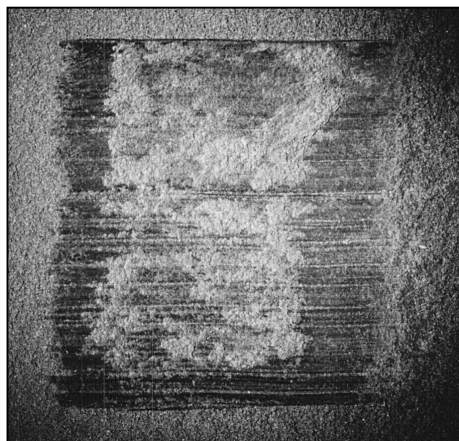
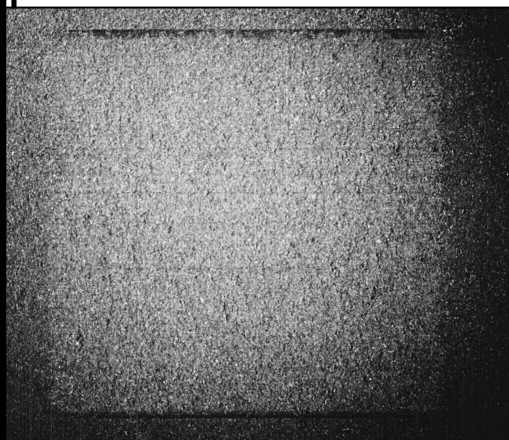
Temp: 80F
 Tip Speed: 155 ft/s
 Incur. Rate: 0.1 mil/s
 Incur. Depth: 40 mils
 Blade Mat'l: 403 SS
 Blade Thick: 150 mils

Low Speed Abradability Test Results

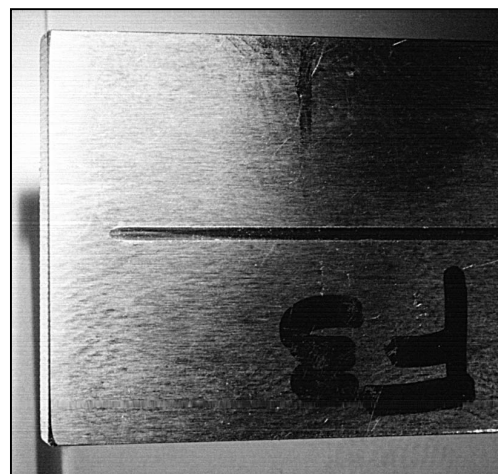
Blade Temperature Rise Not Quantified



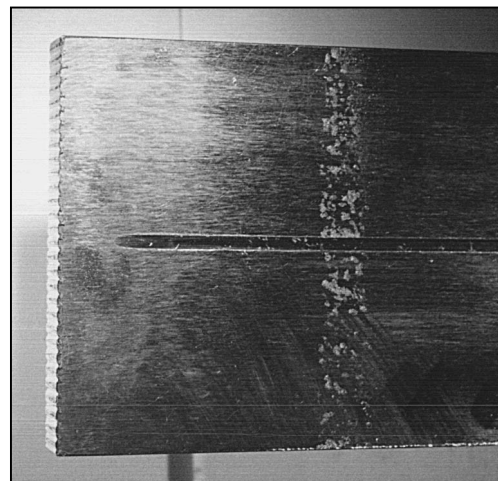
Rub Tracks



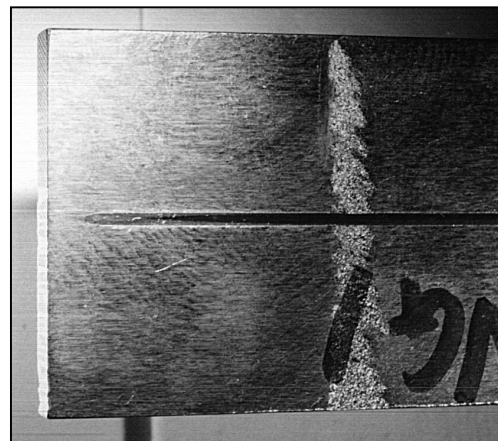
Blades



1500 psi Felt



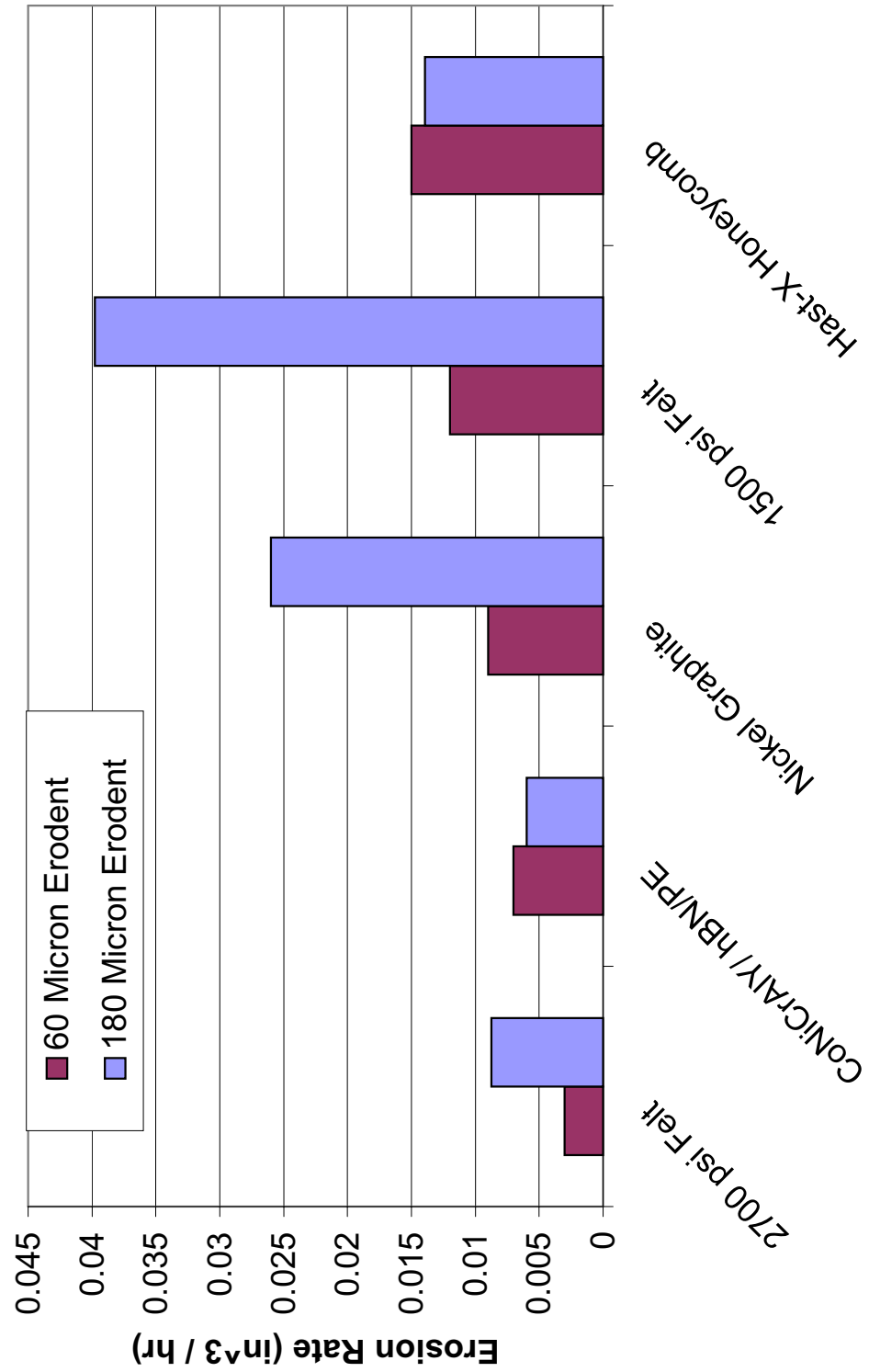
Hast-X Honeycomb



Nickel Graphite

Erosion Test Results

Temp: 70F
 Eroder:: Al2O3
 Gas Vel: 425 ft/min
 Angle: 20 deg
 Feed Rate: 10 g/min
 Duration: 30 min



Conclusions

- Abradable Materials Are Promising For Use In Industrial Gas Turbines
- Feltmetal[®] Can Be Tailored To Meet Specific Application Requirements

Future Work

- Low Speed Rub Blade Temperature
- Continued Parametric Testing
(Temp, Materials, Erodent Size, etc)
- Knife Edge Geometries
- Establish Industry Standards For
Erosion And Abradability Testing

HIGH TEMPERATURE METALLIC SEAL DEVELOPMENT

Amit Datta
Advanced Components and Materials, Inc.
E. Greenwich, Connecticut

D. Greg More
The Advanced Products Company
North Haven, Connecticut

High Temperature Metallic Seal Development

Dr. Amit Datta, President,
Advanced Components & Materials, Inc.

Mr. D.Greg More, Engineering Manager,
The Advanced Products Company

Advanced

Outline

- Challenges
- Development Approach
- Stress Relaxation Studies
- Future Plans for Seal Testing

Advanced

Challenges

- Current Metallic Seals are Made of γ' Hardened Superalloys
- Application Limitation Above γ' solvus
- No Suitable Metallic Seal Above 1300 °F for Long-term Operation

Advanced

Current Challenges

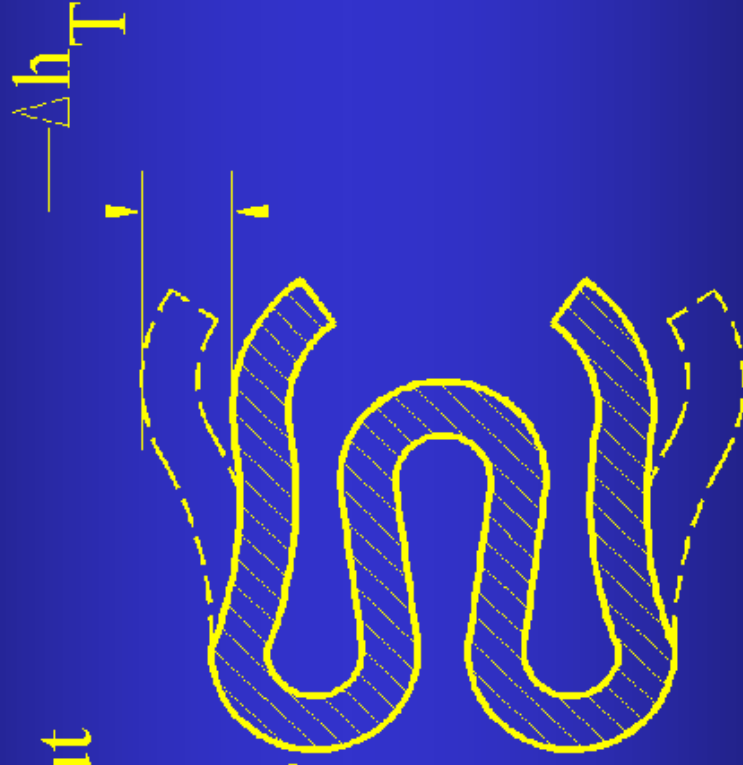
- Stress Relaxation about

γ' solvus

- Seal Compression Δh_T is relaxed as Δh_{PL}

Increases with
Time and
Temperature

- $\Delta h_T = \Delta h_{EI} + \Delta h_{PL}$
Sealing Force $\propto \Delta h_{EI}$



Advanced

Development Approach

- Screen Metallic Alloys Using ASTM E-328 Stress Relaxation Tests in the 1600-1800 °F Range
- Fabricate and Evaluate Seals in the 1600-1800 °F Range

Advanced

Development Approach

Candidate Materials:

- Oxide Dispersion Strengthened Alloys
 - PM 1000, MA-956, MA-754
- Refractory Alloys
 - Mo/Re, TZM, Mo/W, Proprietary Composite Alloy

Advanced

Development Approach

- Challenges
- Manufacturing Process Development
Joining and Forming
- Cost-effective Oxidation Protection
Scheme for Refractory Alloys

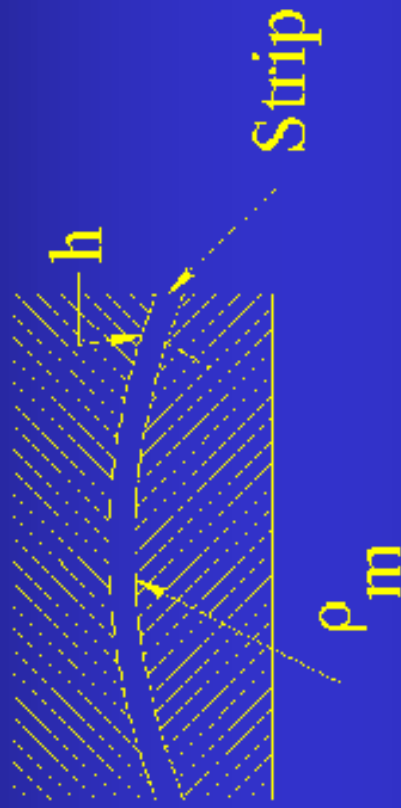
Advanced

Stress Relaxation Studies

- ASTM E-328 Test:

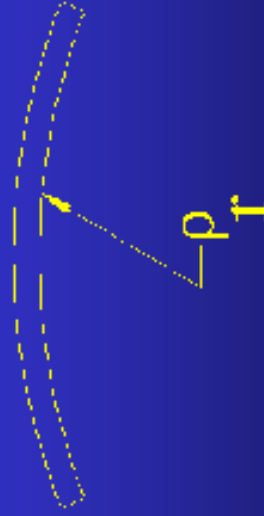
ρ_m - mandrel radius

ρ_r - relaxed radius



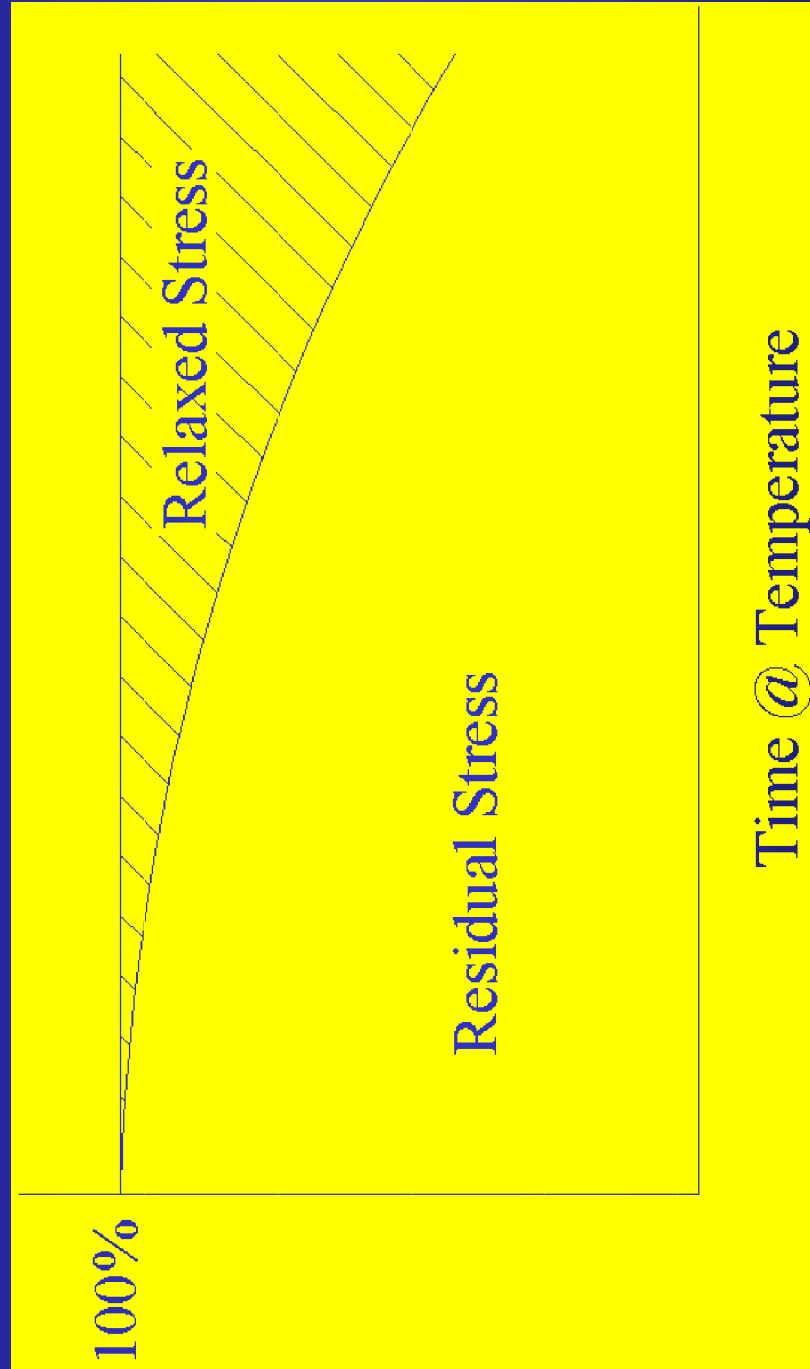
Residual Stress:

$$\sigma_{EI} = E \cdot h / 2 \left(1 / \rho_m - 1 / \rho_r \right)$$



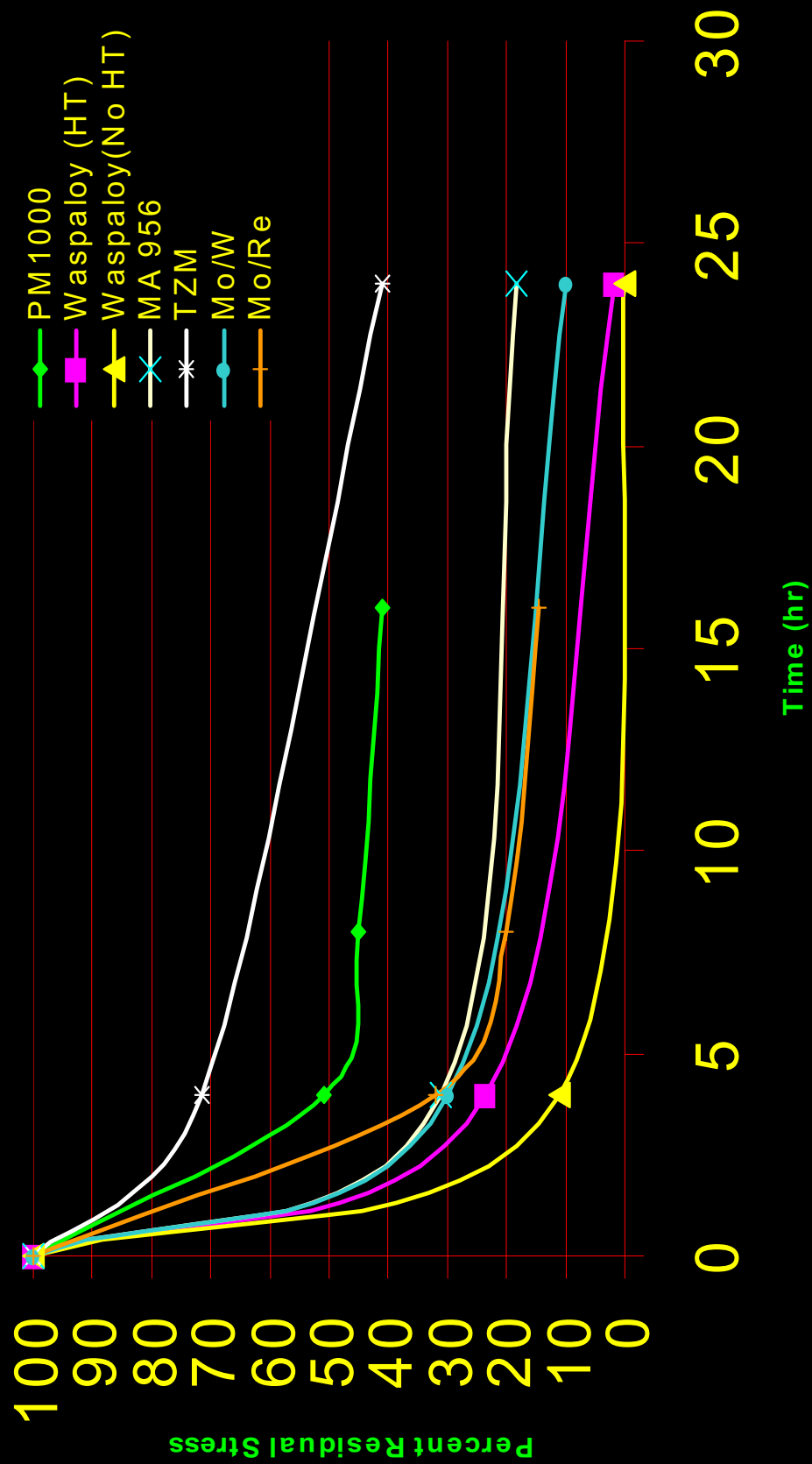
Advanced

Stress Relaxation Studies

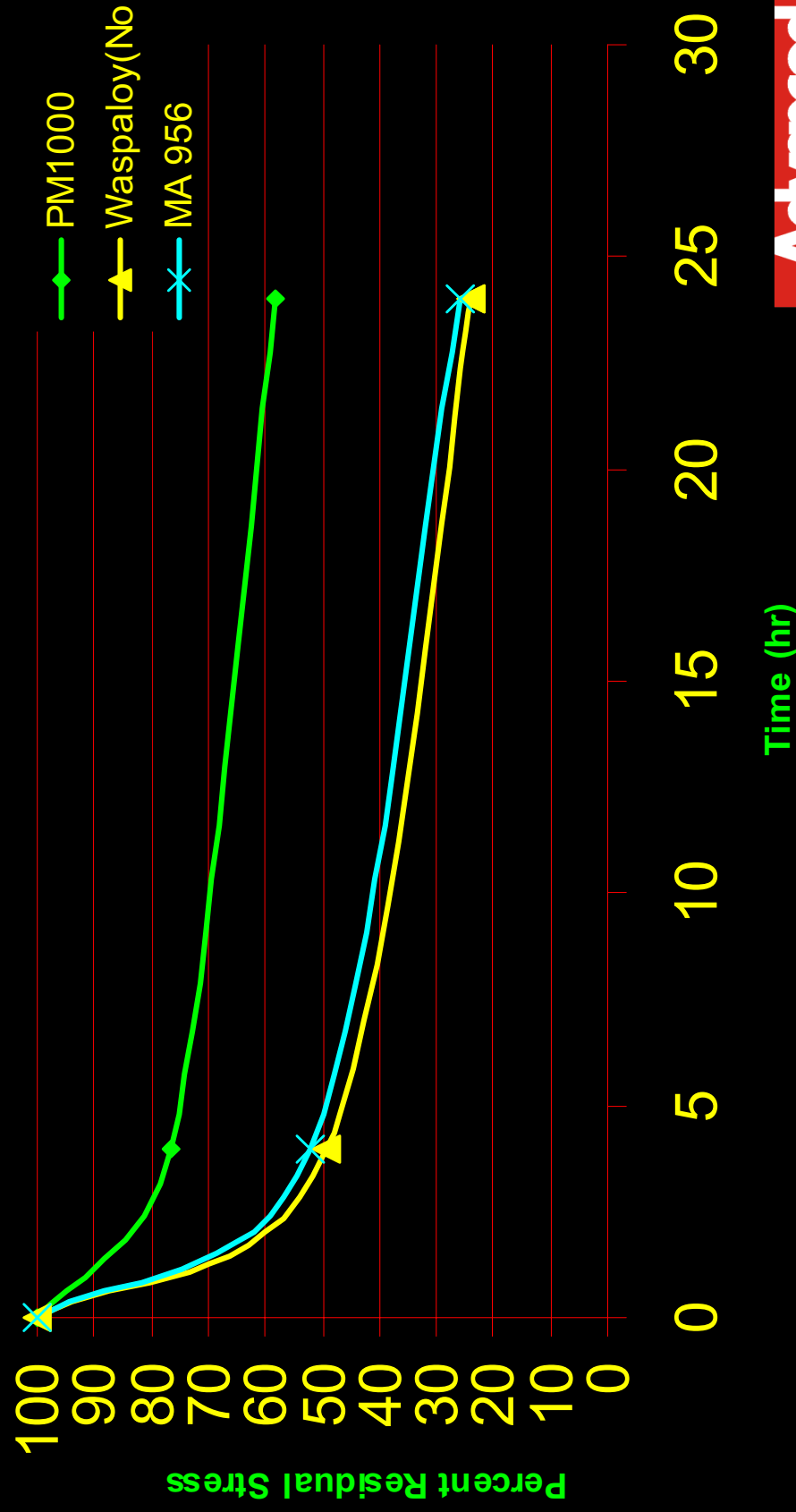


Advanced

Stress Relaxation Studies at 1800 °F



Stress Relaxation Studies at 1600 °F



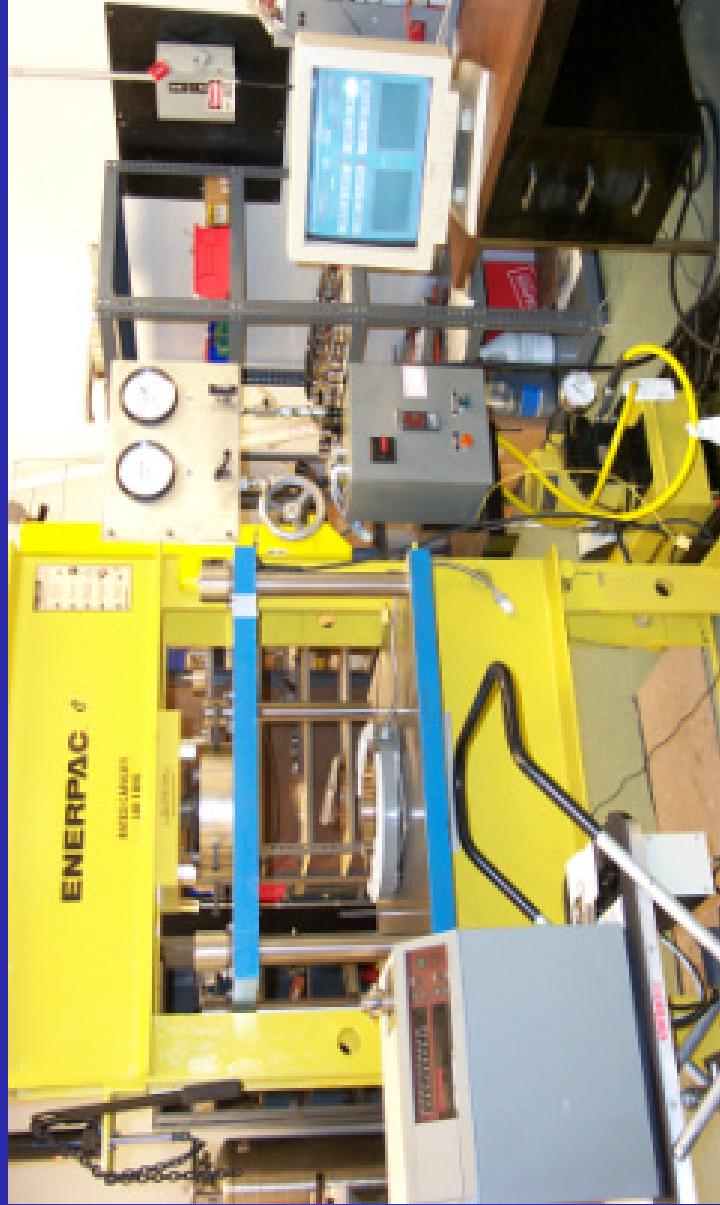
Advanced

Plans for Seal Testing

- Seal Cross Section will be Selected Based on Produceability
- Sealing Performance will be Evaluated in the Temperature Range 1600-1800 °F

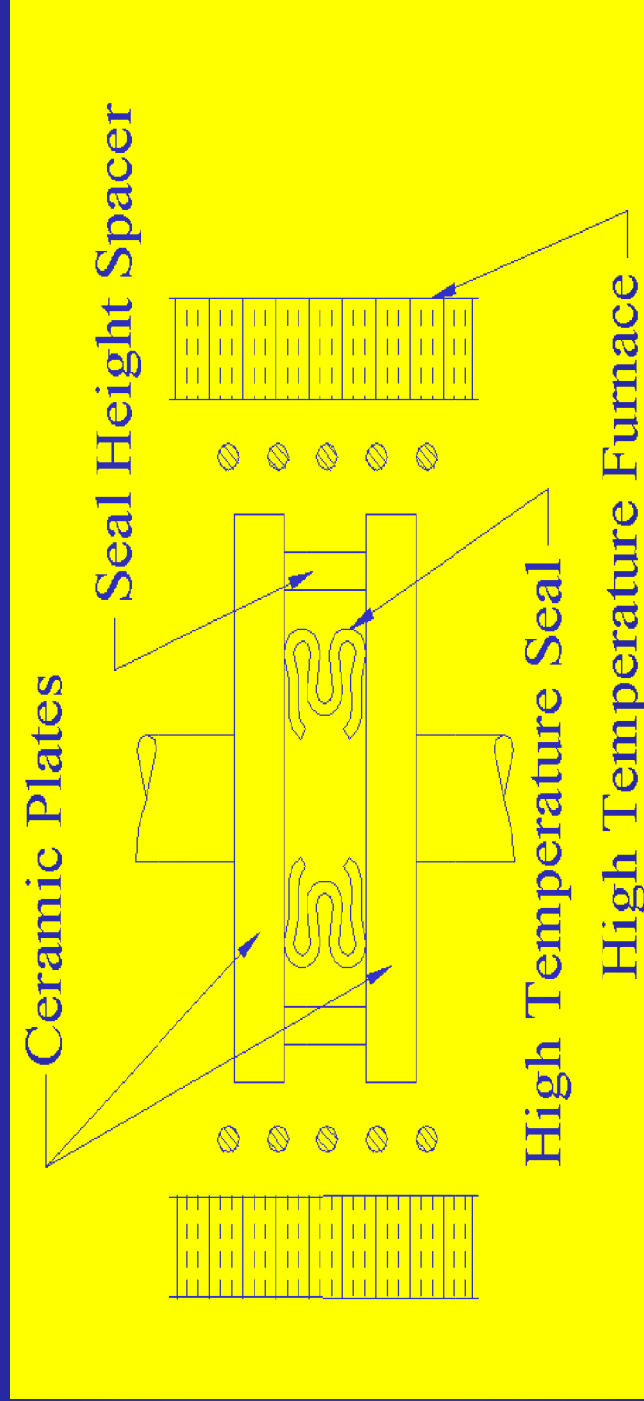
Advanced

Plans for Seal Testing Test Rig



Advanced

Plans for Seal Testing



- Monitor Seal Height Change and Leakage as a Function of Temperature and Time

Advanced

Ratios of Yield Strength to Elastic Modulus at 1800 °F

Alloy	σ_y (ksi)	E (ksi)	σ_y/E (10^{-3})
Waspaloy	20	21×10^3	0.95
PM 1000	28	14×10^3	2.00
MA 956	15	14×10^3	1.07
MA 754	--	--	--
TZM	80	32×10^3	2.75
Mo/W	32.4	35×10^3	0.95
Mo/Re	50	53×10^3	0.94

For short-term duration at temperature, elastic spring back increases as σ_y/E increases

Advanced

In Summary

- Completed ASTM type stress relaxation testing
- Identified several materials with superior stress relaxation characteristics
- Proceeding with high temperature seal development and testing, utilizing findings and materials from initial phases of testing

Advanced

INVESTIGATION OF A SHROUDED ROTOR-STATOR DISK CAVITY

Ram P. Roy, G. Xu, and J. Feng
Arizona State University
Tempe, Arizona



Gas Turbine Heat Transfer Laboratory,
Mechanical & Aerospace Engineering

**INVESTIGATION OF A SHROUDED ROTOR-STATOR
DISK CAVITY**

R. P. Roy, G. Xu and J. Feng

Arizona State University
Department of Mechanical and Aerospace Engineering
Tempe, AZ 85287-6106

NASA Seal/Secondary Air System Workshop
October 25-26, 2000

OBJECTIVES

TO UNDERSTAND:

1. TIME-AVERAGE AND UNSTEADY PRESSURE FIELDS IN THE MAIN-STREAM GAS PATH AND DISK CAVITY
2. VELOCITY FIELD IN THE MAIN GAS PATH AND DISK CAVITY
3. INGESTION OF MAIN GAS INTO THE DISK CAVITY
4. CONVECTIVE HEAT TRANSFER IN THE DISK CAVITY
5. EFFECTIVE RIM SEAL CONFIGURATIONS

APPROACH TAKEN:

EXPERIMENTS AND CFD SIMULATION

EXPERIMENTS PRESENTED

$\underline{\text{Re}_\phi}$	$\underline{\text{Re}_m}$	$\underline{\beta}$	$\underline{c_w}$	$\underline{c_{w, fd}}$
5.16×10^5	5.0×10^5	19.5°	0	8140
5.16×10^5	5.0×10^5	19.5°	1504	8140
5.16×10^5	5.0×10^5	19.5°	7520	8140

Re_m = main-stream flow Reynolds number, = $\rho V_m b / \mu$

Re_ϕ = disk rotational Reynolds number, = $\rho \Omega b^2 / \mu$

c_w = nondimensional mass flow rate of secondary air, = $\dot{m} / \mu b$

$c_{w, fd}$ = nondimensional free disk pumping mass flow rate, = $0.219 \text{Re}_\phi^{0.8}$

CONVECTIVE HEAT TRANSFER AT ROTOR DISK SURFACE

Local convective heat transfer coefficient:

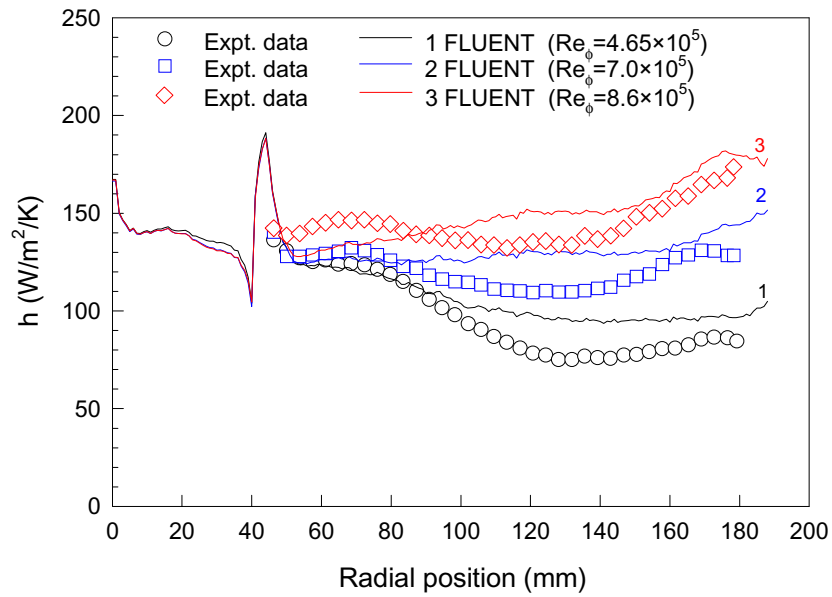
$$h(r) = \frac{q_{w,ro,conv}''(r)}{T_{w,ro} - T_{ref}(r)} = \frac{q_{w,ro}''(r) - q_{w,ro,rad}''}{T_{w,ro} - T_{ref}(r)}$$

Local Nusselt number:

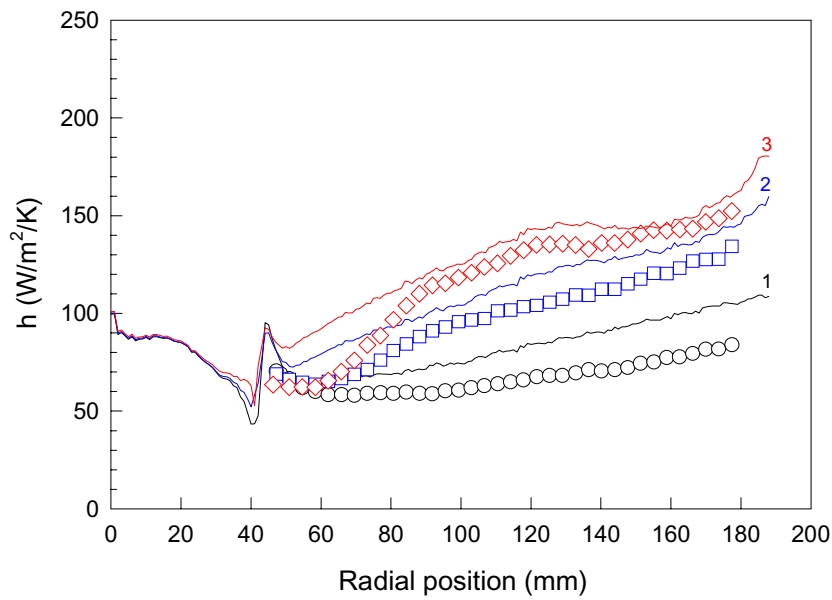
$$Nu_r \equiv \frac{h(r)r}{k_{air}}$$

Local rotational Reynolds number:

$$Re_{\phi,r} \equiv \frac{\rho \Omega^2 r^2}{\mu} = \left(\frac{r}{b}\right)^2 Re_{\phi}$$

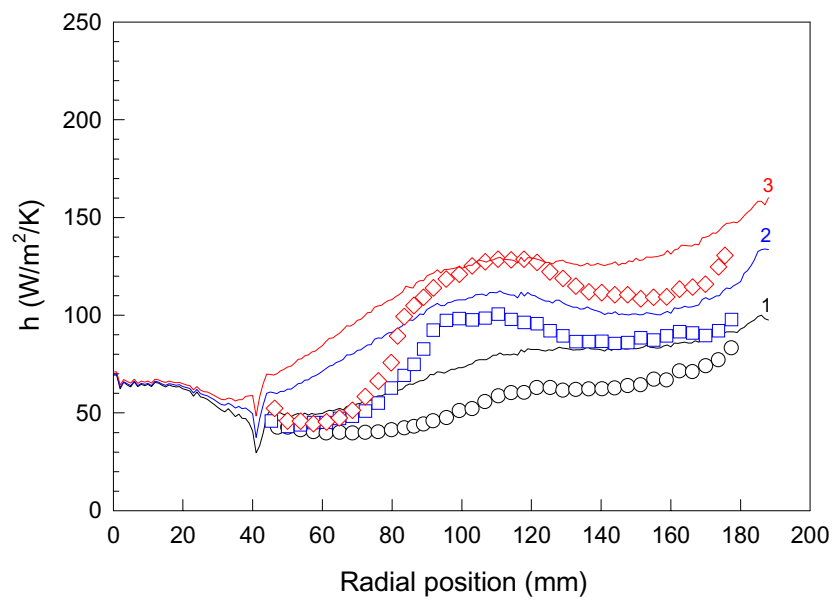


(a) $c_w=7520$

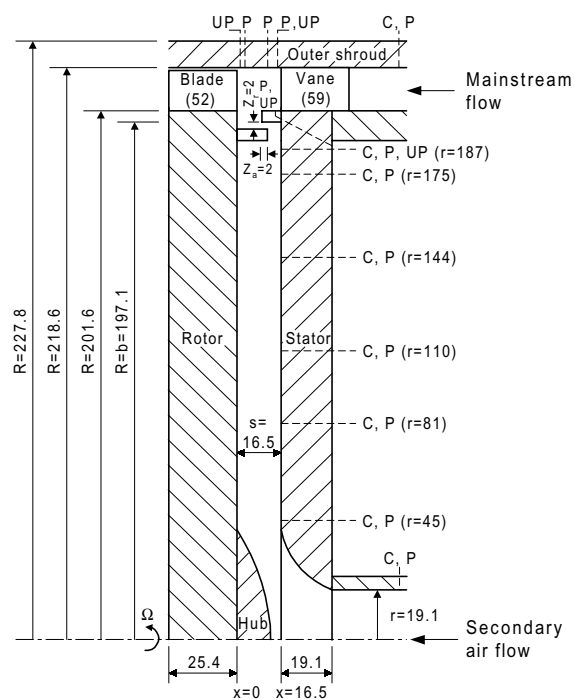


(b) $c_w=3008$

Effect of rotor disk speed on the convective heat transfer coefficient distribution

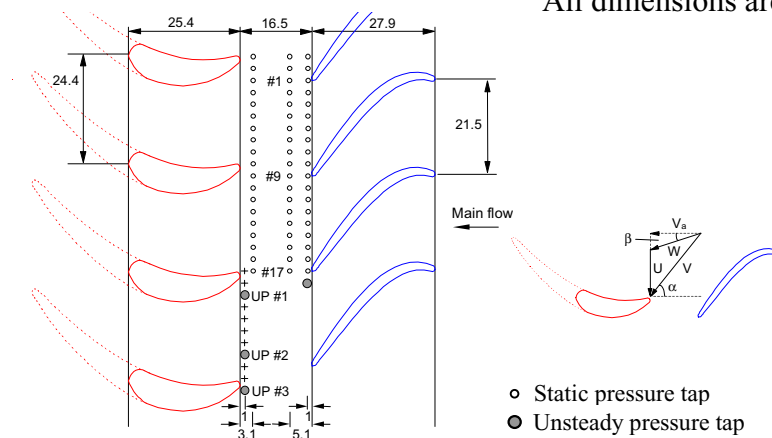


(c) $c_w=1504$



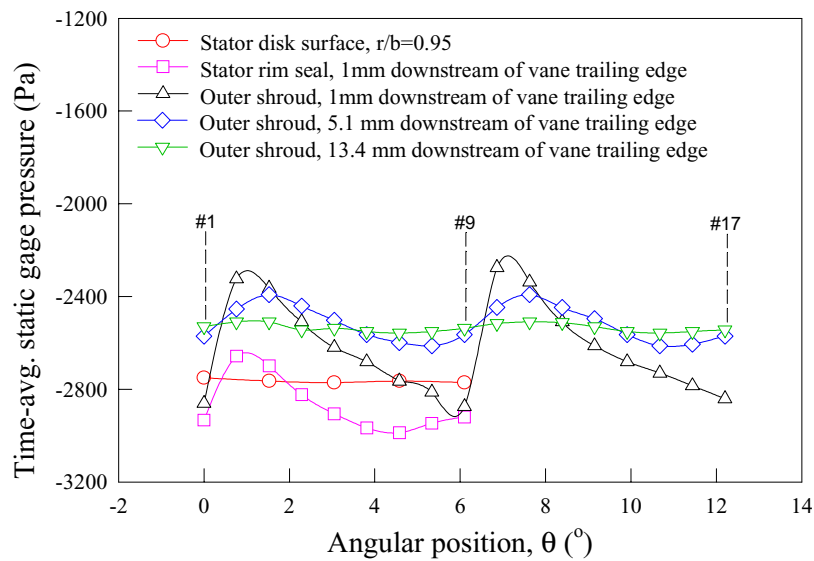
(a) The disk cavity

All dimensions are in mm

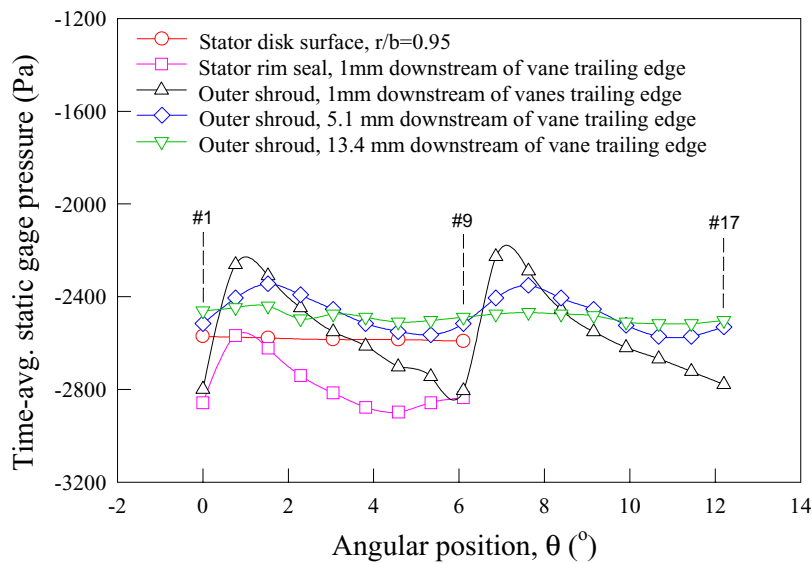


(b) Schematic of blades and vanes

The rotor-stator system (C: tracer gas concentration tap, P: static pressure tap, UP: unsteady pressure tap)

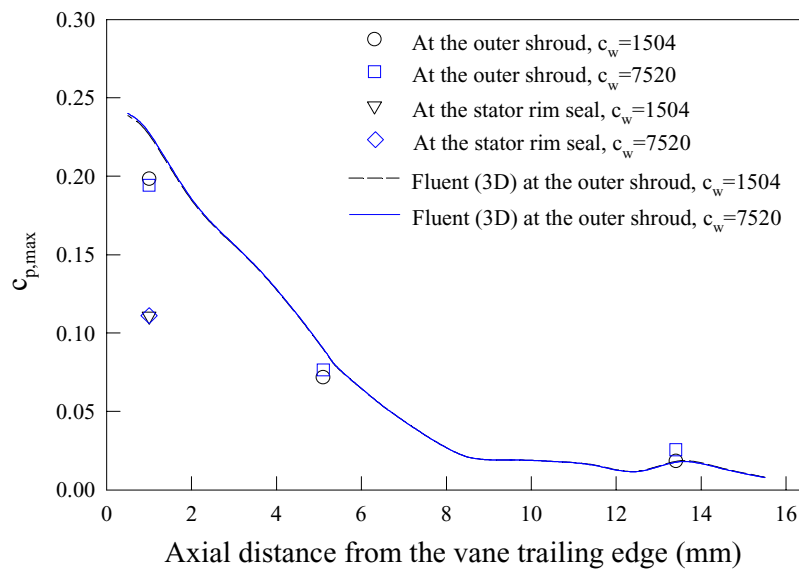


(a) $c_w=1504$

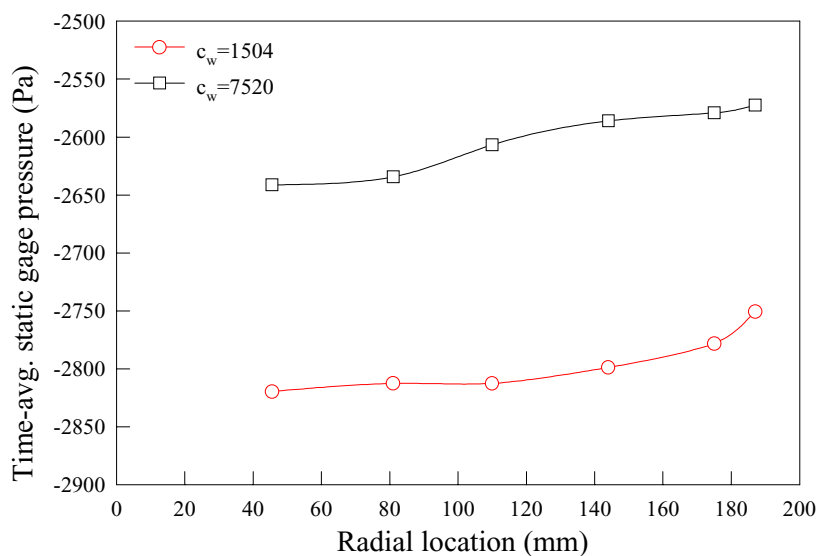


(b) $c_w=7520$

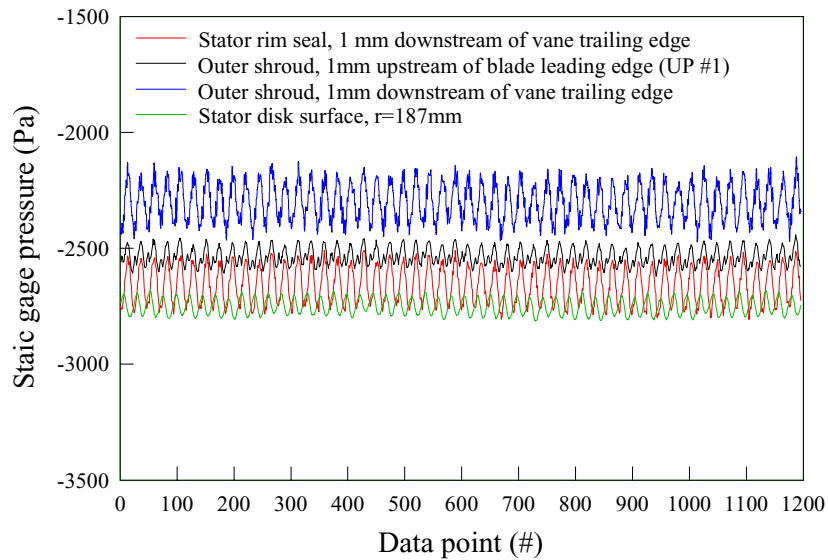
Measured circumferential distributions of time-average static pressure at the outer shroud, stator disk rim seal, and stator disk surface near its rim ($Re_\phi=5.16 \times 10^5$, $Re_m=5.0 \times 10^5$)



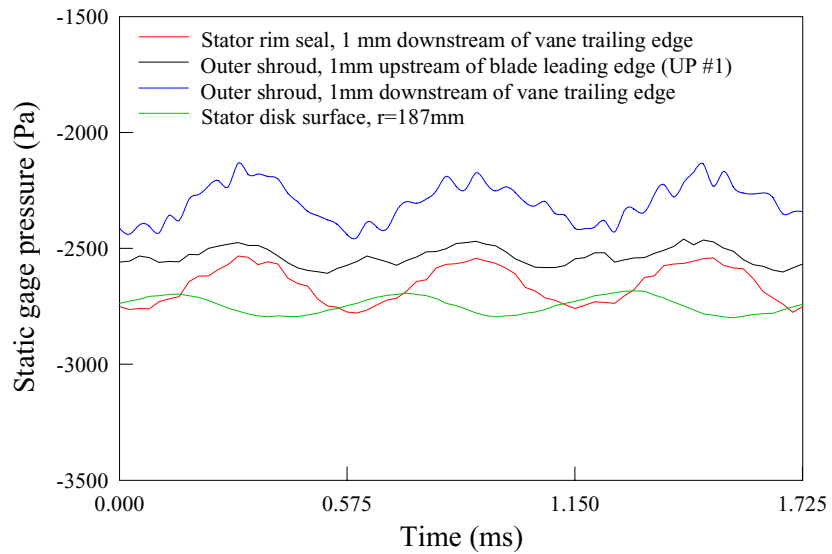
Time-average static pressure circumferential asymmetry coefficient at the main gas path outer shroud and stator rim seal ($Re_\phi=5.16\times10^5$, $Re_m=5.0\times10^5$)



Radial distribution of static pressure at the stator disk surface for two secondary air flow rates ($Re_\phi=5.16\times10^5$, $Re_m=5.0\times10^5$)

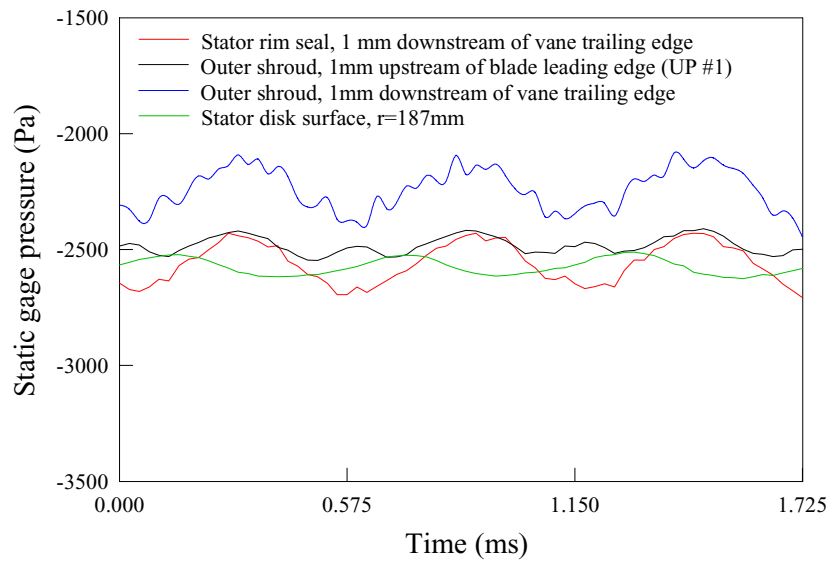


(a) $c_w=1504$ – one revolution of rotor disk

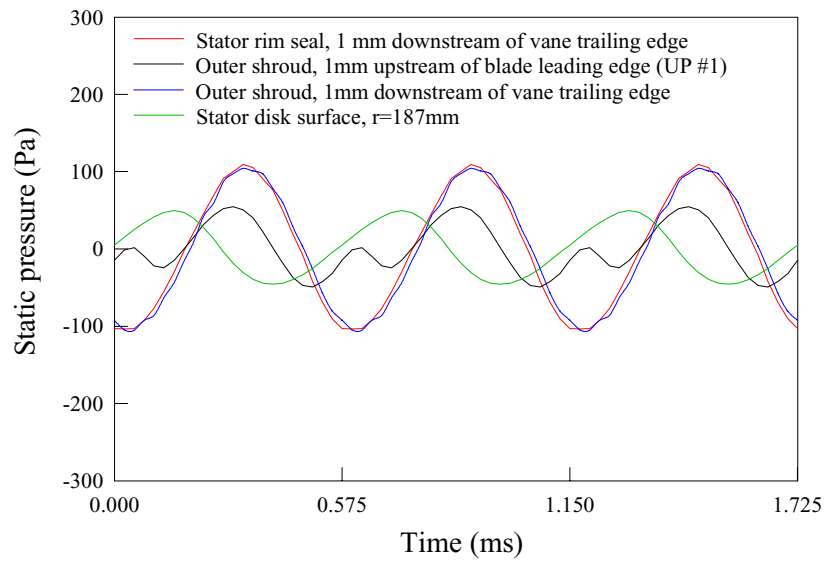


(b) $c_w=1504$ – three blade passages

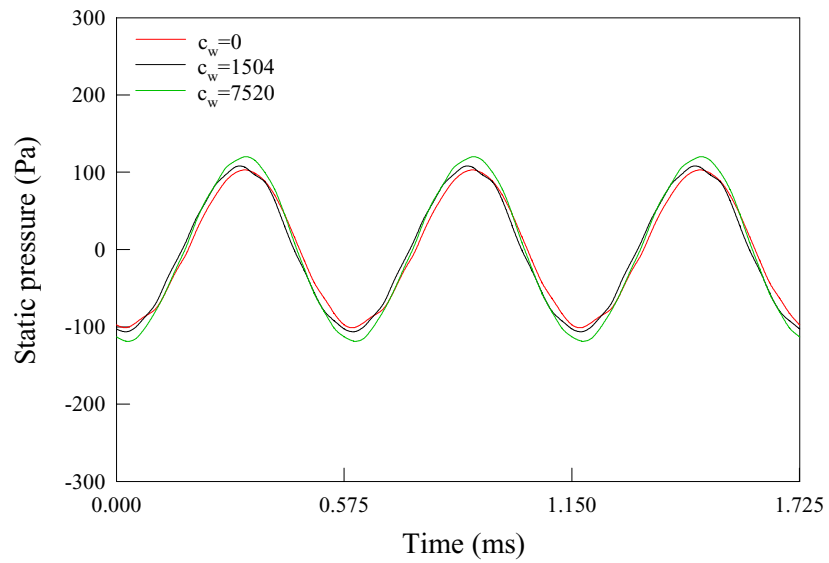
Ensemble-average unsteady static pressure at the outer shroud, rim seal of stator disk, and stator disk surface near the rim ($Re_\phi=5.16 \times 10^5$, $Re_m=5.0 \times 10^5$)



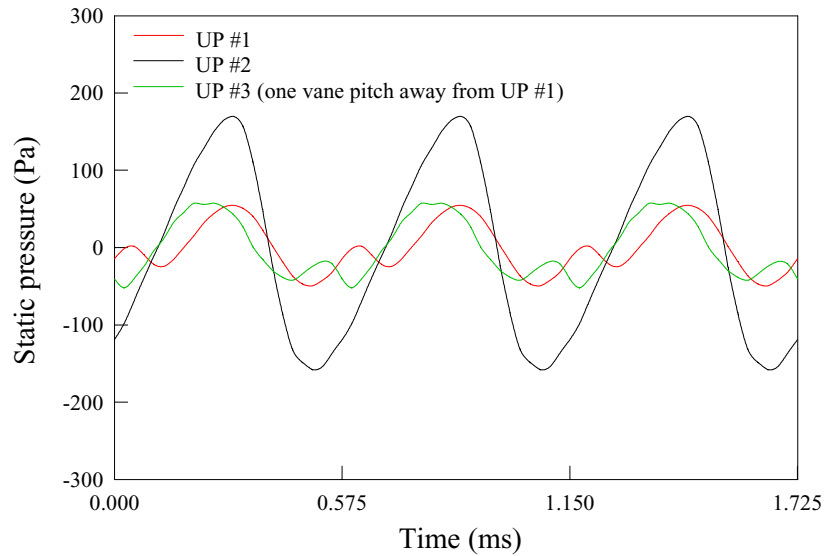
(c) $c_w=7520$ – three blade passages



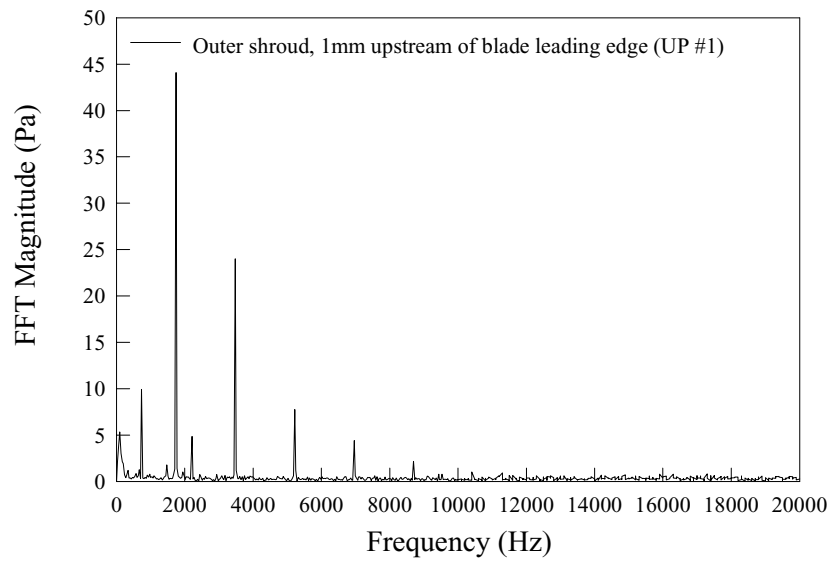
Blade-periodic static gage pressure at the outer shroud, stator disk rim seal, and stator disk surface near its rim ($Re_\phi=5.16 \times 10^5$, $Re_m=5.0 \times 10^5$, $c_w=1504$) – three blade passages



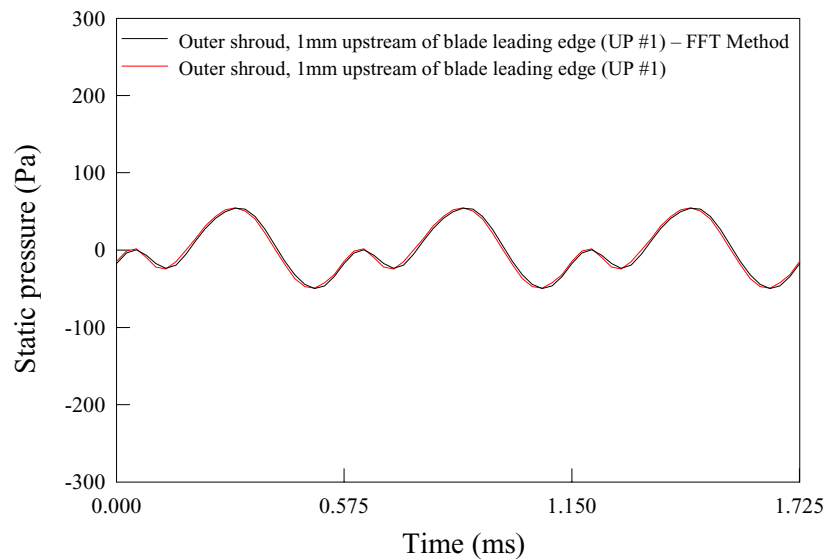
Effect of secondary air flow rate on blade-periodic static pressure at the stator disk rim seal 1 mm downstream of vane trailing edge ($Re_\phi=5.16 \times 10^5$, $Re_m=5.0 \times 10^5$) – three blade passages



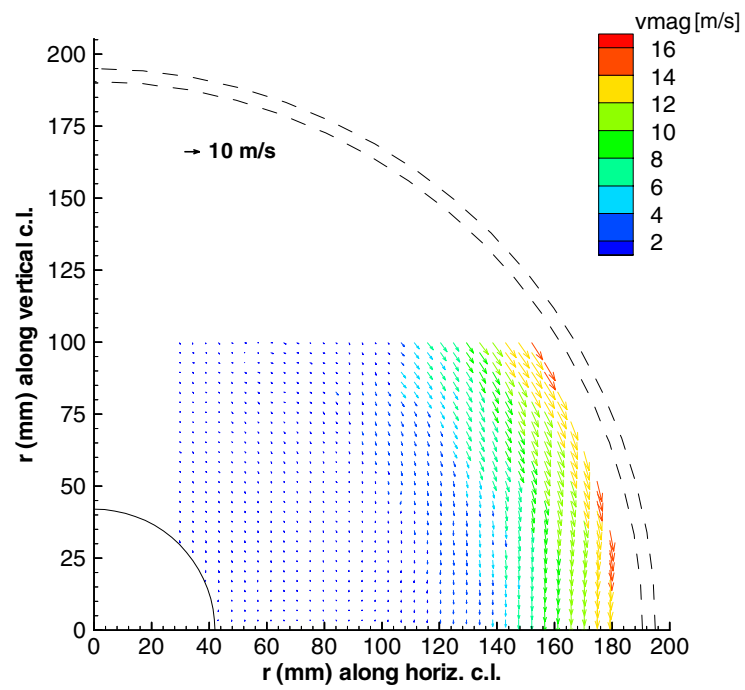
Circumferential variation of blade-periodic static pressure at the outer shroud 1 mm upstream of blade leading edge ($Re_\phi=5.16 \times 10^5$, $Re_m=5.0 \times 10^5$, $c_w=1504$) – three blade passages



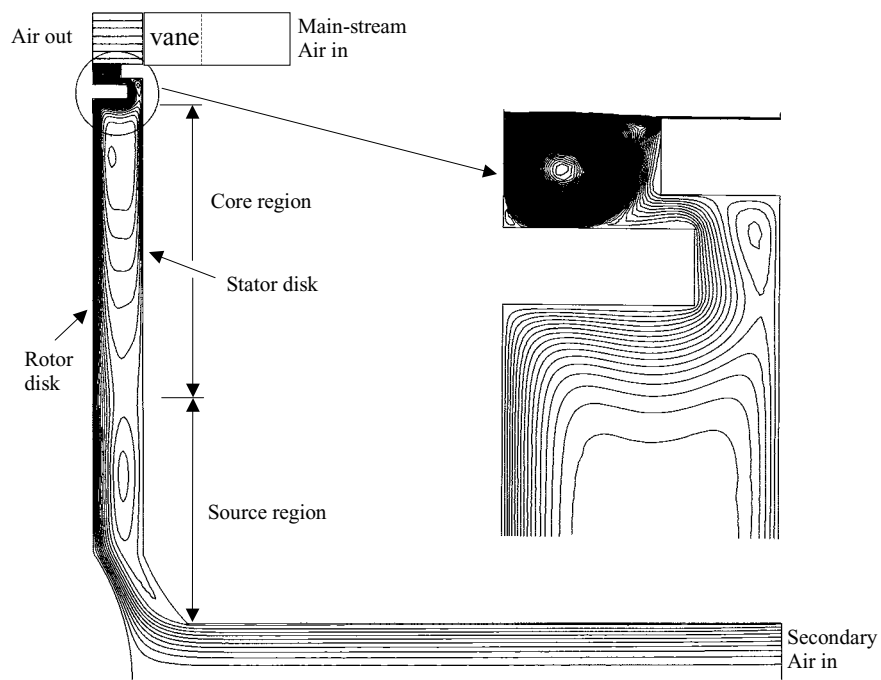
Frequency spectrum of the ensemble-average static pressure fluctuation at the outer shroud 1 mm upstream of blade leading edge ($Re_\phi=5.16 \times 10^5$, $Re_m=5.0 \times 10^5$, $c_w=1504$)



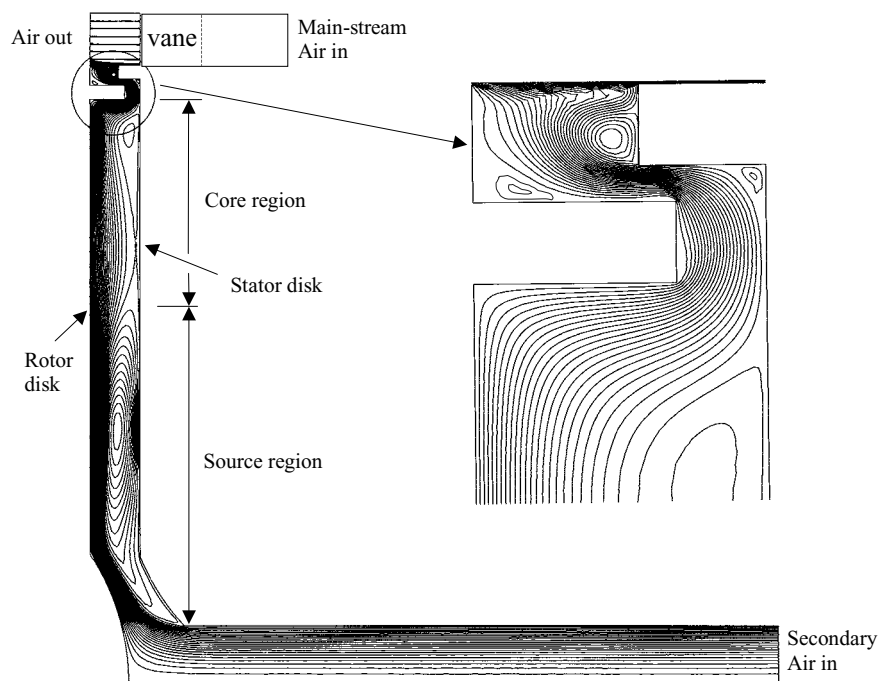
Comparison of FFT method with decomposition method: blade-periodic static pressure at the outer shroud 1 mm upstream of blade leading edge ($Re_\phi=5.16 \times 10^5$, $Re_m=5.0 \times 10^5$, $c_w=1504$) – three blade passages



r - ϕ plane map of the fluid time-average velocity in the cavity 3 mm from the stator disk for $Re_\phi=5.16 \times 10^5$, $Re_m=5.0 \times 10^5$, $c_w=1504$

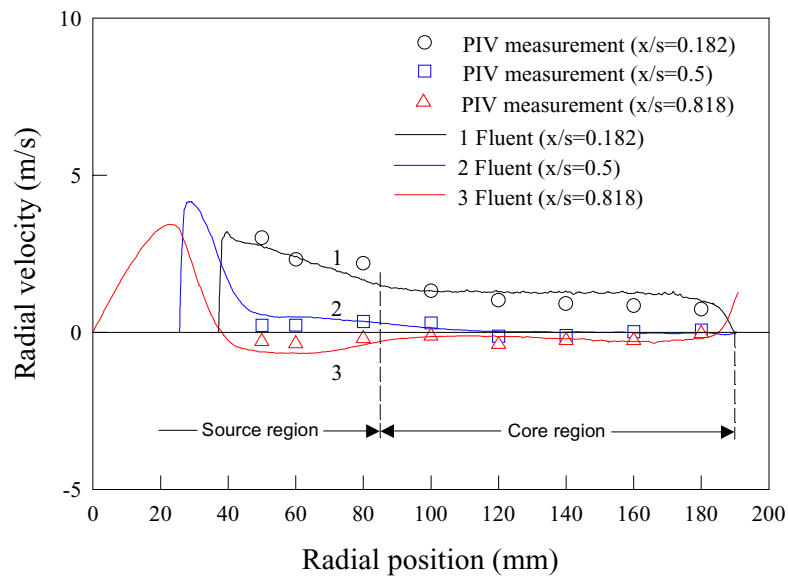


(a) $c_w = 1504$

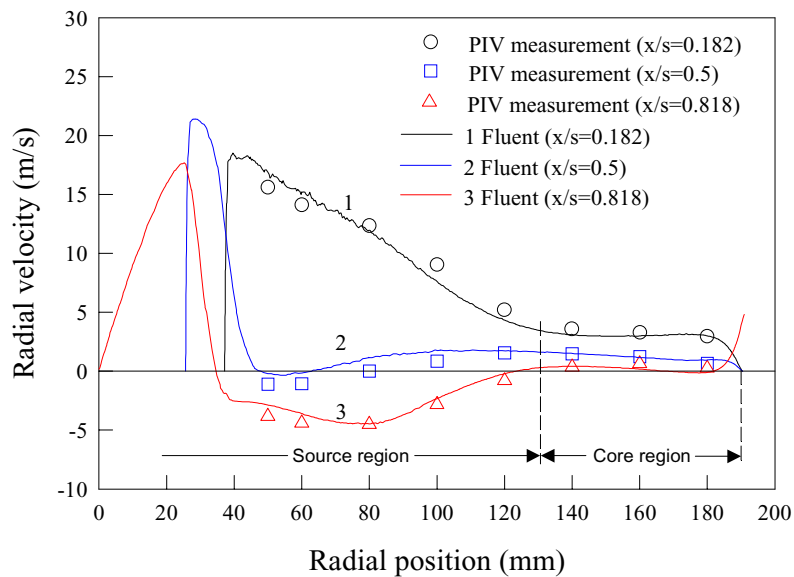


(b) $c_w = 7520$

Computed streamlines for $Re_\phi = 5.16 \times 10^5$, $Re_m = 5.0 \times 10^5$
(steady rotationally-symmetric simulation)

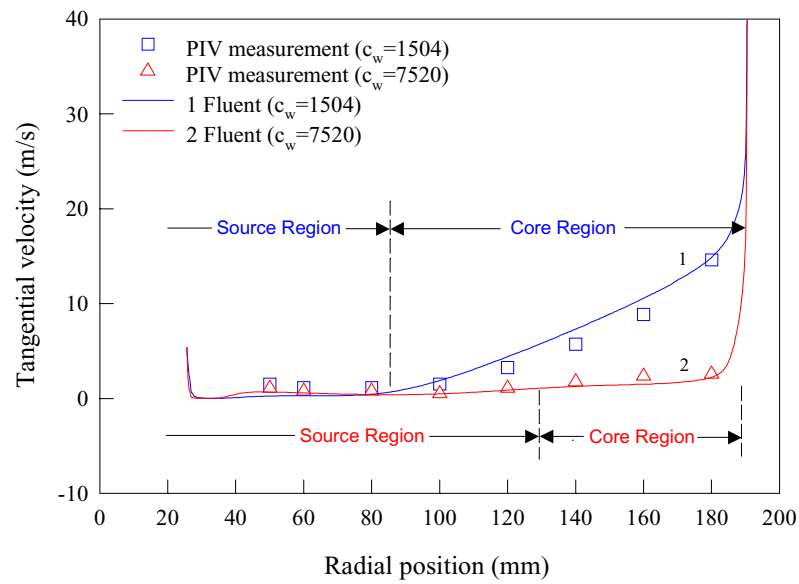


(a) $c_w=1504$

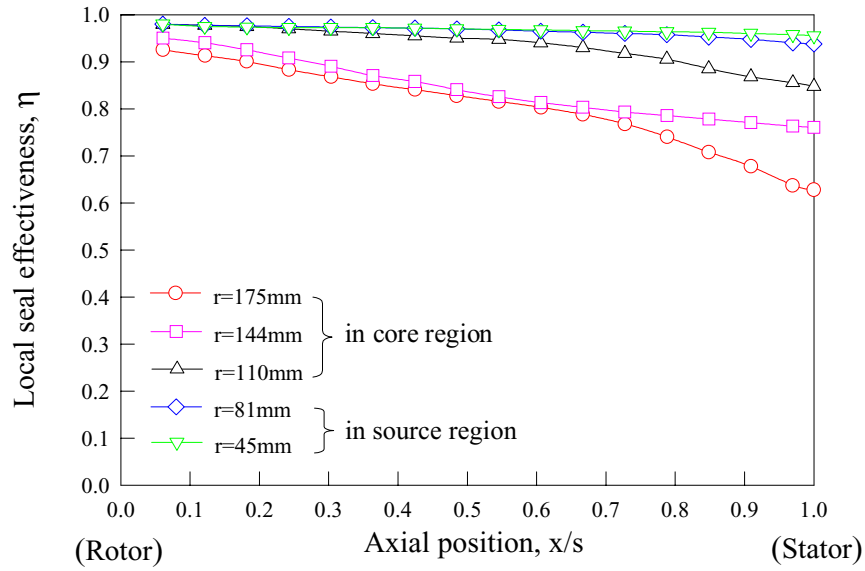


(b) $c_w=7520$

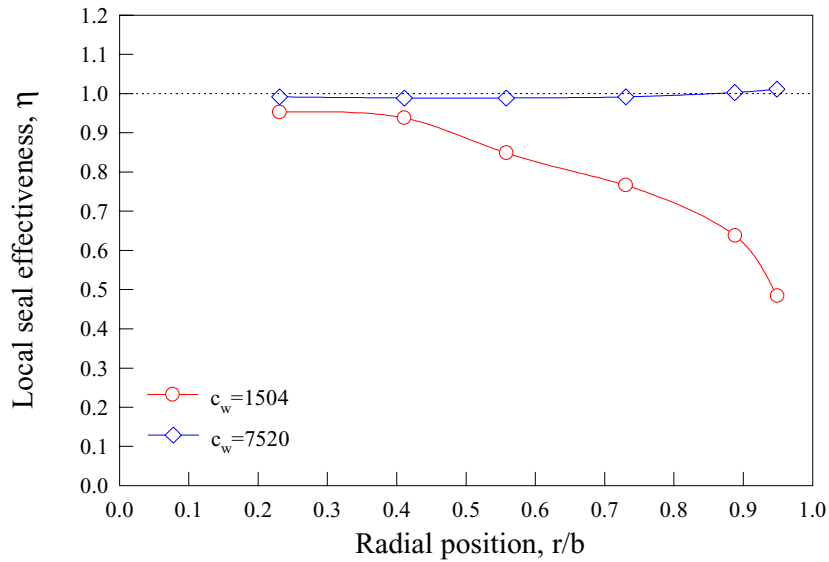
Radial distribution of fluid radial velocities at $Re_\phi=5.16 \times 10^5$, $Re_m=5.0 \times 10^5$



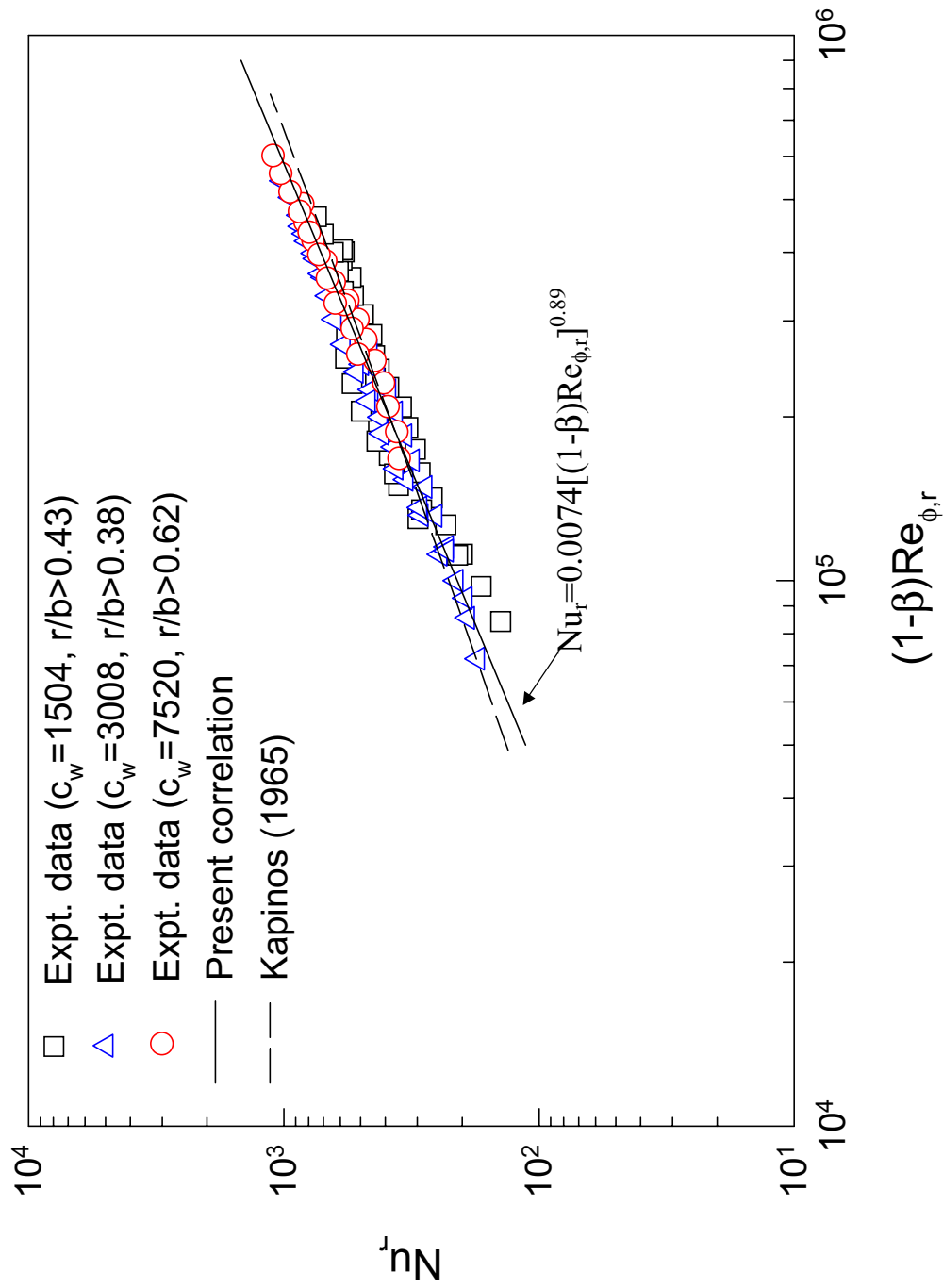
Effect of c_w on the fluid tangential velocity at the cavity mid-axial gap ($x/s=0.5$)
for $Re_\phi=5.16 \times 10^5$, $Re_m=5.0 \times 10^5$



Seal effectiveness distribution in the disk cavity for $Re_\phi=5.16 \times 10^5$, $Re_m=5.0 \times 10^5$, $c_w = 1504$



Seal effectiveness distributions at the stator disk surface for $Re_\phi=5.16 \times 10^5$, $Re_m=5.0 \times 10^5$



Local Nusselt number versus local relative rotational Reynolds number (expt. data and correlation are for the core region and radially outermost part of the source region) – β , core fluid rotation ratio, $= V_\phi/\Omega r$

X-38 SEAL DEVELOPMENT

Donald M. Curry and Ronald K. Lewis
National Aeronautics and Space Administration
Johnson Space Center
Houston, Texas

Jeffrey D. Hagen
Lockheed Martin Space Operations
Houston, Texas

X-38 Seal Development

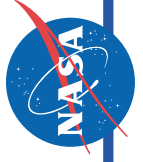
**Donald M. Curry
Ronald K. Lewis
NASA Johnson Space Center
Jeffrey D. Hagen
Lockheed Martin Space Operations**

**2000 NASA Seal/Secondary Air System Workshop
NASA Glenn Research Center
October 25-26, 2000**

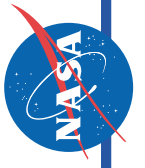
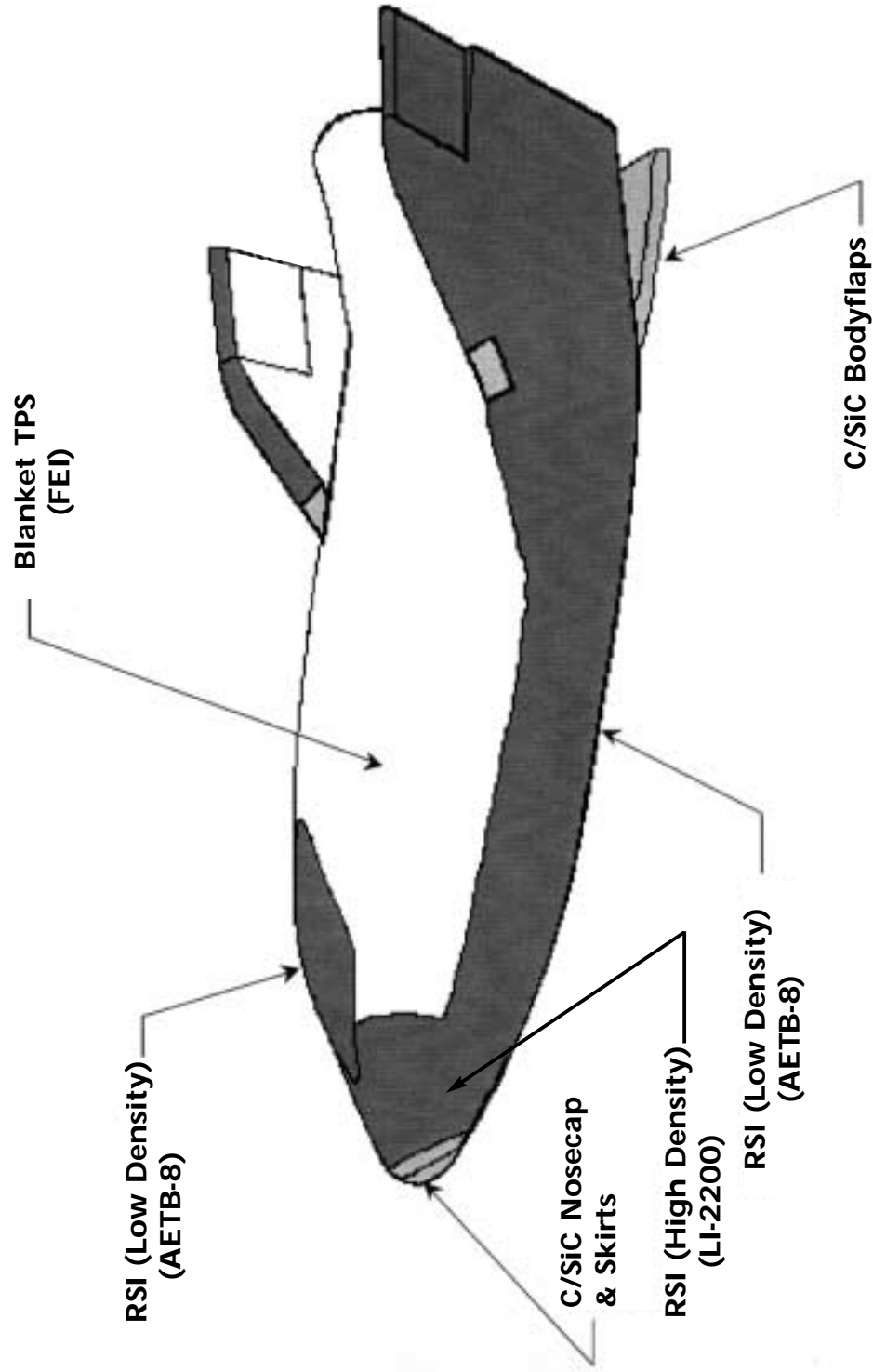


X-38 – Crew Return Vehicle

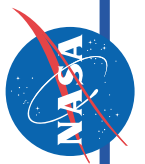
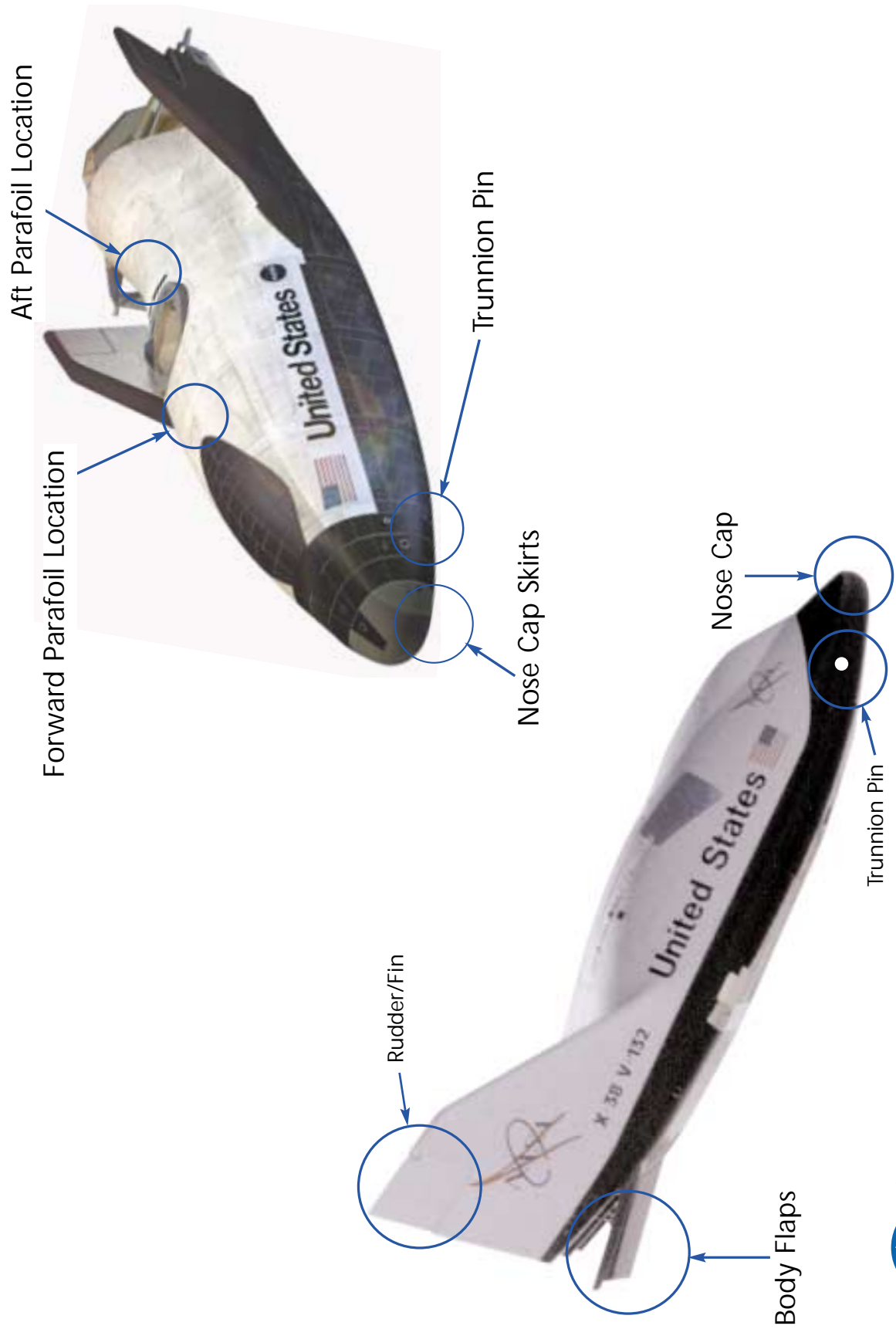
- ❖ An element of the International Space Station (ISS)
- ❖ Three Scenarios
 - ISS catastrophe
 - Emergency medical evacuation
 - Period of Space Shuttle unavailability
- ❖ X-38 Program Purpose:
 - To greatly reduce the costs and schedule for the development of crew Return Vehicles (CRVs) and Crew Transfer Vehicles (CTVs) through the use of the rapid development methodology associated with an X-project
 - Ground Testing
 - Atmospheric Testing
 - Space Flight Testing
- ❖ X-38 Major Milestones
 - Static Test-02/01
 - Primary Structure Completed
 - Vibro/Acoustic Test-11/01
 - TPS Installed
 - V-201 Delivery to KSC-03/02
 - First Flight-STS-114-07/02



X-38 TPS Configuration



X-38 Seal Locations



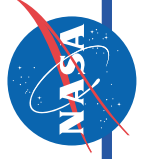
X-38 – TPS Seals

General Seal Requirements

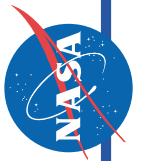
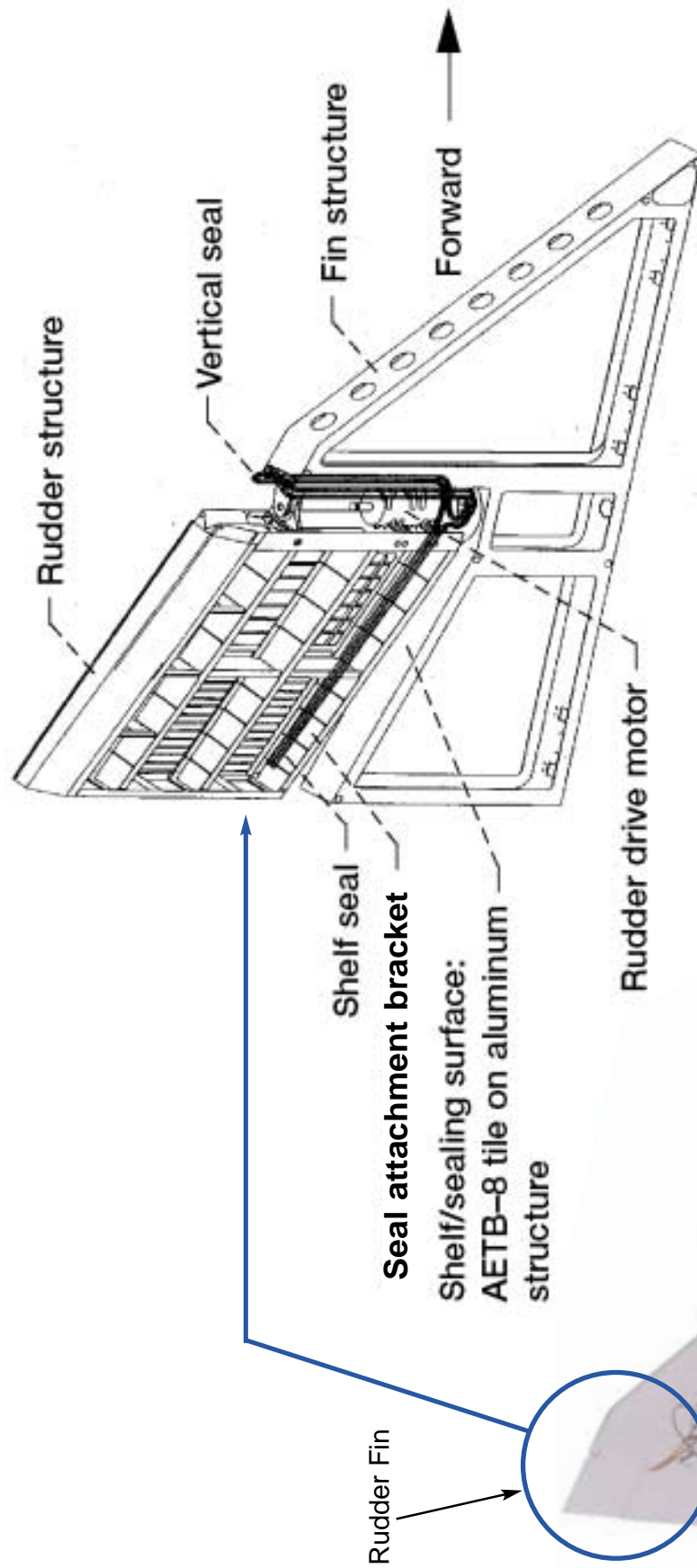
- 1) Single Flight Capability
- 2) High Temperature, Oxidative Environment
- 3) Combined Convective and Radiation Heating
- 4) Different Thermal Expansion of Seal Parts
- 5) Mechanical Load Plus Vibration/Acoustic Loads
- 6) Component Movement and Rotation
- 7) Wear Resistant
- 8) Low Pressure Environment (at Peak Heating)
- 9) Low Permeability to Minimize Leakage

X-38 Design Considerations

- 1) Use a Seal with Flight Heritage (Orbiter)
- 2) Operational Temperature – 1500-3000°F
- 3) Permeability – 1×10^{-10} - 1×10^{-11} Sq. M
- 4) Coefficient of Friction – 1.09-1.17
- 5) Installation Force Limit of 3 lb/in (Installed with 20-30% Seal Deflection)
- 6) Differential Pressures of 350-450 PSF During Peak Heating

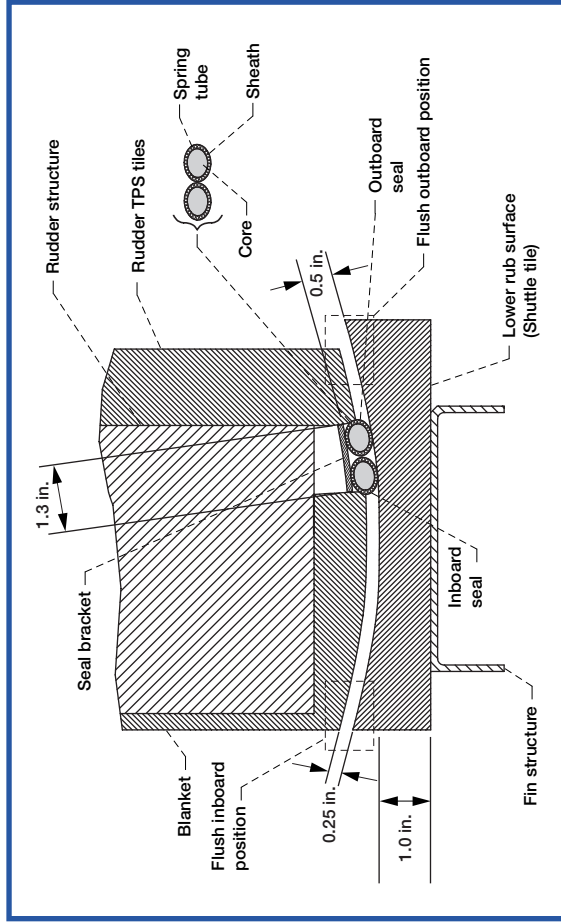


X-38 Rudder/Fin Seal Assembly



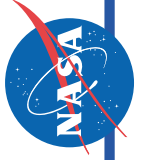
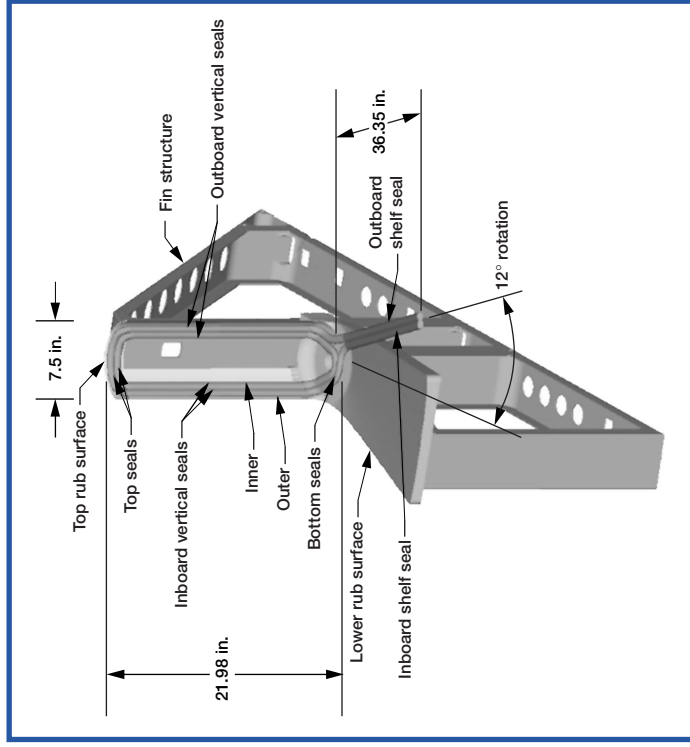
Baseline X-38 Rudder/Fin Seal Design

Cross Section of Rudder/Fin Seal Shelf Location

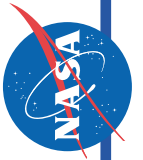
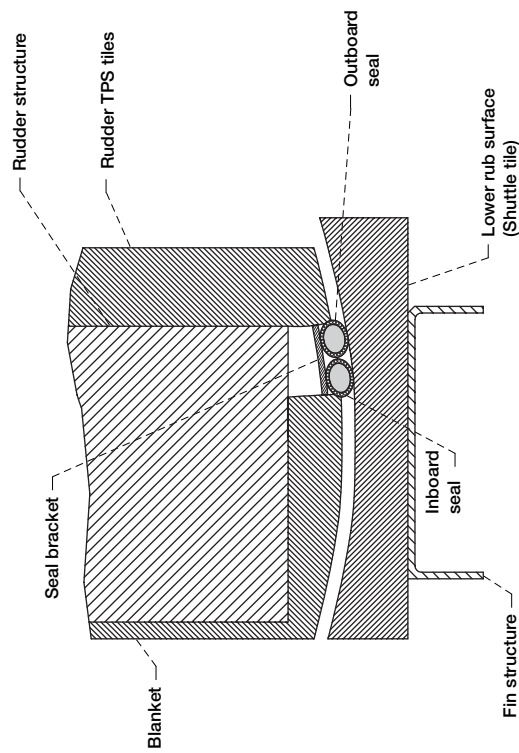
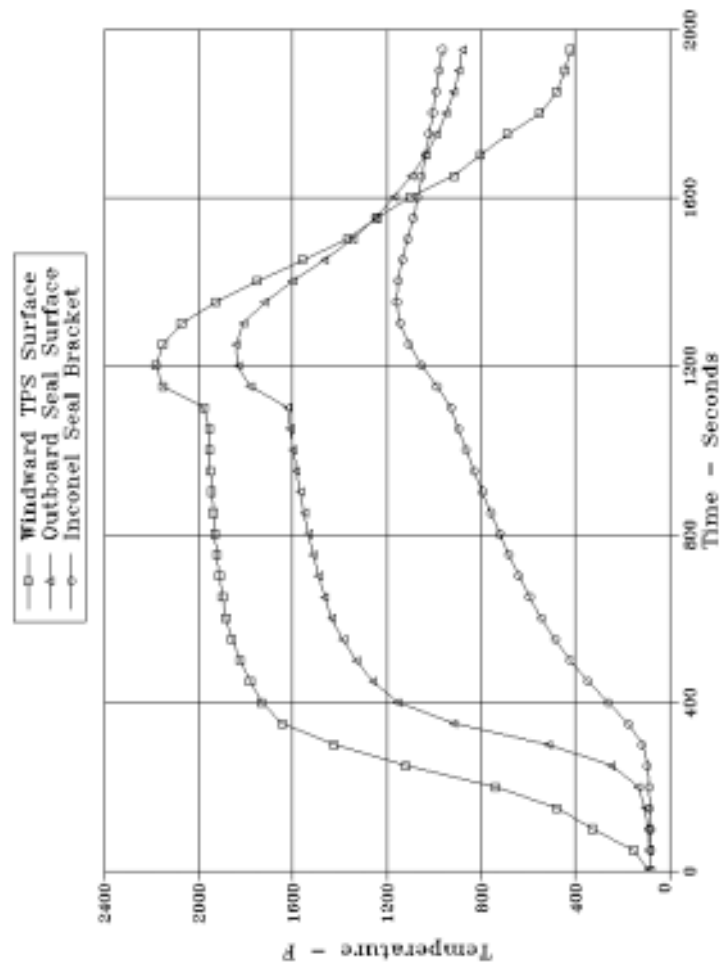


Rudder Shown at Flush Inboard Position

- ❖ Main Seal Components
 - Core: 6 pcf Saffil Insulation
 - Spring Tube: Inconel X-750
 - Sheath: Two Layers of Nextel 312 Fabric
- ❖ Nominal 20% Compression and 0.25-in. Gap

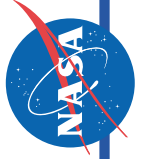


Rudder/Fin Hinge Line Thermal Response

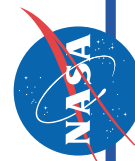
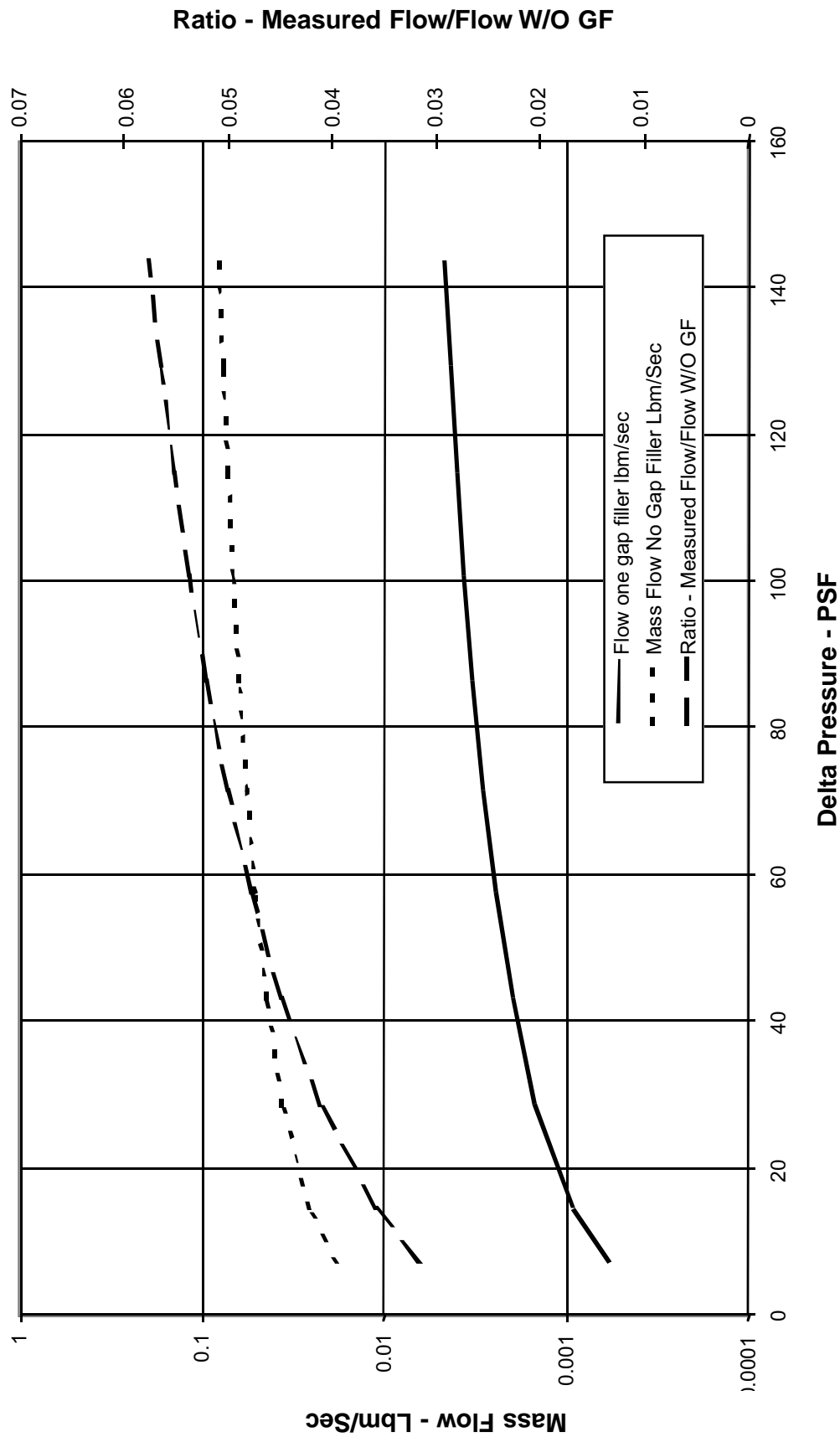


X-38 Rudder/Fin Seal Test

- ❖ Test Conducted at Glenn Research Center (B. Steinetz/P. Dunlap) to Establish:
 - Flow Characteristics of Seal
 - Seal Compression Forces
 - Seal Resiliency
 - Temperature Effects
- ❖ Test Results Indicate:
 - Seal Effective in Blocking Flow Thru Gap
 - Less Than 6% Leakage
 - 20% Seal Compression Results:
 - Unit load of 2.01 lb/in² on rub contact
 - Pre-load of 4.4 lb/in² based on contact seal width of 0.455 in



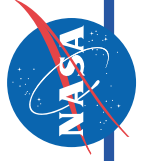
Mass Flow Versus Delta Pressure - Single Gap Filler



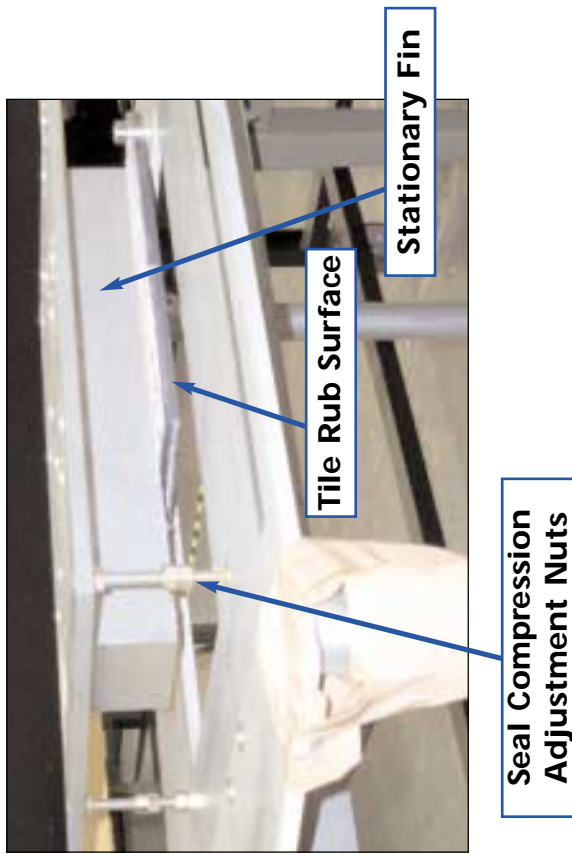
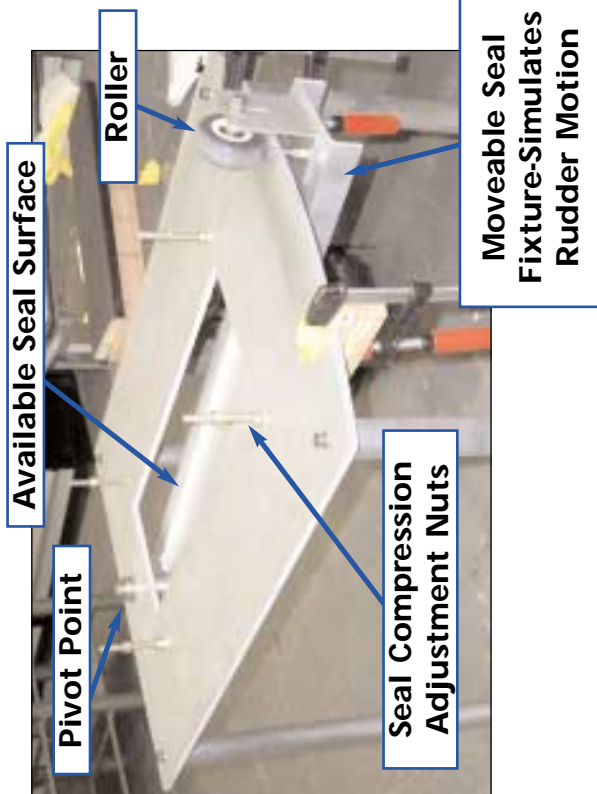
X-38 Rudder/Fin Rub Test

Objective:

- Evaluate Normal Force of Compressed Spring Tube Seal on Sealing Surface
- Determine Frictional Force as Compressed Spring is Moved Over Sealing Surface
- Visually Observe Deformation and Springback Characteristics of Seal as it Engages/Disengages Sealing Surface
- Investigate Wear Performance of Seal with Repeated Cycles



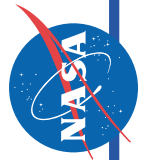
Rudder/Fin Rub Test Assembly



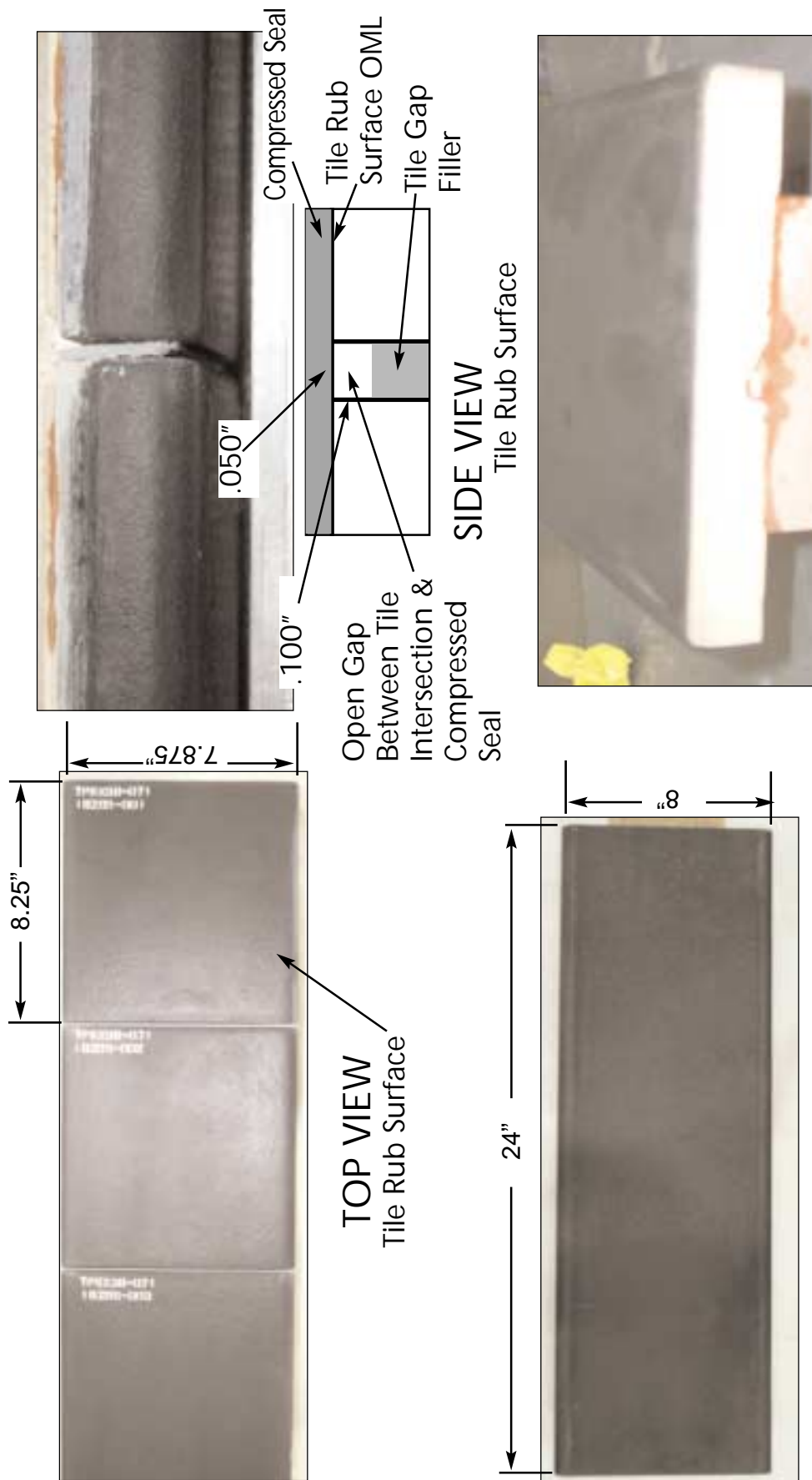
Installed Rudder Seal



Cross Section of Seal



X-38 Rudder/Fin Rub Test



X-38 Rudder/Fin Rub Test

Results:

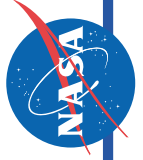
- Initial Test indicated that Coefficient of Friction and Torque required to Rotate Compressed Seal was Less on Northrup Grumman Black Glass Surface Than the Standard RCG/TUFI Coated AETB-8 Tile

- Northrup Grumman CMC
 - Coefficient of Friction: 0.31-0.32
 - Torque: 300-305 in-lb
- RCG/TUFI Coated AETB-8 Tile
 - Coefficient of Friction: 0.48-0.53
 - Torque: 700-800 in-lb

Cyclic Testing Conducted with Tile Rub Surface

- After 100 Cycles of Seal Engage/Disengage Local Failure of Outer Nextel Fabric Associated with Rough Tile
- Removed Rough Tile, Sanded Remaining Two Tiles to Decrease Roughness and Continued Testing Cycle

Continued.....

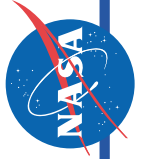


X-38 Rudder/Fin Rub Test

- After 500 Cycles with Smooth Tiles
 - Seal Shows Minor Evidence of Wear (broken fibers)
- After 1000 Cycles with Smooth Tiles
 - Outer Fabric of Seal Failed and Spring Tube was Visible
 - Torque Required to Engage/Disengage Seal was 380 in-lb

Post Test Roughness Measurements

- TUF1/RCG Tile (Rough)
 - 515-574 Micro-Inch RMS
- TUF1/RCG Tile (Sanded)
 - 303-331 Micro-Inch RMS
 - 91 Micro-Inch RMS (Super-Smooth Area)
- Orbiter RCG Baseline Tile
 - 196 Micro-Inch RMS
- Northrop Grumman
 - 282-392 Micro-inch RMS



X-38 Rudder/Fin Rub Test Results



END VIEW

Seal After 100 Cycles with Rough Tile



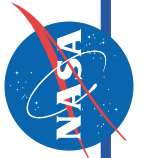
SIDE VIEW



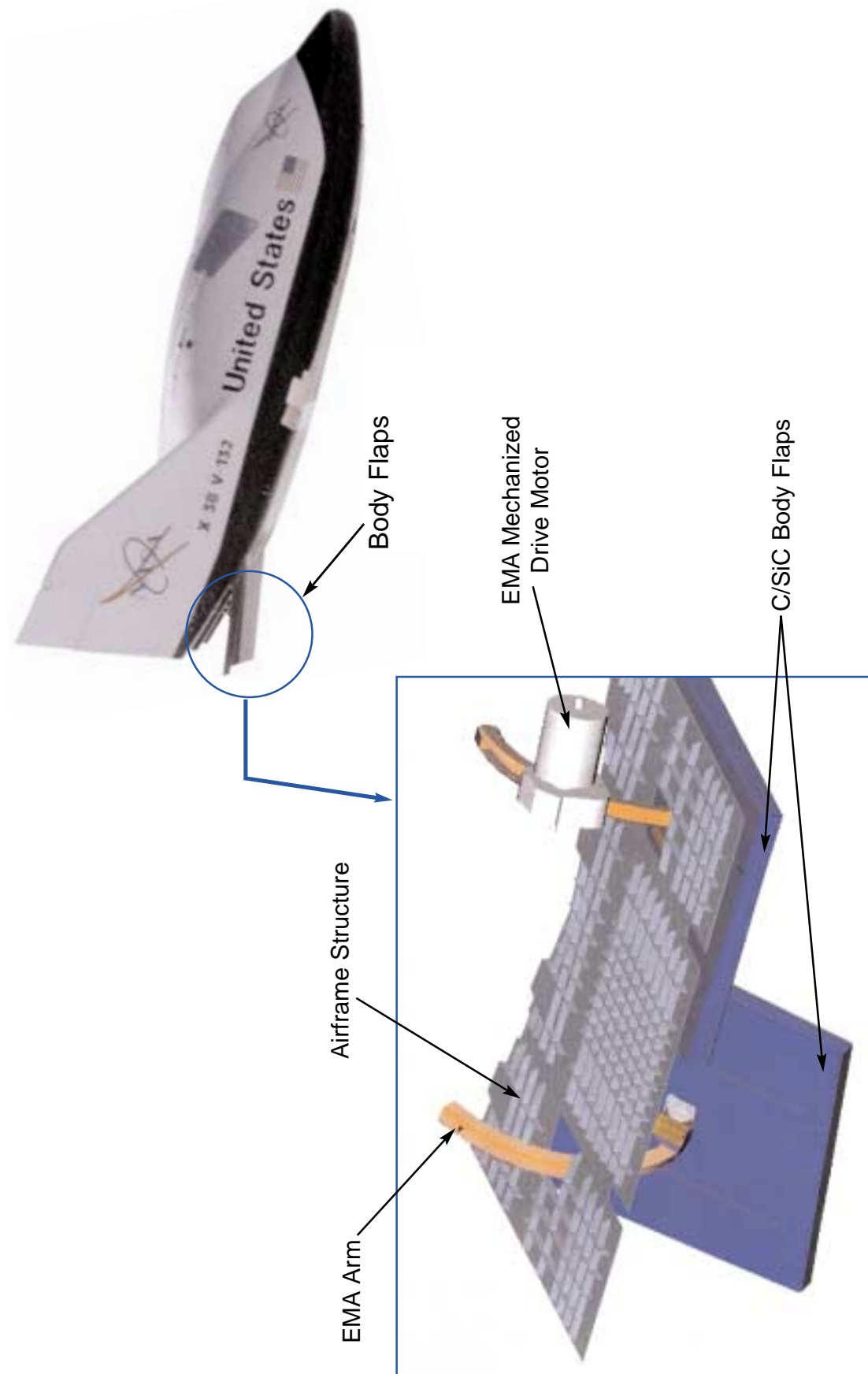
Tile Surface After Sanding



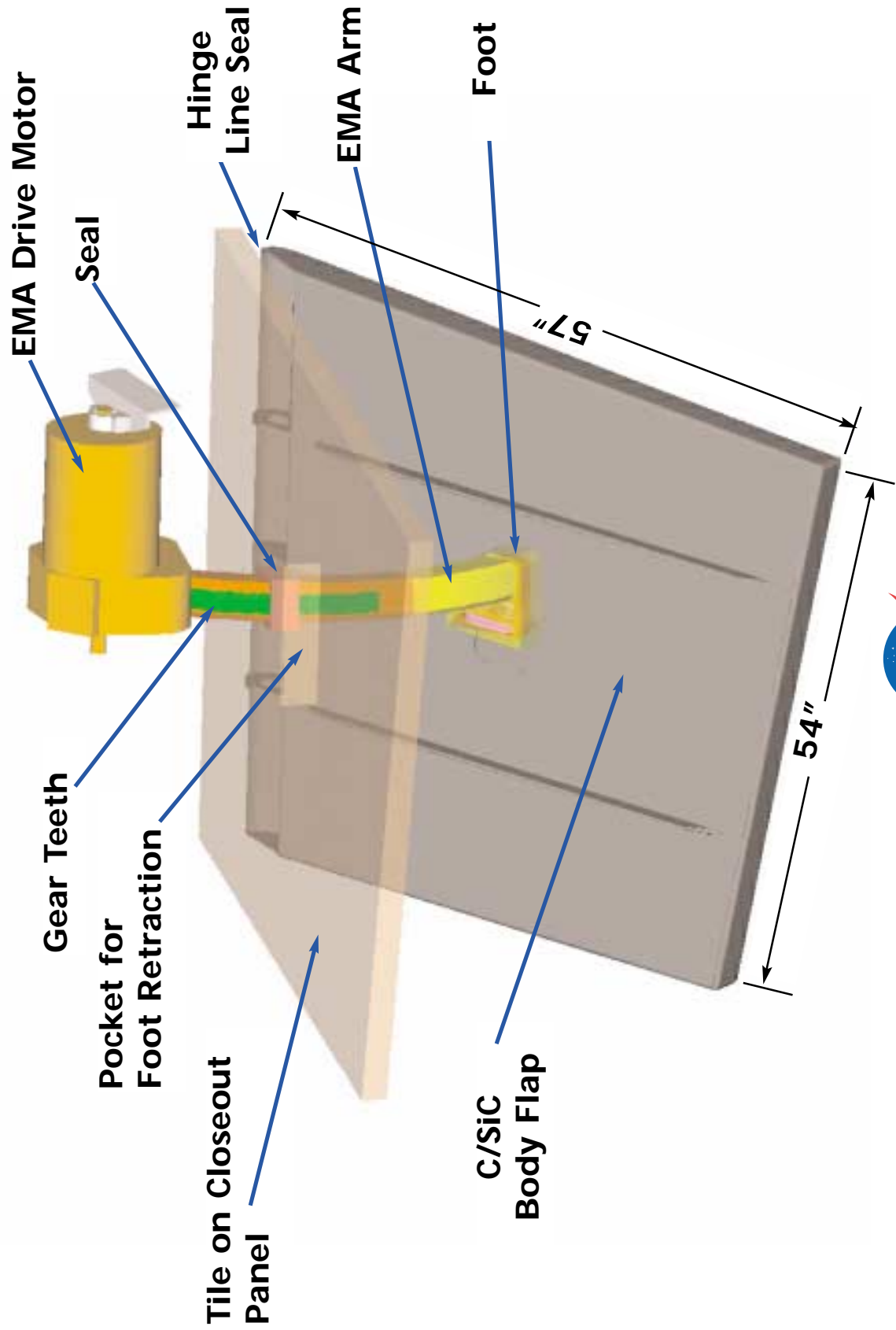
Seal After 1000 Cycles with Smooth Tile



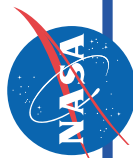
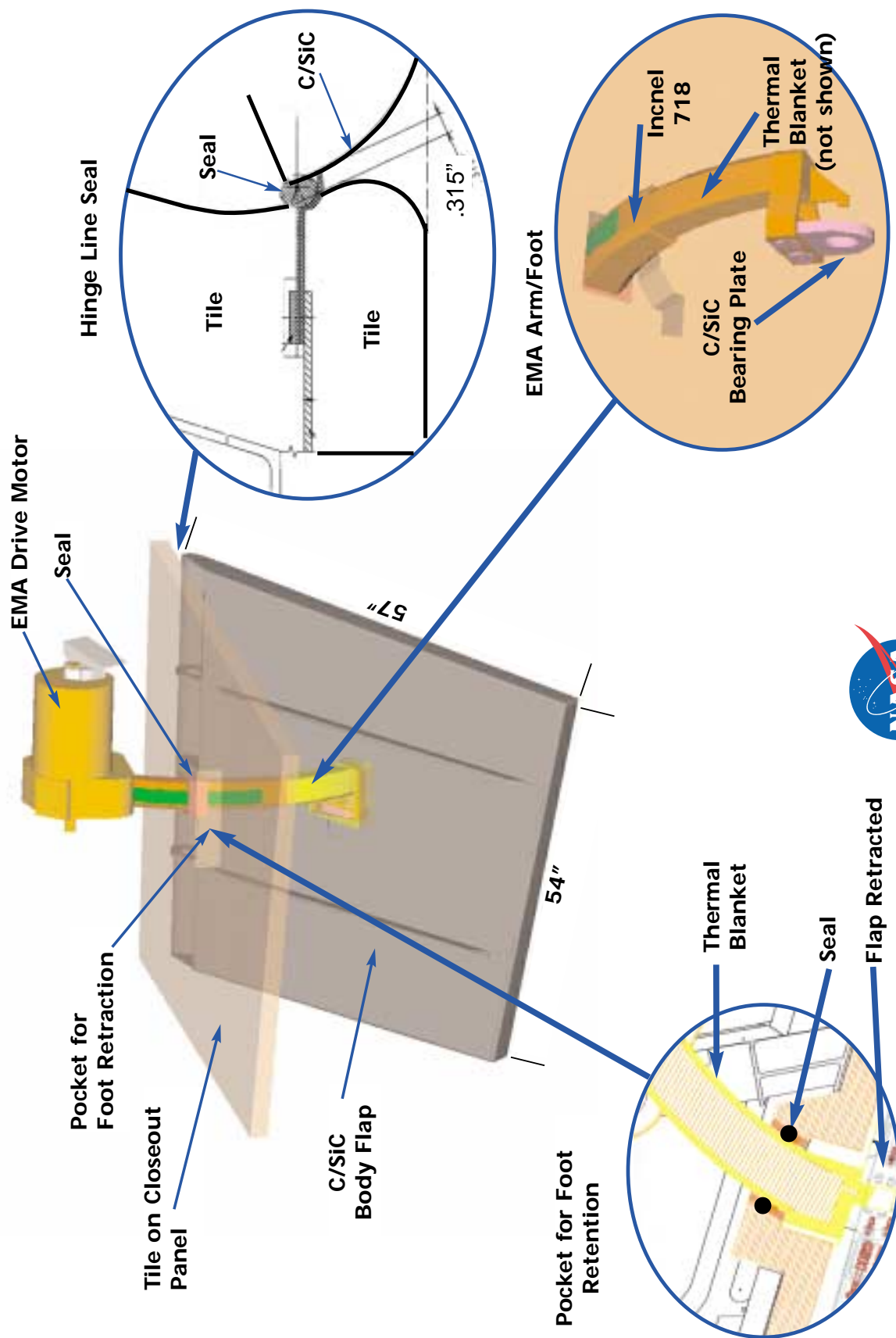
X-38 Body Flap Assembly



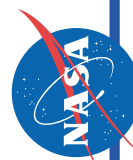
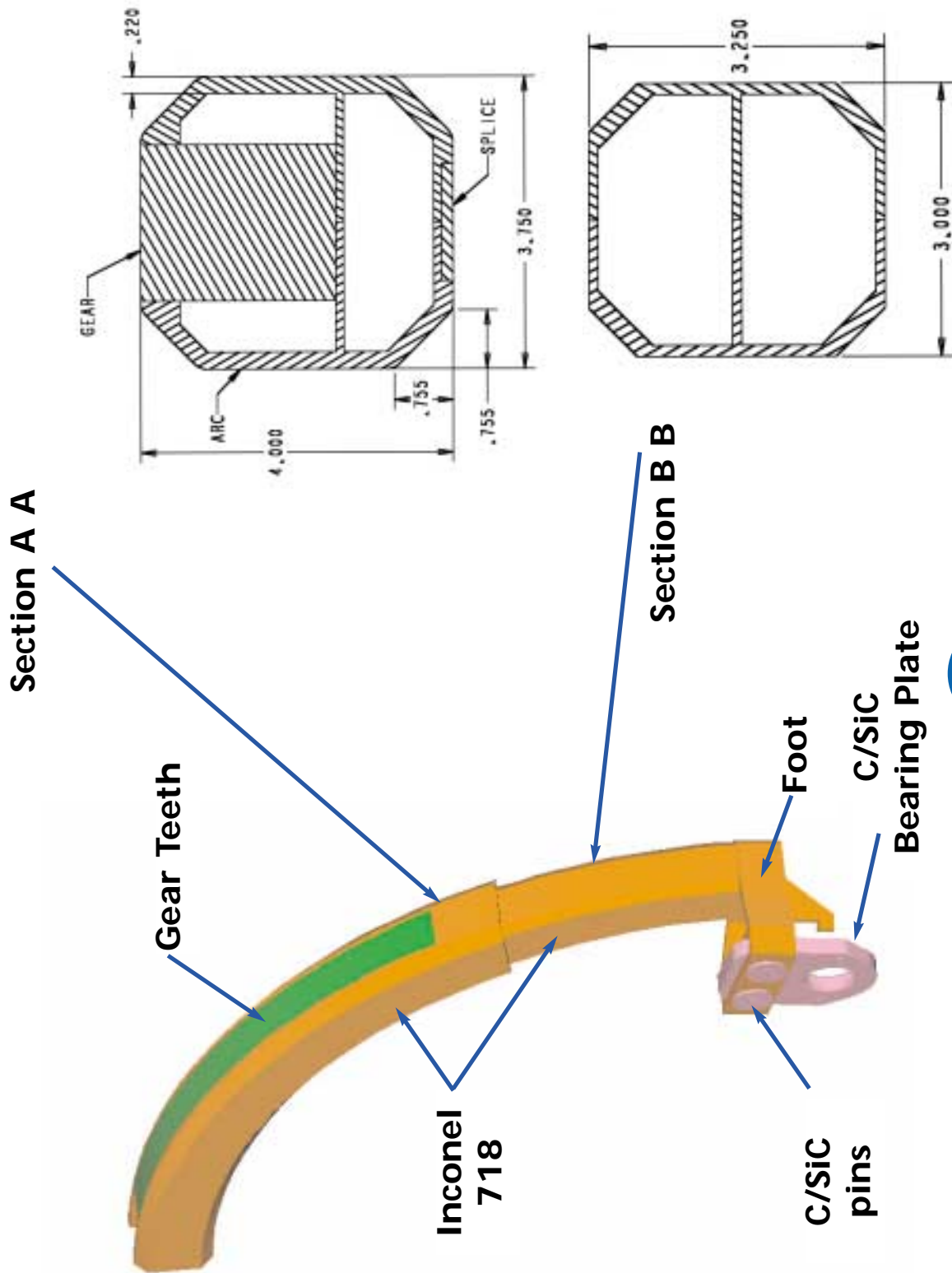
Baseline X-38 Bodyflap Seal Design



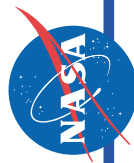
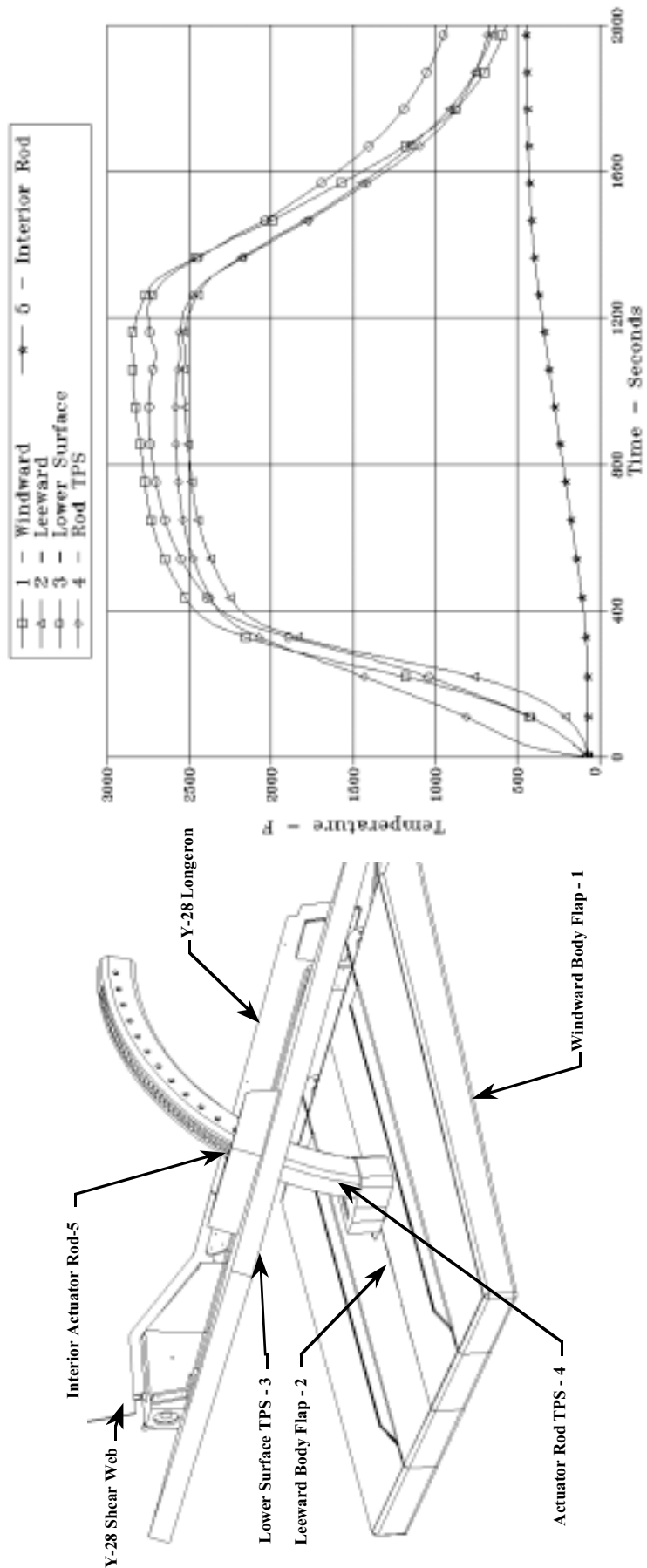
EMA Arm with Thermal Shield



EMA Arm Without Thermal Shield



Body Flap Cavity Thermal Response



Body Flap EMA Arm Thermal Response

Structure

Foot/Arc: Inconel 718

Teeth: Stainless Steel 17-4 PH

TPS

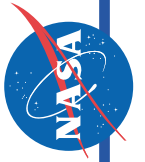
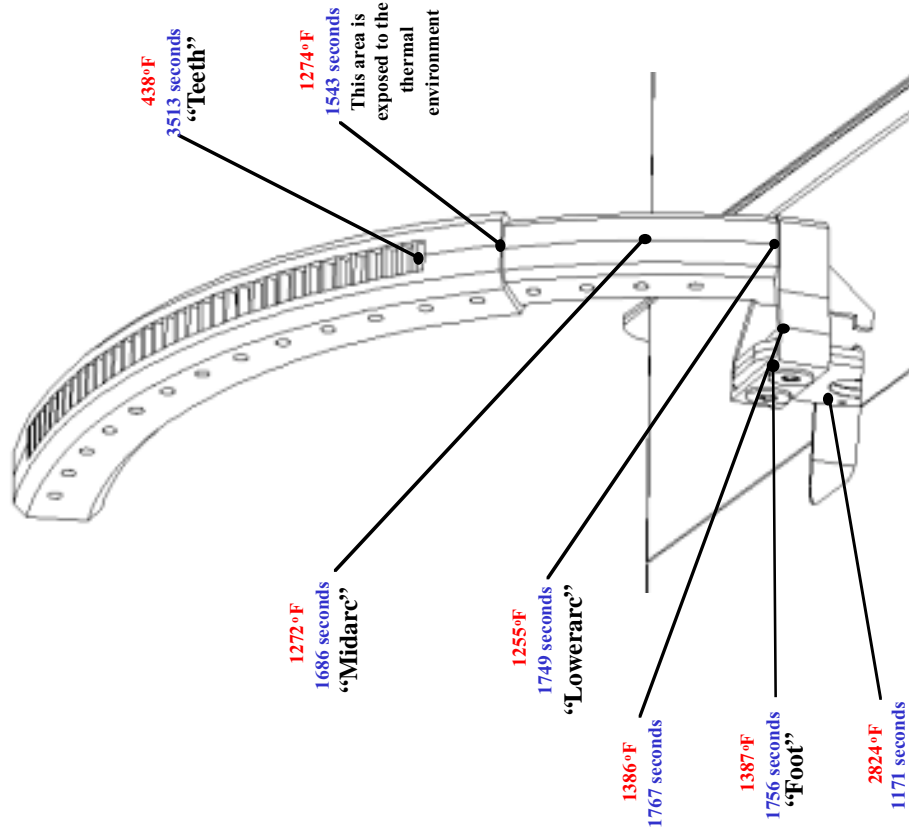
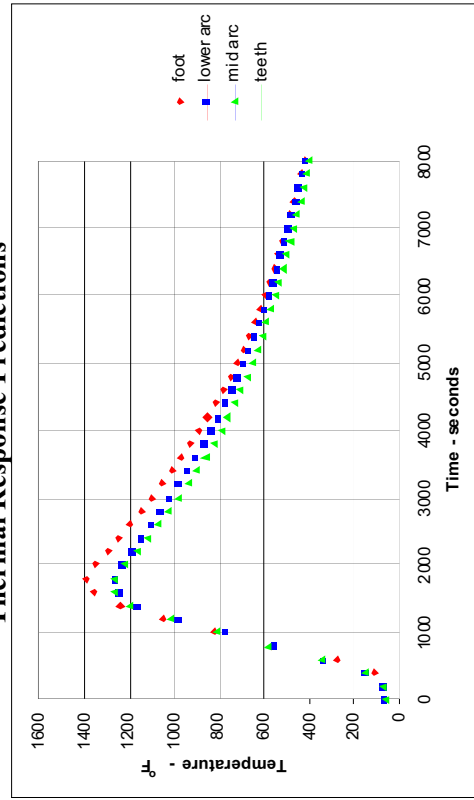
1/2" thick modified HT AFRSI Blanket
(0.54" total thickness)

Heating Environment

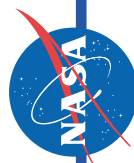
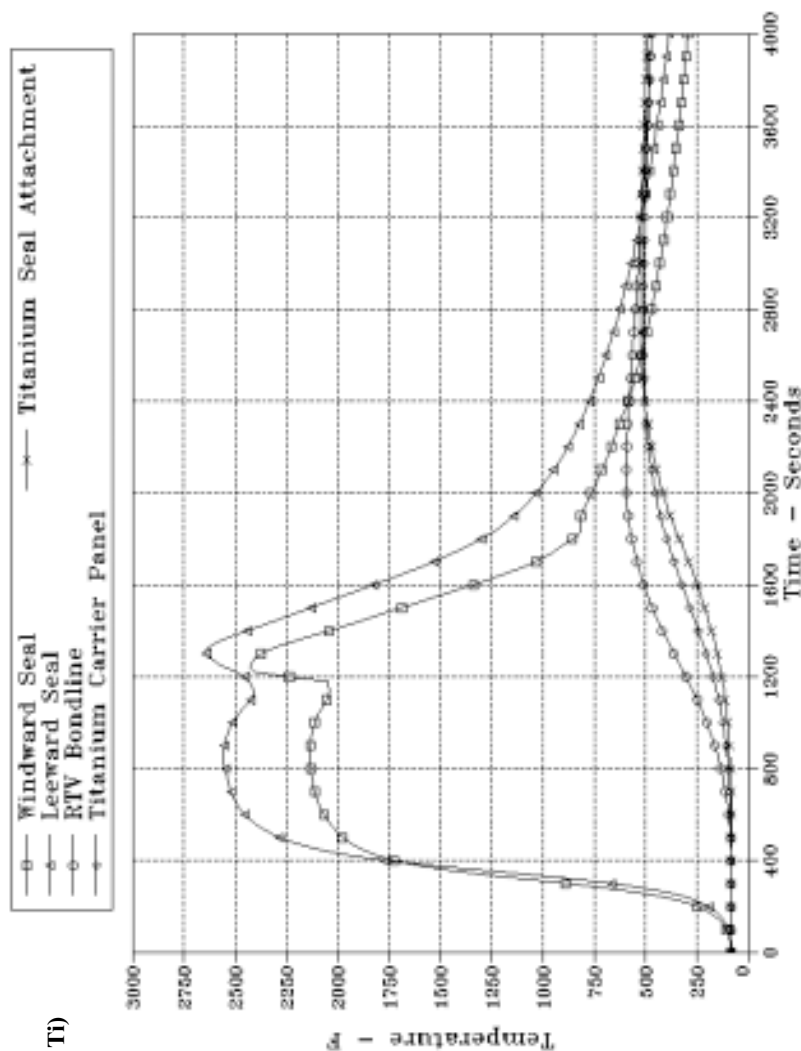
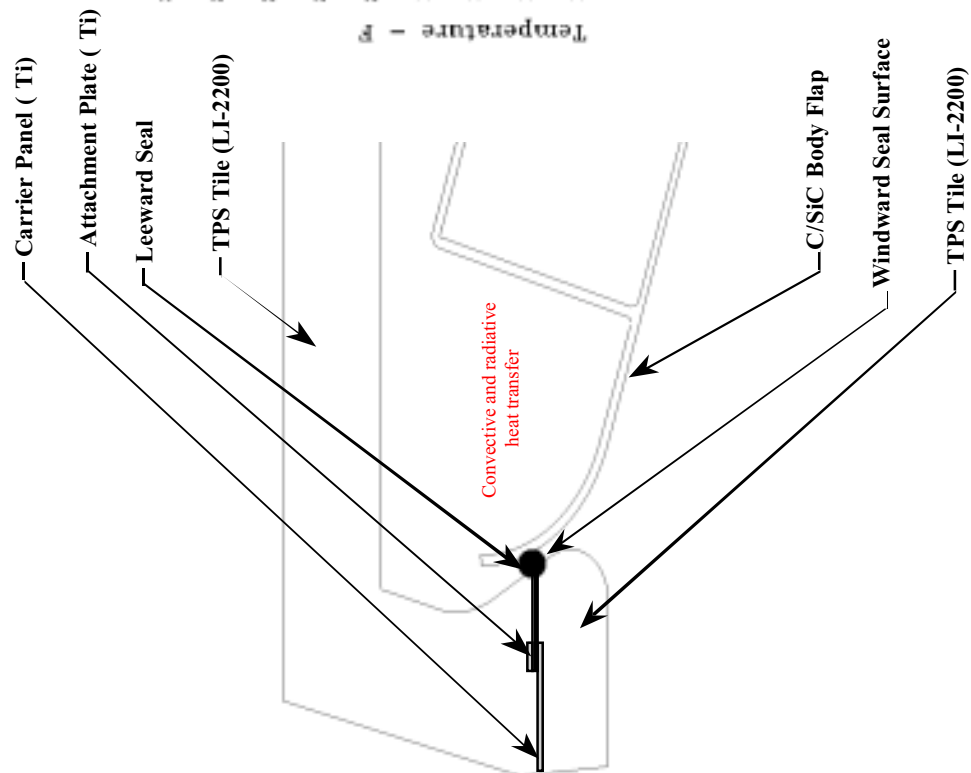
1.0 uncertainty factor applied to all heating

25° flap deflection angle

Thermal Response Predictions

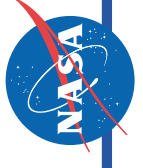


Body Flap Hinge Line Seal Thermal Response



Summary

- ❖ Glenn Research Center Spring Tube Seal Test Established
 - Flow Characteristics
 - Compressed Seal Unit Load/Contact Pressure
 - Resilency
 - Effect of Temperature
- ❖ JSC Rudder/Fin Rub Test
 - Validated Seal Scissor Action Design
 - Provided Coefficients of Friction/Operational Torque
 - Preliminary Coefficient of Friction
 - Engaging/Disengaging Torque Valves
 - Wear Characteristics of Seal
 - Requirement to Fill Open Gap Between Tiles for a Tile Rub Surface Design
- ❖ Future Tests
 - Flow Characteristics
 - Seal Compression Levels of 10% and 0%
 - Seal Degraded from Rub Tests
 - Rub Tests
 - Smooth Tile Rub Surface
 - Redesigned Tile Gap



NASA Facts

National Aeronautics and
Space Administration

Lyndon B. Johnson Space Center
Houston, Texas 77058

International Space Station

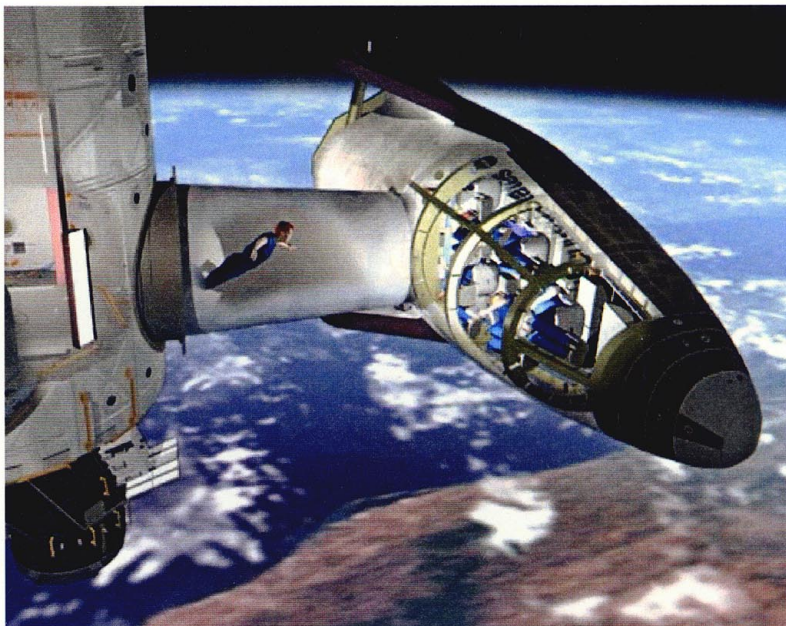


June 2000

The X-38: Low-Cost, High-Tech Space Rescue

A Reliable Lifeboat, Ambulance for the International Space Station

With technologies that blaze a trail for future human spacecraft, NASA's X-38 project is developing -- at an unprecedented low cost -- a prototype rescue vehicle to provide astronauts on the International Space Station an immediate return home in an emergency.



An innovative combination of a shape first tested in the 1970s and today's latest aerospace technology,

An X-38-derived rescue vehicle at the International Space Station. the X-38 already is flying in the actual conditions in which it must perform. Since 1997, increasingly complex, unpowered atmospheric test flights of the X-38 have been under way at the Dryden Flight Research Center in California. An unpowered X-38 space test vehicle, now under construction at the Johnson Space Center in Houston, will fly aboard the Space Shuttle in 2002 and descend to a landing independently. The X-38 is designed to fit the unique needs of a space station "lifeboat" -- long-term, maintenance-free reliability that is always in "turn-key" condition, ready to provide the entire station crew a quick, safe trip home under any circumstance.

In addition to contributions from commercial companies and NASA centers coast-to-coast, international space agencies are participating with the United States in the X-38's development. Contributions to the X-38 are being made by Germany, Belgium, Italy, Netherlands, France, Spain, Sweden and Switzerland and 22 companies throughout Europe.

Pushing the Edge: *Something New, Something Old*

The X-38 couples a proven shape, taken largely from a 1970s' Air Force project called the X-24A, with dozens of new technologies -- the world's largest parafoil parachute; the first all-electric spacecraft controls; flight software developed in a quarter of the time required for past spacecraft; laser-initiated explosive mechanisms for deploying parachutes; and global positioning system-based navigation.

The crew rescue vehicle on the International Space Station will have to be capable of a maintenance-free reliability in orbit never before achieved by a human spacecraft -- an ability to remain attached to the station for up to three years, all the while ready to depart in under three minutes, if needed. After leaving the station, it must be capable of returning a crew home in less than five hours, regardless of bad weather at some landing sites or the station's position when it departs. With medical equipment aboard, the emergency spacecraft will be both a "space ambulance" and a "space lifeboat." And capable of holding up to seven crew members, the rescue craft must have as high a passenger capacity as the space station.

The X-38 turns to the latest technology to meet these demands. Electrically powered spacecraft controls -- rather than maintenance-intensive hydraulic systems more commonly used by today's aircraft and the Space Shuttle -- drastically reduce the X-38's complexity and risks. By using a parafoil for its final descent, the X-38 does not need a long runway at the landing site, opening up many more options around the world as potential sites for a crew's emergency trip home. Laser-fired explosives eliminate a risk that stray electromagnetic interference during the years a rescue vehicle must spend in space could inadvertently cause a malfunction.



Now and Then: Above, the second X-38 test vehicle in free flight above Edwards Air Force Base, CA, in July 1999. Below, Air Force Major Cecil Powell in front of the X-24A in 1971. The X-38 combines a lifting body shape taken largely from the X-24A research with today's cutting-edge technologies.



Low-Maintenance Reliability: A Safe Trip Home in Minutes

Mission Scenario -- Because of illness, a station emergency, or a lack of available transportation, the International Space Station crew enters an X-38 rescue craft and undocks -- in less than three minutes, if necessary, or within 30 minutes under less pressing circumstances. Ground control provides landing site information, or, if needed, the entire descent could be performed independent of ground communications. Within three hours, the engines are fired to deorbit, and the deorbit module is then jettisoned. The rescue vehicle enters the atmosphere at an altitude of about 80 miles, traveling 18,000 miles per hour, half a world away from touchdown. As it descends, the wingless craft generates lift with its body and maneuvers to fly to the landing site. As air pressure increases, body flaps and rudders steer. At 23,000 feet, an 80-foot diameter drogue parachute deploys. As the craft stabilizes, the giant main parafoil begins its deployment and the drogue is cut away. In five stages to ensure a gentle descent, the parafoil slowly opens. Winches pull on lines to steer the parafoil, in the same way a skydiver steers, to the landing site. Landing skids deploy and the craft touches down, dropping at less than five miles an hour with a forward speed of about 40 miles per hour.

X-38 By The Numbers

Crew Rescue Vehicle

Length:	30 feet
Width:	14.5 feet
Cabin:	417 cubic feet
Mass:	24,000 pounds
Crew size:	7 maximum
Mission duration:	Up to 3 years
Launch time:	As low as 3 minutes

Deorbit Propulsion System

Length:	6 feet
Width:	15.5 feet
Mass:	6,000 pounds

Parafoil

Area:	7,500 square feet
Span:	143 feet
Deploy altitude:	23,000 feet



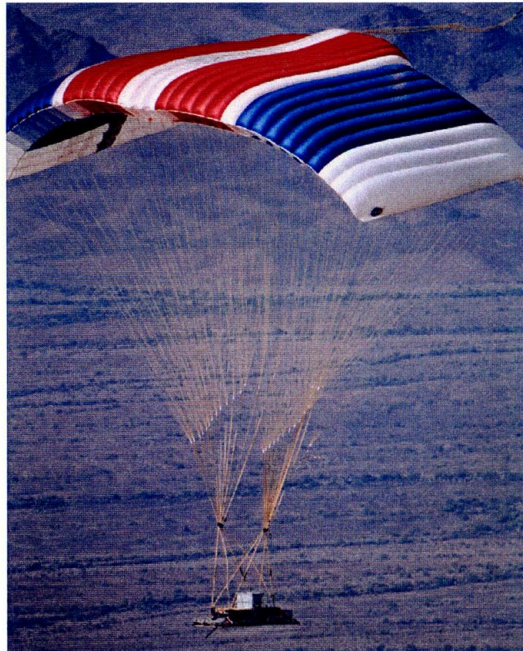
A unique parafoil system guides the X-38 to touchdown at less than 40 miles per hour.

X-38 Technology: *Expanding the Envelope of Spacecraft Design*



- **Electromechanical Actuators:** Small electric motors that weigh only 10 pounds -- yet are powerful enough to move with six tons of force in a fraction of a second -- replace complicated conventional hydraulic systems to power the X-38's flaps and rudders. Hydraulic systems account for up to 25 percent of the annual maintenance on commercial aircraft, and the electrical actuators on the X-38 serve as a forerunner for a technology that has the potential to make flight simpler and safer not only in space but also on Earth.
- **Laser-Initiated Pyrotechnics:** Never before used on a human spacecraft, the explosive charges that deploy the X-38's parachutes are fired using a system of fiber optics and lasers. Using light instead of electricity simplifies the system and reduces the potential for electromagnetic interference during the extended stays the X-38 will experience in orbit.
- **Landing Skids:** Rather than temperature-sensitive tires, the X-38 uses simple skids as landing gear, eliminating the need to watch inflation pressures, brakes, or other complex mechanisms during the years it spends in space.
- **Navigation:** The X-38 uses compact Global Positioning System and electronics technology for its primary navigation system -- never before used as the primary navigation equipment on a human spacecraft -- rather than the complex mechanical navigation platforms used as the primary system aboard the Space Shuttle. The GPS navigation system designed for the X-38 already has been flight-tested as a payload aboard the Space Shuttle.

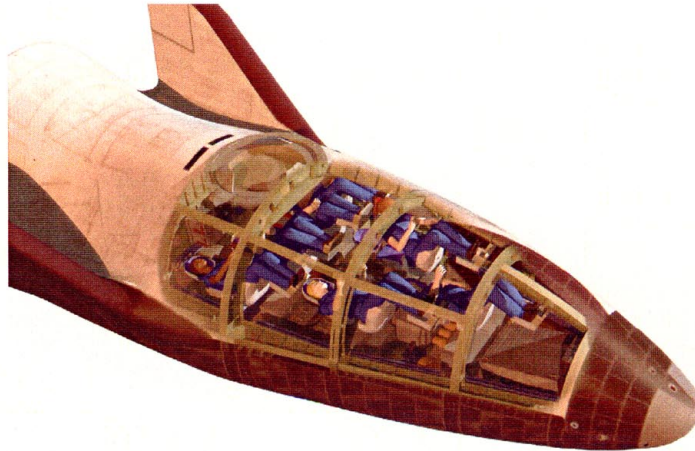
- Lifting Body:** The X-38's special lifting body shape -- a shape that creates lift so the craft can fly even though it has no wings -- is a modified version of a shape tested by the Air Force in the late 1960s and 1970s. The Air Force's previous testing has reduced the costs associated with the X-38. The lifting body shape gives the X-38 the capability to fly to a landing site during its descent, increasing the number of possible landing sites. Two movable fins and body flaps provide steering for the spacecraft as it descends into the atmosphere.
- Parafoil:** A 7,500 square-foot parafoil, the world's largest, allows the X-38 to have great flexibility to get a crew back to Earth quickly with dozens of potential landing sites around the world, eliminating the need for a miles-long runway to accommodate high-speed landings similar to the Space Shuttle. Using the parafoil to glide to its final descent, the X-38 touches down at under 40 miles per hour and skids to a stop in only 150 feet. The giant X-38 parafoil, almost one and a half times as large as the wings of a 747 jumbo jet, may be a technology that finds other uses, including future spacecraft and uses on Earth that require precise landings, such as airdrops of humanitarian aid.



7,500 square-foot parafoil test

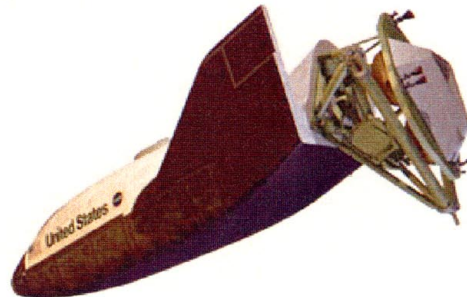
- Life Support:** For reliability, the X-38's life support system uses proven, simple technologies: Lithium batteries already used on many Shuttle-deployed satellites provide electricity. Active cooling of the cabin and electronics is provided by a sublimator technology first used on the Apollo lunar lander. Carbon dioxide is scrubbed from the cabin air using lithium hydroxide canisters that have been used virtually problem-free on all human spacecraft. The fire extinguishing system uses technology commonly found on advanced fighter aircraft. And the communications system is identical to technologies used on most NASA satellites. As a custom-built rescue craft, the X-38 can provide a normal sea-level pressure atmosphere for seven crew members for at least nine hours, twice as long as is required for a worst-case return to Earth.

- **Crew Cabin:** The station "lifeboat" will hold a crew of seven -- the entire crew of the station, ensuring no one is left behind in an emergency -- and be capable of returning to Earth automatically. The crew will be able to take over manual control of some functions, such as



selecting a landing site and steering the parafoil during final descent. The crew will land in a supine position and be subjected to minimal force to protect members that may be sick, injured or deconditioned from long exposure to weightlessness. The crew can monitor the operation of an X-38 rescue vehicle and manually take over using color display screens and controls. The cabin is windowless; exterior views are provided to the crew by television cameras.

- **Thermal Protection System:** The X-38 is protected from the almost 3,000 degrees Fahrenheit experienced during entry into the atmosphere by the same thermal tiles and blankets that protect the Space Shuttle. But, underneath the insulation, the outer skin of the X-38 uses lightweight, superstrong composite materials for the first time. The use of a composite material reduces the amount of flex in the spacecraft's skin and thus simplifies the way tiles are attached, allowing larger tiles to be used.
- **Deorbit Propulsion Module:** The only portion of the X-38 that is not reusable, the deorbit module provides the thrust and orientation control required to begin the rescue craft's descent. Designed for lightweight reliability, the module is built with composite materials, uses a single propellant and has its own set of batteries. To provide adequate backup capability, eight thrusters, each capable of producing 100 pounds of thrust, are fired for about 10 minutes to begin the X-38's descent. If any thrusters fail, the others can be fired longer and maintain a safe trip home for the crew. In addition, eight smaller thrusters, capable of 25 pounds of thrust each, provide orientation control during the deorbit firing. After the engine firings are completed, the module is jettisoned and burns up in the atmosphere.



Taking Flight: Testing That Reduces Risks and Costs

An Unprecedented Efficiency -- The X-38 project is developing a prototype rescue spacecraft for less than a tenth of the cost of past estimates for such a vehicle. Development of the X-38 through the flight of an unpiloted space vehicle in 2002 is estimated to cost about \$150 million. Previous estimates for the development of other station rescue concepts have ranged as high as \$2 billion.



The first two X-38 atmospheric test vehicles, designated V-131 and V-132, during pre- and post-test checkouts and preparation at Dryden Flight Research Center, CA.

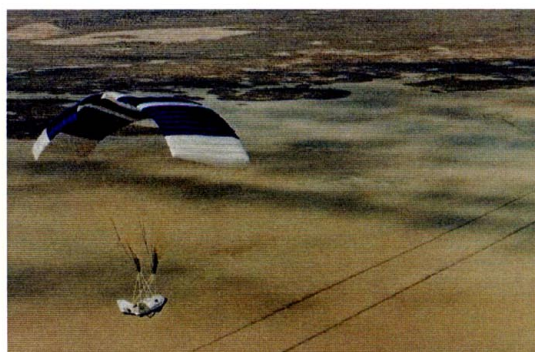
The estimated cost of the entire crew return vehicle project, from development through the construction of four operational spacecraft, ground simulators, spare parts, landing site support facilities and control center capabilities is less than \$1 billion, less than half of the cost to manufacture a single Space Shuttle orbiter. To keep costs low, the X-38's innovative, high-tech development approach uses computerized design, automated fabrication and computerized, laser inspection of many components for the space test vehicle now under construction at the Johnson Space Center in Houston. Rather than seeking early commercial bids on the spacecraft's design, in-depth development and testing of the X-38 is being done largely "in-house" by NASA civil servants. The unusual approach allows NASA personnel to gain a superior understanding of the design, costs, tests, and risks associated with the spacecraft before seeking commercial bids.



Put to the Test -- Testing of the X-38 has been under way since 1995, when over 300 subscale flight tests of the parafoil and lifting body began. Large-scale flight testing began in 1997 when the first X-38 atmospheric test vehicle was flown on "captive carry" tests under the wing of a B-52 aircraft at NASA's Dryden Flight Research Center, California. The same vehicle flew in the first free flight tests in 1998. A second, more sophisticated test vehicle first flew in March 1999 and, in March 2000,

completed a flight from 39,000 feet that intercepted the trajectory of a crew return vehicle returning from space for the first time.

At the U.S. Army's Yuma Proving Ground in Arizona, the X-38 team successfully tested the largest parafoil ever produced, 7,500 square feet, in February 2000. Flight tests that increase in complexity and altitude will continue through at least 2001 with two more X-38 atmospheric test vehicles, leading up to the first X-38 flight in space in the spring of 2002. The X-38 space test vehicle is already under construction at the Johnson Space Center. The unpiloted space vehicle will be carried to orbit in the payload bay of the Space Shuttle, released using the Shuttle's robotic arm and then descend to landing.



Large-scale X-38 atmospheric flight tests have been under way since 1997 and will continue, increasing in complexity and altitude each time, through 2001.

A National and International Partnership -- The X-38 draws on talent and expertise coast to coast in the United States and throughout Europe. Led by NASA's Johnson Space Center in Houston, NASA facilities include: flight testing at the Dryden Flight Research Center, CA; development of the Deorbit Propulsion System at the Marshall Space Flight Center in Huntsville, AL; tile manufacturing and launch processing at the Kennedy Space Center, FL; communications equipment from the Goddard Space Flight Center, MD; wind tunnel testing at the Langley Research Center, Hampton, VA; aerothermal analysis by the Ames Research Center, CA; and electromechanical actuator consultation from the Lewis Research Center, OH. In addition, the U.S. Army provides testing support at the Yuma Proving Ground, AZ; the U.S. Air Force has provided in-flight simulation support; and Sandia National Laboratories has provided parachute systems expertise. Companies with major roles in the project include Scaled Composites, Inc., of Mojave, CA, construction of the atmospheric test vehicle aeroshells; Aerojet Gencorp of Sacramento, CA, construction of the space test vehicle's Deorbit Propulsion Module; Honeywell Space Systems, Houston, development of the flight control software; and Pioneer Aerospace, Inc., of Columbia, MS, fabrication of the parafoil. In addition, the German Space Agency and the European Space Agency are contributing to the project, involving eight countries and 22 companies throughout Europe.



X-38 space test vehicle

RUDDER/FIN SEAL INVESTIGATIONS FOR THE X-38 RE-ENTRY VEHICLE

Patrick H. Dunlap, Jr. and Bruce M. Steinetz
National Aeronautics and Space Administration
Glenn Research Center
Cleveland, Ohio

Donald M. Curry
National Aeronautics and Space Administration
Johnson Space Center
Houston, Texas

Rudder/Fin Seal Investigations for the X-38 Re-Entry Vehicle

**Mr. Patrick H. Dunlap, Jr.
Dr. Bruce M. Steinetz
NASA Glenn Research Center
Cleveland, OH 44135**

**Mr. Donald M. Curry
NASA Johnson Space Center
Houston, TX 77058**

**2000 NASA Seal/Secondary Air System Workshop
October 25-26, 2000**



NASA Glenn Research Center

Background

- **NASA developing X-38 vehicle to demonstrate technologies for crew return vehicle (CRV) for International Space Station. CRV will be “ambulance” for medical emergencies and evacuation vehicle.**
- **X-38 control surfaces (body flaps and rudders/fins) require high temperature seals to:**
 - Limit hot gas ingestion
 - Limit transfer of heat to underlying low-temperature structures
- **NASA Johnson Space Center and Glenn Research Center working together to develop and evaluate rudder/fin seals.**
 - Measure seal flow rates, resiliency, and unit loads in as-received and temperature-exposed conditions
 - Compare measured results to property goals
 - Identify areas for future work

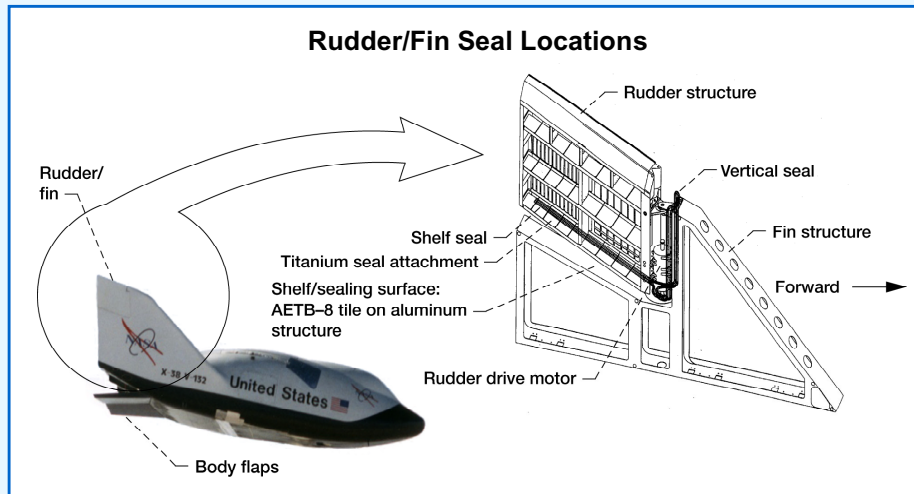


NASA Glenn Research Center

CD-00-80663

NASA is currently developing the X-38 vehicle that will be used to demonstrate the technologies required for a crew return vehicle (CRV) for the International Space Station. The CRV will serve both as an ambulance for medical emergencies and as an evacuation vehicle for the Space Station. Control surfaces on the X-38 (body flaps and rudders/fins) require high temperature seals to limit hot gas ingestion and transfer of heat to underlying low-temperature structures to prevent over-temperature of these structures and possible loss of the vehicle. NASA's Johnson Space Center (JSC) and Glenn Research Center (GRC) are working together to develop and evaluate seals for the rudder/fin control surfaces. The specific objectives of this study are to measure seal flow rates, resiliency, and unit loads in as-received and temperature-exposed conditions and compare the measured results to property goals where applicable. Areas for future work would then be identified.

X-38 Rudder/Fin Seal Assembly

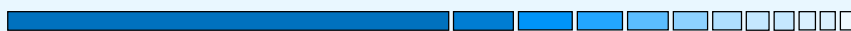


NASA Glenn Research Center

CD-00-80663

This chart shows the X-38 vehicle including the body flap and rudder/fin locations where high temperature seals are required. The figure on the right shows an enlarged view of the rudder/fin seal location. The rudder/fin seals consist of a double seal attached to the surface of the rudder that seals the vertical hinge line and the fin shelf line. The vertical seal loop surrounds and protects the rudder drive motor and the attachments between the rudder and the fin. The shelf seal seals the gap between the bottom surface of the rudder and the shelf of the fin. The seals must allow the rudder to rotate during the entire mission and must accommodate a rudder/fin deflection range of ± 12 degrees. They also must not transmit excessive loads to the AETB-8 (Alumina Enhanced Thermal Barrier – 8 lb/ft³ density) thermal tiles against which they seal so as not to damage the tiles.

Design Requirements for X-38 Rudder/Fin Seals



- **Temperature limits:** Thermal analysis predicted peak seal temperatures of 1900°F (with laminar boundary layer assumption) to 2100°F (with turbulent boundary layer assumption)
- **Pressure drop:** Maximum predicted pressure drop across seal is 56 lbf/ft² (0.4 psi)
- **Flow goal:** Preliminary flow goal of 4.2x10⁻⁵ lbm/sec per inch of seal at 56 lbf/ft²
- **Resiliency:** No specific design requirement. Seals are to maintain contact with sealing surface during maximum heating cycle
- **Seal loads:** Unit load (load per unit inch) is to be less than 5 lbf/in. Contact pressure to be below 10 psi
- **Wear resistance:** Seals must allow rudder rotation without excessive loads on rudder drive motor
- **Life:** Single-use seal



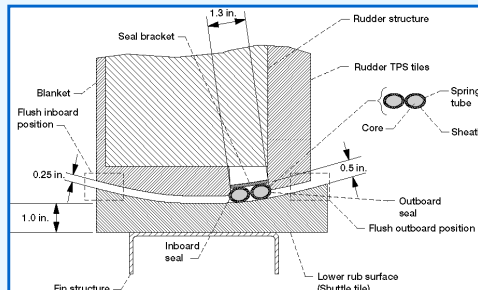
NASA Glenn Research Center

CD-00-80663

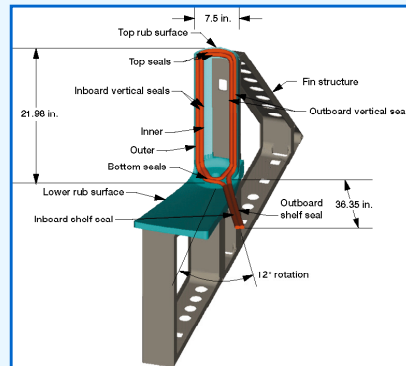
Design requirements were decided upon for the X-38 rudder/fin seals so that test results could be compared to an original set of property goals. An initial thermal analysis performed by JSC predicted peak seal temperatures of 1900°F (with a laminar boundary layer assumption) to 2100°F (with a turbulent boundary layer assumption). The maximum predicted pressure drop across the seal during vehicle re-entry was about 56 lbf/ft² (0.4 psi). An initial seal permeability value was used to calculate a preliminary flow goal along the length of the seal of 4.2x10⁻⁵ lbm/sec per inch of seal at 56 lbf/ft². In terms of seal resiliency, no specific design requirement was set. Designers at JSC only specified that the seals are to remain in contact with the opposing seal surfaces during the maximum heating cycle to prevent flow paths from developing around the seals. Because the seals will seal against Shuttle derived tiles that cannot withstand excessive loads, seal unit loads and contact pressures must be limited to prevent tile damage. Unit loads (load per linear inch of seal) were set to be less than 5 lbf/in, and contact pressures were to be below 10 psi. In terms of wear resistance and life, the seals are single use items that will be replaced after each mission. They also must not experience excessive wear as they are scrubbed over the surface of the fin shelf. Such wear could create loads on the rudder drive motor that would interfere with rudder rotation.

Baseline X-38 Rudder/Fin Seal Design

Cross Section of Rudder/Fin Seal Location



Computer Model of Rudder/Fin Seal



- **Main seal components**
 - Core: 6, 9 pcf Saffil insulation
 - Spring tube: Inconel X-750
 - Sheath: Two layers of Nextel 312 fabric
- **Seals are used on Space Shuttle: main landing gear doors, orbiter external tank umbilical door, payload bay door vents**
- **Nominal 20% compression and 0.25-in. gap**

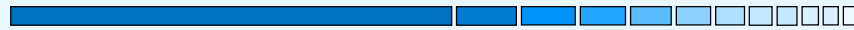


NASA Glenn Research Center

CD-00-80663

This chart shows details of the X-38 rudder/fin seal design. As seen in the figure on the left, the 0.62-in diameter seals are composed of an Inconel X-750 spring tube that is stuffed with Saffil insulation at either 6 or 9 lbf/ft³ (pcf) density. Two layers of Nextel 312 fabric are braided over the spring tube. The 6 pcf design was chosen as the baseline seal design for this application, but the 9 pcf design was also tested for comparison purposes. These seals are currently used in several locations on the Space Shuttle orbiters including the main landing gear doors, the orbiter external tank umbilical door, and the payload bay door vents. The figure on the left shows a cross section of the rudder/fin shelf seal location as seen while standing aft looking forward. The double seals can be seen attached to a bracket in the rudder and compressed against the opposing surface of the fin shelf. The seals are compressed to a nominal 20% compression to seal a 0.25-in gap. The figure on the right shows the entire seal assembly including dimensions for the vertical loop and shelf seal portion. The shelf seals are shown rotated 12 degrees off of the shelf. In this position, a portion of the seals are no longer in contact with the shelf and are exposed to the hot gases that are passing over the vehicle. As the seals are moved back on to the shelf surface, they will be compressed again and must be able to endure the shear forces that they will be subjected to without causing excessive loads on the rudder drive motor.

Test Matrix



Compression Testing

Compression level	20%		25%		30%	
	Primary	Repeat	Primary	Repeat	Primary	Repeat
6 pcf as-received	✓	✓	✓	✓	✓	✓
6 pcf after time at 1900 deg F	✓	✓	✓	✓	✓	✓
9 pcf as-received	✓	✓				

Flow Testing

Gap size	0.25 in				0.13 in			
Compression level	20%		25%		20%		25%	
	Primary	Repeat	Primary	Repeat	Primary	Repeat	Primary	Repeat
Single seal								
6 pcf as-received	✓	✓	✓		✓		✓	
6 pcf after time at 1900 deg F	✓	✓	✓		✓		✓	
9 pcf as-received	✓	✓						
Double seal								
6 pcf as-received	✓							

✓ Checked blocks indicate tests performed

- Each test used a separate seal specimen

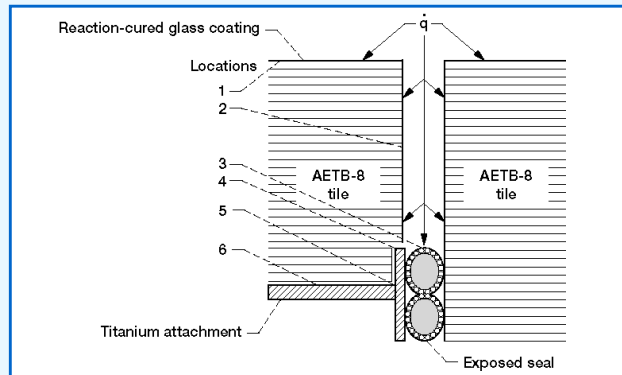


NASA Glenn Research Center

CD-00-80663

This chart shows the matrix of tests that were completed at GRC on the rudder/fin seals. A series of room temperature compression and flow tests were performed on two different seal designs under a variety of test conditions. The checked blocks indicate tests that were performed, and each test used a separate seal specimen. Compression tests were performed to determine the preload and resiliency behavior of the seals. Primary and repeat tests were done at three different compression levels (20, 25, and 30%) on the 6 pcf design in both the as-received state and after temperature exposure at 1900°F. Primary and repeat tests were done at 20% compression on the 9 pcf design in the as-received state for comparison purposes. Flow tests were performed at two different gap sizes (0.25 in. and 0.13 in.) and two different compression levels (20 and 25%). Single seals were flow tested for the 6 pcf design before and after temperature exposure and for the 9 pcf design in the as-received state. A double seal flow test was performed on the 6 pcf as-received seal at 20% compression with a 0.25-in gap.

Thermal Analysis - Rudder/Fin Seal Thermal Model



- Thermal analysis used quasi-2-D representation of tiles (AETB-8 with RCG/TUFI coating), dual seals, and titanium attachment
- Model accounted for conduction, convection, and radiation but no flow through permeable seal. Heat fluxes to seal and gap walls estimated using Nestler gap heating correlations (Nestler, AIAA72-717) using reference heating on windward surface of rudder/fin area as input

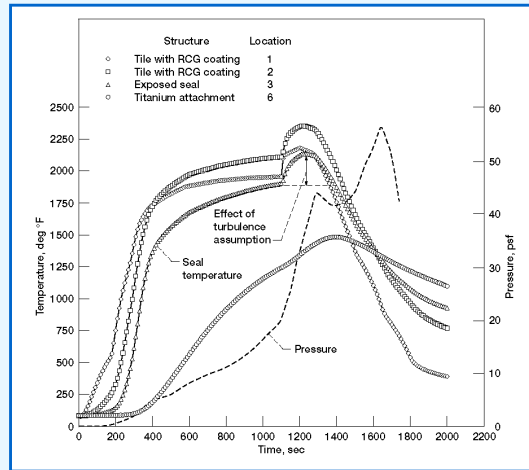


NASA Glenn Research Center

CD-00-80663

This chart shows the thermal model that JSC used to predict temperatures for the rudder/fin seals and surrounding hardware during re-entry of the X-38 vehicle. The model is a quasi-two-dimensional representation of the tiles (AETB-8 with RCG/TUFI coating), the dual seals, and the titanium seal attachment. It accounted for conduction, convection, and radiation down into the seal gap, but it did not account for flow through the permeable seals. We believe that including flow through the seals in the model could effect temperature predictions and result in higher predicted maximum seal temperatures. Heat fluxes to the seal and to the gap walls were estimated using the gap heating relationship presented by Nestler (Nestler, AIAA 72-717). Reference heating conditions on the windward surface of the rudder/fin area during re-entry of the X-38 vehicle were used as the input for the model.

Thermal Analysis- Rudder/Fin Seal Temperature Predictions



- Predicted peak seal temperatures of 1900°F (with laminar boundary layer assumption) to 2100°F (with turbulent boundary layer assumption)
- Predicted peak pressure of 56 lbf/ft²



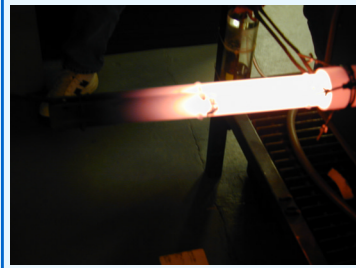
NASA Glenn Research Center

CD-00-80663

The results of the rudder/fin seal thermal analysis performed by JSC are shown in this chart. The plot shows temperature predictions for several locations in the model versus time during re-entry. Also shown is the predicted pressure differential across the seal during re-entry. The third line down shows the predicted seal temperatures. The thermal analysis predicted a maximum seal temperature of 1900°F (with a laminar boundary layer assumption) to 2100°F (with a turbulent boundary layer assumption). The dashed line is the predicted pressure differential across the seal showing a peak pressure of 56 lbf/ft² (psf). The plot shows that the peak seal temperature and pressure are not coincident, but the testing that we performed was done as if they did occur at the same time to simulate worst case conditions.

Temperature Exposure

Temperature Exposure of X-38 Seal



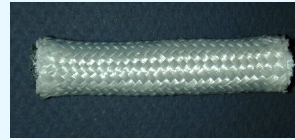
Test Conditions:

- Exposed 6 pcf seals to 1900°F in compressed state for 7 minutes

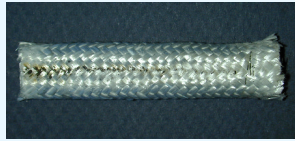
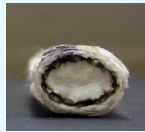
Observations:

- Seals took on elliptical cross section and became stiffer and less flexible
- Loss of resiliency believed to be due to permanent set of Inconel X-750 spring tube (yield strength at 1900°F < 5% of room temperature strength)
- No noticeable changes to Nextel 312 fabric or Saffil batting

As-received



After Temperature Exposure



Seals lost resiliency and took on large permanent set



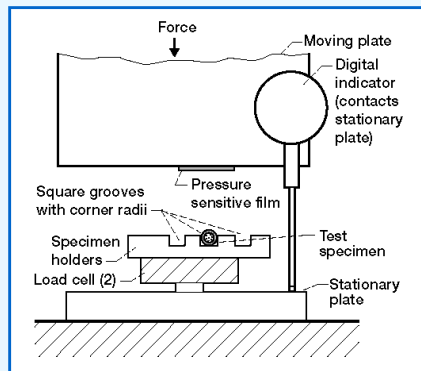
NASA Glenn Research Center

CD-00-80663

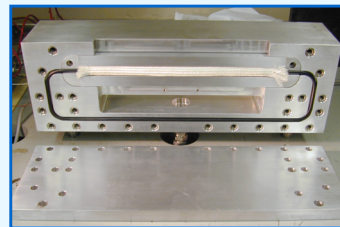
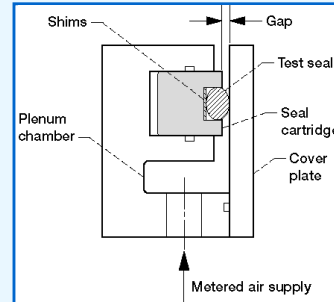
Temperature exposure tests were done on the 6 pcf seal design to simulate exposure to the extreme temperatures predicted by the thermal analysis and to determine the effects that this exposure has on the seals. The tests were conducted by placing specimens into a tube furnace in a compressed state and heating them at 1900°F for seven minutes. The figure on the left shows a hot seal specimen being removed from the furnace in its test fixture. After temperature exposure, the seals took on an elliptical cross section (lower right figure) compared to the circular cross section of an as-received seal (upper right). The seals took on a large permanent set and became stiffer and less flexible than they were before the temperature exposure. We believe that this loss of resiliency is due to permanent set of the Inconel X-750 spring tube whose yield strength at 1900°F is less than 5% of its room temperature strength. There were no noticeable changes after temperature exposure to the Nextel 312 fabric outer sheath or the Saffil batting in the core of the seals. This loss of seal resiliency would be a problem for a reusable vehicle in which the seals must remain resilient after multiple heating cycles. The X-38 only requires single-use seals, though, so this seal design should be resilient enough for one vehicle re-entry.

Test Fixture Schematics

Compression Fixture



Flow Fixture



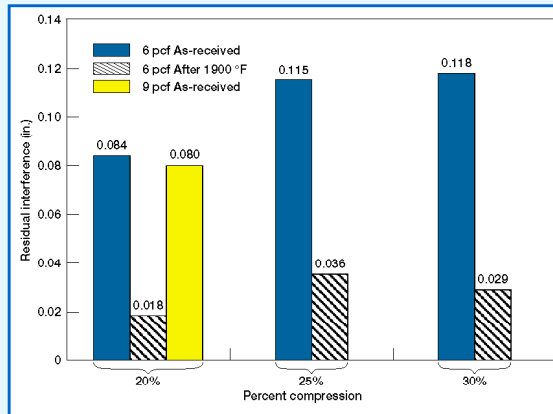
NASA Glenn Research Center

CD-00-80663

This chart shows schematics for our compression (left) and flow (right) fixtures. In the compression fixture, a test specimen is loaded into a stationary grooved specimen holder, and an opposing plate is compressed against the specimen. Load cells behind the specimen holder record the amount of load on the seal, and the displacement of the movable opposing plate against the specimen is shown on a digital indicator. Multiple load cycles are applied to a specimen to remove the effects of hysteresis that accumulate with load cycling. Typically four load cycles are applied to each specimen. A pressure sensitive film mounted on the opposing plate is used to determine the contact width of the specimen as it is loaded. The footprint length and width at the end of the fourth load cycle are used to calculate seal preload or contact pressure. Flow tests are performed using the ambient linear flow fixture shown in the two figures on the right. The fixture is designed so that single or double seals of different diameters can be tested in removable cartridges that are inserted into the main body of the test fixture. Shims are inserted into the groove behind the seal to vary the amount of linear compression on the seal. Spacer blocks of different thicknesses are placed at each end of the cartridge to vary the gap that the seal is sealing between the cartridge and the cover plate. During a test, flow enters through the bottom of the fixture, passes through a plenum chamber, and flows through the gap that the seal is sealing. A flow meter upstream of the fixture measures the flow rate through the seal while the pressure differential across the seal and the temperature upstream of the seal are measured inside the fixture.

Compression Test Results-Resiliency

- Resiliency/springback generally increased with percent compression
- 6 pcf and 9 pcf seals had almost same resiliency
- Large loss of resiliency for temperature-exposed seals
 - Expected cause: Permanent set of Inconel X-750 spring tube
 - Large loss of resiliency a concern for future highly-reusable vehicles with long life requirements



- No specific design requirement for X-38 seal resiliency
- Change in seal gap for rudder/fin seals will be minimal due to floating fittings and attachments



NASA Glenn Research Center

JSC designers deem resiliency acceptable for single-use life requirement

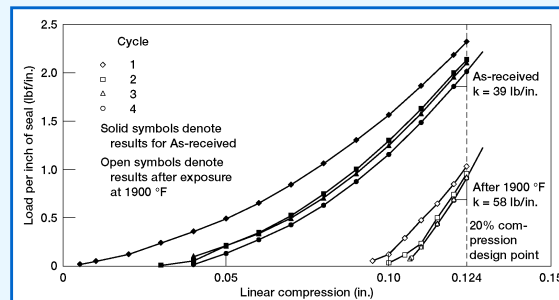
CD-00-80663

This chart shows some of the results of our compression tests. The plot shows the amount of resiliency, or springback, for different test conditions and compression levels. The different color bars are for the 6 pcf design in the as-received state (blue bar), the 6 pcf design after temperature exposure (striped bar), and the 9 pcf design in the as-received state (yellow bar). In the plot, residual interference refers to the amount that a seal springs back after it has been compressed for four load cycles. For example, if the 0.62-in diameter 6 pcf as-received seal is compressed 20% (0.124 in), it springs back for a residual interference of 0.084 in. Thus, the seal has taken a permanent set of 0.040 in. Looking at the results overall, seal resiliency generally increased as the percent compression on the seals was increased from 20% to 25% to 30%. The 6 pcf and 9 pcf as-received seals had almost the seal resiliency at 20% compression. Thus, using the denser core in the 9 pcf design did not add any additional resiliency to this seal design as compared to the 6 pcf design with a less dense core. The temperature-exposed 6 pcf seals took on a large permanent set and lost a large amount of resiliency. Again, this is believed to be due to permanent set of the Inconel X-750 spring tube. The loss of resiliency for this seal design is a concern if this seal is to be used in future highly reusable vehicles with long life and high resiliency requirements. For the X-38 vehicle, there was no specific design requirement, so these seal designs should be resilient enough for a single use. The rudder/fin assembly of the X-38 was designed with floating fittings and attachments, so the change in gap size that the seal is sealing will probably be minimal.

Compression Test Results-Loads

- Unit loads (load per inch of seal) and contact pressures were higher for as-received seals
 - Due to loss of resiliency and smaller contact width for temperature-exposed seals

Load versus Compression Data for 6 pcf Seal



- Temperature-exposed seals were 1.5X stiffer than as-received seals at 20% compression
 - Oxidation and deformation of Inconel X-750 spring tube increased roughness of wires and made seals stiffer
- Unit loads (2 lb/in.) and contact pressures (4.4 psi) below 5 lb/in. and 10 psi limits (Limit loads on Shuttle thermal tiles, AETB-8 with RCG/TUFI coating)

Seal unit loads met goal in both as-received and temperature-exposed conditions



NASA Glenn Research Center

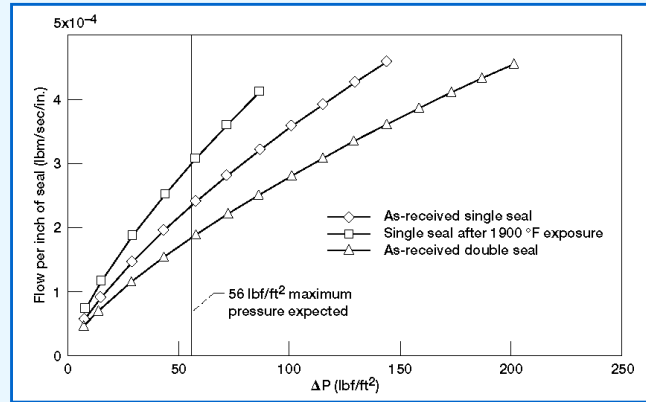
CD-00-80663

This chart shows the results of the loads measured in our compression tests. The plot shows the load versus displacement curves for four load cycles at 20% compression on the as-received and temperature-exposed 6 pcf seals. The plot shows that the seals do take on a permanent set as they are exposed to more load cycles, but the curves for each successive cycle tend to collapse on to each other by the fourth load cycle. It can be seen clearly how much permanent set the temperature-exposed seal has taken on. Using the same starting point for a temperature-exposed seal as for the as-received seal, the opposing plate is moved roughly 0.1 in. before it even contacts the seal for the first few load cycles. This contributed to a difference in loads measured on each seal. The unit loads (load per linear inch of seal) and contact pressures were higher for the as-received seals than for the temperature-exposed seals even though the temperature-exposed seals felt stiffer and less flexible. This was due to the loss of resiliency and smaller contact widths of the seals after temperature exposure. However, the temperature-exposed seals were stiffer than the as-received seals. The slope through the last two data points on the fourth load cycle was 1.5 times larger for the temperature-exposed seals than for the as-received seals at 20% compression. This is believed to be due to oxidation and deformation of the Inconel X-750 spring tube causing the wires to become rougher and less able to slide past each other. All of the seal designs that were tested had unit loads and contact pressures below the 5 lb/in and 10 psi limits that were set to limit loads on the Shuttle thermal tiles that the seals will be in contact with in the rudder/fin application. Thus, these seal designs met the property goals for unit loads and contact pressures.

Flow Test Results-Effect of Temperature Exposure



Flow versus Pressure Data for 6 pcF Seal



- Temperature-exposed seals exhibited 28% higher flow rates than as-received seals at 56 lb/ft²
- Expected cause: Loss of load per unit inch and smaller contact footprint width lead to higher flow rates through seal and sealing contact for temperature-exposed seals

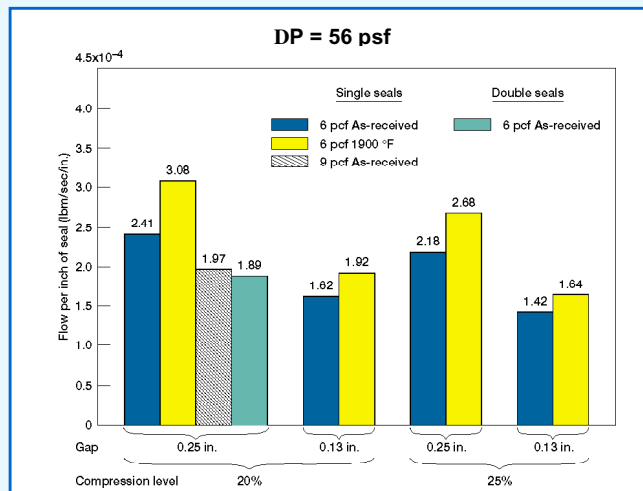


NASA Glenn Research Center

CD-00-80663

This chart shows flow data for the 6 pcF seal design. The flow rate in lbm/sec/in along the length of the seal is plotted versus the pressure differential across the seal for single as-received and temperature-exposed seals and for double as-received seals. This plot shows that temperature exposure of the 6 pcF seals caused an increase in flow rate through the seals of 28% as compared to the as-received seals at a differential pressure of 56 lb/ft². This is believed to be due to the loss of load per unit inch and smaller contact footprint width caused by temperature exposure of these seals. A narrower contact footprint reduces the contact area between the seal and the adjacent structure and leads to higher flow rates through the seals. This plot also shows that adding another seal into the flow path reduced the amount of flow through the seals as compared to only a single seal. This will be discussed further on the next chart.

Flow Test Results



- Flow rates decreased with increase in compression levels and decrease in gap size

- Lower flow rates for as-received 9 pcf seal than for as-received 6 pcf seal

- Denser core in 9 pcf seal blocked more flow

- Flow rates through double 6 pcf as-received seals were 22% lower than for single seals but were 4.5X higher than preliminary flow goal



NASA Glenn Research Center

CD-00-80663

Additional flow test data is presented in this chart. Flow rates are presented for several different seal types and conditions at a pressure differential of 56 lbf/ft². Single seal flow rates are given for 6 pcf as-received (blue bars) and temperature-exposed seals (yellow bars) and for 9 pcf as-received seals (striped bars). Flow data is also given for double 6 pcf as-received seals (green bars). Data is shown for two different compression levels (20 and 25%) and two gap sizes (0.25 in. and 0.13 in.). Flow through the seals decreased as the amount of compression on the seals was increased. This was expected because increasing the amount of compression on the seals closed the gaps and flow paths in their porous structure and allowed less flow to pass through them. Similarly, reducing the gap size from 0.25 in. to 0.13 in. also lowered the amount of flow through the seals. This was also expected because a reduction in gap size decreased the flow area through the seals and further limited the seal area that was in the flow path. Lower flow rates were measured for the as-received 9 pcf seal than for the as-received 6 pcf seal. The denser core of the 9 pcf design blocked more flow through the seal. Flow rates through double 6 pcf as-received seals were 22% lower than for a single seal at the same compression level. Adding a second seal did not cut the amount of flow through the seals in half, but this type of behavior has been observed previously in multiple-seal flow tests (Steinetz, et al., Journal of Propulsion and Power, Vol. 14, No. 6, 1998, pp. 934-940). Flow rates through the double seals were 4.5 times higher than the preliminary flow goal.

Summary and Conclusions

- Exposure of seals in compressed state at 1900°F resulted in loss of resiliency due to permanent set of Inconel X-750 spring tube. Not a problem for single-use seals.
- Unit loads and contact pressures were below 5 lb/in. and 10 psi limits. Low loads required to limit damage to Shuttle thermal tiles.
- Flow rates for double as-received 6 pcf seal about 4.5 times higher than preliminary flow goal
 - Effect of measured flow through porous seal on maximum seal temperature requires further examination
- Seal designs expected to endure peak seal temperatures for single-use life



NASA Glenn Research Center

CD-00-80663

In summary, temperature exposure of these seals in a compressed state at 1900°F resulted in a large loss of resiliency due to permanent set of the Inconel X-750 spring tube. This is not anticipated to be a problem for the single-use X-38 rudder/fin application where the seals can be replaced after each mission. However, these seal designs would not work well in applications where reusable, resilient seals are required that can endure high temperatures without taking on a large permanent set. The unit loads and contact pressures measured for these seals were below the 5 lb/in and 10 psi limits that were set to limit the amount of damage that these seals would cause in adjoining Shuttle thermal tiles on the rudder/fin. Flow rates for double 6 pcf as-received seals were about 4.5 times higher than the preliminary flow goal. We believe that these measured flow rates should be incorporated into the thermal model to see how the effects of seal porosity influence the maximum seal temperature. Overall, these seal designs are expected to endure the peak seal temperatures and anticipated environment for a single-use life in the X-38 rudder/fin application.

Future Work/Recommendations

- Perform more detailed thermal analyses including flow through permeable seal to assess effects on maximum predicted seal temperatures
- Perform additional flow tests representative of application:
 - After scrubbing
 - Under low seal preload conditions (0%, 10% compression)
 - With fabric as opposing surface
- Perform arc jet tests (part of Spaceliner-100 program) and scrubbing tests (at JSC) to assess seal performance under simulated environments

NASA JSC and NASA Glenn are currently evaluating best approaches to address these issues



NASA Glenn Research Center

CD-00-80663

NASA JSC and GRC are currently discussing what additional work will be done to evaluate these seals. GRC has recommended that more detailed thermal analyses be performed to include flow through the permeable seals and to assess how this affects maximum predicted seal temperatures. Additional flow tests will probably be performed to examine seal flow rates after scrubbing, under low preload conditions (0%, 10% compression), and possibly with fabric as the surface in contact with the seals. A series of arc jet tests will be performed as part of the Spaceliner-100 program in which these same seal designs will be used as the baseline designs. JSC is also planning to do more scrubbing tests on these seals. These tests will be done to assess seal performance under simulated environments.

CONTROL SURFACE SEAL DEVELOPMENT FOR FUTURE RE-ENTRY VEHICLES

Chuck Newquist, Juris Verzemnieks, and Peter Keller
The Boeing Company
Seattle, Washington

Control Surface Seal Development for Future Re-Entry Vehicles

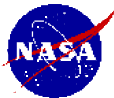
presented at

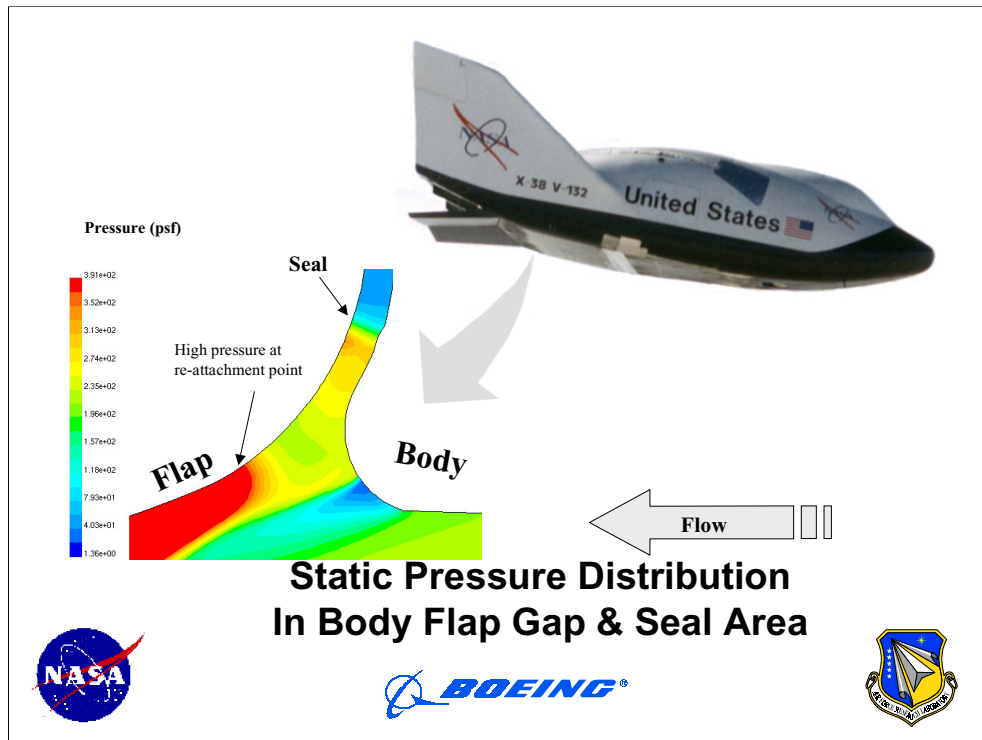
NASA Seal/Secondary Air Delivery Workshop
NASA Glenn Research Center
26 October 2000

Dr. Chuck Newquist 425-234-2662 chuck.newquist@boeing.com

Juris Verzemnieks 425-234-2682 juris.verzemnieks@boeing.com

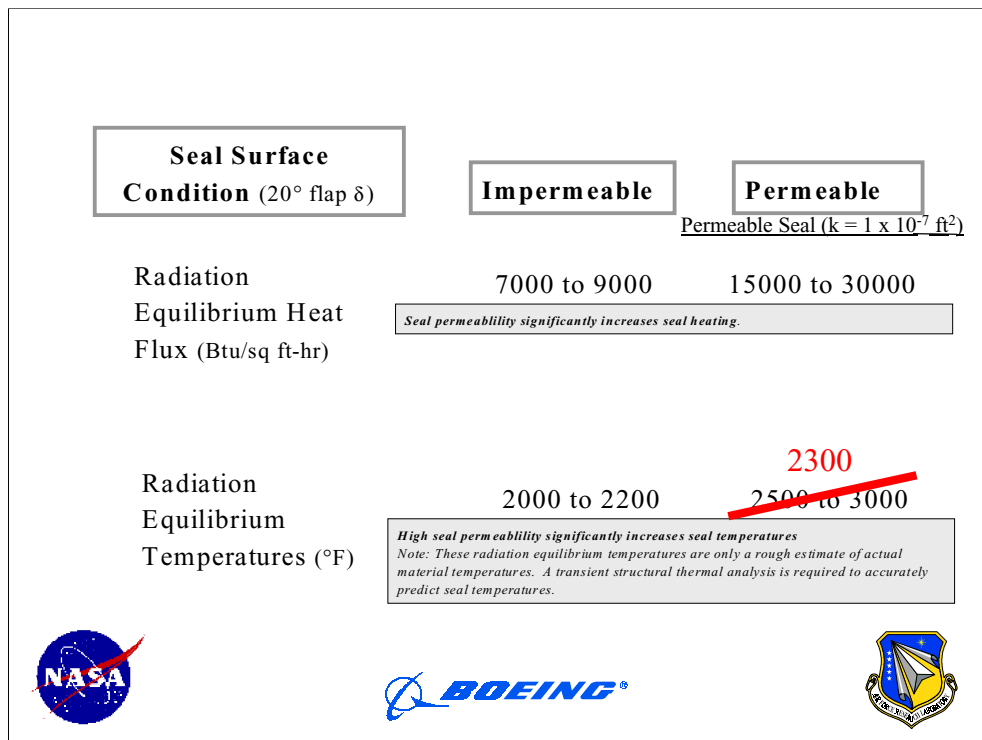
Pete Keller 206-662-1805 peter.c.keller@boeing.com





Phase 1 of this project was presented at this workshop last year. This chart is taken from that presentation and illustrates our modeling analysis. The flow environment was from X-38 re-entry conditions and the physical dimensions were adapted from the X-38 preliminary designs. The thermal modeling was accomplished using FLUENT, a commercially available CFD software package.

We focused on the seal area and two seal conditions: (1) an impermeable seal, and (2) a permeable seal -- permeability, $k = 1 \times 10^{-7} \text{ ft}^2$



The phase one thermal analysis results for radiation equilibrium temperatures is shown in this chart, with an overstrike for the permeable seal case-- a revised estimate for temperatures.

Aerothermal analysis was performed during the first phase of this program using X-38 data and FLUENT, a commercial CFD code. The seal aerothermal environment was estimated with a steady state flowfield solution. Steady state flow solution assumes constant energy flow into the cove sufficient to balance heat flux into seal and structure. An effective seal prevents high flow rates into the cove. However, there was a problem with including porosity as a property of the seal, and resulted in estimated porous-seal temperatures that appeared to be high. Attempts were made to overcome the porosity issue, but temperature estimates as the porosity was decreased to negligible values did result in convergence (at very low porosity) to temperatures that were estimated with an impermeable seal. The thermal analyst's solution is outlined below:

- Determine equivalent mass leakage ratio of permeable bodyflap seal
- Apply Shuttle Orbiter elevon-seal-leakage correlation factors to determine bodyflap thermal environment.
- Apply aerothermal environment to thermal structural model of seal
- Seal-heating prediction methods used on the Shuttle Orbiter were developed in terms of leakage rates. To apply these to a permeable seal, an equivalent leakage rate must be determined.

Leakage rates on our seal designs were determined and resulted in seal temperatures that are estimated now to be in the range of 2300°F. Previous analysis had resulted in seal temperatures on the order of 2650°F

THERMAL ANALYSIS -- Approximate Methods

2-D Analysis with FLUENT

Arcjet Conditions

1. Conduct 2D integrated CFD/structural thermal analysis on test fixture at test conditions
2. Compare predicted pressure and temperatures with test data
3. Adjust analysis parameters to improve correlation with data

Flight Conditions

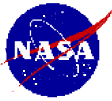
1. Conduct FLUENT analysis with method resulting in best agreement with test data at flight conditions

Limitations and Assumptions

1. FLUENT contains no real gas model, seal temperature analysis conducted by matching flow total temperature
2. Analysis parameters and assumptions which resulted in agreement with test data are assumed to work well for flight conditions

Advantages

1. Relatively fast CFD analysis Integrated flow field and structural heat transfer analysis



Apply Correlations of Test Data

Arcjet Conditions

1. Predict heating and pressure at reference locations on test fixture surface using established 2D boundary layer method
2. Correlate seal and cove temperature data to reference values with relationships developed on previous studies
3. Evaluate applicability of previously developed correlations to current conditions
4. Evaluate assumption of equivalence of leakage and flow through a porous seal

Flight Conditions

1. Predict heating and pressure at reference locations on test fixture surface using established 2D boundary layer method
2. Use correlations of test data to predict seal and surrounding structure aerothermal environments
3. Conduct transient finite element analysis of seal region during reentry to determine seal temperatures

Limitations and Assumptions

1. Correlations developed from test data are assumed to be valid at flight conditions as well

Advantages

1. Rapid analysis method
2. Used successfully before CFD available



The next few charts are about thermal analysis and issues of relating analysis of the arc-jet conditions to those of flight. There are three basic methods for analysis -- these are listed in **bold** type and discussed below.

For all the methods, since there is no data at actual flight conditions, it is assumed that 1) the important parameters in the flow are modeled and 2) that if the method matches data at the test conditions it will also be valid at flight conditions. For the three methods we're looking at those assumptions range from bad to good.

Since **FLUENT** has no real gas model, flows with total temperatures greater than 3000 R will not be modeled correctly. That includes both the arcjet and flight environments. So, this violates assumption (1) above. But it is able to analyze complex flow fields relatively quickly and I think can give us good indications of the trends due to seal porosity and other parameters.

Correlations of the arcjet data will inherently include the real gas effects in the arcjet. So this should be an improvement over the FLUENT predictions. But it still assumes the real gas and chemistry effects in the arcjet can be extrapolated to flight. This violates assumption (2) to some degree.

The Ames CFD work will use a sophisticated model of the air chemistry which I expect is based on a lot of theory and high temperature chemical data. The important aspects of the flow field are certainly modeled and the assumption that the methods will also be valid at flight conditions has probably been shown for Shuttle and other flight data. So I think we can claim a high amount of confidence in flight predictions made with this method.

THERMAL ANALYSIS -- Higher Order Method

Non-Equilibrium Air 3D CFD Analysis

(NASA ARC Reacting Flow Environments Branch)

Arcjet Conditions

1. Conduct 3D non-equilibrium CFD analysis for test geometry and conditions drawing on experience of modeling arcjet flows
2. Validate method with measured pressure, temperature and LIF data

Flight Conditions

1. Conduct 3D non-equilibrium CFD analysis of vehicle geometry at flight conditions using identical air chemistry model as used for test conditions
2. Apply CFD aerothermal environment to finite element model of vehicle seal region to determine reentry temperature histories

Limitations and Assumptions

1. Requires significant time, effort and experience

Advantages

1. Highest fidelity analysis
2. Benefits from Reacting Flows Branch experience in modeling arcjet flows



(continued)

Collaboration with NASA-Ames Research Center RFE Branch has resulted in suggested Aerothermal Analysis Tasks of Benefit to Advanced High Temperature Seals program. The object is to use the most sophisticated analysis of the arc-jet flow field in order to be able to make the best extrapolation of arc-jet test data to flight conditions. The following tasks are being discussed:

- 1) Investigate relationship between boundary layer enthalpy profile and thickness forward of control surface gap and enthalpy of flow entering gap at test conditions
- 2) Investigate relationship between control surface deflection angle, Mach number, control surface pressure and pressure at seal at test and flight conditions
- 3) Produce high fidelity CFD solution at test conditions for comparison to test data and approximate methods
- 4) Predict seal and cove aerothermal reentry environments with methodology validated at arcjet conditions

THERMAL ANALYSIS -- Summary

- Analysis assumes that:**
- 1) the important parameters in the flow are modeled.
 - 2) that if the method matches data at the test conditions it will also be valid at flight conditions.

How Do the Methods of Analysis Compare ?

FLUENT

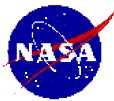
- FLUENT has no real-gas model
- However, it can quickly analyze complex flow fields and give us good indication of trends due to porosity, etc.

Correlations of Arc-Jet Data

- Will inherently include real-gas effects.
- However, it still assumes that real-gas and chemistry effects can be extrapolated to flight.

NASA-Ames CFD

- Uses sophisticated model of gas chemistry
- Can claim a high degree of confidence in flight predictions.



SEAL DESIGN

Baseline Seals -- Orbiter, X-33, X-38

Standard Bulb

Nextel™ 312 & 440 for the braid/fabric over the metal spring and the fiber fill.

Inconel™ metal alloy spring -- woven multi-wire

Saffil™ fiber for the fill material -- vary bulk density

Advanced Bulb Seal

Nextel™ 440 for the braid/fabric over concentric layers of Nextel™ 440 sleeving

Next Generation Seals

TBD -- based in part on arc-jet test results



Baseline seals have been selected from the experience of Shuttle Orbiter and numerous design programs for small re-entry vehicles such as X-38, X-33, and X-37.

Nextel 312 materials are capable of long-term service only to temperatures of around 1600F. For capability to temperatures of 2000 to 2200F ceramic fiber products using Nextel 440 material are included.

The standard spring device (again based on 1600F performance) has been Inconel wire (multi stranded) that is woven into a spring. Steinetz and Dunlap in the study for the previous presentation in this workshop investigated bulb seal resilience to temperatures of 1900F and found that the standard bulb seal construction with the Inconel spring permanently deforms at temperatures of 1800 to 1900F. We have baselined the construction designs of the Steinetz and Dunlap study because of the extensive flow and compression testing performed in that study.

The advanced bulb seal configuration that we will test uses a design that was introduced during the development of X-38. This design uses a core fill of concentric Nextel sleeving to form a resilient seal that shows promise at elevated temperatures.





Next generation seals will consider other features such as refractory metal foils or springs and ceramic composite elements to retain resiliency and lower the permeability. Of course these designs will be based in part on the results of arc-jet testing.




TEST OBJECTIVES:

- **Validate thermal model at two gap sizes** (*0.25 and 0.375 inch -- 0.625 dia. seal*)
- **Evaluate Arc-Jet performance of:**
 - **Baseline** Shuttle seals with Nextel 312 (2 layers of braid cover), Inconel spring tube, and 6 & 9 lb/ft³ Saffil core fill
 - **Advanced Seals** with Nextel 440 (2 layers braid cover + 1 layer braid with 5HS cover), Inconel spring tube, and 6 and/or 9 lb/ft³ Saffil core fill
 - **Next Generation** Seal Designs
- **Evaluate wear resistance at RT of candidate seals against TUFI-RCG coated TPS Tiles; and, Where Possible, perform high temperature wear resistance cyclic testing.**



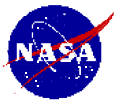
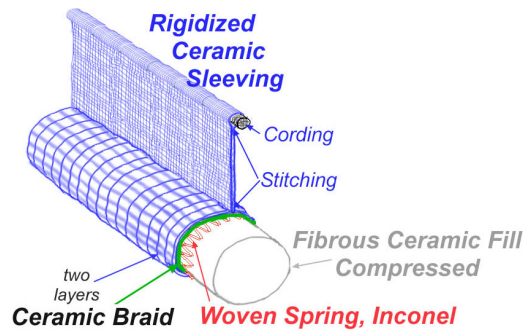
The test objectives are presented in this chart. They are to validate the thermal modeling, evaluate performance of the baseline and advance seal materials discussed in the previous chart, and to evaluate wear resistance at room temperature against TUFI-RCG coated tiles. Because of the articulation of the test fixture we will gain some idea of high temperature wear behavior -- we will perform cyclic movements where appropriate.

High Temperature Structural Seals							Arc-Jet Tests			Lab Environment		
Test Matrix Components							CMC Aug	Run #	Temp/Press	Hi Temp Cyclic Wear	RT Wear in Arc- Jet Fixture	Flow Resistance @ GRC
Seal Configuration	DESCRIPTOR											
	#1	#2	#3	#4	#5	#6						
	Material	Fabric/Braid	weave	Knitted wire Spring	Mat Fill	Fill (lb/ft ³)	Attachment to fixture					
Braid is two layers, unless stated other							Check-Out Run					
							Establish operating envelope Determine angle limits of this fixture in Arc-Jet facility Measure cover pressures and T's as function of elevon					
Baseline ~ Single  0.625 inch dia SEAL GAP = 0.25 inch COMPRESSION = 20% Diametrically	Nextel 312	Braided sleeving	Inconel -- 0.53 inch diam	Saffil	6	CMC stiffened "tail" attached by sewing; held in fixture with small-corded- bulb.	1	Measure elevon surface temperatures as function of el				
	Nextel 312	Braided sleeving		Saffil	6		2	X		X		
	Nextel 312	Braided sleeving		Saffil	9		3	X		X		
	Nextel 440	Braided sleeving		Saffil	9		4	X		X	X	
	Nextel 440	Braided sleeving		Saffil	9		5	X	X			
Baseline ~ Double  	Nextel 312	Braided sleeving		Saffil	6		6	X		X		
	Nextel 440	Braided sleeving		Saffil	9		7	X		X	X	
	Nextel 312	Braided sleeving		Saffil	6		8	X		X		
	LARGER GAP -- 0.375 inch -- Run #8											
Concentric Braid Fill single 	Nextel 440	SHS fabric over concentric 1/8, 1/4, 1/2 inch diameter braid sleeving	N/A	N/A	N/A	Overwrap fabric forms tail, with cording at interior side of cross-section; stiffen with CMC matrix.	9			X	X	
							END of BASELINE & ADVANCED SEAL TESTS					
	Nextel 440	440 Braided sleeving over concentric 1/8, 1/4, 1/2 inch diameter braid sleeving	N/A	N/A	N/A	Tail formed from One inch diam. Braid with cording at interior side; stiffen with CMC matrix.	10			X	X	



This table lists the parameters describing the seal configuration for the first 10 arc-jet test runs. We plan to begin with the single bulb seal configuration and also include the double seal configuration. We will conclude this series with the Nextel 440 concentric sleeving core design. The variables to be tested will be the exterior covering -- compared will be 5 Harness satin fabric to the standard braided sleeving. As described later we will use the fabric so that we have an exposed face where the majority of yarns are parallel to the sliding direction.

Single Bulb Seal Configuration



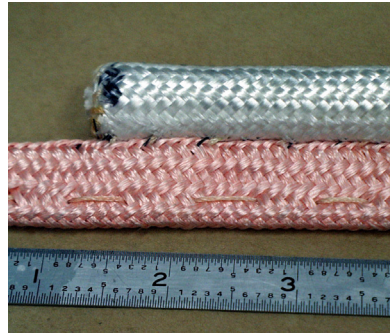
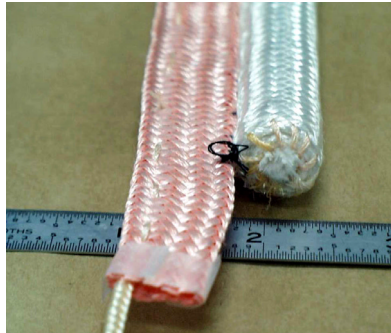
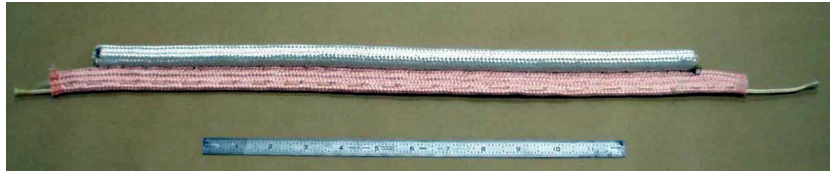
Attachment of bulb seals to the thermal protection system structure is very important. We selected a method of attachment that is all ceramic and uses the basic bulb seal element combined with braided fiber products; then finished with a selective rigidization using a proprietary Boeing ceramic coating/matrix material.

We used a 1/2 inch Nextel 440 braided sleeve into which we sewed a stretched Nextel 440 1/8 inch diameter sleeve into one side. This flattened sleeveing was attached to the bulb seal (locating the joint with a tool having the fixture contour) by sewing with Nextel 440 thread. The seal and attachment fixture is then heat treated to remove the sizing before placing into the molding tool for densification and rigidization.

We considered metallic attachment, silicone bonding, ceramic cements and rejected them because of service temperature limitations, and the desire to have an easily replaced unit. The same concept works as well for a fabric over-wrapped bulb seal.

SEAL FABRICATION

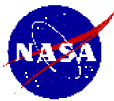
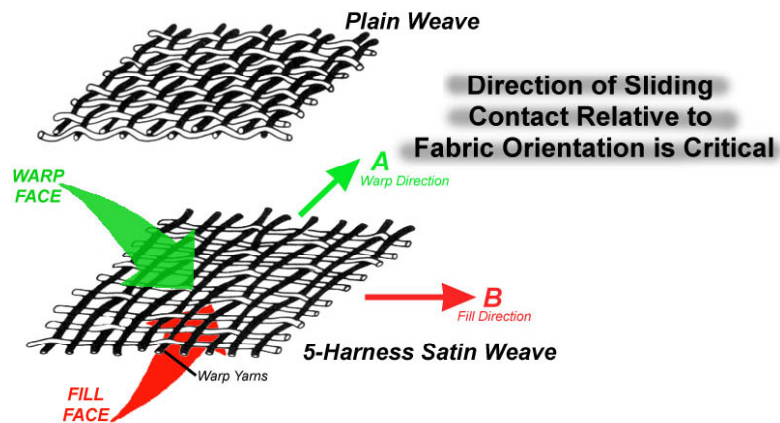
Ready for Sizing Burn-Out & Tail Rigidization



The first test article seal (Nextel 312 braid, Inconel spring, and 9 lb/ft³ core Saffil) with the attachment sleeve. This unit includes the stitching which is barely visible against the bulb seal in the photo at the lower right. The ends of the attachment sleeving will be trimmed to the proper length after the rigidization process is complete.

The black thread (photo lower left) is cotton and was used as a temporary fabrication aid. It disappears during the sizing removal process. The lower right photo also shows a black marking of ink from the fabrication sequence.

Direction of Sliding Contact Relative to Fabric Orientation



The direction of sliding contact with a ceramic fabric is critical. Experience indicates that sliding contact on a fabric face in the parallel direction of the floating yarns results in less damage than perpendicular to them.

This chart illustrates some of the definitions involved with this discussion -- such as warp and fill faces of a 5-harness satin weave fabric.

Arc-Jet Testing & Fixture

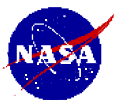
- **Arc-Jet testing of seals in a unique, articulating fixture.**
- **Use NASA-Ames PTF (*Panel Test Facility*)**

20 MW

Pressure of 20 torr (approximately 80,000 ft of altitude)

Convective heating rate = 0.5 to 75 Btu/ft²-sec

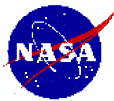
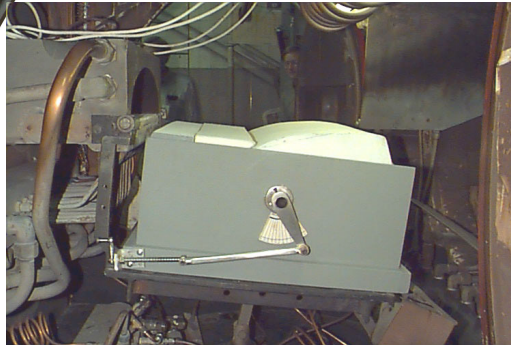
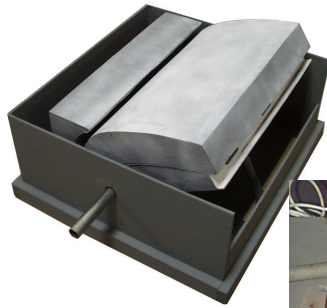
Mach No. 5.5



The program team designed a unique, articulating control surface element as an Arc-Jet test fixture for the NASA-ARC PTF .

The pressure of 20 torr is the chamber pressure -- the dynamic pressure on the control surface element and seal will be higher and a function of the deflection angle.

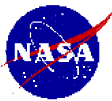
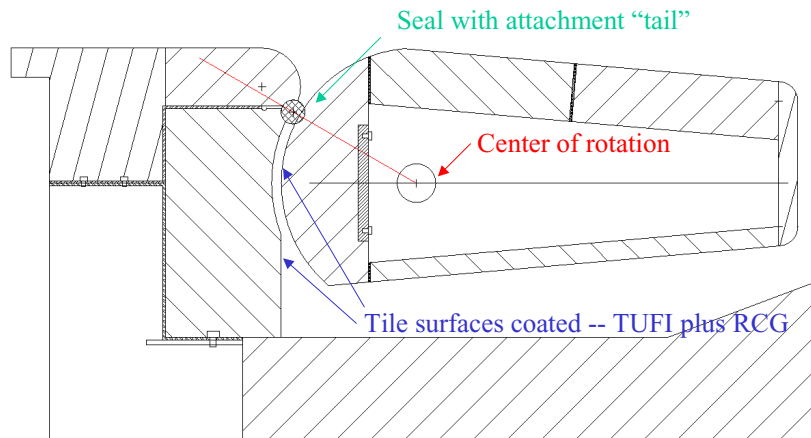
Mock-Up of Arc-Jet Test Fixture



This chart shows the mock-up of the test fixture that was fabricated for the first phase of this project. It was a model for design check-out in the arc-jet, and to work out the fine details including actuator location and alignment of fixture with arc-jet fittings. It turned out to be an invaluable tool for the design process and elicited significant suggestions and enthusiasm from the staff of the facility.

Drawing -- Arc-Jet Test Fixture

Showing Tile Segments



This is the nearly final iteration of the drawing for the actual arc-jet fixture components. There is a change from this drawing of the side view -- the joints of the tile segments are now stepped.

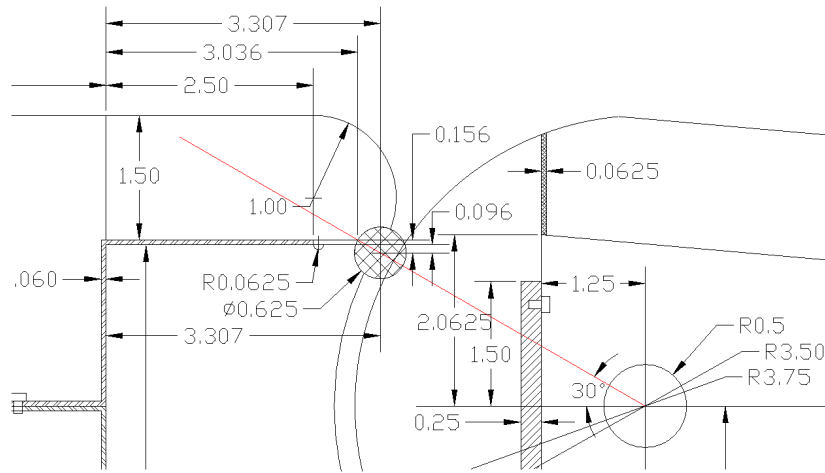
The fixture is designed so that the components can be easily disassembled (*and re-assembled*), especially the front section that holds the seal element. The front piece (Silfrax with the lip) lifts out and the metal framing can be unbolted and the seal holder lifted out -- without removing the articulating elevon section. The tested seal can then be removed and replaced with the next test article.

The tiles are mounted on metal carrier plates for ease of assembly and replacement.

The exposed tile surfaces (made of AETB-16) are coated with TUF1 and overlaid with the RCG coating for a robust and smooth, glassy surface.

A total of 32 thermocouples will be installed for thermal data collection -- six thermocouples in potentially sensitive, critical areas will be monitored in real-time. An IR camera and optical pyrometers are also available. In addition 6 pressure transducer taps will be recording pressure data during the arc-jet runs.

Drawing -- Arc-Jet Test Fixture



The seal element is held in place mechanically. The small, corded bulb on the end of the tail is locked in by the TPS tile sections. A friction fit of the flat portion of the tail is held between the tile sections.

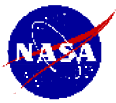
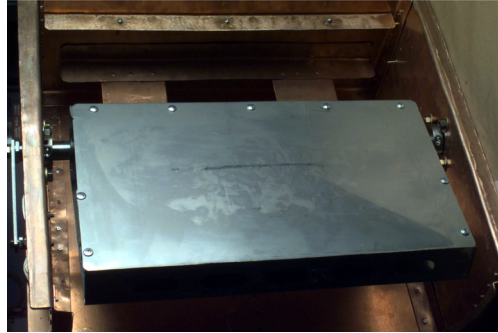
Arc-Jet Test Fixture -- Metallic Structure



The box that holds the stationary tile assembly is made of copper sheet and will be cooled by circulating water coils on the exterior. The stainless steel metallic structure for the elevon element is clearly shown. The actuating lever will be mechanically articulated to move the elevon to the required deflection angle.

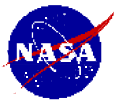
The maximum angle of deflection may be limited by deflection of the arc-jet flow onto thermally sensitive areas of the chamber. This will be investigated during the first test run.

Arc-Jet Test Fixture -- Metallic Structure



Another view of the metallic components. This view is toward the front (the arc-jet nozzle) and shows the top of the elevon support structure.

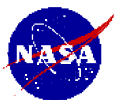
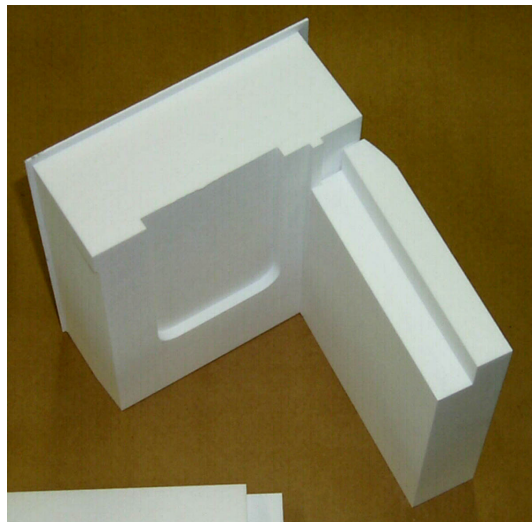
Elevon Nose Section Machined from AETB-16 At NASA-Ames Ceramics Lab



A nose section of the elevon tiles being milled for the at NASA-ARC. The front radius is being shaped.

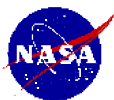
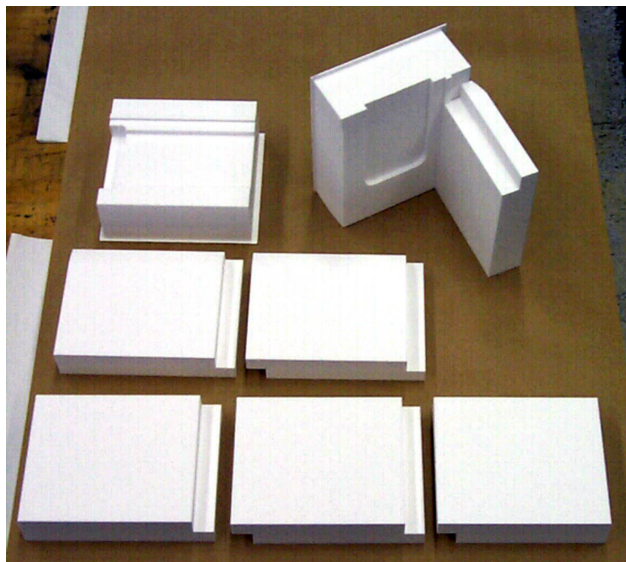
The AETB-16 material for the tiles was supplied by Boeing, Huntington Beach with support by the Boeing X-37 program.

Tile Sections Machined from AETB-16
Partially finished Nose section and top surface tile



A close-up view of a finished top surface tile butted up to a partially completed nose section tile (the front radius remains to be milled). Note the stepped joints and the recessed area for the nose-tile carrier plate.

Tile Sections Machined from AETB-16

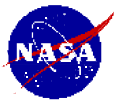


Nose section tile blanks (partially completed) along with elevon surface tiles.

All pieces are AETB-16 tile material.

SUMMARY

- Thermal analysis efforts are being coordinated with NASA-ARC in a cooperative effort for relating arc-jet environment of the seal to flight environment
- An articulating arc-jet test fixture has been designed and nearly completed
- Baseline seals have been designed and fabricated
- An all-ceramic attachment method has been designed and developed
- Arc-jet testing is scheduled for November



THERMAL BARRIERS

Dennis Barber
Oceaneering Thermal Systems
Houston, Texas

Thermal Barriers
Oceaneering Thermal Systems
Dennis Barber
October 2000



NASA Seal/Secondary Air Flow System Workshop
OTS Thermal Barriers

10/25/2000

Contents

- **Introduction**
- **Key Parameters**
- **OTS Thermal Barriers**
 - **Tile**
 - **Blanket**
- **Closing**



NASA Seal/Secondary Air Flow System Workshop
OTS Thermal Barriers

10/25/2000

Introduction

- The thermal barrier designs included in this presentation were developed for Orbital Sciences Corp., Dulles, VA and Kistler Aerospace Corp., Kirkland, WA



NASA Seal/Secondary Air Flow System Workshop
OTS Thermal Barriers

10/25/2000

Introduction of launch vehicles that use the presented thermal barrier designs

Introduction

- **OTS projects involving thermal barrier design, fabrication, and test**
 - **Orbital Sciences X-34**
 - **Lockheed Martin Skunkworks X-33**
 - **Kistler Aerospace K1**
- **RLVs require doors in the external surface of the vehicle**
 - **Locations include: landing gear, umbilical connections, compartment venting, payload compartments**
 - **Design Elements**
 - **Open and/or close during the flight which can include ascent, on orbit and reentry phases**
 - **Perimeter gaps are relatively large due to hinged action and tolerances**
 - **TPS includes thermal barriers at the door perimeter gaps to prevent excess heating of the vehicle structure and pressure seals due to hot gases entering the gaps**
 - **Pressure seals are typically present at the door structure to prevent gas flow into the vehicle due to delta P**



NASA Seal/Secondary Air Flow System Workshop
OTS Thermal Barriers

10/25/2000

Projects supported by Oceaneering Thermal Systems

Key features of RLV doors that drive thermal barrier designs

Introduction

- **Panels (for reference only - not part of this presentation)**
 - **Locations include: umbilical connections, maintenance access and ground operations**
 - **Typically removed on the ground during vehicle turnaround**
 - **Can have blanket TPS simply snug fit to surrounding TPS or include a perimeter Gap Filler**



NASA Seal/Secondary Air Flow System Workshop
OTS Thermal Barriers

10/25/2000

Key features of RLV doors that drive thermal barrier designs

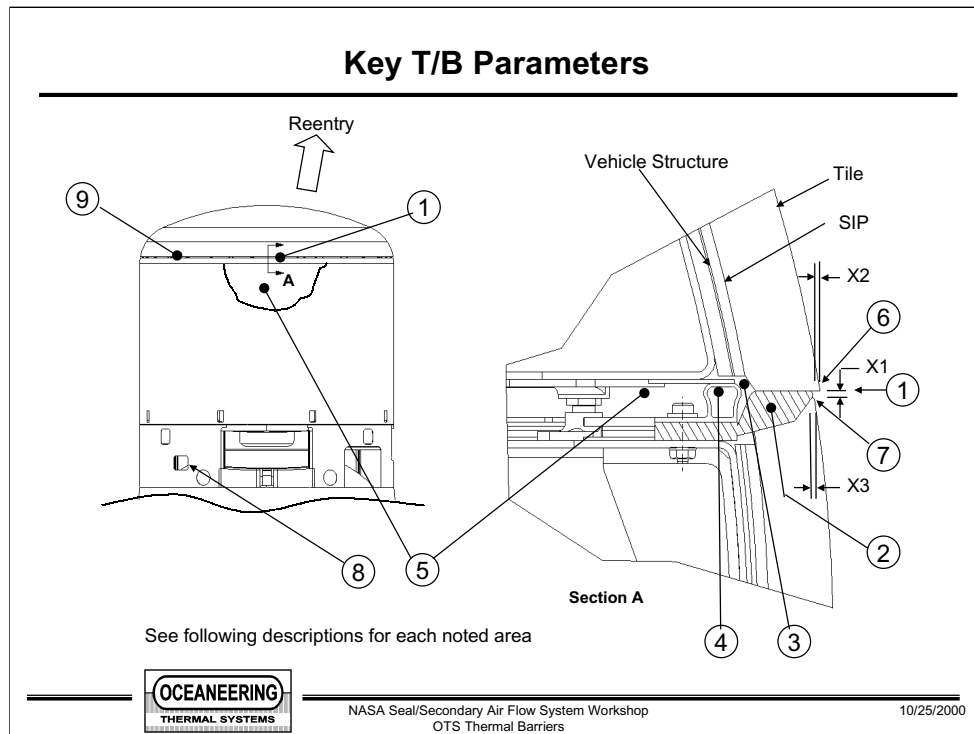


Illustration for a description of typical thermal barrier functions

Thermal Barrier Parameters

(1) Gap in surface of OML at perimeter of an actuated door

- Reentry causes heating at gap surface
- Applicable design parameters are heat, temperature, local pressure and delta pressure across and along T/B

(2) and (9) Thermal Barrier (T/B)

- Fills the gap between structure TPS and door TPS
- Provides thermal insulation for underlying structures
- Restricts air flow in the gap parallel and transverse to T/B length
- Compensates for wider gaps and larger gap tolerances than gaps in acreage TPS
- Maintain gap side wall contact to prevent unrestricted air flow into cavity (3)
 - “sneak” flow occurs through cavity (3) if there is a pressure differential between two locations (1) & (9) and there is a lack of wall contact at each location



NASA Seal/Secondary Air Flow System Workshop
OTS Thermal Barriers

10/25/2000

Parameters affecting typical thermal barrier functions

Thermal Barrier Parameters

(3) Cavity between T/B and pressure seal

- Size minimized to limit amount of total heat when this space is repressurized
- Size minimized to restrict flow parallel to T/B
- Structure along this cavity will absorb and dissipate small heat flow

(4) Pressure (Environmental) Seal

- Prevent flow through the T/B caused by pressure differential between (1) and (5)

(5) Vehicle inner volume

- Vented during ascent and reentry via vents (8)
- Vent (8) is typically closed during maximum reentry heating period
- Analyze components exposed to direct flow from the vent



NASA Seal/Secondary Air Flow System Workshop
OTS Thermal Barriers

10/25/2000

Parameters affecting typical thermal barrier functions

Thermal Barrier Parameters

(6) & (7) Forward and aft sides of TPS gap

- Increasing OML step (X2) increases protuberance heating
- Wider gap (X1) increases protuberance heating
- Wider gap (X1) exposes additional T/B materials to heating which increases total heat absorbed by the T/B
- Wider gap (X1) increases heating to the sides of gap
- Gap side walls see heating due to radiation from opposing wall (radiation trap)
- Deeper gaps (X3) increase gap wall heating due to reduced view factor to space
- Allowable step is primarily relative to the local boundary layer thickness
- Allowable gap width is primarily relative to the local flowfield pressure gradients and the surface geometry



NASA Seal/Secondary Air Flow System Workshop
OTS Thermal Barriers

10/25/2000

Parameters affecting typical thermal barrier functions

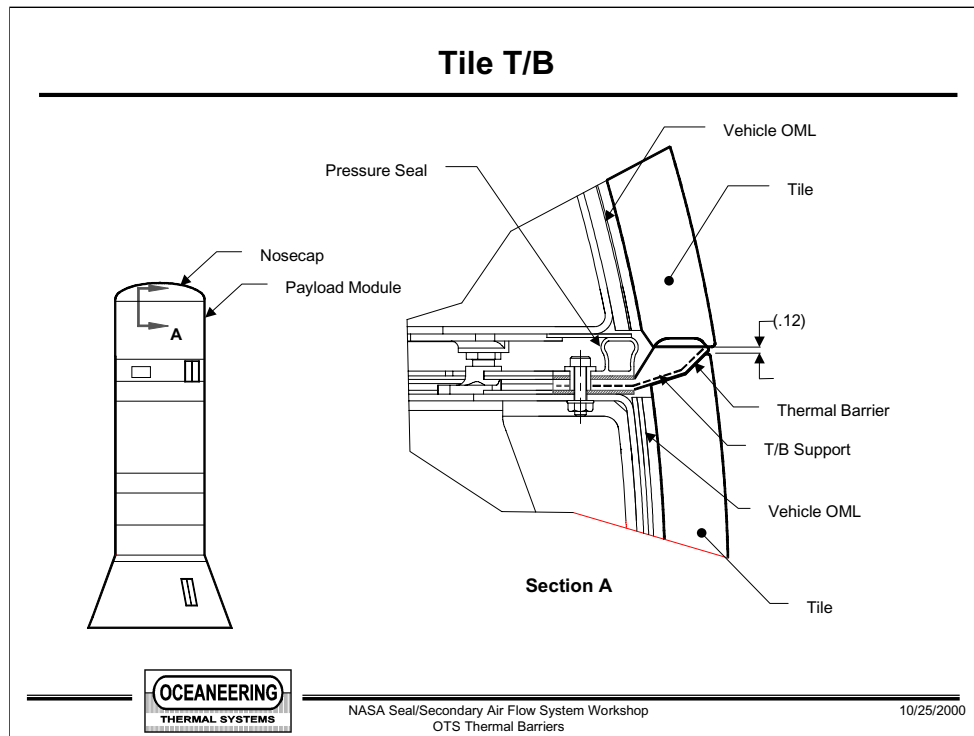


Illustration of a tile to thermal barrier interface

Tile T/B

Design

- Typically windward side use
- Compressed between TPS tile
- Multiple Nextel sleeves w/ Inconel mesh tubes filled with Saffil
- T/B support to maintain position w/o the use of adhesives
- TPS surface temperature capability up to 2400°F
- Maximum structure temperature = 350°F
- Heating from orbital reentry near vehicle leading edge
 - Design similar to nose gear door T/B on the Space Shuttle

Status

- Development unit built to develop manufacturing techniques
- Compression testing of development unit performed to confirm loads and seal location stability
- 2D thermal analysis is complete
- Arc jet testing is planned



NASA Seal/Secondary Air Flow System Workshop
OTS Thermal Barriers

10/25/2000

Design and status of a tile to thermal barrier interface

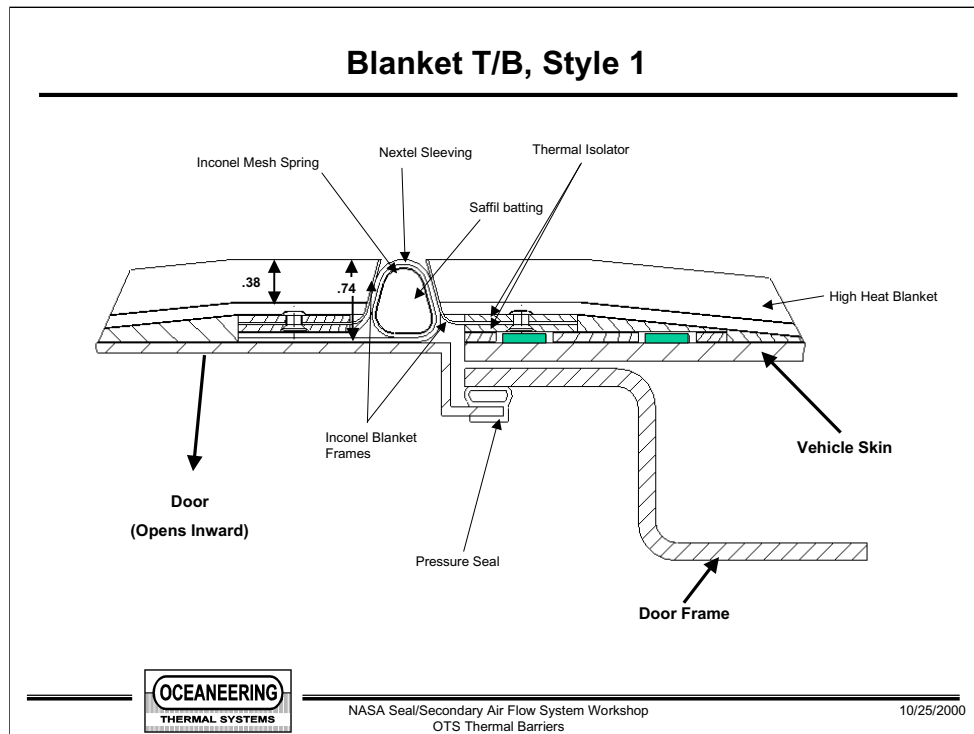


Illustration of a blanket to thermal barrier interface

Blanket T/B, Style 1

Design

- Leeward or windward side use
- External Inconel reinforced blanket edges to compress T/B
- Inconel sandwiched to thermally isolate from RTV
- Single Nextel sleeve, Inconel mesh tube and Saffil
- Inward opening door
- TPS surface temperature up to 1250° F as shown, 1500° F being evaluated
- Maximum structure temperature = 350° F
- Heating durations for reentry from orbit
- High Heat Blanket (HHB) is Nextel 440 OML with Saffil Insulation

Status

- Concept complete
- 2D thermal analysis complete
- Development unit planned
- No thermal testing planned



NASA Seal/Secondary Air Flow System Workshop
OTS Thermal Barriers

10/25/2000

Design and status of a blanket to thermal barrier interface

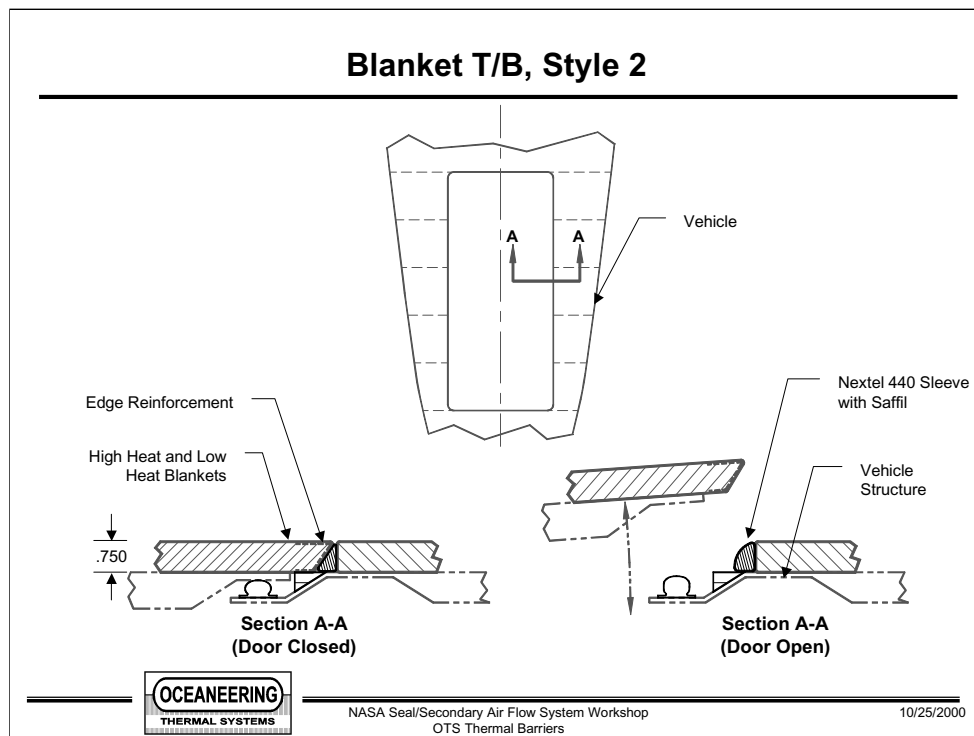


Illustration of a blanket to thermal barrier interface

Blanket T/B , Style 2

Design

- Leeward or windward side use
- Internal reinforced blanket edges to compress T/B
- Nextel 440 sleeve and Saffil
- Outward opening door
- TPS surface temperature up to 1000° F for LHB, 1700°F for HHB
- Maximum structure temperature = 300°F
- Heating durations for suborbital reentry
- Low Heat Blanket (LHB) is Astroquartz OML with Q-Felt insulation

Status

- Design qualified and drawings released
- Flight units built and delivered
- Arc jet testing complete
- Installation and flight planned



NASA Seal/Secondary Air Flow System Workshop
OTS Thermal Barriers

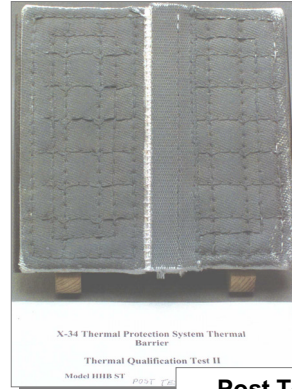
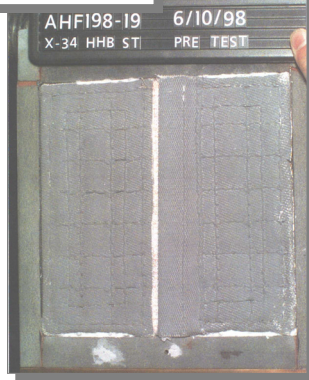
10/25/2000

Design and status of a blanket to thermal barrier interface

Blanket T/B, Style 2

- Arc Jet test coupons for Style 2 T/B
- Aerodynamic Heating Facility at NASA ARC
- Test results indicate T/B protected the structure

Pre Test



Post Test



NASA Seal/Secondary Air Flow System Workshop
OTS Thermal Barriers

10/25/2000

Description and photos of thermal barrier arc jet test coupon

Tile Thermal Barrier Test Fixture

- T/B test articles up to 24 inches long
- Replaceable interface plates for different T/B designs
- Load cell readout for compression loads
- Indicator for deflection measurements



NASA Seal/Secondary Air Flow System Workshop
OTS Thermal Barriers

10/25/2000

Description and photos of a thermal barrier compression test fixture

Space Shuttle Tile T/B Inspection

Procedure

- **Mylar pull test**
 - Initial installation
 - Mylar strip pulled from between the tile and T/B at the center of every tile - nose gear (NG), main gear (MG) and external tank (ET)
 - Performed every flight
 - NG door due to potential changes from high heating
 - ET door because black RTV is recoated on T/B every flight
 - MG door is not checked every flight
- Flow path checks are performed every flight at NG, MG, ET door tile
 - Consists of pushing a .010 shim between the T/B and tile to ensure no gaps exist
 - Checks made along full length of each tile



NASA Seal/Secondary Air Flow System Workshop
OTS Thermal Barriers

10/25/2000

Description of Space Shuttle thermal barrier installation inspection

Closing

Updates in work for thermal barriers on the next generation launch vehicles

- Enhanced durability to reduce replacement
- Enhanced reliability to reduce inspection needs



NASA Seal/Secondary Air Flow System Workshop
OTS Thermal Barriers

10/25/2000

Thermal barrier upgrades in work for next generation RLVs

OVERVIEW OF THERMAL BARRIER/SEAL DEVELOPMENT AT HI-TEMP INSULATION

James Joyce and Sieg Bork
Hi-Temp Insulation, Inc.
Camarillo, California

AFRSI blankets and high temperature gap fillers and seals, originally developed for use on the Space Shuttle, have significantly improved for use on new generation reusable launch vehicles. This presentation will focus on:

- Original designs used on the Space Shuttle.
- Advanced designs developed for use on the X-33.
- Additional advancements for future use on reusable launch vehicles.

This presentation will provide an overview of thermal barrier / seal development at Hi-Temp Insulation.

Preview:

This presentation is organized into the following three sections.

- Hi-Temp Insulation Inc. (Brief Description).
- Current and advanced designs for Ceramic Textile Insulation (AFRSI).
- Advanced designs for high temperature gap fillers and seals.

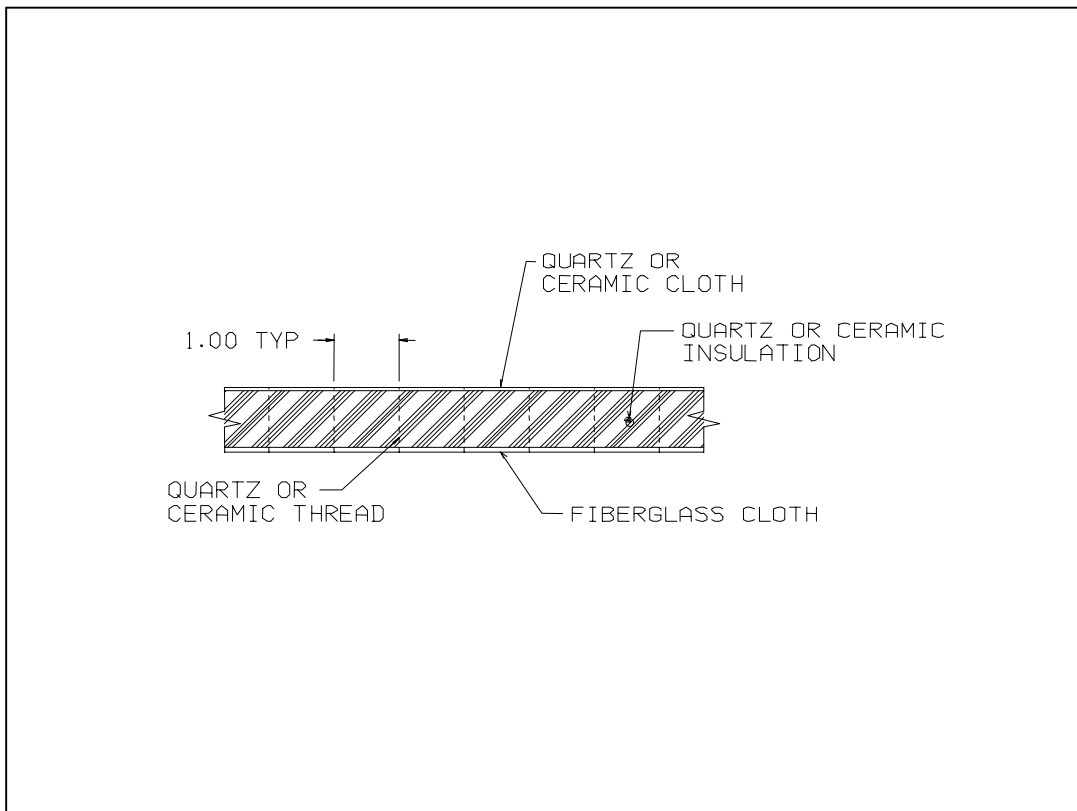
Hi-Temp Insulation has provided the Aircraft, Missile and Space Industries with the most innovative designs and dependable products since 1972. Specializing in solving thermal and acoustical problems, our niche is defined by extreme temperatures and limited space/weight, requiring the most efficient insulating materials.

The products we offer are divided into four categories:

1. Metal foil covered insulation blankets are used for protection at high temperatures when fluid resistance and increased durability are critical.
2. Coated cloth, (typically coated with silicone), covered insulation blankets are used in environments under 450°F, and are both fluid resistant and flexible. Adding a ceramic cloth layer, these blankets stop a 2000°F flame for 15 minutes with no burn-through.
3. Film covered insulation blankets offer the same advantages as the coated cloth products, while being lighter weight. These products are used in environments to 600°F.
4. Sewn or quilted insulation blankets are typically used when operating temperatures are over 1200°F. It is this division of Hi-Temp Insulation that fabricated the AFRSI blankets and seals.

Program	Application - Insulate the...	Customer
Space Shuttle	We provide over 70 percent of the insulation for this program.	Boeing (Rockwell) USBI
Delta II & III	Rocket Nozzle, Gimble Boot, Roll Engines, Blast Tube and Wire Harness Assemblies.	Boeing
Delta IV	Main Nozzle, Roll Nozzle, Exhaust Nozzle, and Drain Lines.	Boeing
Atlas 2AR	Helium Tanks, Engine, Fuel Lines and Oxygen Lines.	Lockheed Martin
Atlas 2ARS	Rocket Nozzles, Turbine Exhaust Duct, and Oxygen Fuel Lines.	Lockheed Martin
Atlas III	Engine Nozzle, and LO2 Inlet	Lockheed Martin
RS-68	Hot Ducting, Turbine Duct, Turbine Exhaust Duct, Lox Pump, Fuel Pump and Gas Generator.	Boeing (Rocketdyne)
X-33	Engine, Thermal Protection System (Metal Foil Blankets and AFRSI Blankets), High Temperature Seals.	Boeing (Rocketdyne) Rohr Industries
Space Station	Designing quilted Kevlar / Nextel insulation blankets for protection from micro-meteors.	Boeing (Space)
Satellites	MLI blankets	Lockheed Martin Boeing (Space)

Hi-Temp Insulation participates in most major Space programs. Listed are some of these programs.



Low temperature advanced flexible reusable surface insulation (AFRSI) is currently used on the upper or leeward surfaces of both the Space Shuttle and the X-33. The AFRSI blankets are rated for continuous use to 1400°F, while reducing the bond line temperature to 300°F.

- Insulation - Quartz Felt.
- Outside fabric facing - Quartz cloth.
- Inside fabric facing - Fiberglass cloth.

High temperature AFRSI is currently used on both the leeward surface between the vertical fins and on the base of the X-33. The higher temperatures in these areas are due to the close proximity to the thermal plume from the aero-spike engines. The high temperature AFRSI is rated for continuous use to 2200°F while reducing the bond line temperature to 300°F.

- Insulation - Ceramic fiber.
- Outside fabric facing - Ceramic cloth.
- Inside fabric facing - Fiberglass cloth.

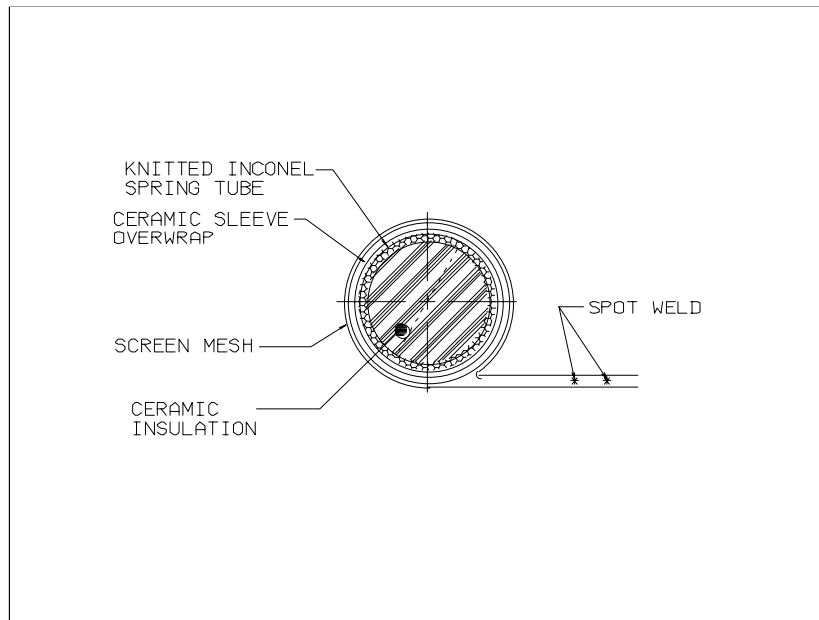
Impact resistant tiles are part of a Boeing shuttle upgrade program. Advanced ceramic textile insulation blankets were recently installed to protect the wing leading edge from meteorite impacts. We added layers of ceramic cloth to the current wing leading edge insulation blanket design. This reduces the higher temperatures generated from the impact of meteorites on the shuttle surface, and from the torch conditions that the penetrations in the TPS system create.

On the space station TPS system, we added layers of both ceramic cloth and kevlar cloth. The ceramic cloth cooled the meteorite during impact, and the kevlar, layered behind the ceramic cloth, stopped the penetrations.

Working with NASA-Ames Research Center, and increased durability and impact resistant ceramic textile insulation was developed called DurAFRSI. This blanket is a hybrid metallic / ceramic insulation that provides both impact resistance and thermal protection.

- Insulation - Ceramic fiber.
- Outside facing - hybrid metallic / ceramic cloth.
- Inside facing - Fiberglass cloth.

Typically, each of the AFRSI blankets discussed are bonded to a composite or aluminum surface with RTV 560. The TPS system must reduce temperatures to protect both the bond line and the vehicle surface. Also, the blankets are typically waterproofed using a process that individually coats each of the insulation fibers preventing the AFRSI from absorbing water. Finally, after installation, a protective ceramic coating is added to the outer surface of the AFRSI blankets.



One very significant difference between the Space Shuttle thermal protection system and the X-33 TPS system is that the X-33 has a “hot-frame” requirement. Since the frame expands and contracts during flight, the TPS system incorporates a variety of seals between the insulation panels to accommodate this movement. The high temperature seal types can be generally grouped into four categories; gap filler, spring seal, spring “P” seal, and screen reinforced seal.

Gap filler seals are the simplest seals we fabricate. They provide good compression but have poor resiliency. They include a ceramic sleeve filled with ceramic insulation. The insulation density varies from 3 to 9 PCF depending on the performance requirements.

- Outer surface – Quarts or Ceramic fabric.
- Core – Ceramic insulation.

To improve the seal’s resiliency, an Inconel knitted spring tube is added. The knitted spring tube is overwrapped with a lightweight ceramic sleeve and stuffed with an appropriate density of ceramic insulation. By adding the knitted spring tube and varying the insulation density, we control the seal’s thermal efficiency, compressive ability, and it’s resiliency or “spring back” characteristics.

- Outer surface – Inconel knitted spring tube overwrapped with lightweight ceramic cloth
- Core – Ceramic insulation.



Hi-Temp Insulation Inc.



Hi-Temp Insulation, Inc. provides the Aircraft, Missile and Space Industries with the most innovative designs and the very best products used to solve thermal and acoustical problems.

The leader in new material use and fabrication techniques; our products are designed to meet the challenge of today's sophisticated requirements.

Our modern 134,000 sq. ft. facility includes a comprehensive range of equipment, storage space, test labs, and manufacturing capability.

Our equipment includes many special machines such as rigidizing rollers for strengthening metal foils; special heated platen press for bonding structural components; heat-sealing machines; seam and spot welders for light gage stainless steel and inconel; high temperature ovens for shaping resin impregnated fabrics; and sewing machines for quilting up to two inches thick.

Specialists in metal foil, soft goods and sewn insulation designs; we have gained considerable experience by providing solutions for a variety of demanding applications.

As a full service manufacturer, Hi-Temp Insulation provides its customers with...

Customer Service

- Our sales and support staff are prepared to meet with you throughout the United States and worldwide to discuss your technical requirements.

Research and Development

- We continue to pursue numerous research and development projects including the best available products for high temperature and fire stop applications.

Engineering

- We have a comprehensive engineering facility which undertakes the complete design and manufacture of products from basic performance requirements.

Production

- We are small enough to be flexible and responsive, and large enough to manufacture a quality product that will satisfy your high standards of production.

Quality Control

- Our strict quality control procedures, satisfying the requirements of DI-9000, ISO-9000 and FAR21.303, track the fabrication process from material selection through final packaging, assuring that critical specifications are met.

AFRSI blankets and high temperature gap fillers and seals, originally developed for use on the Space Shuttle, have significantly improved for use on new generation reusable launch vehicles. This presentation will focus on:

- Original designs used on the Space Shuttle.
- Advanced designs developed for use on the X-33.
- Additional advancements for future use on reusable launch vehicles.

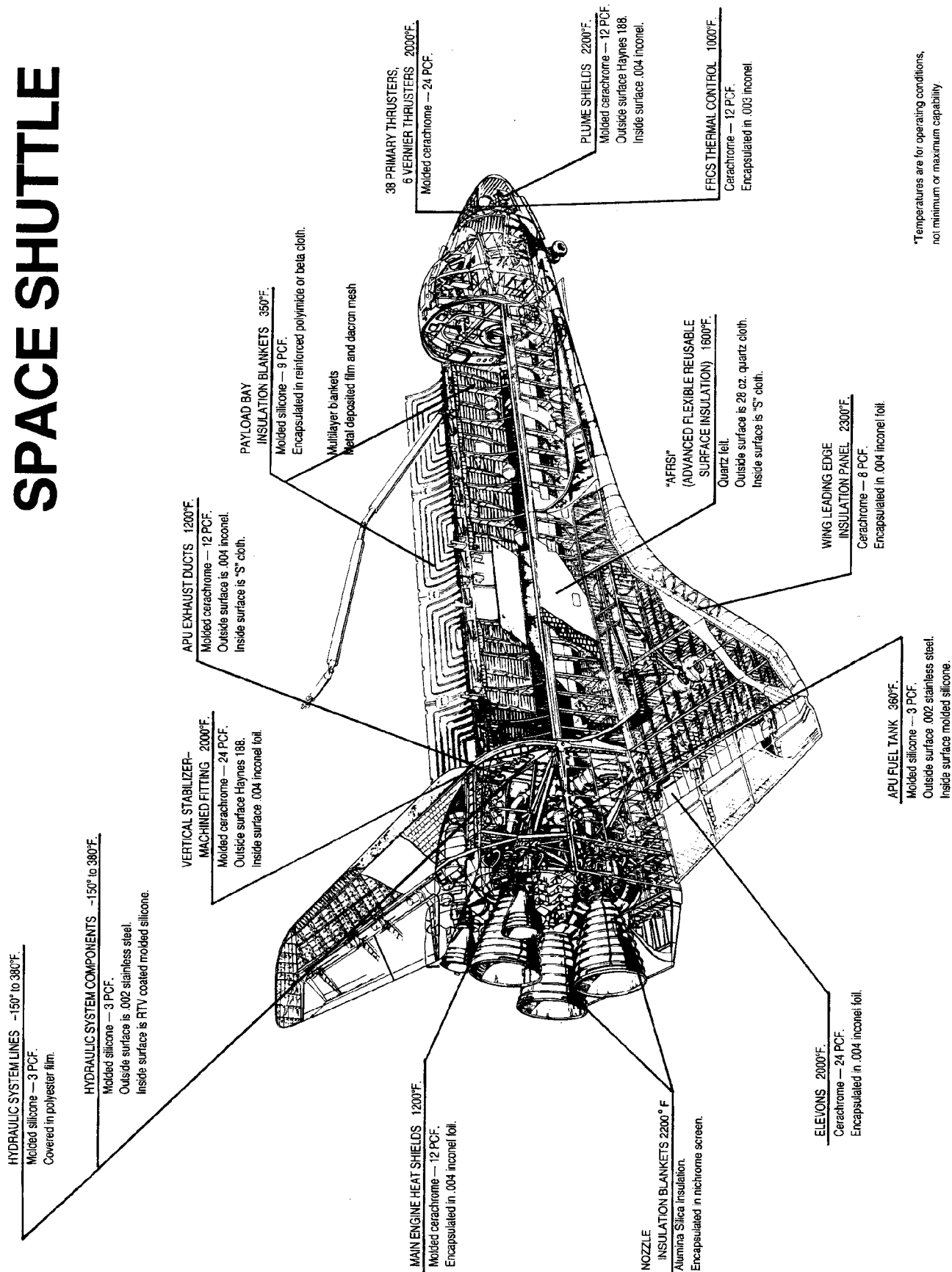
Preview:

This presentation is organized into the following three sections.

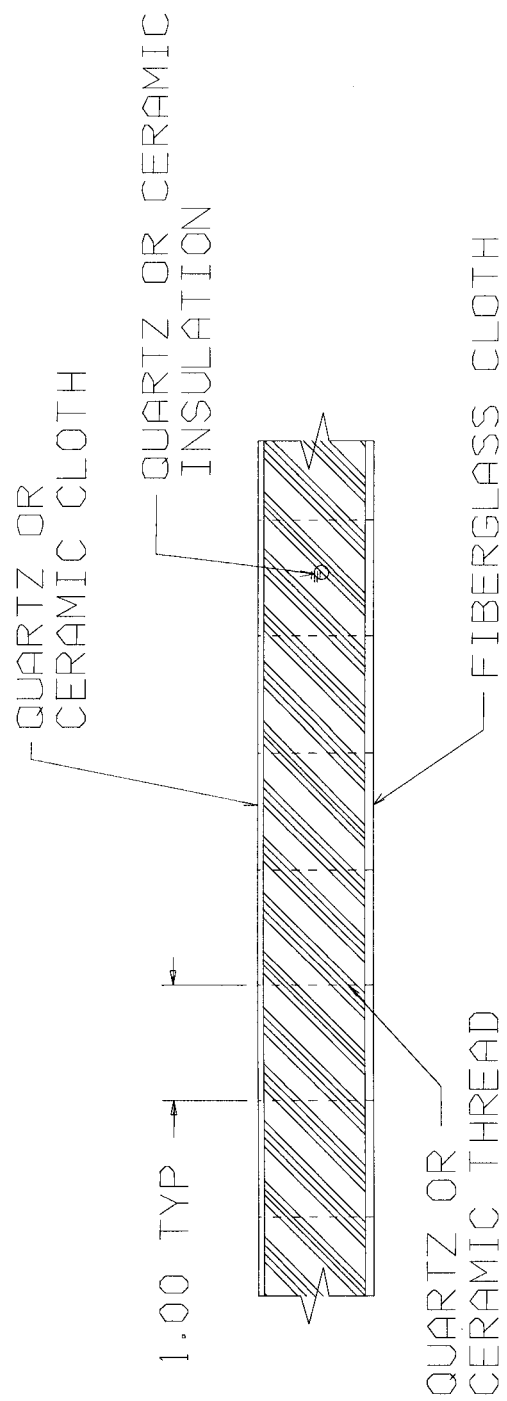
- Hi-Temp Insulation Inc. (Brief Description).
- Current and advanced designs for Ceramic Textile Insulation (AFRSI).
- Advanced designs for high temperature gap fillers and seals.

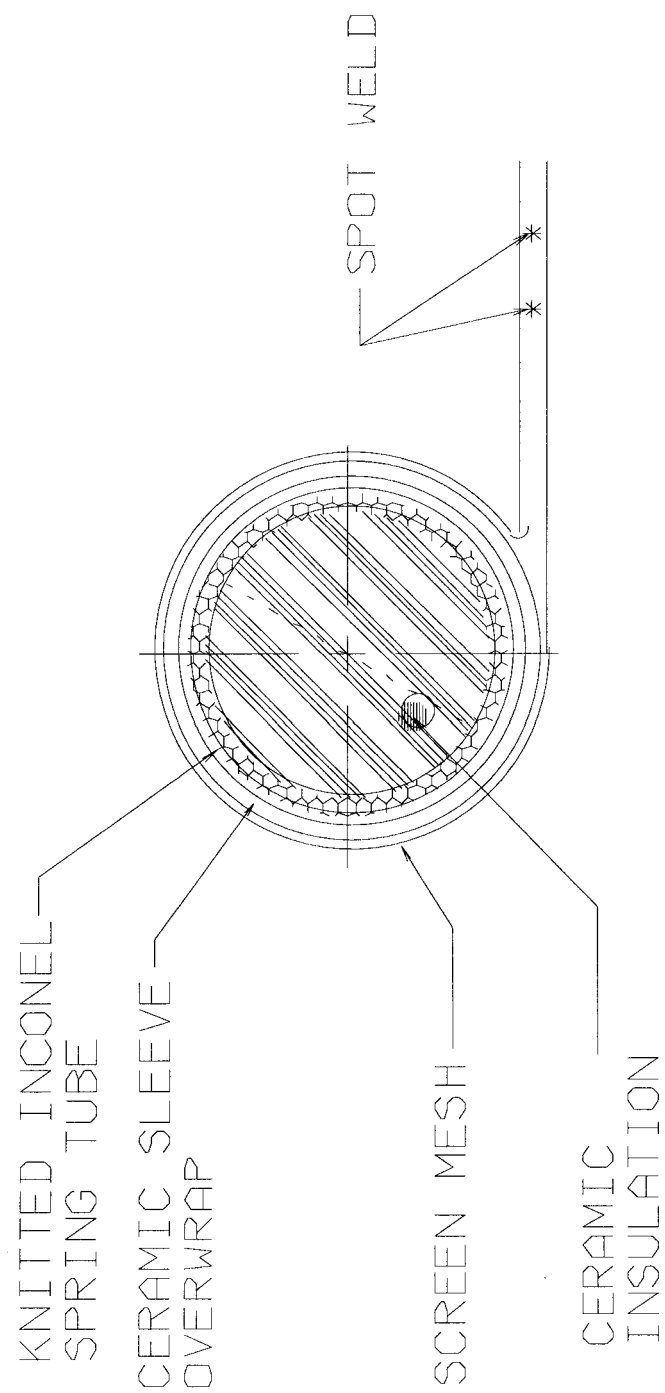
Program	Application - Insulate the...	Customer
Space Shuttle	We provide over 70 percent of the insulation for this program.	Boeing (Rockwell) USBI
Delta II & III	Rocket Nozzle, Gimble Boot, Roll Engines, Blast Tube and Wire Harness Assemblies.	Boeing
Delta IV	Main Nozzle, Roll Nozzle, Exhaust Nozzle, and Drain Lines.	Boeing
Atlas 2AR	Helium Tanks, Engine, Fuel Lines and Oxygen Lines.	Lockheed Martin
Atlas 2ARS	Rocket Nozzles, Turbine Exhaust Duct, and Oxygen Fuel Lines.	Lockheed Martin
Atlas III	Engine Nozzle, and LO2 Inlet	Lockheed Martin
RS-68	Hot Ducting, Turbine Duct, Turbine Exhaust Duct, Lox Pump, Fuel Pump and Gas Generator.	Boeing (Rocketdyne)
X-33	Engine, Thermal Protection System (Metal Foil Blankets and AFRSI Blankets), High Temperature Seals.	Boeing (Rocketdyne) Rohr Industries
Space Station	Designing quilted Kevlar / Nextel insulation blankets for protection from micro-meteors.	Boeing (Space)
Satellites	MLI blankets	Lockheed Martin Boeing (Space)

SPACE SHUTTLE



*Temperatures are for operating conditions, not minimum or maximum capability





Summary:

This presentation focused on the following three topics.

- **Hi-Temp Insulation** - uses the most efficient materials to protect from extreme temperatures.
- **Current and advanced designs for AFRSI** - quilted quartz, ceramic and metallic materials used as TPS on reusable launch vehicles.
- **Advanced designs for high temperature gap fillers and seals** - quartz and ceramic facings with inconel knitted spring tube and ceramic insulation, optimize both compression and resiliency.

ROPE SEAL DEVELOPMENTS

Bruce Bond
Albany International Techniweave, Inc.
Rochester, New Hampshire

John Xia
Siemens Westinghouse

Margaret Kowal
University of New Hampshire
Durham, New Hampshire

Rope Seal Developments

- Co-authored by:
 - Bruce Bond - Albany Techniweave
 - John Xia - Siemens Westinghouse
 - Margaret Kowal - University of New Hampshire

Albany International Techniweave



The work presented here includes information gained from a number of experiments conducted on a standard Albany Techniweave Style 9024 rope seal. The information contained herein is shared with the permission of Siemens Westinghouse. A special note of appreciation goes to Margaret Kowal of the University of New Hampshire for her assistance in this effort. Margaret is in her second year of a Masters in Chemical Engineering at UNH and is funded by a joint program between the University of New Hampshire and Albany Techniweave.

Style 9024

- Nominal OD - 0.375 inches
- Core - Nextel 312, fiber volume 45%
- Core Construction - multi-layered braid
- Outer sheath - Haynes 188

Albany International Techniweave



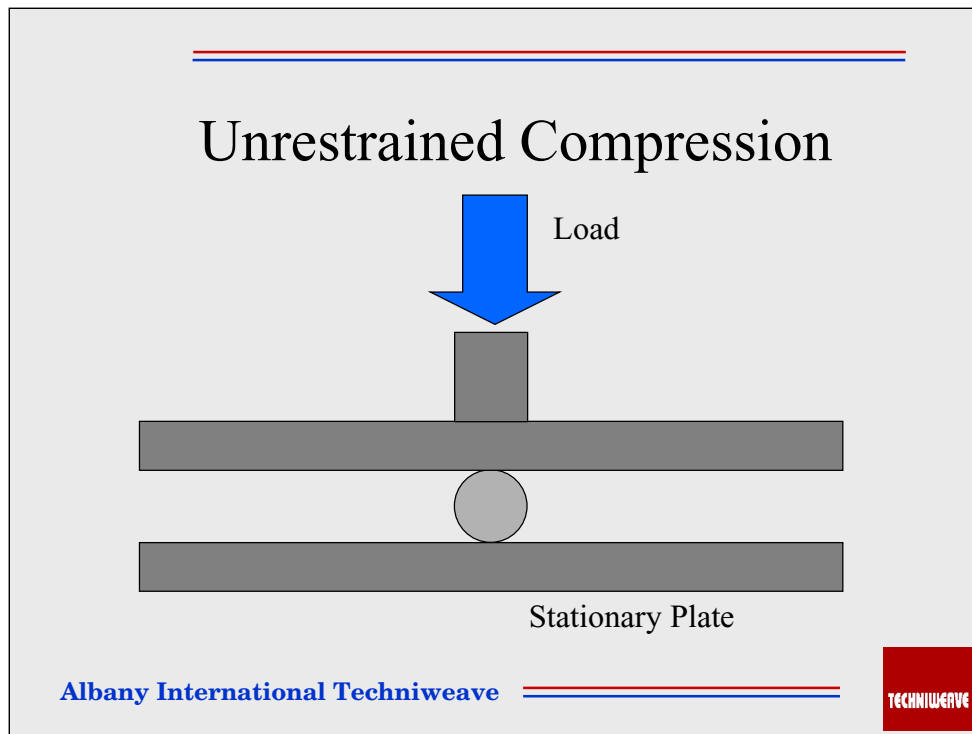
The AIT Style 9024 is a hybrid rope seal consisting of a multi-layered braided core of Nextel™ 312 yarns with an overbraid of Haynes™ 188 wire. The wire protects the fragile ceramic yarns in abrasive environments.

Experiments Conducted

- Unrestrained compression
- Compression in grooves to fixed volumes (105% of original seal x-section)
- Compression in .360 wide groove with varying depths to fixed max loads

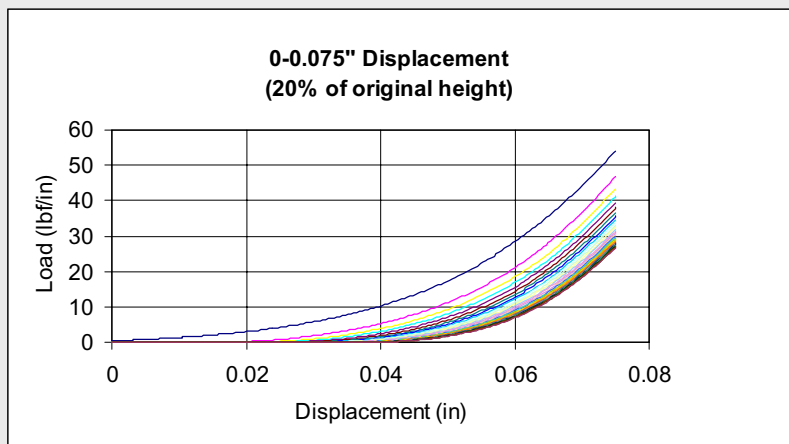
Albany International Techniweave





Unrestrained compression was conducted between two flat plates using an Instron™.

Typical 30 Cycle Load Curve

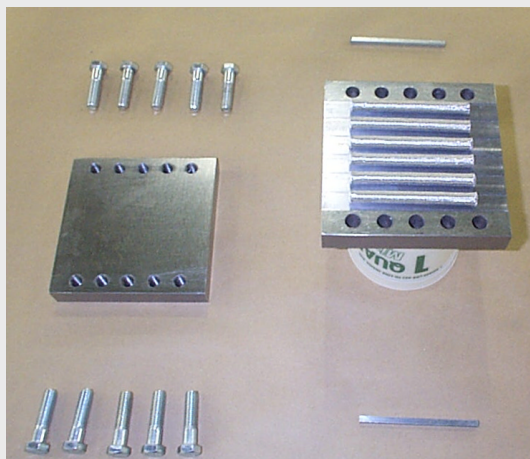


Albany International Techniweave



Cyclical loadings to a fixed displacement show a decreasing rate of change in the load required and the amount of recovery.

Compression and Impregnation

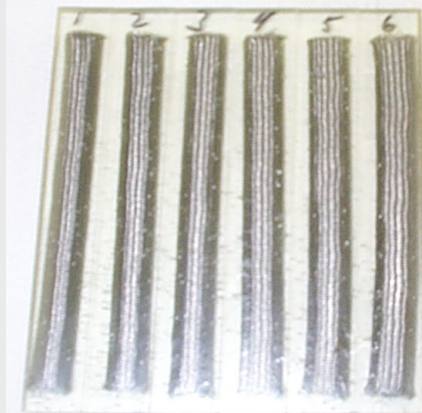


Albany International Techniweave



A fixture consisting of a plate with grooves and a smooth plate was used to compress six seal samples between 5 and 30 percent of the original seal diameter.

Seal Shape Captured in Epoxy

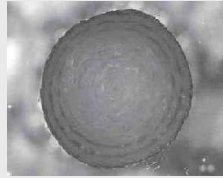


Albany International Techniweave

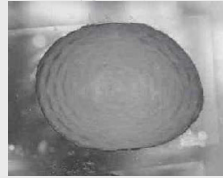


The seals were imbedded in an epoxy resin to fix their shape.

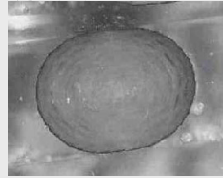
Seal X-Section



As Built



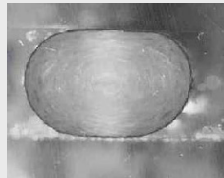
5% Compression



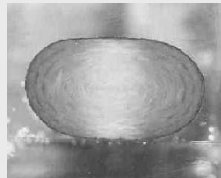
10% Compression



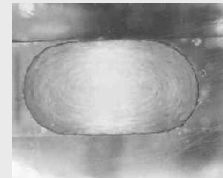
15% Compression



20% Compression



25% Compression



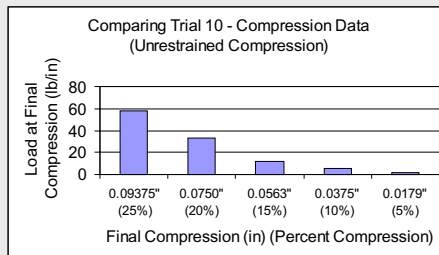
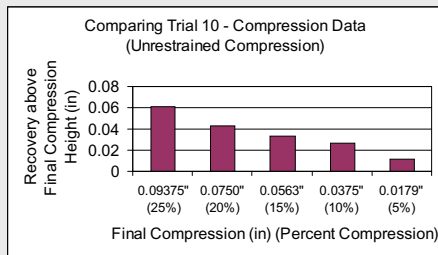
30% Compression

Albany International Techniweave



The potted seals were sectioned, photographed and the cross sectional area measured. The seals exhibited a decrease in cross section with increasing compression and hence an increase in fiber volume. In contrast, elastomeric seals would have a constant cross section.

Comparison of 10th Cycle Curves



Albany International Techniweave



In some instances a rope seal will be required to seal between two flat surfaces. The above graphs show the recovery and loads as a function of the percent compression as based on the original diameter.

Compression to Fixed Volumes (0.117 sq. in)



Width	0.371"	0.396"	0.495"	0.446"
Depth	0.313"	0.296"	0.235"	0.262"

*Note, photos are for demonstration purposes only; testing was performed one seal at a time

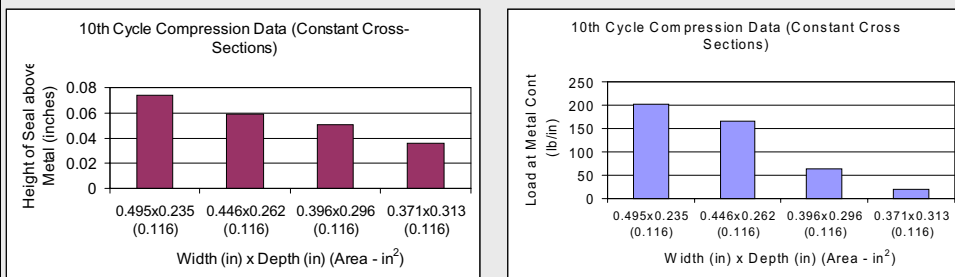
**Note, 1st set of grooves are slightly off scale from 2nd set of grooves in this slide

Albany International Techniweave



Seal samples were subjected to repeated compressions in grooves with constant cross section and varying dimensions.

Comparison of 10th Cycle Curves

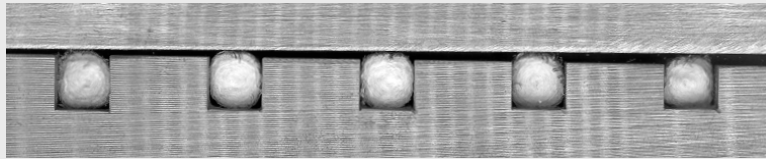


Albany International Techniweave



In some instances the anticipated loads would be sufficient to ensure metal to metal contact. The graphs above show the recovery of the seal and the loads required to make metal to metal contact for various configurations where the cross section of the groove has been held constant.

Compression with Changing Volume (Constant Width)



Width:	0.360"	0.360"	0.360"	0.360	0.360"
Depth:	0.356"	0.338"	0.319"	0.319"	0.300"
Area:	0.128 in ²	0.122 in ²	0.115 in ²	0.115 in ²	0.108 in ²
	0.101 in ²				

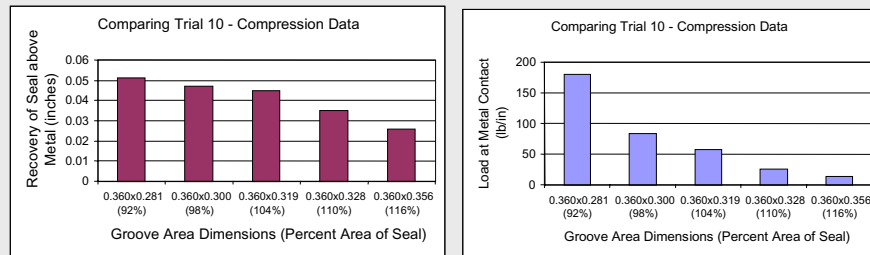
*Note, photos are for demonstration purposes only; testing was performed one seal at a time

Albany International Techniweave



In certain applications it is desirable to place the seal in a groove which is slightly narrower than the diameter of the seal to facilitate installation and retention during assembly. A family of curves can be established using different loads per linear inch and various groove depths..

Comparison of 10th Cycle Curves



Albany International Techniweave



In some instances the anticipated loads would be sufficient to ensure metal to metal contact. The graphs above show the recovery of the seal and the loads required to make metal to metal contact for various groove depths where the width is held to a 0.360 inches.

Compression to a Fixed Load



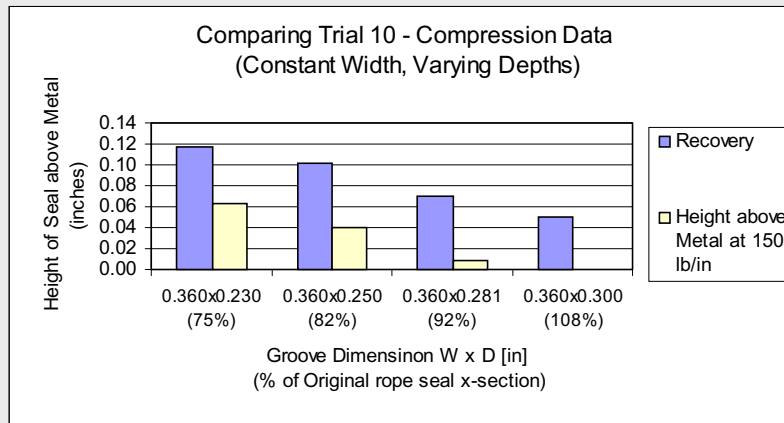
*Note, photos are for demonstration purposes only; testing was performed one seal at a time

Albany International Techniweave



The seals were compressed using various grooves where the load was limited to certain maximums as measured in pounds/inch of seal length.

Comparison of 10th Cycle



Albany International Techniweave



This graph shows the recovery and the final height above the metal surface for various groove configurations where the maximum load was 150 lb./linear inch.

Summary

- Cyclical compressions appear to approach a stable load / deflection curve
- Resiliency is a function of both the amount of compression and the groove configuration
- Specific applications may require specific testing

Future Work

- Room temperature leak testing
 - Fixed groove, varying amounts of compression
 - Effect of architecture on leakage
- Testing of other seals
 - .050” - 0.500”
 - Nextel-312, 440, 550, 610, 710

Albany International Techniweave



The next area of investigation is to evaluate the effect of compression and architecture on leakage at room temperature. The work will be extended to include our other standard seals and a wide range of potential fibers and architectures.

NASA GRC CRYOGENIC SEAL TEST RIG CAPABILITY


Margaret Proctor
National Aeronautics and Space Administration
Glenn Research Center
Cleveland, Ohio



NASA GRC Cryogenic Seal Test Rig Capability

Presented by
Margaret Proctor

2000 NASA Seal/Secondary Air System Workshop
October 25–26, 2000



NASA Glenn Research Center

CD-00-80970

It has been about 6 years since any cryogenic seal tests were run at NASA GRC. The Cryogenic Components Lab, where the cryogenic seal test rigs are located, has been shutdown due to the impending expansion of the Cleveland Hopkins International Airport. The current plan is to move the Cryogenic Components Lab (CCL), Cells 1 and 2 to NASA Plumbrook in Sandusky, Ohio. The purpose of this presentation is to inform the seal community of the cryogenic seal test rig capabilities available at NASA GRC for planning of future programs.

Cryogenic Seal Test Rigs at NASA GRC



1. Lox Seal Test Rig

Designed and built by Mechanical Technology Inc. under NASA Contract NAS3-23260 to test seals for liquid oxygen turbopumps.

2. Cryogenic Brush Seal Test Rig

- **Originally designed and built by Rocketdyne under NASA contract to test low thrust pumps.**
- **Modified by NASA to test brush seals in LN₂ and LH₂.**

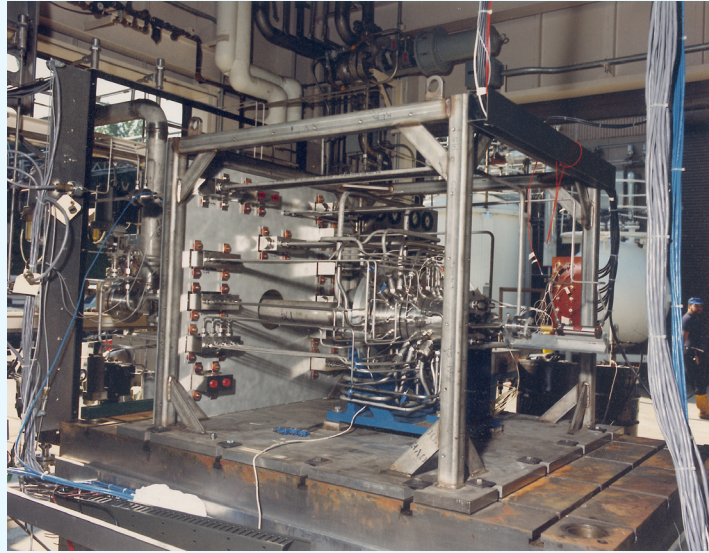


NASA Glenn Research Center

CD-00-80970

Two test rigs are available to test cryogenic seals. The Lox Seal Test Rig was designed and built by Mechanical Technology, Inc. under a NASA contract to test seals for liquid oxygen turbopumps. The Cryogenic Brush Seal Test Rig was originally designed and built by Rocketdyne under a NASA contract to test low thrust pumps. NASA then modified the rig to test brush seals in liquid nitrogen and liquid hydrogen.

Lox Seal Test Rig

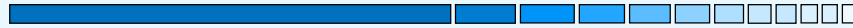


NASA Glenn Research Center

CD-00-80970

This photograph shows the Lox Seal Test Rig as it was installed in Stand C at the Rocket Engine Test Facility. Some initial testing was conducted. Due to conflicts with other test stands at the Rocket Engine Test Facility, it was decided to move the Lox Seal Test Rig to the Cryogenic Components Lab, Cell 1 (CCL-1). About half way through the facility build-up at CCL-1, funding resources were cut. The Lox Seal Test Rig components are stored in cabinets.

Lox Seal Test Rig Capabilities



- 50-mm and 20-mm seal hardware
- Face seal or ring seals
- 750-psi LN₂ or Lox seal supply
- 200-psi GHe seal supply
- 100,000-rpm maximum shaft speed (depending on seal)
- 100-hp GN₂ turbine drive, overhung, radial inflow
- Axial vibration can be imposed via thrust bearing control

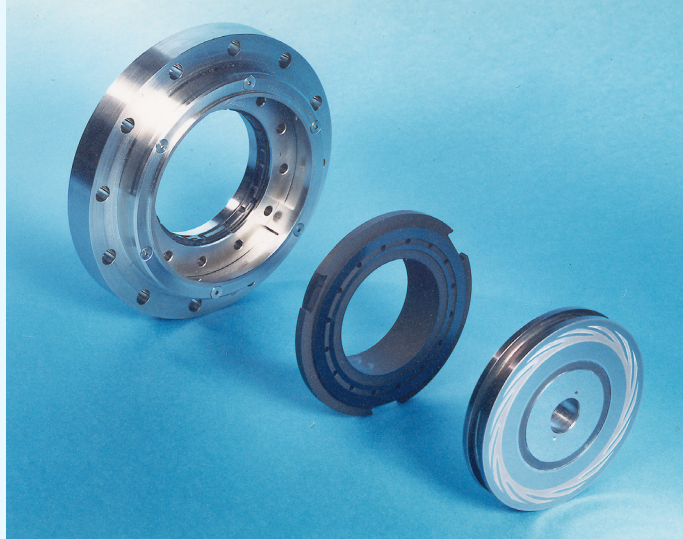


NASA Glenn Research Center

CD-00-80970

The Lox Seal Test Rig was designed to test both 50-mm and 20-mm seal hardware. These two sizes are representative of the shaft sizes used in turbopumps for launch vehicles and orbital transfer vehicles, respectively. Both face seals and ring seals can be tested. Lox spiral-grooved face seals and Rayleigh-step, helium-buffered ring seals were designed and fabricated for testing in this rig. The rig and test facility was designed for 750-psi liquid nitrogen or liquid oxygen seal supply. This high pressure LN₂ or Lox also supplies the hydrostatic bearings. No testing has been done with lox. When testing the helium buffer seal, up to 200 psi gaseous helium can be supplied to the seal and liquid nitrogen is supplied to the hydrostatic bearings. Shaft speeds up to 100,000 rpm can be attained depending on which seal rotor is being used. The maximum shaft speed is 100,000 rpm for 20-mm Lox and helium seals; 56,000 rpm for 50-mm Lox seal and 70,000 rpm for 50-mm helium seal. The rig is powered by an overhung, radial inflow, 100-hp gaseous nitrogen turbine drive. Axial vibrations can be imposed by controlling the thrust bearing. The rig was designed to provide axial shaft vibrations up to +/- 0.005 inch with a frequency of 10 Hz.

Lox Spiral Groove Face Seal

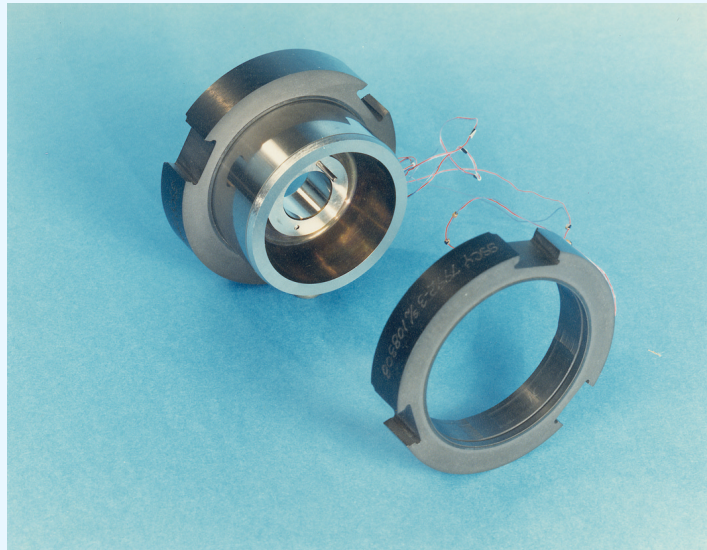


NASA Glenn Research Center

CD-00-80970

This photograph of the Lox Spiral Groove Face Seal shows a stationary carbon ring (center) and the spiral groove rotor (right). The carbon ring is held in the seal holder (left).

Raleigh-Step Helium Buffer Seal

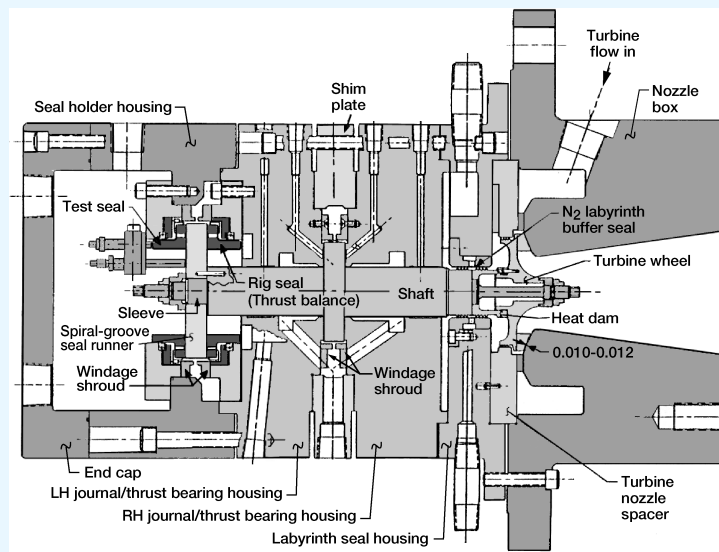


NASA Glenn Research Center

CD-00-80970

The Raleigh-step Helium Buffer Seal is comprised of a rotor and two carbon rings. Helium is supplied to a space between the two carbon rings. Helium then leaks axially through the gap between the carbon rings and the rotor. On the inner diameter of each carbon ring are four shallow pockets, which generate a hydrodynamic lifting force during shaft rotation. This lifting force prevents the seal from contacting the rotor and wearing the seal.

Lox Seal Test Rig



NASA Glenn Research Center

CD-00-80970

This cross section of the Lox Seal Test Rig has a pair of face seals installed on either side of the spiral groove seal runner mounted on the left end of the shaft. Lox or LN2 is supplied to the outer diameter of the seal runner. The Lox or LN2 leaks radially inward through the seal. The inboard seal is a slave seal to balance axial loads on the shaft. Its leakage flow enters a drain in the LH journal/thrust bearing housing. The test seal is the outboard seal and its leakage exits through the end cap. Two proximity probes are shown. One measures the axial motion of the test seal, the other measures the motion of the seal runner. The difference between these two measurements provides the clearance. This approach to tracking the seal clearance is not very accurate due to thermal gradients. Therefore, proximity probes have been flush mounted in the test seal to directly measure the clearance between the seal and the seal runner. The shaft is supported by two hydrostatic journal bearings which are supplied with either Lox or LN2. A hydrostatic thrust bearing located approximately in the middle of the shaft controls axial shaft motion. Gaseous nitrogen drives the radial inflow turbine mounted on the right end of the shaft. A GN2 labyrinth buffer seal keeps LN2 from entering the turbine cavity.

Lox Seal Test Rig During Test



NASA Glenn Research Center

CD-00-80970

This photograph shows the Lox Seal Test Rig during a test.

Cryogenic Brush Seal Test Rig Capabilities

- 2-in.-diameter bore seals
- 5 brushes at one time - use long, low speed runner
maximum speed 40,000 rpm
- 1 brush at a time - use short, high speed runner
maximum speed 65,000 rpm
- 800-psig MAWP of rig
- Maximum Delta-P across seal is 300 psi due to balance piston capability
- LH₂ or LN₂
- 14 seal temperature measurement locations
- 14 seal pressure measurement locations
- 3 proximity probes measure rotor orbit

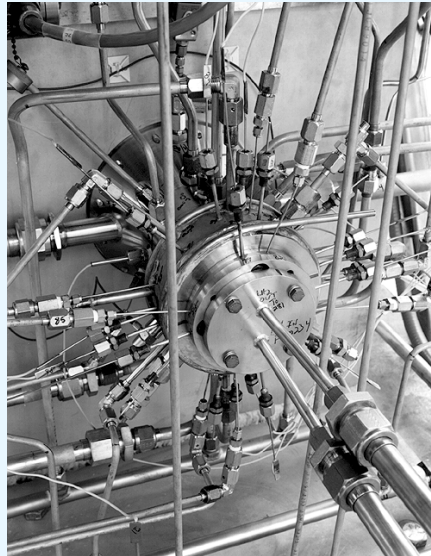


NASA Glenn Research Center

CD-00-80970

The Cryogenic Brush Seal Test Rig was designed to test 2-inch diameter bore brush seals. Up to five brushes can be tested at one time using a long, low speed seal runner, which has a maximum shaft speed of 40,000 rpm. A short, high speed runner can be used to test at speeds up to 65,000 rpm. With this runner only one brush seal can be tested. Special seal spacers were used to allow pressure and temperature measurements between seals to study staging effects. The rig has a maximum allowable working pressure of 800 psig. However, the maximum pressure drop across the seal that can be attained during rotation is 300 psi due to the balance piston capability. Either liquid hydrogen or liquid nitrogen can be used in this rig. There are fourteen temperature and fourteen pressure measurement locations. Three proximity probes are used to measure the seal runner orbit.

Cryogenic Brush Seal Tester Installation



NASA Glenn Research Center

CD-00-80970

This is a photograph of the Cryogenic Brush Seal Tester as it is installed in the Cryogenic Components Lab, Cell 2 (CCL-2) and as viewed from the test seal end of the rig.

Typical Brush Seal

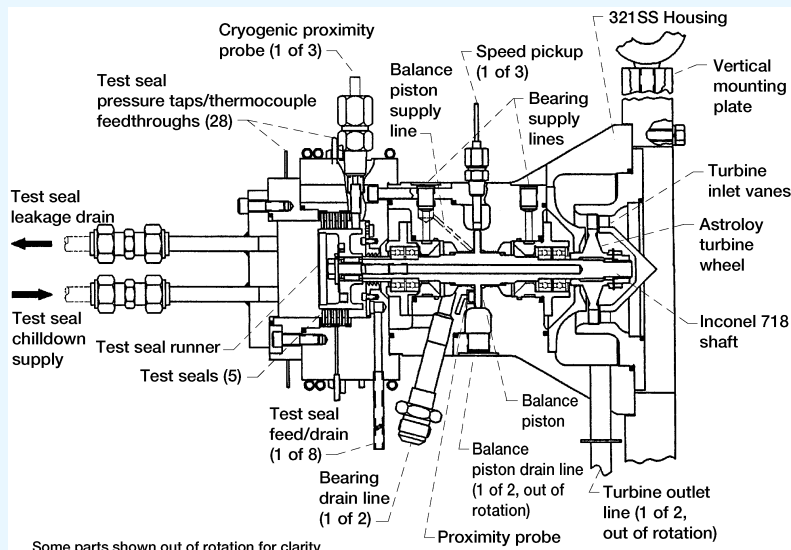


NASA Glenn Research Center

CD-00-80970

This is a typical brush seal. It is made of a pack of metal wire bristles at an angle to the radius of the inner diameter and sandwiched between an upstream sideplate (visible in photo) and a downstream sideplate (not visible). The bristles are typically 0.002 to 0.003 inch in diameter and flex like a cantilevered beam during shaft growth or excursions.

Cross Section of Cryogenic Brush Seal Tester

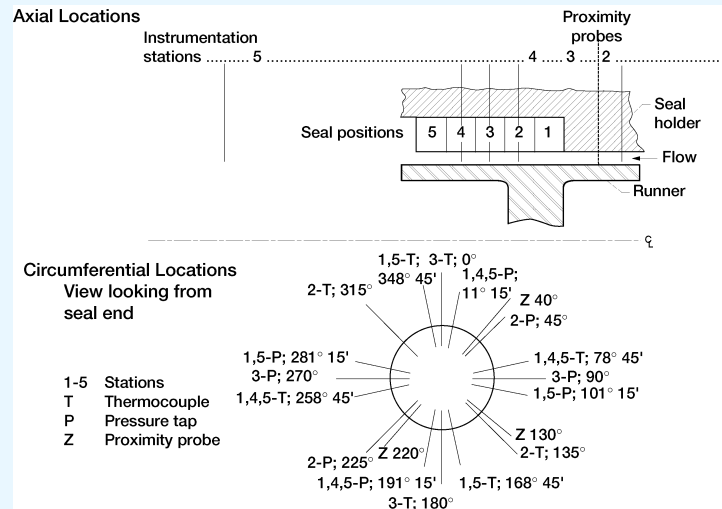


NASA Glenn Research Center

CD-00-80970

This cross section of the Cryogenic Brush Seal Tester shows the shaft is supported by two pairs of ball bearings. A balance piston is located between these bearings to balance out the axial loads due to the pressure drop across the seal. The rig is driven by a gaseous nitrogen or hydrogen, full-admission, axial-flow turbine depending on the test fluid. The long, low speed seal runner is shown attached to the left end of the shaft. Five test seals are shown. The test fluid (LN₂ or LH₂) is supplied to the inboard, high-pressure side of the seal runner. It then passes through a perforated plate, which is integral with the test-seal-end labyrinth seal, to steady the flow. In tests where the brush seal leakage was low, it was necessary to bypass some flow out of the seal supply cavity to keep the rig cold enough.

Location of Brush Seal Positions and Instrumentation Stations Low-Speed Runner Shown

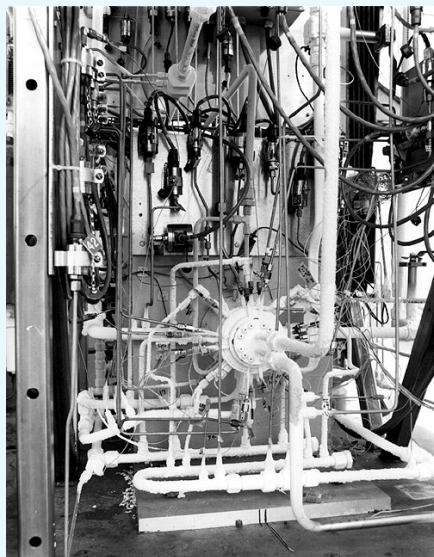


NASA Glenn Research Center

CD-00-80970

This shows the location of the pressure, temperature, and proximity measurements. Spacers with holes for instrumentation can be put in seal positions 2, 3, and 4 to measure interstage conditions.

Cryogenic Brush Seal Tester During Test



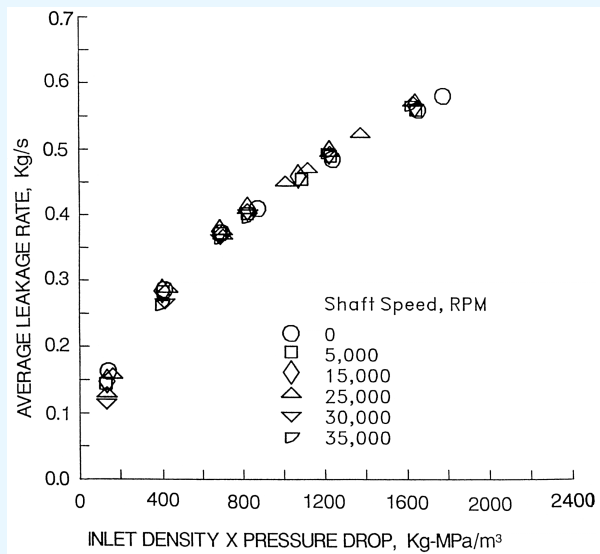
NASA Glenn Research Center

CD-00-80970

Self-explanatory.

12-Tooth Labyrinth Seal in LN₂

0.13-mm Radial Clearance

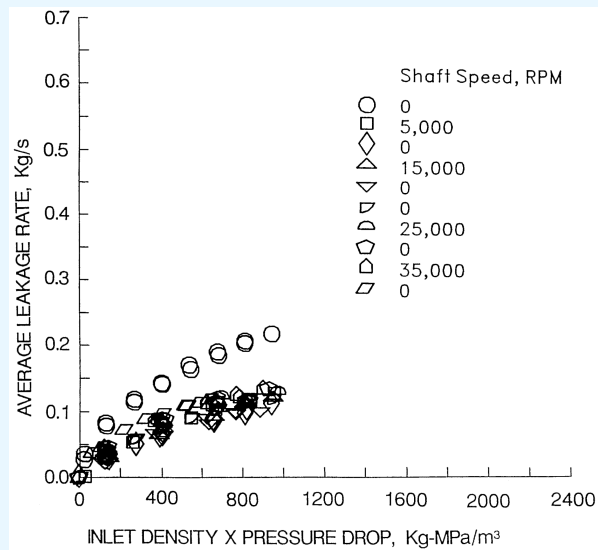


NASA Glenn Research Center

CD-00-80970

This is a plot of leakage rate vs. inlet density times pressure drop for a 12-tooth labyrinth seal in liquid nitrogen. The seal had a radial clearance of about 0.005 inch.

Single Brush Seal in LN₂ 0.11-mm Radial Interference

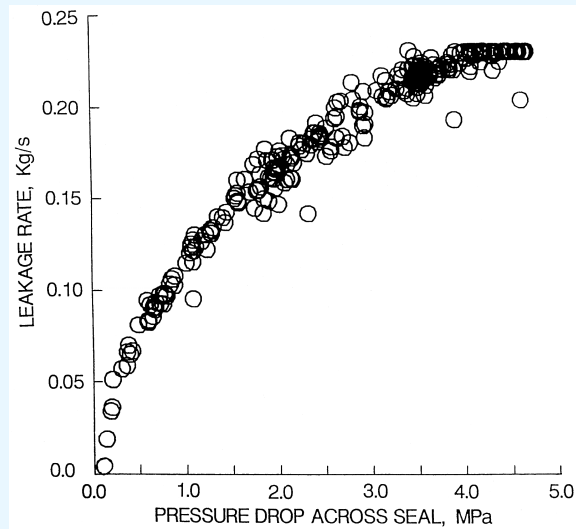


NASA Glenn Research Center

CD-00-80970

The leakage rate of a single brush seal in liquid nitrogen is about one-half to one-third that of the 12-tooth labyrinth seal with a radial clearance of 0.005 inch. Note that the data shown as circles, taken at 0 rpm, was the first pressurization of the seal. Subsequent data shows a lower leakage rate and indicates that some rotation is needed to fully seat the seal.

Blowout Test of a Single Brush Seal in LN₂ at Zero rpm



NASA Glenn Research Center

CD-00-80970

A blowout test was done of a single brush seal in liquid nitrogen at zero rpm. Blowout means that the bristles bend in the axial direction to the point where they no longer contact the shaft. It was anticipated that if blowout were to occur, then the leakage rate would suddenly increase. As can be seen, there was no indication of blowout at pressure drops across the seal up to 3.8 Mpa (550 psid). The leveling out of data above 3.8 Mpa is due to the pressure transducers being at their maximum reading limit.

Tribological Performance Summary for LH₂ Brush Seal

35,000 rpm

SEAL RUNNER COATING	ACCUMULATIVE TEST DURATION (min)	ACCUMULATIVE LINEAR SLIDING DISTANCE (Km)	ACCUMULATIVE BRISTLE WEAR (μm)	MAXIMUM RADIAL SEAL RUNNER WEAR (μm)
INCONEL-718 (UNCOATED)	43	213	64	-17 (DEPOSITED)
CrC	51	223	25	6
Cr+TEFLON	28	86	(NEGLIGIBLE)	(NEGLIGIBLE)
ZrO ₂	47	222	5	90

65,000 rpm

SEAL RUNNER COATING	ACCUMULATIVE TEST DURATION (min)	ACCUMULATIVE LINEAR SLIDING DISTANCE (Km)	ACCUMULATIVE BRISTLE WEAR (μm)	MAXIMUM RADIAL SEAL RUNNER WEAR (μm)
INCONEL-718 (UNCOATED)	38	300	41	-17 (DEPOSITED)
CrC	58	450	38	20
Cr+TEFLON	66	577	56	12
ZrO ₂	48	337	18	85



NASA Glenn Research Center

CD-00-80970

Wear testing was done for an uncoated Inconel 718 rotor, a rotor coated with chrome carbide, a rotor coated with chrome carbide and impregnated with Teflon, and a rotor coated with zirconium oxide. Testing was done at both 35,000 rpm and 65,000 rpm. Bristle material was deposited on the uncoated Inconel 718 rotor at both speeds. The zirconium oxide coating had the most wear at both speeds. The chrome carbide coating had small amounts of wear, but the chrome carbide coating impregnated with Teflon had negligible wear at 35,000 rpm and less wear than the chrome carbide alone at 65,000 rpm. The Teflon has a lubricating effect, but does wear away.

For more details see NASA TM 107203, "Wear Characteristics of Three Rotor Coatings for Application to Brush Seals Operating in Liquid Hydrogen," by James F. Walker and Margaret P. Proctor, 1995.

For more details about the Cryogenic Brush Seal Test Rig, see NASA TP 3536, "Brush Seals for Cryogenic Applications Performance, Stage Effects, and Preliminary Wear Results in LN2 and LH2," by Margaret P. Proctor, et. al., 1996.

OVERVIEW OF CMC DEVELOPMENT ACTIVITIES IN NASA'S ULTRA-EFFICIENT ENGINE
TECHNOLOGY (UEET) PROGRAM

Dave Brewer
National Aeronautics and Space Administration
Glenn Research Center
Cleveland, Ohio

UEET

National Aeronautics &
Space Administration
Glenn Research Center



***Overview of CMC Development Activities in NASA's
Ultra-Efficient Engine Technology (UEET) Program***

***2000 NASA Seal/Secondary Air System Workshop
Cleveland, Ohio
October 26, 2000***

Dave Brewer

NASA Glenn Research Center

The primary objective of the UEET Program is to address two of the most critical propulsion issues: performance/efficiency and reduced emissions. High performance, low emissions engine systems will lead to significant improvement in local air quality, minimum impact on ozone depletion and level to an overall reduction in aviation contribution to global warming. The Materials and Structures for High Performance project will develop and demonstrate advanced high temperature materials to enable high-performance, high efficiency, and environmentally compatible propulsion systems



Vision:

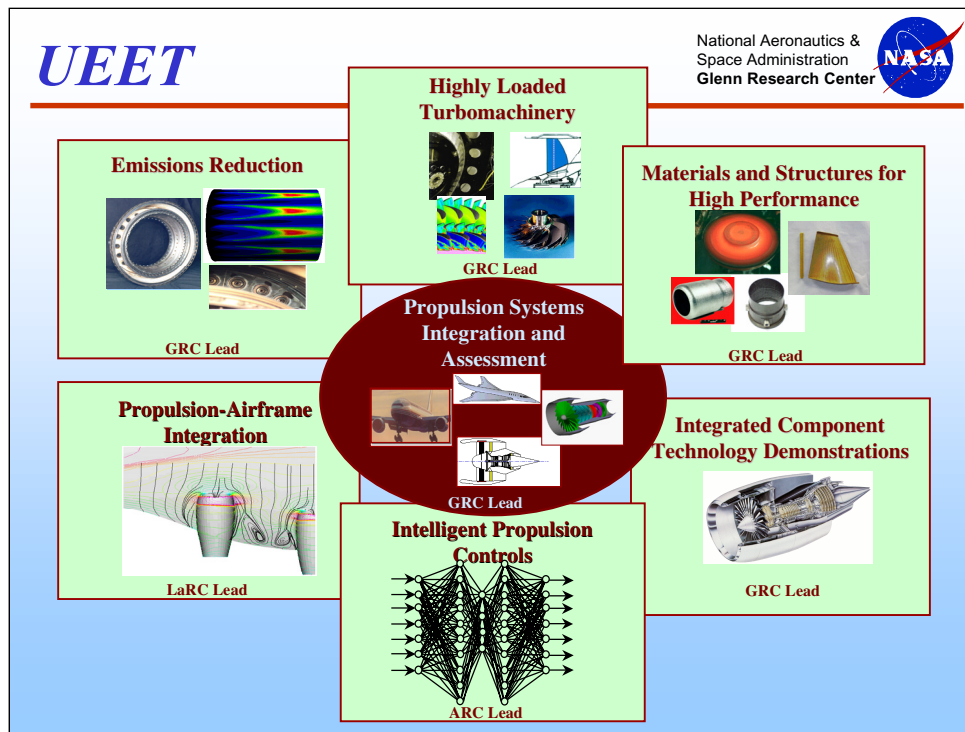
Develop and hand off revolutionary propulsion technologies that will enable future generation vehicles over a wide range of flight speeds.

Goals:

Propulsion technologies to enable increases in efficiency and therefore fuel burn reductions of up to 15 % (equivalent reductions in CO₂)

Combustor technologies (configuration and materials) which will enable reductions in LTO NO_x of 70% relative to 1996 ICAO standards.

The material and structural technologies developed in this project will contribute toward achieving the two primary UEET program goals—(1) take-off and landing NO_x emissions reduction of 70% and (2) overall fuel savings of 8 – 15%. Technologies developed in this project include ceramic matrix composite (CMC) combustor liners and turbine vanes, advanced disk alloys, turbine blade material systems, high temperature polymer matrix composites (PMC), and innovative lightweight materials and structures for static engine structures



The UEET Program is comprised of seven major components or tasks. Research in the areas of Emissions Reduction, Highly Loaded Turbomachinery, Propulsion Systems Integration and Assessment, Integrated Component Technology Demonstrations and finally Materials and Structures for High performance is lead from Glenn Research Center. Langley and Ames lead research in the areas of Propulsion-Airframe integration and Intelligent Propulsion Controls, respectively. The annual budget for the total program is approximately \$50M/year. The Material and Structures task funding is approximately \$14M/year out of the total program funding.



Disk Alloy



Ceramic Matrix Composites

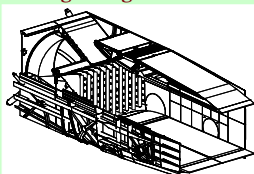


Polymer Matrix Composites

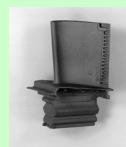


Materials and Structures for High Performance

Lightweight Nozzle



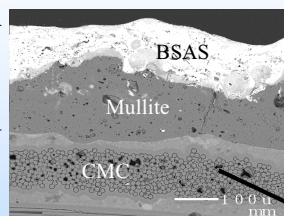
Turbine Blade System



There are five areas of research within the Materials and Structures for High Performance Task: Disk Alloy, Polymer Matrix Composites (which was not continued in FY 01), Turbine Blade System, Lightweight Nozzle Materials and the focus of this presentation, Ceramic Matrix Composites. Ceramic Matrix Composites receives funding support of approximately \$4M/year of the \$14M/year in Materials and Structures support.

UEET CMC Development Initiated From 9/99 EPM Material

Environmental
Barrier Coating
(EBC)

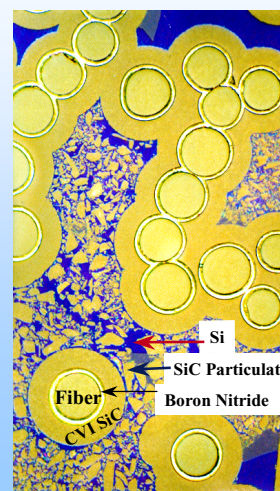


Composite Characteristics:

- Stoichiometric SiC fiber (Sylramic™ from Dow Corning)
- Si-doped BN fiber coating
- Slurry cast melt infiltration process
- EBC for surface recession resistance

Key Composite Properties for 9/99 Material:

- Thermal conductivity at 2200 °F - 8.5 BTU/hr.ft.°F
- 20 ksi stress capability for long-term life at 2200 °F



Dense composite

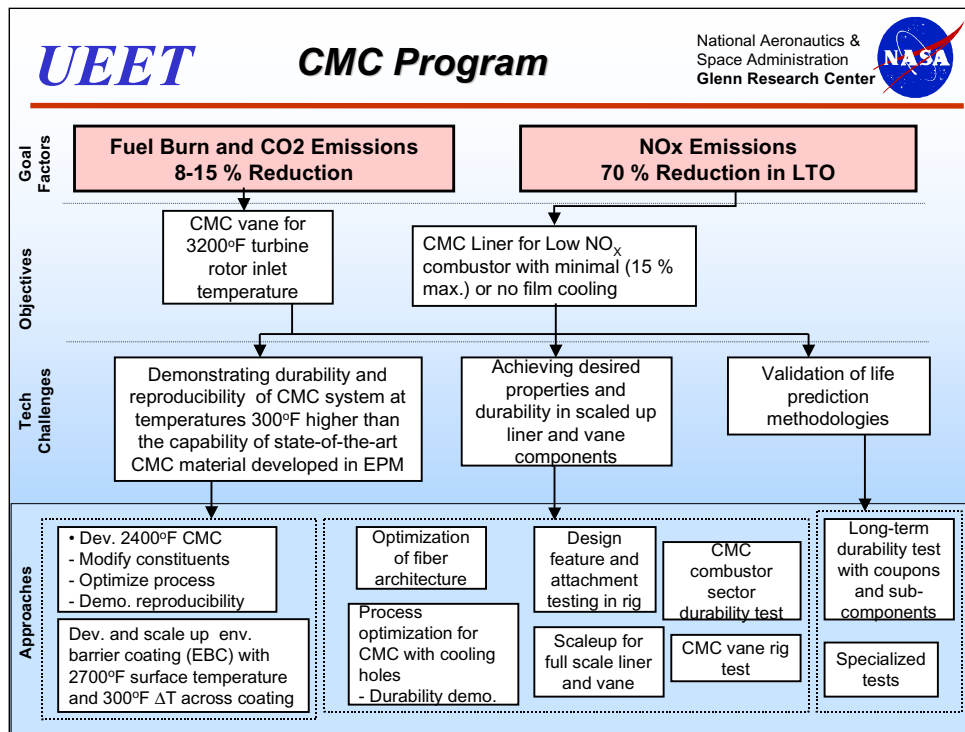
The genesis for the current Ceramic Matrix Composite (CMC) material program came from the Enabling Propulsion Materials (EPM) program, which was part of the High Speed Research (HSR) program. The EPM program came to conclusion at the end of FY99 with a CMC material system developed for a supersonic gas turbine combustor liner for the the High Speed Civil Transport. The material, developed under EPM was a silicon carbide fiber, silicon carbide matrix, SiC/SiC, composite manufactured by Honeywell Advanced Composites. The fiber, used to improve fracture toughness, was a near stoichiometric SiC. The operating goals for the liner material, under EPM, were 9,000 hours of operation at 2200°F at realistic liner thermal and mechanical stresses. Because the basic constituent of the composite, silicon carbide, reacts with combustion products at operating temperatures, and environmental barrier coating was developed to improve the surface recession resistance of the material system and increase the hot side temperature capability to 2300°F.



- Develop ceramic matrix composite (CMC) material system and process for low NO_x combustor liner and turbine vane
- Demonstrate properties in components
- Demonstrate durability of liner/vane sub-components in rig tests.
- Demonstrate 2400 °F CMC and 2700 °F environmental barrier coating (EBC) system for combustor liner and vane



- Achieve desired durability at 2400 °F in HSR-EPM developed SiC/SiC composite without developing a new fiber
- Develop environmental barrier coating with long-term stability for coating surface temperature of 2700 °F and ΔT of 300 °F across the coating
- Achieve properties in complex combustor and vane components



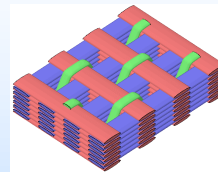
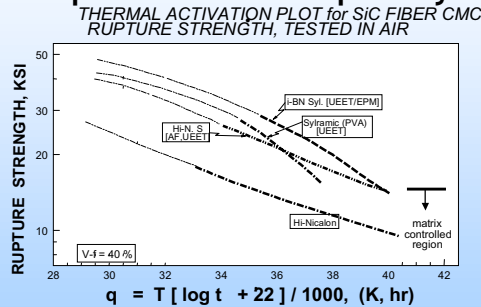
The UEET program will develop a 2700°F CMC system, which will consist of a 2400°F CMC material and an EBC with 2700°F surface temperature capability. A combined EBC/TBC coating system will be developed that can provide 300°F temperature gradient across the coating. The development of 2400°F CMC material will be closely coordinated with parallel IHPTET efforts. Process optimization and scaleup activities will be undertaken to demonstrate reproducibility of CMC properties in components. Long-term durability of liner subcomponents and components will be demonstrated in combustor sector tests. Advanced manufacturing processes will be developed to fabricate complex vanes. Fiber architecture and attachment/joining schemes will be developed for turbine vanes. Long-term durability of the vane system will be demonstrated in rig tests.

Micromechanics-based life prediction methodologies will be developed for CMC components and validated through laboratory and rig tests. Mechanical characterization in support of life prediction model development will include tensile, fatigue, creep, interlaminar, thermal gradient, and multi-axial benchmark tests. Specialized test methods will be developed as required. Life prediction models will be incorporated into design and analysis tools for component design.

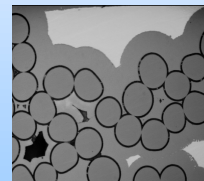


2400 F Material Development

Improve Material Capability



Optimize Fiber Architecture

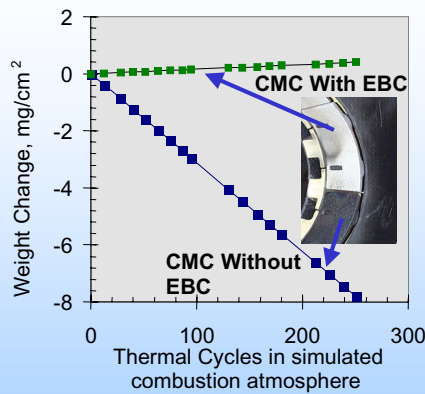


Improve Process Reproducibility

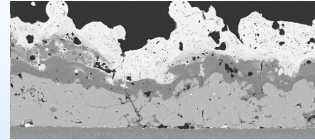
Fiscal Year



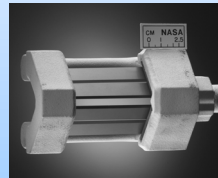
To meet the performance goals for advanced combustor liners and inlet turbine vanes in future military and civilian gas turbine engines, certain factors associated with the constituents of the SiC/SiC CMC system will require further optimization. These include optimized fiber architectures and improved materials and processes for the reinforcing SiC-based fiber, the BN-based interphase coating, and the melt-infiltrated SiC-based matrix. Under EPM and UEET-FY00, it was shown that there is a wide range of compositions, geometries, and processes for the constituents, and that microstructural optimization of these factors is quite complex due to many beneficial and adverse physical, chemical, and mechanical interactions that can occur between the constituents. This complexity is further enhanced on the macrostructural level where fiber architectures have to be optimized to yield maximum performance for each small volume element of complex-shaped CMC components.



Coating Improvements



New Compositions



Improve Environmental Resistance

High Pressure Burner Rig

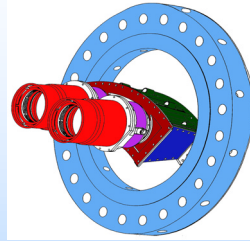
Fiscal Year



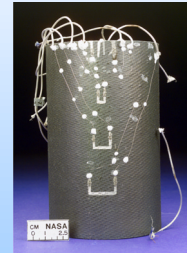
Key limitations of BSAS-based EPM EBC's are low upper temperature limit (~ 2550 °F) and rapid increase of thermal conductivity under thermal exposure. For thin (<10 mil) EBC's required for vane application, a very low thermal conductivity EBC is necessary to achieve the 300 °F ΔT goal while satisfying the thickness requirement. Very low thermal conductivity YSZ top coat is a promising approach. Other approaches include incorporation of nano particles or nano layers.



Thermal gradient Rig



Sector Rig 1000 hr durability

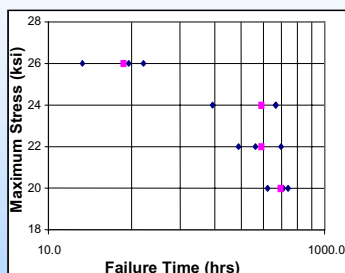


Instrumentation

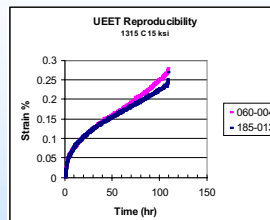


CMC component design features, such as improved component attachments and novel ply splice technology, will be evaluated via mechanical testing. Test capability for the lean transition zone combustor liners of the sector rig will be developed in the High Pressure Burner Rig. The combustion rig in NASA's test cell CE-9 will be used to evaluate a modified attachment for the SiC/SiC rich zone liners. Material Assessments will be conducted in the High Pressure Burner Rig to study the effects of temperature, pressure and complex gas chemistries on UEET developed CMCs and coatings. Coupon testing will be used to decouple effects of temperature, pressure, stress, and combustion environment on material behavior. Vanes concepts, including tubes, will also be tested. A combustor liner component, the lean transition section from the sector rig, will be adapted to the High Pressure Burner Rig.. The Thermal Gradient Rig facility will be used to simulate in-service combustor liner conditions by imposing pure thermal stress distributions in fiber reinforced silicon carbide cylinders. Studies will be performed on combustor liner material to assess the effects of thermal gradients as a function of composite fabrication and cylinder architecture.

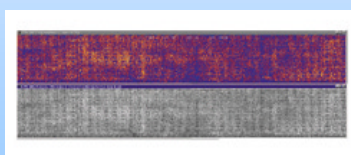
2200 F LCF for 9/99 Material



CMC Durability Data



Physical Property Plots



NDE

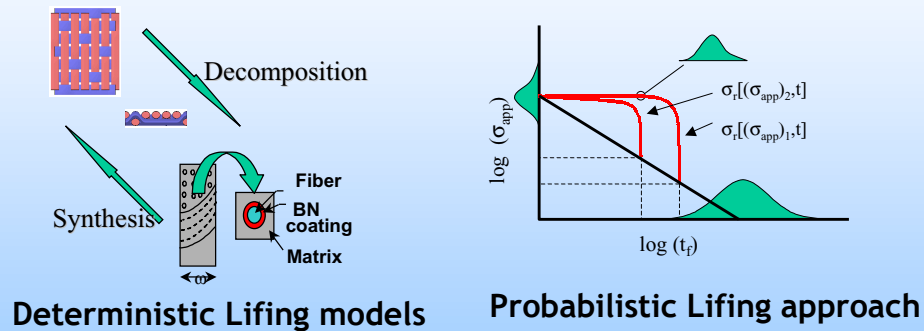
Fiscal Year



Commercial implementation of the melt infiltration ceramic matrix composite, as a 2400F aerospace material, requires a rigorous engineering assessment and statistical characterization of the physical properties, time dependent behavior, environmental durability, and high cycle fatigue response of the 01/01 material. Factors affecting the potential use of the material will be the reliability of this assessment which will quantitatively examine the material processing reproducibility, the fidelity of supporting experimental tests, and the experimental database size available to determine the realistic statistical variation of mechanical properties



Physics based Modeling Approaches



Micro-mechanics based CMC material behavior model development will begin by evaluating NASALIFE and PCGINA/CEMCAN developed under EPM as well as other in-house codes like GENOA. Constituent material degradation behavior due to temperature, stress, fatigue, creep, environment etc. will be addressed and incorporated in the micro-mechanics approach. Models permitting the computation of micro-stresses/strains in local regions will be developed for the Linear Elastic Regime first and subsequently be extended to cover the entire stress/strain regime. Overall stress/strain behavior of the CMC will be predicted and verified/validated with experimental data.

A Probabilistic Life Model will be formulated for multi-axial fatigue based on a three parameter Weibull distribution,. Experimental data will be used to calibrate the model first for uniaxial loading and then for multi-axial loading. The validated/verified multi-axial fatigue model for CMC's will be incorporated in a standalone code that can be utilized by designers/analysts



- **2400 °F CMC material**
- **2700 °F environmental barrier coating (EBC)**
- **1000 hr liner and vane durability rig demonstration**
- **Vane rig design feature test**
- **Validated physics based life prediction models**



- The UEET Program will provide the revolutionary technologies needed to enable future turbine engine propulsion systems for a wide variety of aerospace vehicles.
- Systems requirements studies done with the U.S. industry will provide key inputs to determining the long term direction for the program.
- The UEET Program content will be adjusted on a regular basis so as to pursue the highest payoff technology set.
- The UEET Program will partner wherever appropriate with NASA Base R&T Programs to transition technologies.
- The UEET Program will actively seek partners to carry the technologies to a TRL6 to enable timely transitions to future industry application specific designs.

OVERVIEW OF NASA STUDIES ON HIGH-TEMPERATURE CERAMIC FIBERS

James A. DiCarlo and Hee Mann Yun
National Aeronautics and Space Administration
Glenn Research Center
Cleveland, Ohio

INTRODUCTION

- NASA, DOD, and DOE are currently looking to the NASA UEET Program to develop ceramic matrix composites (CMC) for hot-section components in advanced power and propulsion systems
- Success will depend strongly on developing ceramic fibers with a variety of key thermostructural properties, in particular, high as-produced tensile strength and retention of a large fraction of this strength for long times under the anticipated CMC service conditions.
- Current UEET approach centers on selecting the optimum fiber type from commercially available fibers since the costs for development of advanced fibers are high and the markets for high-temperature CMC have yet to be established.

OBJECTIVE

Present a brief overview of NASA-UEET studies aimed at

- Developing a general property base for ceramic fibers
- Selecting fibers for high-temperature structural CMC.

OUTLINE

- Key fiber property requirements for CMC components
- Commercial fibers of current CMC interest
- NASA testing for fiber strength versus time, temperature, environment
- NASA modeling of fiber results for CMC applications
- Status of fiber selection for high-temperature CMC
- Environmental issues for SiC-based CMC and fibers
- Potential for SiC fibers as seal materials

KEY FIBER AND CMC PROPERTY REQUIREMENTS FOR HOT-SECTION COMPONENTS

- ***High Capability for Complex CMC Shapes:***
will typically require 2D/3D fiber weaving/braiding and thus implies Small-diameter (<20 μm), Continuous-Length fibers which in turn implies Fine-Grained Polycrystalline fibers.
- ***High CMC Strength Retention at all temperatures after matrix cracking in oxygen and moisture-containing environments:***
implies fibers with Oxide- and Silicon-based Compositions
- ***High CMC Ultimate Tensile Strength***
- ***High CMC Strength Retention under stress up to 2400°F***
- ***High CMC Transverse and Axial Thermal Conductivity***
- ***High CMC Creep Resistance up to 2400°F***

SMALL-DIAMETER COMMERCIAL FIBERS WITH OXIDE- AND SILICON-BASED COMPOSITIONS

(Diameters 10 to 15 μm ; Grain sizes ~3 to 500 nm)

FIBER TYPE	SOURCE	PROCESS	COMPOSITION
Oxide-based			
Nextel 610	3M	Sol Gel	Al_2O_3
Nextel 720	3M	Sol Gel	Al_2O_3 + Mullite
Silicon-based			
Nicalon	Nippon Carbon	Polymer/Pyrolysis	SiC + Si-O-C
Hi-Nicalon	Nippon Carbon	P/P (radiation cure)	SiC + C
Hi-Nicalon S	Nippon Carbon	P/P (radiation cure)	SiC + trace C
Sylramic	Dow Corning	P/P (sinter)	SiC +trace (B+ Ti)
Tyranno SA	UBE	P/P (sinter)	SiC +trace Al_2O_3

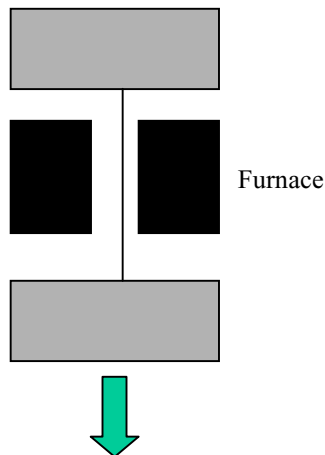
TESTS TO EVALUATE FIBER STRENGTH RETENTION DURING SIMULATED CMC SERVICE

Typical Test Variables:

stress, stress rate,
temperature (20 to 1400°C) , temperature warm-up rate,
gauge length (~25 to 100 mm), environment (air or argon)

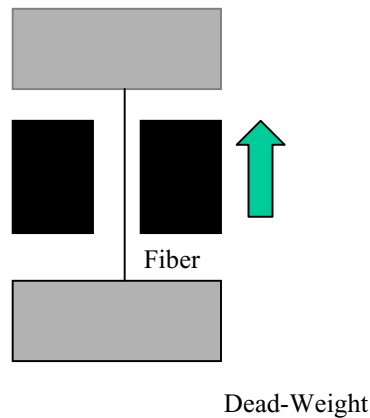
Typical Mechanical Tests

Fast-Fracture



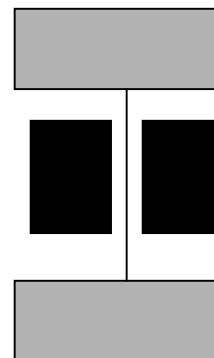
Stress Rate = Constant
Temperature = Constant
Measure Fracture Stress

Slow Warm-up



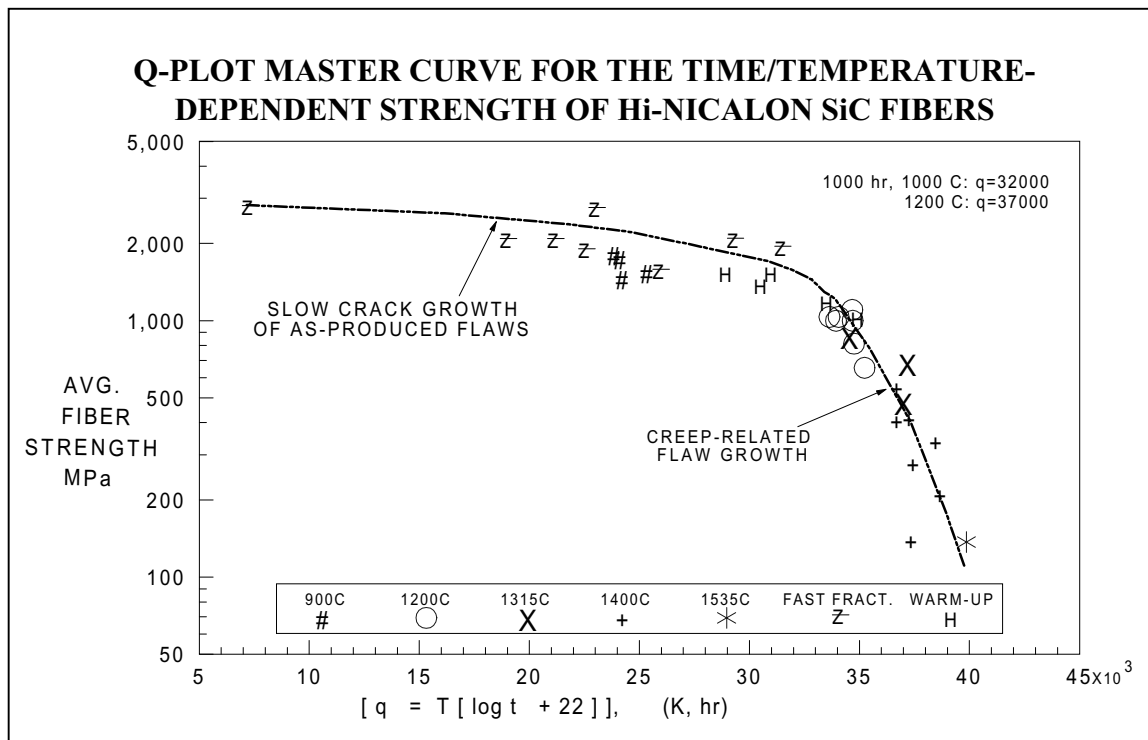
Stress = constant
Temperature Rate = Constant
Measure Fracture Temperature

Stress-Rupture



Stress = constant
Temperature = Constant
Measure Creep,
Fracture Time

At NASA Glenn, the strength properties of a variety of oxide and SiC-based fibers have been measured from 20 to 1400°C under air and argon environmental conditions [1-7]. Air was used to simulate fiber exposure to oxidizing conditions, such as for cracked CMC in combustion environments; while argon simulated the inert conditions for fibers in an uncracked CMC. The measurements were made on single fibers across a time range from ~0.01 to over 100 hours using three types of tests: fast-fracture (constant temperature and constant rate of stress change), slow warm-up (constant stress, constant rate of temperature change), and stress rupture (constant stress and constant temperature).

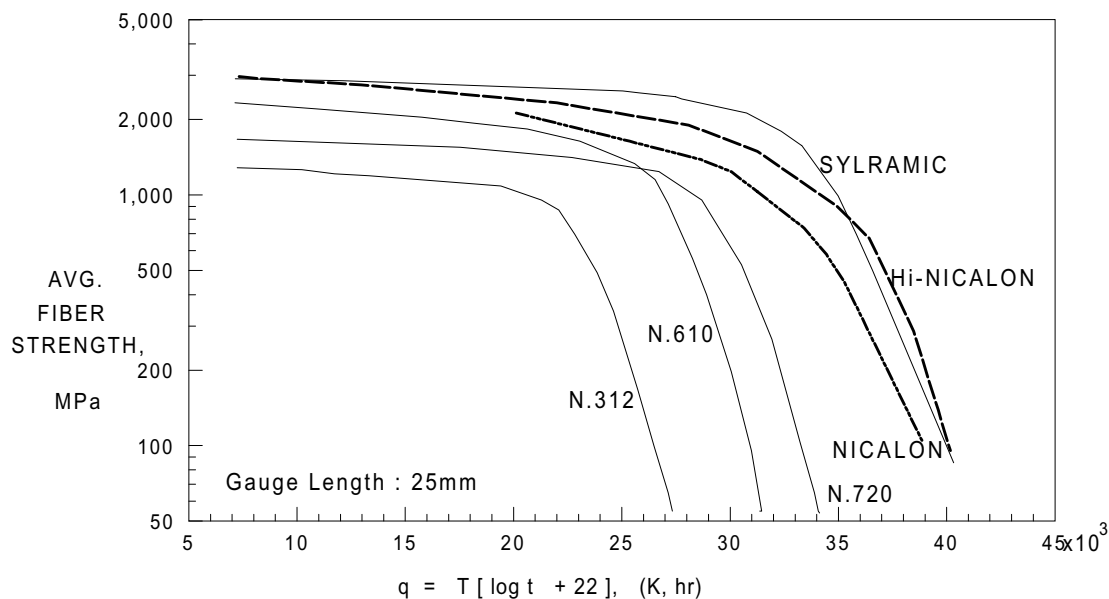


Using simple thermal-activation theory [5, 8], it was determined the single-fiber strength results from the three tests for each fiber type could be combined into a single master curve or q-plot which describes the applied stress at fracture (fiber strength) versus the time-temperature dependent parameter q given by

$$q \equiv Q / 2.3R = T (\log t + 22) .$$

Here Q is the effective activation energy for time-dependent fiber fracture, R is the universal gas constant (8.314 J/mol-K), and T (kelvin) is the absolute temperature at fiber fracture. For the stress-rupture tests, t (hours) is the fiber rupture time. By applying slow crack growth theory for the time conditions of the other tests [5], $q = 18.3 T$ for the fast-fracture tests and $q = 20.2 T$ for the slow warm-up tests.

Q-PLOT MASTER CURVES FOR THE TIME/TEMPERATURE-DEPENDENT STRENGTH OF OXIDE AND SiC-BASED FIBERS



The q-plots, shown here and the previous slide, for ceramic fiber tensile strength versus time and temperature have many important basic and practical implications. First, on the basic level, all curves have the same shape with increasing q ; that is, an initial section with a small negative slope (Region I), and a remaining section with a much larger negative slope (Region II). This behavior is typical of the rupture of monolithic ceramics in which at low temperatures, as-produced flaws grow slowly in size (slow crack growth); whereas at high temperatures, creep mechanisms aid in the more rapid growth of the same flaws or in the nucleation and growth of new micro-cracks and cavities.

On the practical side, the q- plots indicate that fiber strength values throughout Region I depend directly on the fiber's as-fabricated strength at room temperature ($q \approx 7000$). That is, the entire Region I section moves up in strength when as-produced flaws are reduced in size or frequency. Alternatively, the Region I curves would move up or down if the test gauge lengths were smaller or greater, respectively, than the ~25 mm length used to generate the curves. In addition, the q-plots clearly indicate the greater thermostructural capability of the SiC fibers over the oxide-based fibers both in Regions I and II. The Region I advantage is related to the higher fracture toughness of SiC; while the Region II advantage is primarily due to slower diffusion processes in the SiC-based fibers. Finally, the curves allow the prediction of fiber strength behavior if any four of the following five application variables are known: stress, stress rate, temperature, temperature rate, and time [5].

APPLICATION OF CERAMIC FIBER q-PLOTS FOR MODELING MAXIMUM CMC STRENGTH

- Assume a **cracked** CMC under constant uniaxial stress σ_c at a constant temperature T in an air environment. If V_f^* is the effective fiber volume fraction bridging the through-thickness cracks in the stress direction, CMC strength can be predicted from:

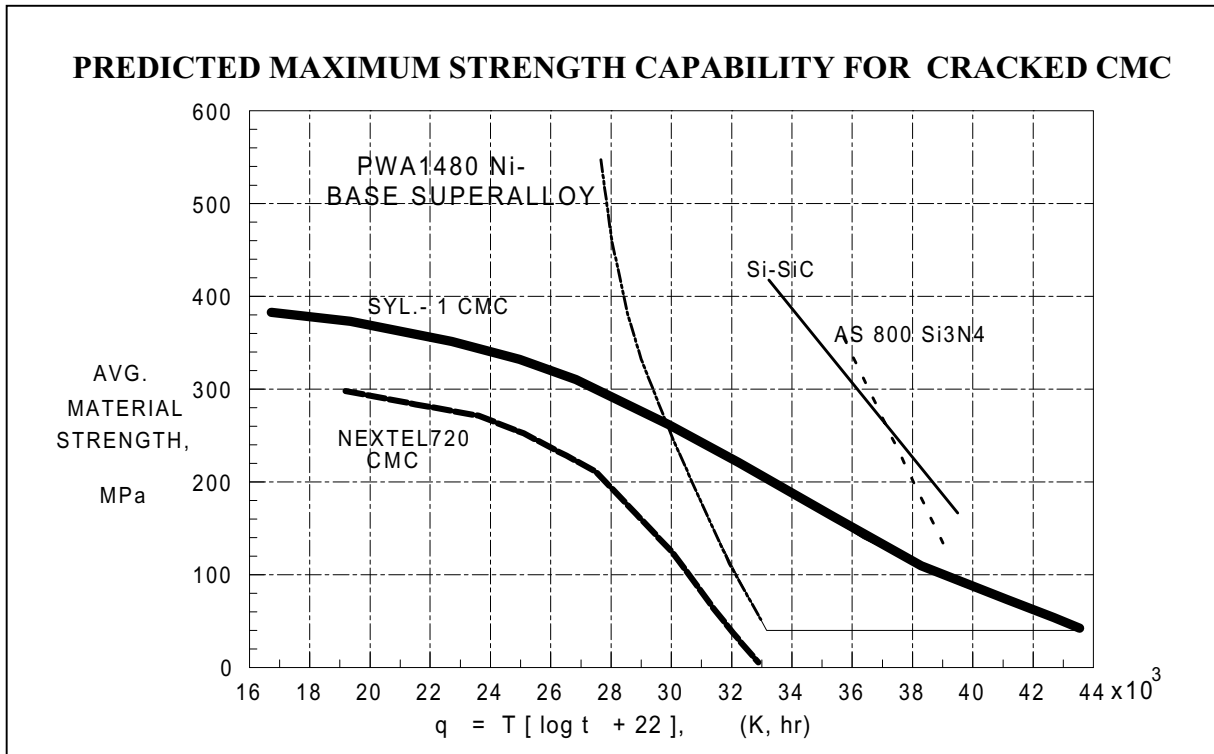
$$\sigma_c = V_f^* \sigma_B(t, T, L_e)$$

Here σ_B is the average strength of the fiber bundles within the cracks, and L_e is the effective bundle gauge length within the cracks.

- When interfacial conditions and bundle fracture statistics are taken into account, a good approximation for $\sigma_B(L_e)$ is the average strength of individual fibers measured at ~25 mm gauge length; so that

$$\sigma_c \approx V_f^* \sigma_f(q, 25 \text{ mm})$$

One very important CMC application condition is that in which the composite contains through-thickness matrix cracks that are bridged by the fiber reinforcement. These cracks could have developed during CMC fabrication due to a thermal expansion mismatch between the fibers and matrix, or during CMC service due to some random overstress or the need for a high design stress. For a simple CMC strength model, one might assume that the application requires the cracked CMC to experience a relatively constant uniaxial stress σ_c at a constant temperature T in an air environment. Then as described above, one can use the fiber q-plots, $\sigma_f(q, 25 \text{ mm})$, and the effective fiber volume fraction V_f^* within a cracked CMC to predict its maximum tensile strength capability as a function of application time and temperature. A variety of recent CMC studies have confirmed the validity of this modeling approach for cracked CMC under simple test conditions [9].



An important advantage of CMC strength modeling using fiber q-plots is that it gives insight into how CMC will perform at high temperatures in comparison to competing structural materials. For example, the above slide displays maximum strength behavior predicted for cracked CMC reinforced by Nextel 720 and Sylramic(1) fibers, the most creep and rupture resistant oxide- and SiC-based fibers examined to date at NASA. For this slide, 0/90 woven composites were assumed with a typical total volume fraction of 40% so that $V_f^* = 20\%$. Also shown are the measured strength behavior for one of the highest-temperature nickel-based superalloys currently available and for SiC and Si₃N₄ monolithic ceramics. It can be seen that the CMC with the best oxide-based fiber barely competes with the superalloy in the creep-rupture regime; whereas the CMC with the SiC-based fiber has the potential for much better thermostructural performance than both materials (hatched area). On the other hand, the SiC-reinforced CMC does not outperform the Si-based monolithics, which follows simply from a reduced volume fraction (i.e., 20 versus 100%). However, in contrast to CMC, the monolithics suffer from catastrophic failure upon local material fracture and also cannot be reliably fabricated into large and complex-shaped components.

**KEY PROPERTIES OF NEAR-STOICHIOMETRIC SiC FIBERS FOR
HIGH-TEMPERATURE CMC APPLICATIONS**

Trade Name	Hi-Nicalon S	Tyranno SA (1,2,3)	Sylramic	Sylramic (1,2)
Max. Process Temperature	~ 1600°C	> 1700°C	> 1700°C	> 1700°C
Average Diam., μm	13	8-10	10	10
Second Phases	trace O + C	trace Al ₂ O ₃	trace B + Ti	Reduced B, trace Ti
Average Grain Size, nm	< 100	≥ 150	~ 100	> 100
Avg. Surface Roughness, nm	< 10	~ 10	~ 10	~ 27
Thermal Cond. W/m ² .°C at R.T	18	65	46	> 46

Given the goals of the UEET Program to develop CMC hot-section components with as high a thermostructural capability as possible, the results of the fiber testing and modeling studies have clearly pointed to the use of SiC fibers in general and pure stoichiometric SiC fibers ($C/Si = 1$) in particular. This is based primarily on observations that impurities such as oxides degrade SiC fiber creep resistance and result in fiber strength degradation upon their decomposition and reaction with SiC at high temperatures; while excess carbon in the SiC fiber can reduce its oxidation resistance and thermal conductivity. Thus current UEET focus is centered on down-selection from the commercial near-stoichiometric SiC fibers listed in the above slide. As indicated in Slide 2, these fibers are produced by three different manufacturers primarily from the pyrolysis and sintering of polymer-derived precursor fibers. As shown in the above slide, the polymer, pyrolysis, and sintering routes are different enough to affect the impurity content and grain size within the final fiber microstructures. These two factors are critical to high-temperature fiber performance because they significantly affect fiber strength retention, creep resistance, and thermal conductivity [6]. Generally the best structural and conductivity performance is obtained for high purity SiC fibers with grain sizes between 100 and 500 nm. At the present time, in lieu of complete property data from SiC/SiC composites, the Sylramic(1) fiber with reduced boron is displaying the best combination of desirable properties. This fiber type was developed at NASA Glenn by treating the commercial Sylramic fiber in such a manner so as to reduce the creep-prone boron sintering aid in the fiber grain boundaries, while at the same time forming an in-situ boron nitride layer on the fiber surface [7]. As explained on the next slide, approaches such as these will be required to achieve and maintain the high thermostructural performance available in the stoichiometric SiC fibers, particularly in oxidizing environments.

POTENTIAL STRENGTH DEGRADING MECHANISMS FOR SiC/SiC CMC AND SiC FIBERS IN COMBUSTION ENVIRONMENTS

- Above ~2000°F, silica rapidly forms on SiC surfaces, which then vaporizes due to moisture-induced volatilization of silicon hydroxides. The SiC surface recesses and the material loses cross-sectional area and load-bearing capability [10].

Current solution: Oxide environmental barrier coatings (EBC) such as aluminum silicates, which minimize silicon exposure and reactivity with combustion environments.

- From ~1000 to 2000°F, oxygen penetrates into CMC through matrix cracks, which then attacks the fiber interfacial coating and forms thin silica layers on internal SiC fiber surfaces. Silica bonds the fibers to the matrix and to each other, so that when the matrix or one weak fiber in a tow breaks, neighboring fibers fracture at low stress.

Current solution: Interfacial coatings such as silicon-doped BN, which rapidly form oxide glasses that inhibit oxygen penetration away from the matrix cracks.

POTENTIAL FOR SiC FIBER TOWS AS SEAL MATERIALS

Key Benefits in Relation to Oxide-based Fibers:

- Intrinsic strength and elasticity retention to above 2000°F

Key Performance Issues:

- Above ~1000°F, silica formation on fiber surfaces and fiber-fiber bonding, resulting in loss of tow flexibility and strength
- Above ~2000°F, surface recession and dimensional reduction in moisture-containing combustion environments

Possible Solutions:

Protective fiber coatings (deposited or in-situ formed) that are high-temperature oxides or convert to high-temperature oxides which

- display low surface diffusion and intrinsic bonding and/or
- slowly ablate in combustion environments

References

1. DiCarlo, J.A., "Property Goals and Test Methods for High Temperature Ceramic Fibre Reinforcement", *Ceramics International*, Vol. **23**, 1997, pp. 283-289.
2. Yun, H.M., Goldsby, J.C., and DiCarlo, J.A., "Tensile Creep and Stress-Rupture Behavior of Polymer Derived SiC Fibers", *Ceramic Transactions*, Vol. 46, 1994, pp. 17-28.
3. DiCarlo, J.A., Yun, H.M., and Goldsby, J.C., "Creep and Rupture Behavior of Advanced SiC Fibers", *Proceedings of ICCM-10*, 1995, Vol. VI: Microstructure, Degradation, and Design, Poursartip, A. and Street, K.N., Eds, pp. 315-322.
4. Yun, H.M., Goldsby, J.C., and DiCarlo, J.A., "Environmental Effects on Creep and Stress-Rupture Properties of Advanced SiC Fibers", *Proceedings For HTCMC-2, II*, Evans, A.G. and Naslain, R., Eds., *Ceramic Transactions*, Vol. 57, 1995, pp. 331-336.
5. Yun, H.M. and DiCarlo, J.A., "Time/Temperature Dependent Tensile Strength of SiC and Al₂O₃-Based Fibers", *Ceramic Transactions*, Vol. 74, 1996, pp. 17-26.
6. DiCarlo, J.A. and Yun, H.M., "Microstructural Factors Affecting Creep-Rupture Failure of Ceramic Fibers", *Ceramic Transactions*, Vol. 99, 1998, pp. 119-134.
7. Yun, H.M. and DiCarlo, J.A., "Comparison of the Tensile, Creep, and Rupture Strength Properties of Stoichiometric SiC Fibers", NASA/TM – 1999-209284.
8. DiCarlo, J.A., Yun, H.M., and Morscher, G.N., "Models for the Thermostructural Properties of SiC Fibers", *Proceedings for HTCMC-2*, Ceramic Transactions **57**, 1995, pp. 343-348.
9. DiCarlo, J.A. and Yun, H.M., "Factors Controlling Stress-Rupture of Fiber-Reinforced Ceramic Composites", *Proceedings of ICCM-12*, Paris, France, 1999.
10. Smialek, J.L., Robinson, R.C., Opila, E.J., Fox, D.S., and Jacobson, N.S., "SiC and Si₃N₄ Recession Due to SiO₂ Scale Volatility under Combustor Conditions", *Adv. Composite Mater.*, Vol. 8, No. 1, 1999, pp. 33-45.

HIGH TEMPERATURE CERAMIC FIBER DEVELOPMENT AND TRENDS

David Wilson
3M
St. Paul, Minnesota

High Temperature Ceramic Fiber Development and Trends

David Wilson

**3M Specialty Fibers & Composites Department
St. Paul, MN**

3M

Introduction

Nextel™ industrial fibers (Nextel 312, 440, 550)

- based on Al_2O_3 - SiO_2 - B_2O_3 system
- textiles for flame barrier/thermal insulation

Nextel™ composite fibers (Nextel 610, 650, 720)

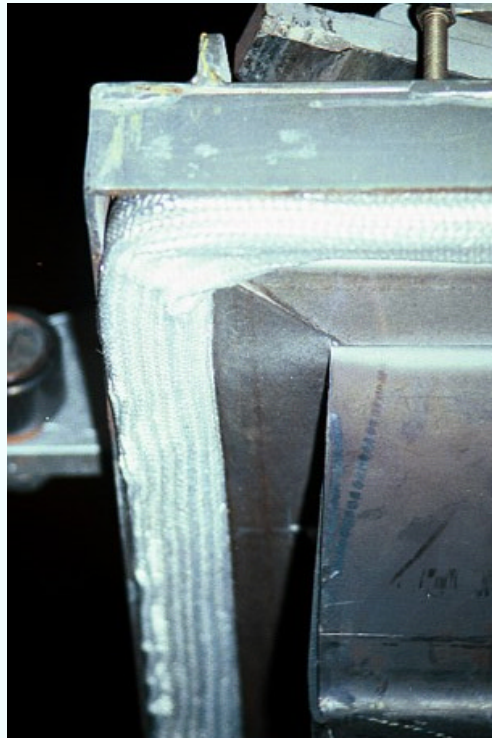
- based on α - Al_2O_3
- improved stability, high temperature properties
- composite reinforcement

New high temperature fibers

- YAG
- advanced mullite



Nextel™ Furnace Door Seals



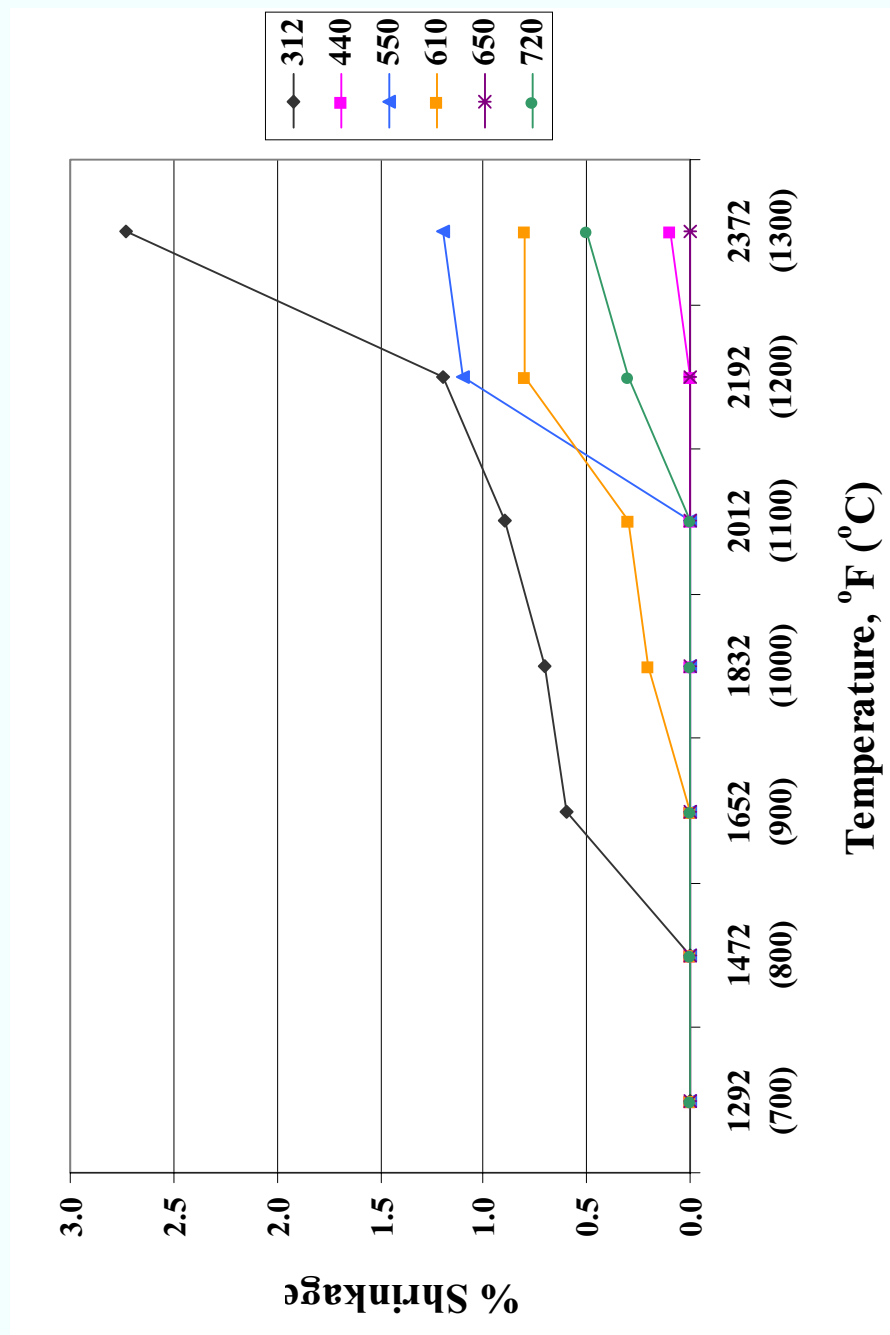
3M

Nextel™ Industrial Fibers

Property		Nextel™ 312	Nextel™ 440	Nextel™ 550
Chemical Composition	wt. %	62 Al ₂ O ₃ 24 SiO ₂ 14 B ₂ O ₃	70 Al ₂ O ₃ 28 SiO ₂ 2 B ₂ O ₃	73 Al ₂ O ₃ 27 SiO ₂
Crystal Phase		9Al ₂ O ₃ ·2B ₂ O ₃ + Amorph.	γ-Al ₂ O ₃ + Amorph. SiO ₂	γ-Al ₂ O ₃ + Amorph. SiO ₂
Tensile Strength (25.4 mm gauge)	MPa (Ksi)	1700 (250)	2000 (300)	2000 (300)
Elastic Modulus	GPa (Msi)	150 (22)	190 (28)	193 (28)
Density	g/cc	2.7	3.05	3.03
Roving Denier: Filament Count		600: 420 900: 420 1800: 780	700: 420 1000: 420 2000: 780	700: 420 1000: 420 2000: 780
Thermal Expansion (100-1100°C)	ppm/°C	3 (25-500°C)	5.3	5.3

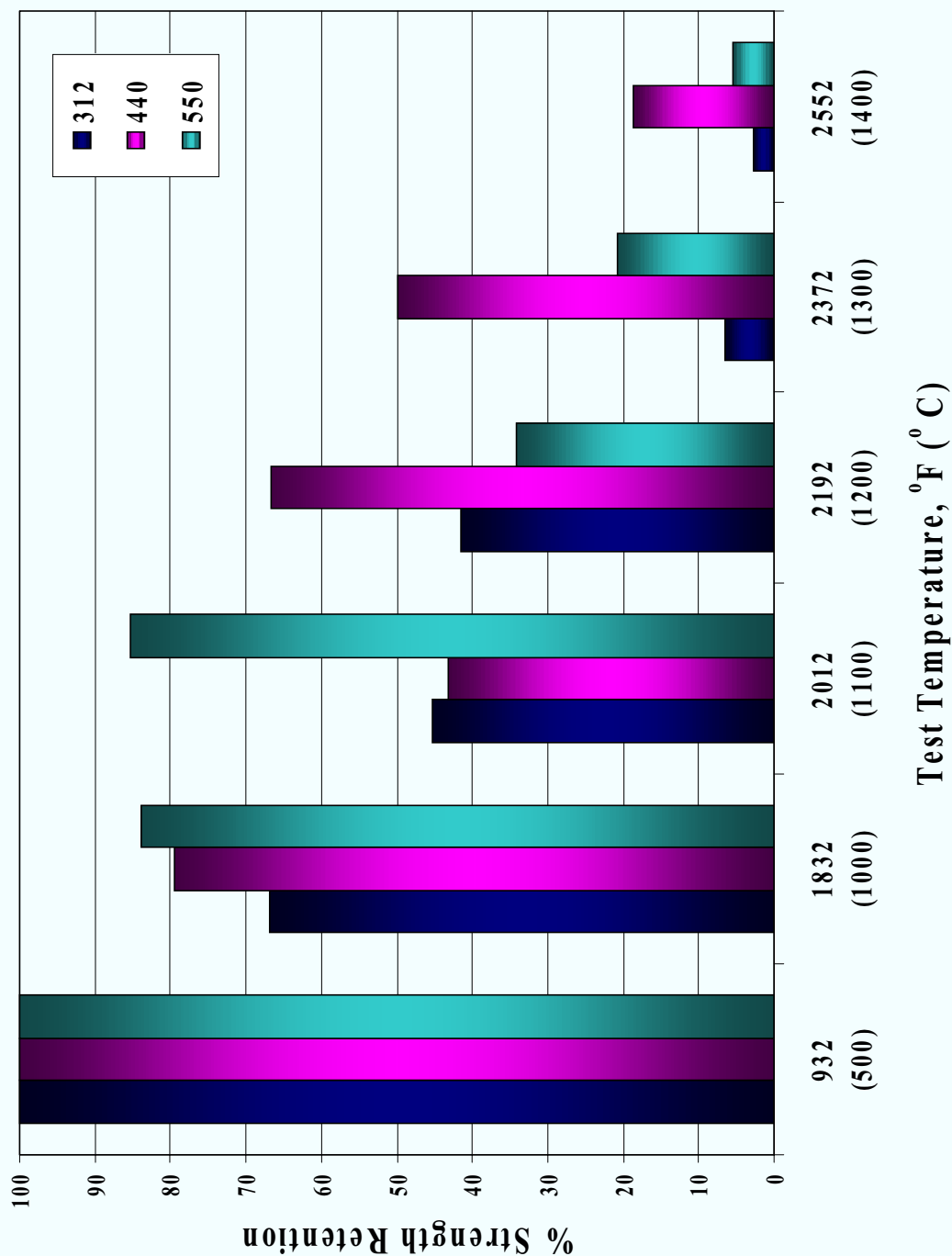
3M

Nextel™ Shrinkage vs. Temperature



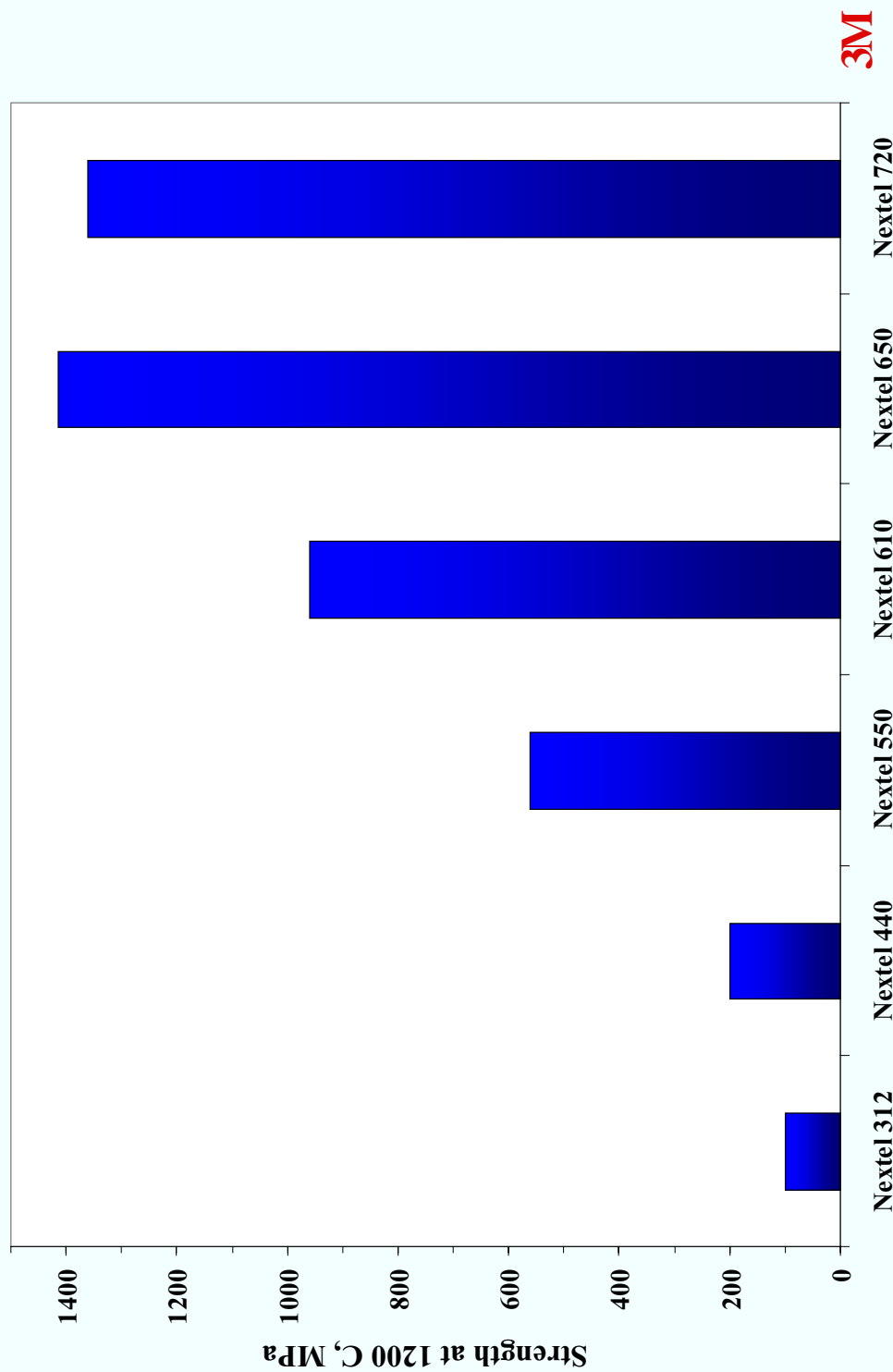
3M

Nextel™ Industrial Rovings: Strength Retention after 100hr thermal aging



3M

High Temperature Strength of Nextel™ Fibers is Increasing

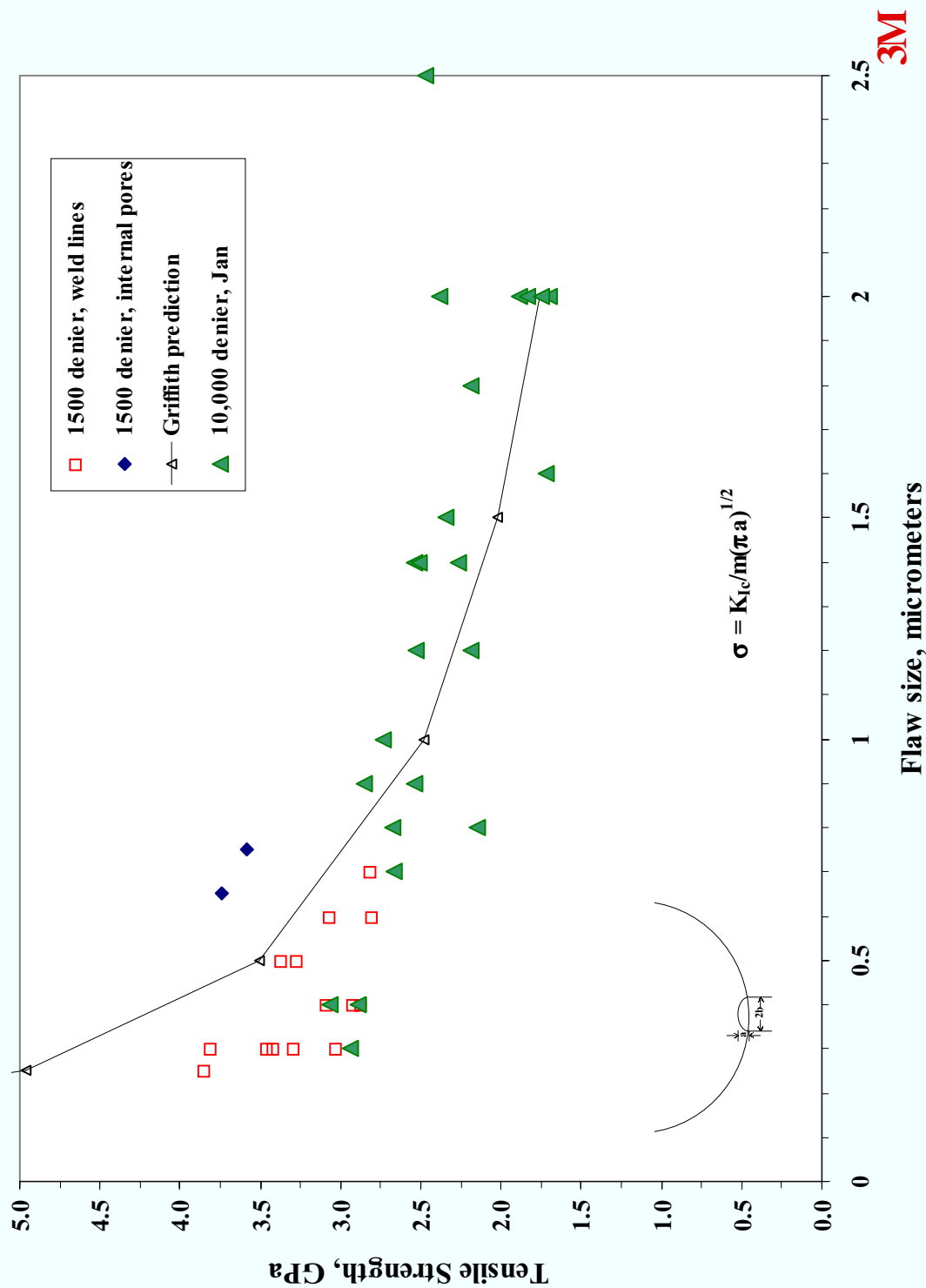


Nextel™ Composite Fibers

Property		Nextel™ 610	Nextel™ 650	Nextel™ 720
Chemical Composition	wt. %	>99 Al ₂ O ₃	89 Al ₂ O ₃ 10 ZrO ₂ 1 Y ₂ O ₃	85 Al ₂ O ₃ 15 SiO ₂
Crystal Phases		α-Al ₂ O ₃	α-Al ₂ O ₃ + cubic ZrO ₂	α-Al ₂ O ₃ + mullite
Tensile Strength (25.4 mm gauge)	GPa (Ksi)	3.3 (470)	2.5 (360)	2.1 (300)
Tensile Modulus	GPa (Msi)	373 (55)	358 (52)	260 (38)
Density	g/cc	3.9	4.1	3.4
Thermal Expansion (100-1100°C)	ppm/ °C	7.9	8.0	6.0
Max Use Temperature (1% strain/ 69 MPa/1000 hr)	°C	1000°C	1080°C	1150°C
Roving Denier: Filament Count		1500: 420 3000: 780 10000: 2600	3000: 780	1500: 420 3000: 780

3M

The strength of Nextel 610 fiber is inversely proportional to flaw size

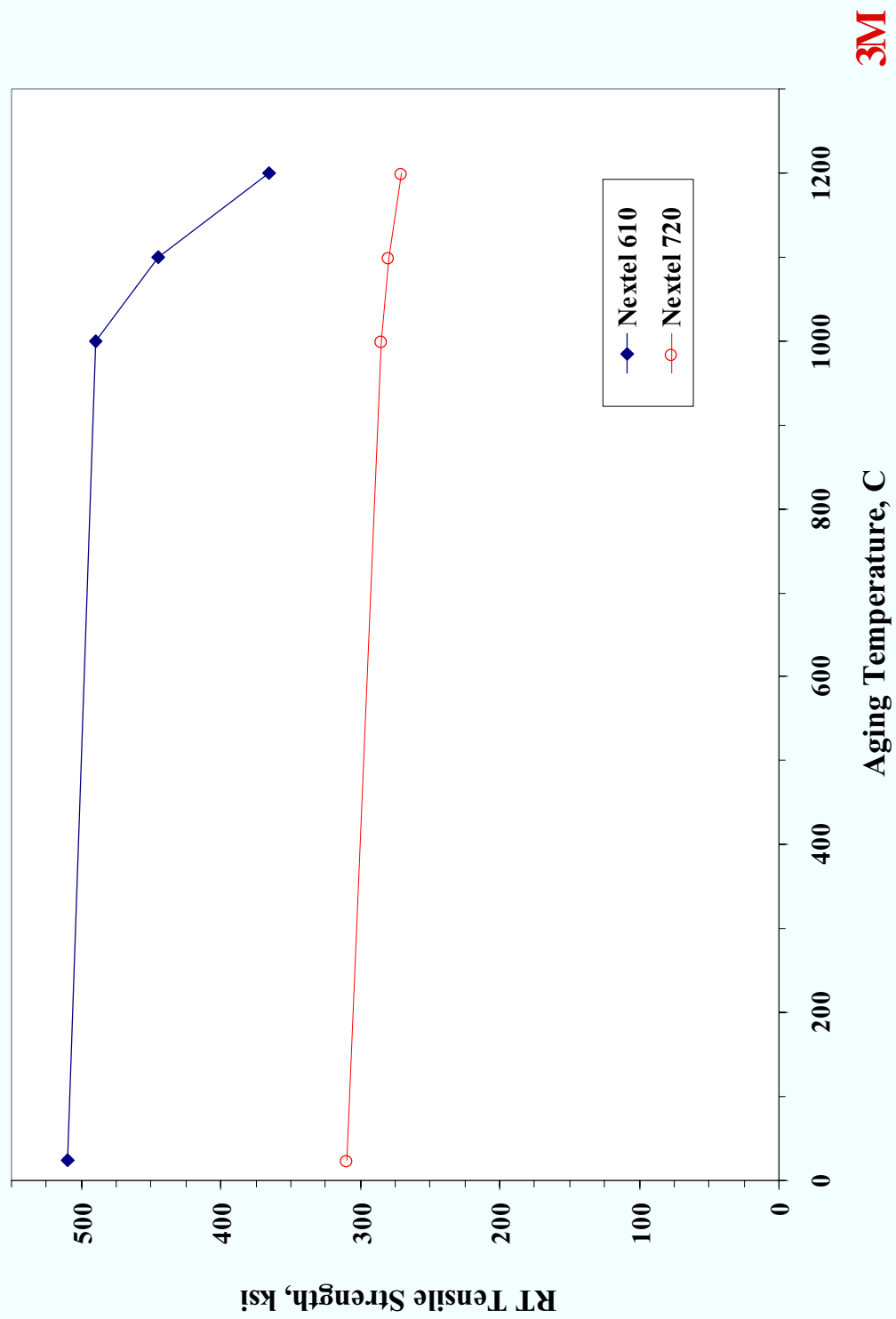


Nextel 720 fiber was developed for high temperature composite reinforcement

- 85% Al_2O_3 - 15% SiO_2 composition intermediate between alumina and alumina-silica fibers
- Interpenetrating α - Al_2O_3 -mullite microstructure reduce grain growth, degradation at high temperature
- Large ($0.5\text{ }\mu\text{m}$) grains of mullite provide excellent creep resistance and hot strength
- Lower thermal expansion, modulus reduce thermal stresses

3M

**Nextel™ composite fibers retain
good strength after 1000 hrs at 1200°C**



3M

Summary of Nextel fiber attributes

Nextel™ 312:	Lowest cost, best textile properties
Nextel™ 440:	Good strength retention > 1200°C, good textile properties
Nextel™ 550:	Better chemical resistance, good strength to 1100 °C
Nextel™ 610:	Highest strength, high modulus, excellent chemical stability
Nextel™ 650:	High strength, better creep resistance, less shrinkage
Nextel™ 720:	Best creep resistance, high temperature strength retention

3M

Summary

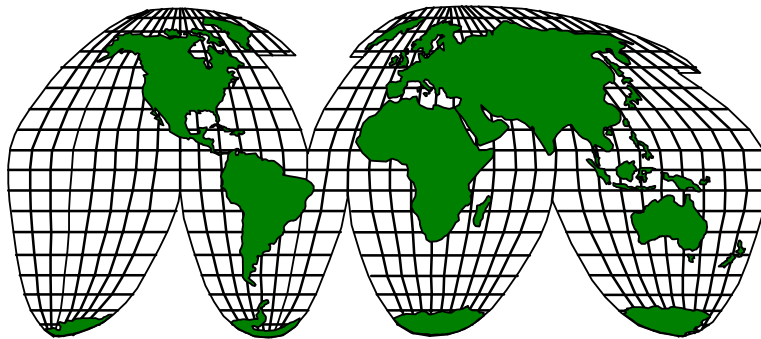
- **Family of Nextel fibers available for both industrial and composite applications**
- **Composite fibers represent new opportunities in high temperature capability**
- **Opportunities exist for further improvements in fiber temperature performance**
 - Nextel 650 fiber was recently developed for applications at 1100°C in corrosive environments
 - YAG fibers under development



AN INTRODUCTION TO TRIZ

Dana W. Clarke, Sr.
Ideation International Inc.
25505 West 12 Mile Road
Suite 5500
Southfield, Michigan 48034
Ph: 248-353-1313
Fax: 248-353-5495
www.ideationtriz.com

An Introduction to TRIZ



**A Different Point of View:
Systematic and Structured Innovation for Everyone**



Solving Problems with Mathematics

Why can we all do math – add, subtract,
multiply, divide and more?

Was this always possible for all people?
Why is it possible for all people today?





Mathematics

A Science

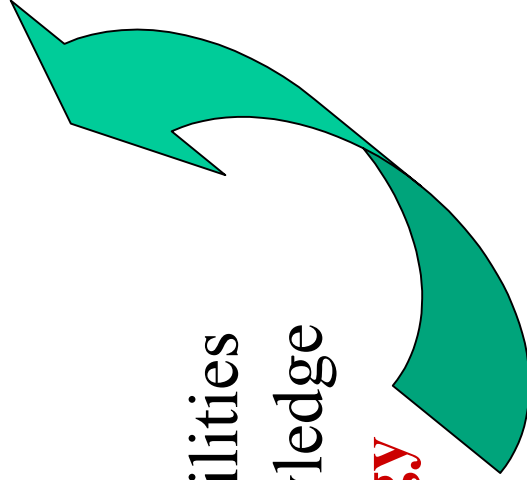
Calculators & Computers

Theoretical Foundation,

Algorithms,

Operators, etc.

$$\text{Results} = P_c \times P_{kn} \times (1+M) \times (1+T)$$



P_c = Personal Capabilities

P_{kn} = Personal Knowledge

M= Methodology

T = Tools



What about Creative Problem Solving and Innovation?

Who was your teacher?

What courses did you take?

What are your structured methods and tools?

Step-by-step how do you invent / innovate?



What is TRIZ?

- Russian acronym for the **Theory of Inventive Problem Solving**
- Systematic, structured way of thinking
- Science
- Results of over 50 years of research analyzing over 2 million worldwide patents within **all engineering disciplines**



Why TRIZ was Created

- To be a systematic step-by-step procedure
- To guide an inventor through the solution space and to direct him or her to the area with the best (ideal) solutions
- To provide an inventor with reliable and repeatable results that do not depend on personal (psychological) issues
- To prove knowledge (patent information) can be accessed
- To verify that accumulation of human innovation experience is possible

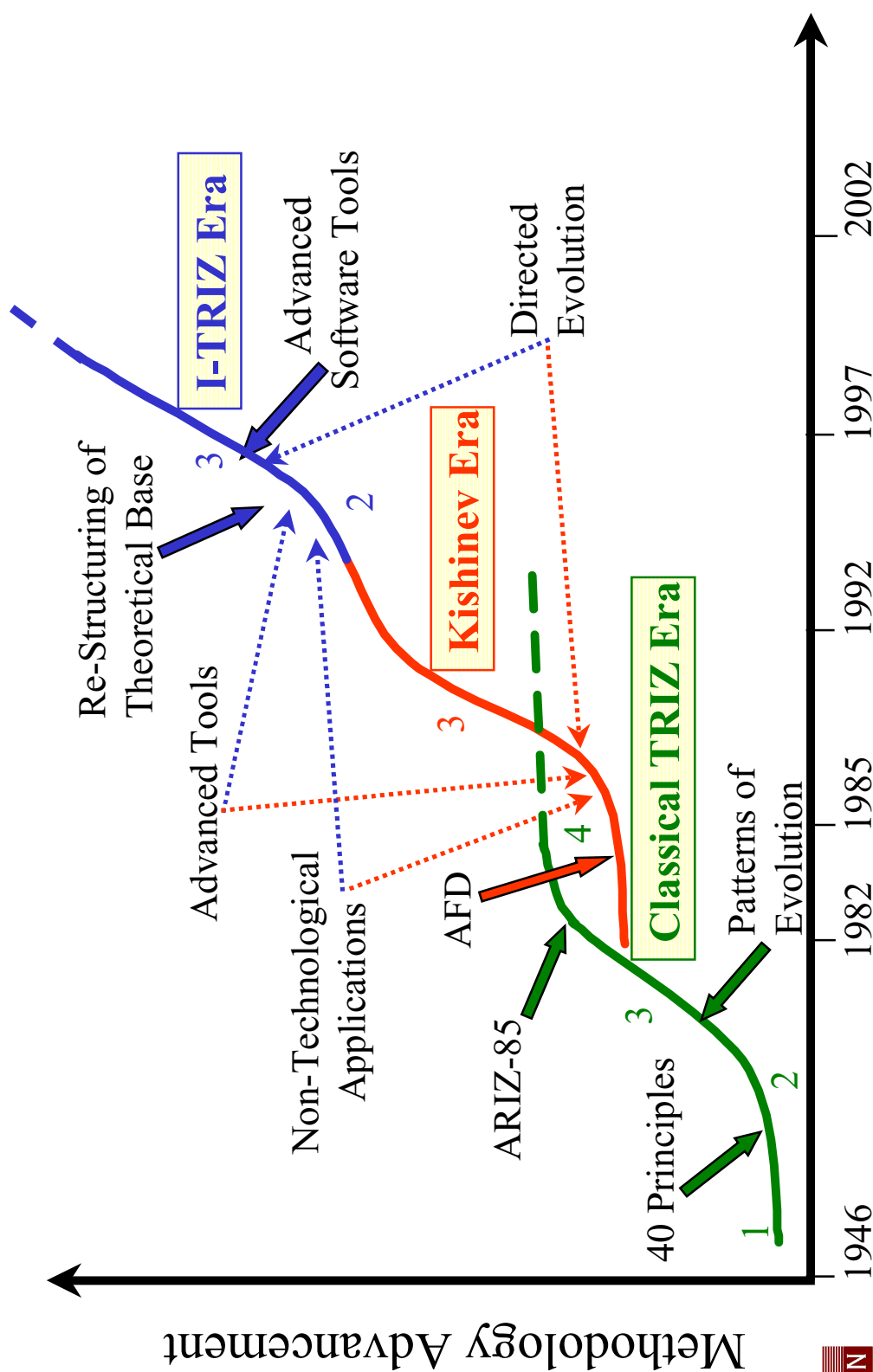


What is I-TRIZ?

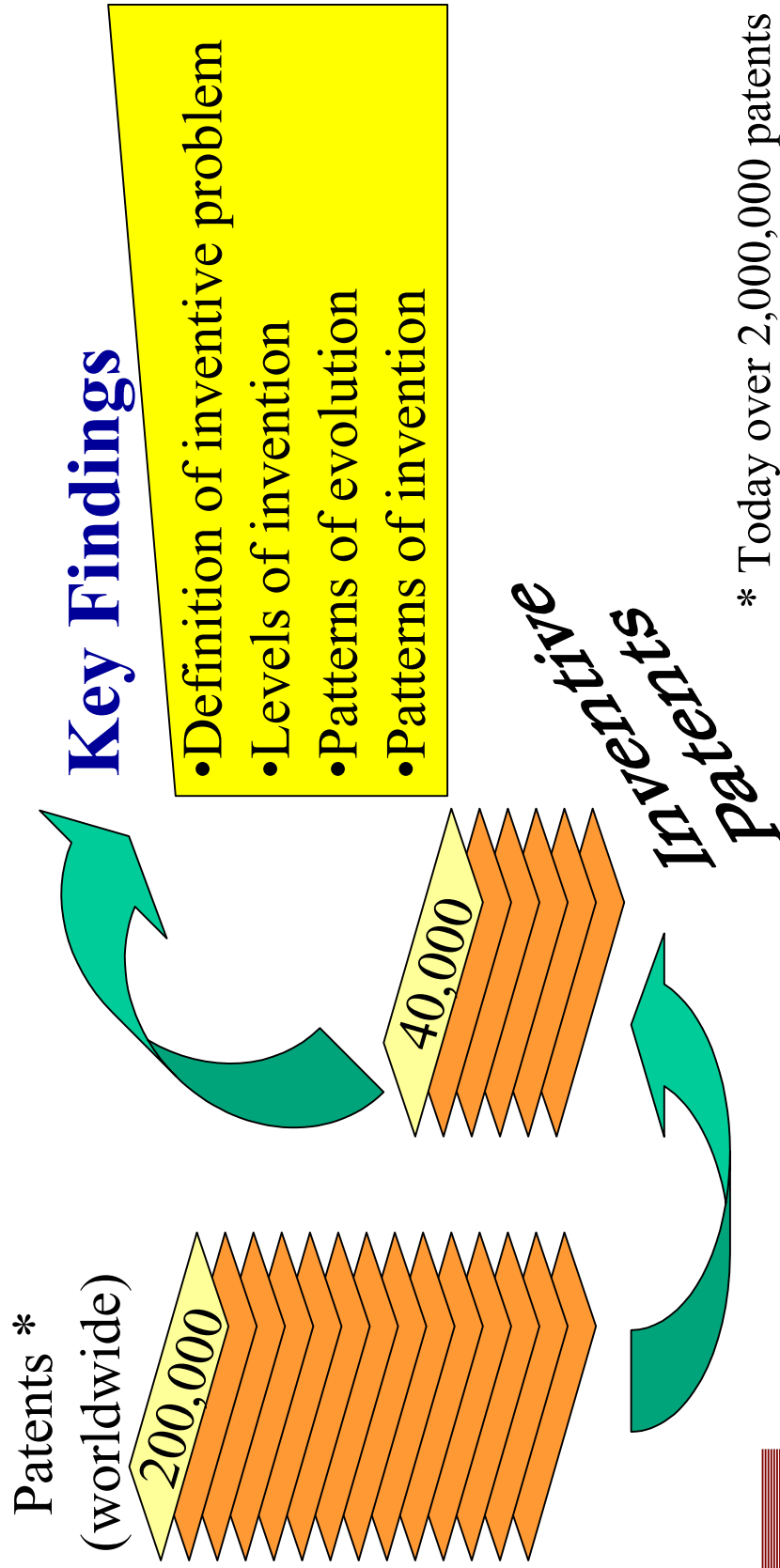
“Practical Application” of the Theory of Inventive Problem Solving



Evolution of TRIZ To I-TRIZ



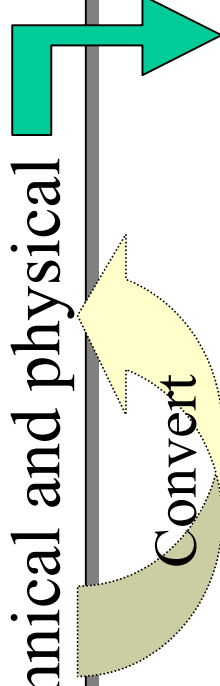
TRIZ's Foundation is Based on Technology Rather than Psychology



What is an Inventive Problem?

- Involves one or more contradictions
- Suggests no known ways or means of solution

There are two types of contradictions:
technical and physical



Apply 4 principles

- Separation in time
- Separation in space
- Separation between the parts & the whole
- Separation upon conditions



Levels of Solution

- **Level 1: Apparent solution (no invention)**
 - Established solutions; well-known and readily accessible
- **Level 2: Improvement**
 - Small improvements of an existing system, usually with compromise
 - Bifocal glasses, beeper
- **Level 3: Invention inside the paradigm**
 - Essential improvement of an existing system
 - Automatic transmission, radio telephone
- **Level 4: Invention outside the paradigm**
 - A concept for a new generation of an existing system, based on changing the principle by which the primary function is performed
 - Jet aircraft, integrated circuit
- **Level 5: Discovery**
 - Pioneering of an essentially new system
 - Laser, radio, airplane



Patterns of Invention

- Altshuller recognized that the same fundamental problem (contradiction) had been addressed by a number of inventions in different areas of technology
- He also observed that the same fundamental solutions were used over and over again, often separated by many years
- He reasoned that if the latter inventor had had knowledge of the earlier solution, their task would have been straightforward
- He sought to extract, compile, and organize such information



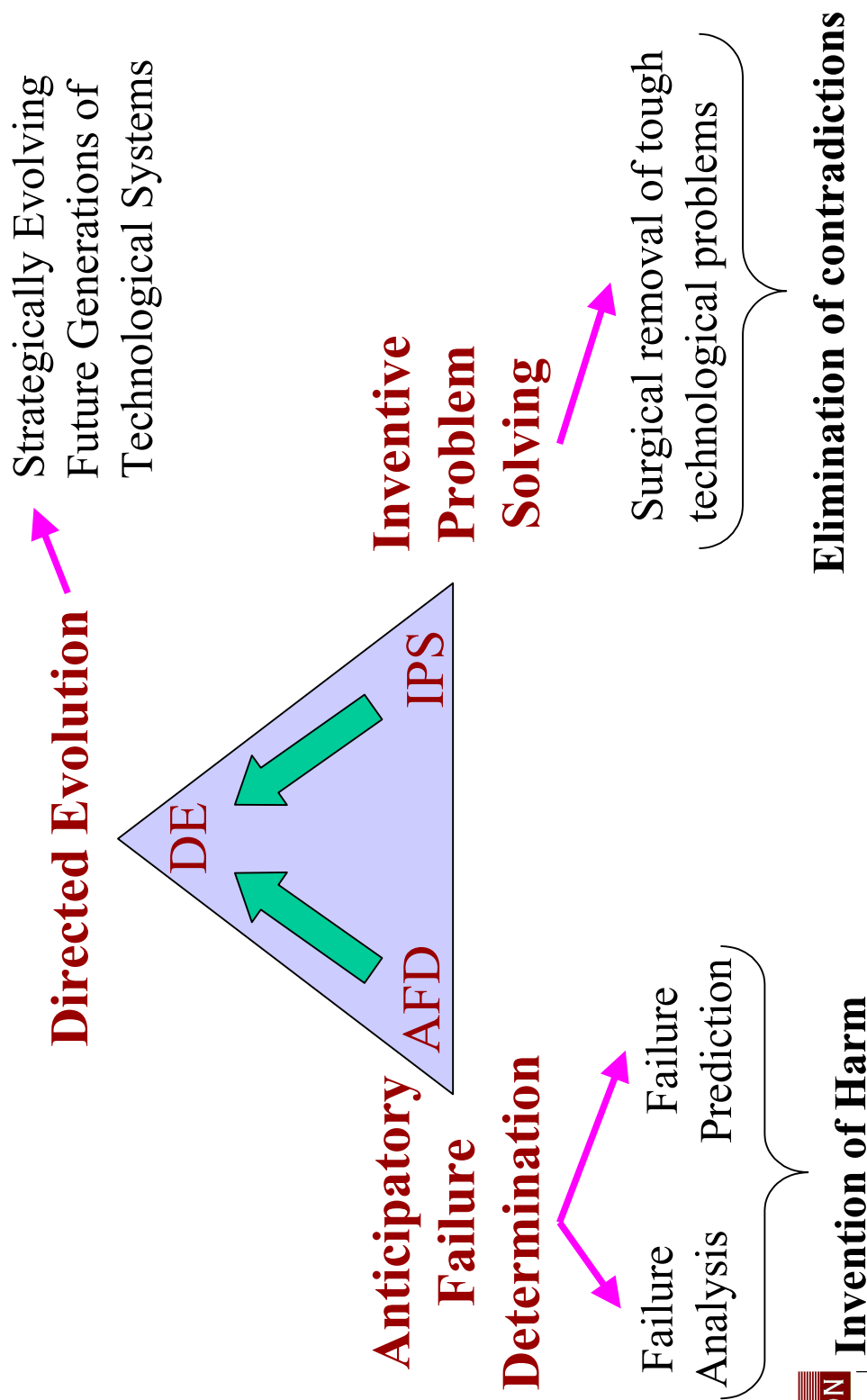
Patterns of Evolution -- The Primary TRIZ Postulate

- Engineering (technological) systems evolve not randomly, but according to objective patterns
- These patterns can be revealed from the patent fund and purposefully used for systems development without numerous blind trials





I-TRIZ Applications & Related Tools



Structured Process for Inventive Problem Solving

Step	Action	Contents	Software Supported
1	Document the problem	Complete and analyze the Innovation Situation Questionnaire (ISQ)	✓
2	Formulate the problem	Develop exhaustive set of Directions for Innovation	✓
3	Prioritize Directions for Innovation		✓
4	Develop Concepts	Develop an exhaustive set of Solution Concepts utilizing various knowledge-base tools	✓
5	Evaluate Results & Plan Implementation	Select Solution Concepts and develop an implementation plan	✓



I-TRIZ Based Invention/Innovation A Science

Computers & Software

Theoretical Foundation,

Algorithms,

Operators, etc.

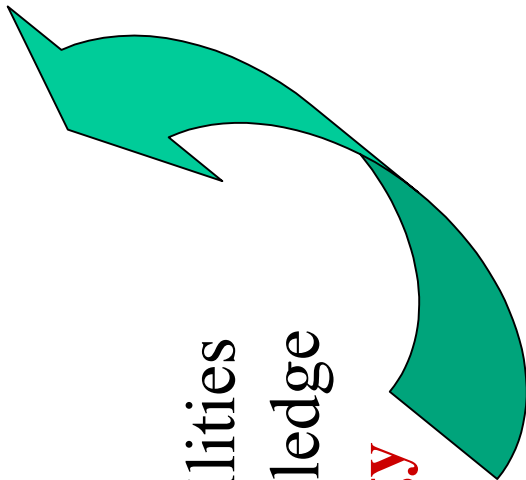
$$\text{Results} = P_c \times P_{kn} \times (1+M) \times (1+T)$$

P_c = Personal Capabilities

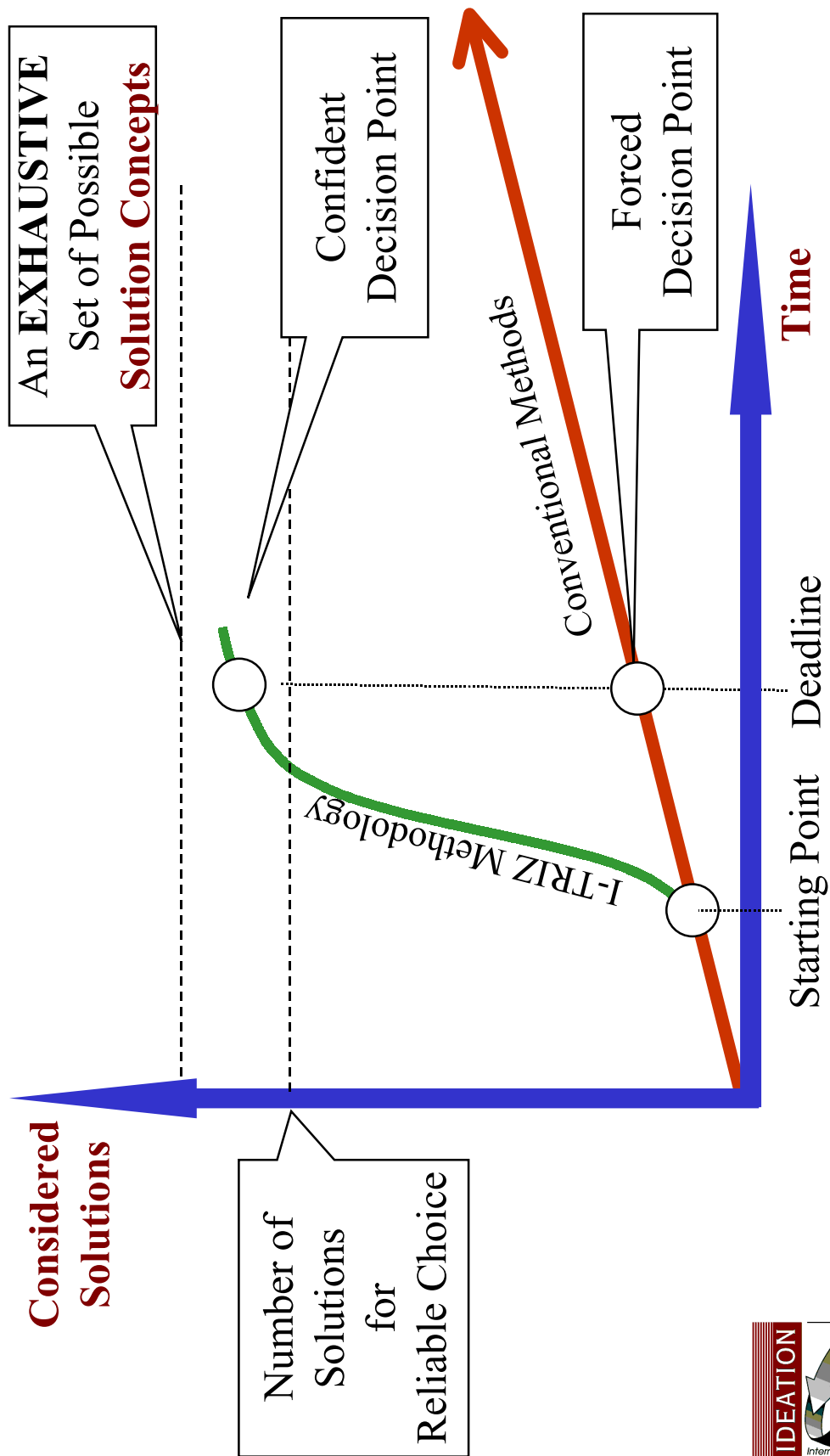
P_{kn} = Personal Knowledge

M= Methodology

T = Tools



Methods and Tools Provide Innovation Leverage





Breadth of Inventive Problem Solving Projects

(Over 10,000 Different Solutions Developed in Last 7 Years)

Industries	Industries
• Automotive	• Paper
• Food	• Ship Building
• Agriculture	• Medical
• Electronics	• Software
• Chemical	• Communications
• Oil	• Other
• Aviation/Aerospace	



Examples of Cost Reduction Projects

- Pentagon – US Army
 - Personnel Reductions
- Boeing
 - C-17
 - Weapon Delivery System
- Allied Signal
 - Compressor
- Dead Sea Bromine
 - Water Cooling
- Helen of Troy
 - Hair Clippers
- Advanced Cardiovascular
 - Medical Devices
- Ford
 - Wind Tunnel
 - Brakes
- Rockwell
 - Golf Cart Brakes
- Navistar
 - Mirror
- Amoco
 - PTA & Processing Plant
- GM
 - Seat (wear and cost)



Examples of Anticipatory Failure Determination Projects


Failure Analysis Projects

- Chemical Industry
 - Reactor Explosion
 - Toxic Chemical Release
 - Tower Fire
 - Chemical Processing Failures
 - Chemical Exposure Issues
 - Hydrogen Compressor Failures
- Automotive Industry
 - Brakes
 - Transmissions
 - Seat Covers
- Trucking Industry
 - Fuel Tank Rotation
 - Fuel Tank Level

Failure Analysis Projects (cont.)

- Aviation / Helicopters
 - Material Defects
 - Passenger Safety
 - Systems Failures
- Oil Industry
 - Wet Gas Valve Failures
- Fluid Systems
 - Water Pumps
 - Hazardous Materials Pumps

Failure Prediction Projects

-  Critical post-concept development step following many Inventive Problem Solving and Directed Evolution projects.



Examples of Directed Evolution Projects

- **Chemical Industry**
 - New Generation of Existing Chemical Processing Plant
 - Processing of New Chemical
- **Heavy Equipment**
 - Lifting Cranes
- **Automotive Industry**
 - Parking Brakes
 - Doors
 - Cable Applications
- **Medical Industry**
 - Surgical Instrumentation
- **Fluid Systems**
 - Water Pumps
 - Hazardous Materials Pumps
- **Materials Development**
 - Super Absorbent Fibers
 - Plastics
 - Packaging
- **Oil Industry**
 - Control of Oil Production
- **Commercial Products**
 - Sanitary Products
 - Foot Massagers
 - Electric Shavers
 - Hair Care Products
 - Combs, Hair Dryers, Curling Irons, Hair Clippers



Presentation by:
Dana W. Clarke, Sr.
TRIZ Scientist
Ideation International Inc.
25505 West 12 Mile Road
Suite 5500
Southfield, Michigan 48034
Ph: 248-353-1313
Fax: 248-353-5495
dclarke@ideationtriz.com
www.ideationtriz.com



REPORT DOCUMENTATION PAGE			Form Approved OMB No. 0704-0188	
Public reporting burden for this collection of information is estimated to average 1 hour per response, including the time for reviewing instructions, searching existing data sources, gathering and maintaining the data needed, and completing and reviewing the collection of information. Send comments regarding this burden estimate or any other aspect of this collection of information, including suggestions for reducing this burden, to Washington Headquarters Services, Directorate for Information Operations and Reports, 1215 Jefferson Davis Highway, Suite 1204, Arlington, VA 22202-4302, and to the Office of Management and Budget, Paperwork Reduction Project (0704-0188), Washington, DC 20503.				
1. AGENCY USE ONLY (Leave blank)		2. REPORT DATE October 2001		3. REPORT TYPE AND DATES COVERED Conference Publication
4. TITLE AND SUBTITLE 2000 NASA Seal/Secondary Air System Workshop			5. FUNDING NUMBERS WU-706-85-37-00	
6. AUTHOR(S) Bruce M. Steinetz and Robert C. Hendricks, editors				
7. PERFORMING ORGANIZATION NAME(S) AND ADDRESS(ES) National Aeronautics and Space Administration John H. Glenn Research Center at Lewis Field Cleveland, Ohio 44135-3191			8. PERFORMING ORGANIZATION REPORT NUMBER E-13062-1	
9. SPONSORING/MONITORING AGENCY NAME(S) AND ADDRESS(ES) National Aeronautics and Space Administration Washington, DC 20546-0001			10. SPONSORING/MONITORING AGENCY REPORT NUMBER NASA CP-2001-211208-VOL1	
11. SUPPLEMENTARY NOTES Proceedings of a conference held at and sponsored by NASA Glenn Research Center, Cleveland, Ohio, October 25-26, 2000. Responsible person, Bruce M. Steinetz, NASA Glenn Research Center, organization code 5950, 216-433-3302.				
12a. DISTRIBUTION/AVAILABILITY STATEMENT Unclassified - Unlimited Subject Categories: 37, 16, and 99 Available electronically at http://gltrs.grc.nasa.gov/GLTRS This publication is available from the NASA Center for AeroSpace Information, 301-621-0390.			12b. DISTRIBUTION CODE	
13. ABSTRACT (Maximum 200 words) The 2000 NASA Seal/Secondary Air System Workshop covered four main areas: (i) overviews of NASA-sponsored Ultra-Efficient Engine Technology (UEET) and Access to Space Programs, with emphasis on program goals and seal needs; (ii) review of turbine engine seal issues from the perspective of end users such as United Airlines; (iii) reviews of sealing concepts, test results, experimental facilities, and numerical predictions; and (iv) reviews of material development programs relevant to advanced seals development. The NASA UEET overview illustrates for the reader the importance of advanced technologies, including seals, in meeting future engine system efficiency and emission goals. GE, Pratt & Whitney, and Honeywell presented advanced seal development work being performed within their organizations. The NASA-funded GE/Stein Seal team has successfully demonstrated a large (3-ft. diam) aspirating seal that can withstand all anticipated pressures, speeds, and rotor runouts anticipated for a GE90 L.P. turbine balance piston location. GE/Stein Seal are fabricating a full-scale seal to be tested in a GE-90 ground test engine in early 2002. Pratt & Whitney and Stein Seal are investigating carbon seals to accommodate large radial movements anticipated in future geared-fan gearbox locations. Honeywell presented a finger seal design being considered for a high-temperature static combustor location incorporating ceramic finger elements. Successful demonstration of the braided carbon rope thermal barriers to extreme temperatures (5500 °F) for short durations provide a new form of very high temperature thermal barrier for future Shuttle solid rocket motor nozzle joints. The X-37, X-38, and future highly reusable launch vehicles pose challenging control surface seal demands that require new seal concepts made from emerging high-temperature ceramics and other materials.				
14. SUBJECT TERMS Seals; Numerical code flow; Experimental; Design			15. NUMBER OF PAGES 493	
			16. PRICE CODE	
17. SECURITY CLASSIFICATION OF REPORT Unclassified	18. SECURITY CLASSIFICATION OF THIS PAGE Unclassified	19. SECURITY CLASSIFICATION OF ABSTRACT Unclassified	20. LIMITATION OF ABSTRACT	